Divalent Digestion:
Insight in Intestinal Ion Transport

Anke Lameris

Divalent Digestion:
Insight in Intestinal Ion Transport

Proefschrift

ter verkrijging van de graad van doctor
aan de Radboud Universiteit Nijmegen
op het gezag van de rector magnificus prof. mr. S. C. J. J. Kortmann,
volgens besluit van het college van decanen
in het openbaar te verdedigen op dinsdag 4 februari 2014
om 12.30 uur precies

door

Anke Ludovica Louise Lameris
Geboren op 25 december 1984
te Grubbenvorst

Promotoren
    Prof. dr. J. G. J. Hoenderop
    Prof. dr. R. J. M. Bindels

Manuscriptcommisie
    Prof. dr. J. Drenth
    Prof dr. M. Ritskes-Hoitinga
   Dr. Stan van de Graaf *(AMC)*

Table of contents

1

Introduction

Calcium and magnesium: chemistry, physics and biology

Calcium (Ca^{2+}) and magnesium (Mg^{2+}) are of vital importance for many physiological functions, which include muscle contraction, neuronal excitability, bone formation, and enzymatic activity. Therefore, it is essential that their concentration throughout the body is tightly regulated. There are many similarities in the homeostatic regulation of Ca^{2+} and Mg^{2+} with respect to the involved organs, the hormones modulating their transport and mobilization, as well as the sensing mechanisms monitoring their concentration [1, 2]. However, despite the similarities in their homeostasis, there are also some important chemical and physical differences between both elements, which have great biological and physiological consequences.

Chemical and physical properties
Both Ca^{2+} and Mg^{2+} belong to the Group 2 elements within the periodic table. This group consists of the alkaline earth metals; a number of elements with similar chemical properties. Basic chemistry rules teach us that the atomic number of an element is identical to the number of protons in its core, meaning that Ca^{2+} and Mg^{2+} consist of 20 and 12 protons, respectively [3]. Since atoms have no overall electrical charge, the number of negatively charged electrons always equals the number of positively charged protons. The 20 electrons of Ca are divided over 4 shells surrounding the core, for Mg the 12 electrons are divided over 3 shells (Figure 1A) [3]. Ions are formed when electrons are lost from the relatively unstable outermost electron shell in order to reveal the, chemically more stable, full shell of electrons underneath. When ionized, both Ca and Mg will lose the 2 negatively charged electrons in their outer shell, turning them into positively charged divalent cations; Ca^{2+} and Mg^{2+} [4]. The size of these ionized atoms is represented by their ionic radius. For Mg^{2+}, the ionic radius (0.65 Å) is among the smallest of all cations, and it is approximately 30% smaller than the ionic radius of Ca^{2+} (0.99 Å) [5]. When ions are dissolved, water molecules form a sphere around the ion due to the electro-negative charge of the oxygen in the water molecule, which directs towards the positively charged ion. Because the attraction of water molecules around an ion depends on the ion's density of charge, smaller ions attract more water molecules. The hydrated radius of Mg^{2+} (4.76 Å) is, therefore, much bigger than that of Ca^{2+} (2.95 Å) (Figure 1B) [5]. These differences become even more prominent in the actual three-dimensional environment, meaning hydrated Mg^{2+} is approximately 400 times larger than its ionic form. In contrast, the hydrated volume of Ca^{2+} is only ±25 times bigger than its ionic volume [5].

A

B
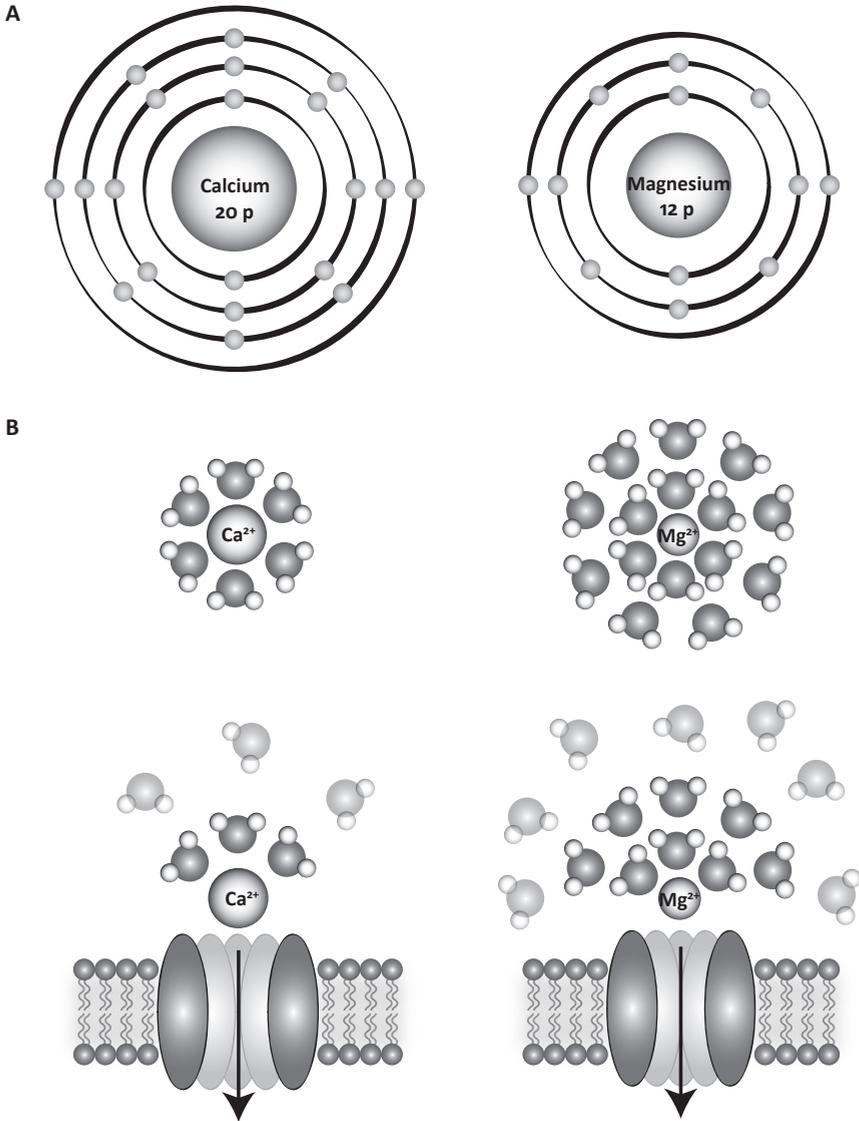
Figure 1 A. Ca and Mg atoms with protons and electrons **B.** When passing a transporter, Ca^{2+} is able to easily shed its single hydration shell so the dehydrated ion will fit through the pore. Mg^{2+} on the other hand, first has to shed two layers, which is highly energy consuming (simplified model, adapted from [4]).

This bulky hydrated volume of Mg^{2+} has serious consequences for its biological function. Most transport proteins for example, require complete dehydration of an ion before it can to pass through the pore of the protein [6]. Mg^{2+} poses two problems in this situation. First, a transporter needs to be able to recognize and interact with the hydrated ion, which is harder when the hydration shell around a cation is bigger. Second, when the cation has been recognized, all water molecules surrounding it need to be removed before it can pass through the membrane via the pore of a transport protein. The relative strength of the interaction between the surrounding water molecules and the cation makes it harder to strip the hydration shell from the Mg^{2+} ion compared to for example a Ca^{2+} ion [6]. These differences in hydration between Ca^{2+} and Mg^{2+} explain a lot of the peculiarities in the biological characteristics of Mg^{2+}, including its often antagonistic behavior to Ca^{2+}, despite their similarities in chemical reactivity and charge.

Biological functions

The roles of Ca^{2+} in biology range widely. As a major component of our bones, Ca^{2+} helps to support and protect our body. Ca^{2+} is also extremely important in cellular function, as it is one of the most important second messengers involved in many intracellular signaling cascades. There are many biological processes that depend on Ca^{2+}, including muscle contraction, neuronal transmission, cellular motility and fertilization. Other biochemical roles of Ca^{2+} include the regulation of enzyme activity, permeability of ion channels and activity of pumps [7]. Mg^{2+} has been suggested to play a role in nearly every physiological system, due to its activity as a Ca^{2+} antagonist, it role in energy transfer and its function in membrane stability [8]. In addition, over 300 enzymes require the presence of Mg^{2+} as a cofactor for their catalytic action [6]. When interacting with enzymes or substrates, Mg^{2+} either takes part in the chemistry of the catalytic reaction or alters the conformation of the enzyme or substrate thereby allowing a reaction to take place. Mg^{2+} frequently acts as a natural Ca^{2+} antagonist, mostly due to its ability to block Ca^{2+} channels [9]. In addition, Mg^{2+} plays a role in the stability of polyphosphate compounds in the cell [10]. Adenosine triphosphate (ATP), the most important source of energy for many cellular processes, must be bound to a Mg^{2+} ion in order to be biologically active [11]. Since ATP is required to fuel glucose utilization, synthesis of proteins and nucleic acids, and many other processes, Mg^{2+} is of vital importance for maintenance of normal cellular function.
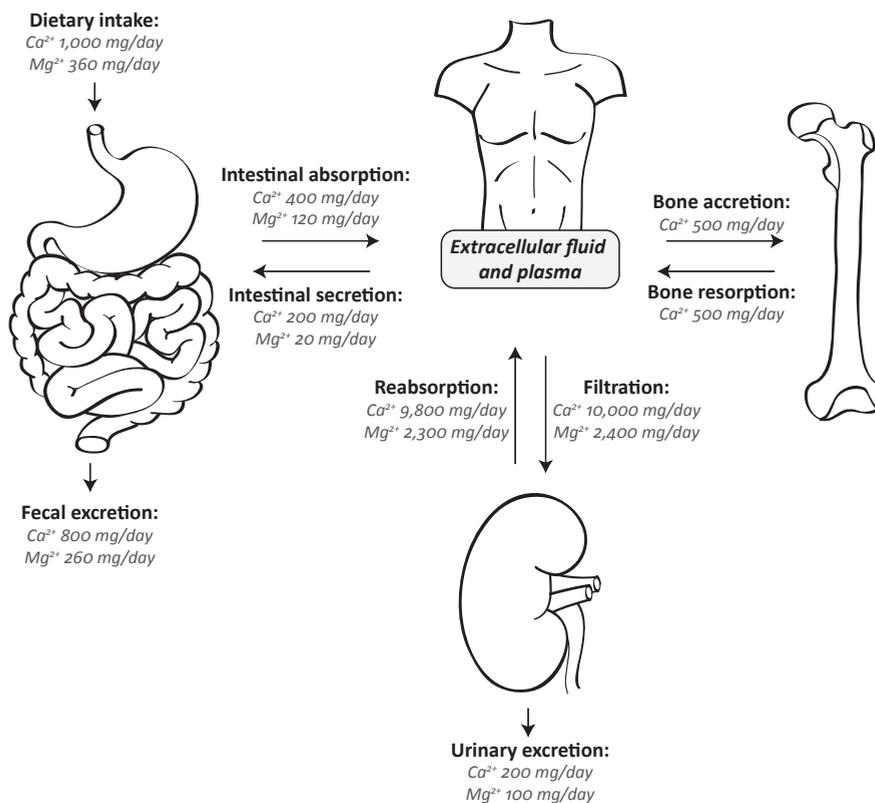
Metabolism

Our body contains about 1,260 gram of Ca^{2+}, 99% of which is stored in bone together with phosphate in the form of calcium-hydroxylapatite ($Ca_{10}(PO_4)_6(OH)_2$)

[12]. The remaining 1% resides intracellularly and in the extracellular fluid (ECF), which includes the blood compartment. Plasma Ca^{2+} levels are tightly controlled within a narrow range, usually between 2.2 and 2.6 mmol/L [13]. It should be noted, however, that only 50% of plasma Ca^{2+} is present in its biologically active, ionized form. The remainder is bound to proteins such as albumin (40%) or complexed to anions such as bicarbonate, citrate and phosphate (10%) [13]. Within the cell, less than 1% of the total intracellular Ca^{2+} exists in a free ionized form, resulting in a low intracellular concentration of 0.1 µmol/L [14]. These low concentrations of free intracellular Ca^{2+} are necessary to avoid the formation of precipitates with phosphate. In addition, the low intracellular concentration is essential to enable Ca^{2+} to function as a second messenger. To maintain a low intracellular Ca^{2+} concentration, Ca^{2+} is actively pumped out of the cytosol and into the extracellular space, endoplasmic reticulum (ER), and mitochondria. In addition, Ca^{2+} can be bound to proteins such as calbindins, which act as Ca^{2+}-buffers keeping intracellular Ca^{2+} concentrations low [15]. The entry of Ca^{2+} into the cell via plasma membrane channels and the release of Ca^{2+} from intracellular stores can trigger a rapid and local increase in the cytoplasmic Ca^{2+} level up to 0.5–1.0 µmol/L, which is important in Ca^{2+} signaling [14].

The total amount of Mg^{2+} in our body is approximately 24 gram, which is much lower than that of Ca^{2+} [16]. Approximately 53% of the total amount of Mg^{2+} in the body is stored in bone, 46% is located in tissues such as muscle and the remaining 1% is located in the extracellular fluid [12]. The plasma Mg^{2+} concentration is tightly regulated, in healthy individuals plasma Mg^{2+} levels should range between 0.7 and 1.1 mmol/L. Like Ca^{2+}, total plasma Mg^{2+} consists of three fractions. Generally, 55-70% is present in the biologically active, free ionized form, 20-30% is bound to intracellular proteins, and 5-15% is complexed to anions [13]. The total intracellular concentrations of Mg^{2+} can vary between 5 and 20 mmol/L, depending on the type of tissue [16]. Most of the intracellular Mg^{2+}, however, is bound to organic molecules such as ATP or localized within organelles such as the mitochondria or the ER. The free intracellular Mg^{2+} concentration is maintained between 0.5 and 1 mmol/L, and shows little fluctuations despite large variations in the concentration of total intracellular or extracellular Mg^{2+} [16]. This means, the concentration gradient driving transport between the extracellular and intracellular compartments is low.

Since dietary intake is the only source of Ca^{2+} and Mg^{2+} for the body, intestinal absorption is of key importance to avoid depletion and keep our bodily stores filled. The Recommended Dietary Allowance (RDA) is the daily dietary intake level of a nutrient considered sufficient by the US Food and Nutrition Board, as it

Figure 2 Homeostasis of Ca²⁺ and Mg²⁺ metabolism is maintained by the concerted action of the intestine, the bone and the kidneys.

should meet the daily requirements of 97.5% of healthy individuals. For Ca^{2+}, the RDA is 1,000 mg/day [17]. Ca^{2+} can be found milk and dairy products, but also in nuts and seeds, in tofu and in certain vegetables. From the daily intake of 1,000 mg of Ca^{2+}, around 400 mg is absorbed by the intestine (Figure 2). Approximately 200 mg is excreted into the intestine, resulting in a fecal excretion of 800 mg of Ca^{2+} per day and a net absorption of 200 mg [17]. Approximately 500 mg of all the Ca^{2+} which is stored in our bones is freely and quickly exchangeable with the ECF [14]. In the kidneys, 10,000 mg of Ca^{2+} is filtered on a daily basis, 9,800 mg is, however, reabsorbed from the pro-urine along the nephrons, resulting in a final urinary excretion of 200 mg Ca^{2+} per day. The RDA for Mg^{2+}, which is 360 mg/day, is considerably lower compared to that of Ca^{2+} [6]. Foods with a particularly high Mg^{2+} content include green leafy vegetables, legumes, nuts, seeds and unrefined

grains. From the 360 mg of Mg^{2+} that is ingested on a daily basis, approximately 120 mg is absorbed (Figure 2). However, 20 mg is secreted into the intestinal lumen, resulting in a net absorption of 100 mg and a fecal excretion of 260 mg Mg^{2+}. In the kidneys, 2,400 mg of Mg^{2+} is filtered from the blood on a daily basis. 2,300 mg is, however, reabsorbed along the nephron, resulting in a final urinary excretion of 100 mg per day [12].

The balance between the absorption of Ca^{2+} and Mg^{2+} via the intestine, their exchange with bone and their excretion via the kidneys should be neutral in normal, healthy individuals, meaning that the total bodily content remains stable. Disturbances of Ca^{2+} and Mg^{2+} homeostasis can have serious biological consequences. In order to maintain a neutral balance, the transport of Ca^{2+} and Mg^{2+} across epithelial layers in various organs is tightly regulated by the interplay of various transport mechanisms and hormones.

Epithelial transport of Ca^{2+} and Mg^{2+}

Epithelial cell layers separate compartments of different compositions such as the intestinal lumen or the lumen of the nephron and the interstitial space or blood compartment. The movement of solutes, ions, and water across these epithelia can take place via either a transcellular route, involving the passage of the apical and basolateral plasma membranes, or via a paracellular route, directly connecting the luminal compartment with the interstitial space. The absorption of Ca^{2+} and Mg^{2+} via the transcellular pathway is saturable, takes place via specialized transporters and can be regulated by several calciotropic and magnesiotropic hormones [18]. Transport via the paracellular pathway is non-saturable, concentration depended, and mainly driven by electrochemical gradients. Together, these two routes determine the distinct transport properties of a certain tissue.

Transcellular transport
Transcellular transport generally requires three consecutive steps. First, ions enter the epithelial cell from the luminal compartment via specific influx proteins on the apical side of the cell. Second, ions are bound to specialized intracellular carrier proteins that facilitate the diffusion across the cytoplasm from the apical area towards to the basolateral membrane. Third, the ions are extruded out of the cell and into the interstitial fluid via ion exchangers and/or pumps on the basolateral side of the epithelial cell [19, 20]. Transport of Ca^{2+} and Mg^{2+} across the apical membrane of epithelial cells is considered to be the rate-limiting factor in

the transcellular transport pathway [18]. Therefore, members of the transient receptor potential channel (TRP) superfamily are essential for the maintenance of Ca^{2+} and Mg^{2+} balance as they facilitate the entry of these cations from the intestinal and renal lumina into the cell [18].

Ca^{2+} entry across the apical membrane of the renal and intestinal epithelial cells is facilitated by TRP Vanilloid 5 and 6 channels (TRPV5 and TRPV6), respectively [21]. Once transported into the cell, Ca^{2+} is bound to calbindin proteins, which function as a buffer and facilitate diffusion of the Ca^{2+} ions towards the basolateral membrane [22]. In the intestine, calbindin-D_{9K} is responsible for this process whereas in the kidney calbindin-D_{28K} is predominant [20]. By buffering intracellular Ca^{2+} levels, calbindins maintain the low intracellular Ca^{2+} levels that facilitate a continuous chemical inward driving force at the apical membrane [15]. At physiological intracellular Ca^{2+} concentrations, calbindins are saturated with Ca^{2+} [23]. Consequently, Ca^{2+} signaling can occur during and independently of transcellular Ca^{2+} movement [24]. At the basolateral side of the cell, efflux of Ca^{2+} takes place against a considerable electrochemical gradient. In the intestine, extrusion of Ca^{2+} across the basolateral membrane takes place via a plasma membrane Ca^{2+}-ATPase named PMCA1b. In the kidney, a Na^+/Ca^{2+} exchanger (NCX1) uses the electrochemical gradient of Na^+ to extrude Ca^{2+} [20].

The key players involved in transcellular transport of Mg^{2+} are less well defined than those responsible for transcellular transport of Ca^{2+}. TRP Melastatin 6 and 7 cation channels (TRPM6 and TRPM7) are thought to be responsible for Mg^{2+} transport across the apical membrane into the cell [25]. TRPM6 is most abundantly expressed in the intestine, kidney and lung, whereas TRPM7 is ubiquitously expressed [26]. Transport of Mg^{2+} from the tubular or intestinal lumen into the cell is, therefore, considered to be mediated predominantly via TRPM6, whereas TRPM7 seems responsible for cellular Mg^{2+} homeostasis. A role for TRPM7, and even of TRPM6/TRPM7 heterotetrameric complexes in the apical influx of Mg^{2+} has, however, also been suggested [27, 28]. Specific Mg^{2+}-binding proteins involved in cytosolic diffusion have not been identified to date. The calbindin proteins, primarily responsible for cytosolic Ca^{2+} transport, have been shown to also bind Mg^{2+}, but the physiological relevance of this observation remains to be determined [29]. The molecular identity of the basolateral extrusion mechanism for Mg^{2+} remains to be defined as well [30]. Since extrusion of Mg^{2+} must occur against an electrochemical gradient, the process most likely depends on a primary or secondary active form of transport, implicating a role for a Mg^{2+} pump and/or a Na^+/Mg^{2+} exchanger [31, 32].

Paracellular transport

Over the last decade, the scientific view on paracellular transport has been changed to a great extent with the identification of various proteins that contribute to the sealing of epithelial cell layers as a part of tight junction structures. These tight junctions have two basic functions. First, they form a fence, which prevents diffusion of membrane proteins from the basolateral to the apical side and vice versa, thus ensuring cell polarity [33]. Second, the tight junctions represent a transepithelial barrier, which determines the permeability of the paracellular pathway to ions and water [33]. Depending on the functional requirements of an epithelium, there may be small or large amounts of water and small solutes flowing passively through the paracellular junctions. Tight junctions consist of several types of integral transmembrane proteins, including occludin, tricellulin, and members of the claudin family [34]. The claudin family consists of a family with at least 26 members ranging in molecular mass from 20–28 kD. All claudins have a similar membrane topology of four transmembrane domains, with cytosolic amino- and carboxy-termini [35]. The first extracellular loop of each claudin is longer and more hydrophobic than the second extracellular loop and is considered to be responsible for determination of the paracellular charge selectivity [36]. The extracellular loops of claudin molecules make homophilic and heterophilic interactions with the extracellular loops of other claudin molecules in adjacent cells [35]. These interactions create either barriers against, or pores for, the passage of selective molecules in the paracellular pathways. The different claudin family members exhibit distinct tissue-, cell-, developmental stage-, and disease-specific expression patterns [33, 37].

So far, the involvement of claudins in Ca^{2+} and/or Mg^{2+} homeostasis in the kidney has been clearly demonstrated for three specific claudins. Patients with mutations in CLDN16, the gene encoding claudin 16, suffer from familial hypomagnesemia with hypercalciuria and nephrocalcinosis (FHHNC, OMIM 248250) [38]. Patients with mutations in CLDN19, encoding claudin 19, have similar clinical features as patients with FHHNC, with additional of occular abnormalities (OMIM 248190) [39]. Expression of both claudin 16 and claudin 19 is restricted to a part of the nephron named the thick ascending limb (TAL) [38, 40]. Here they form a highly cation-specific paracellular channel together, able to transport Mg^{2+} as well as Ca^{2+} [41]. The third claudin family member that is associated with Ca^{2+} and/or Mg^{2+} homeostasis is claudin 14. A recent genome-wide association study has identified CLDN14 as a major risk gene for the development of hypercalciuric nephrolithiasis [42]. Like claudin 16 and 19, claudin 14 is localized in the TAL, where its expression level seems to vary depending on dietary Ca^{2+} content [43]. This suggests a regulatory role for claudin 14 in renal Ca^{2+} handling. Interestingly,

claudin 14 seems to block the paracellular cation channel formed by claudin 16 and 19, thereby reducing Ca^{2+} reabsorption in the TAL [43]. It was shown that high dietary Ca^{2+} intake down regulates the expression level of specific microRNAs (miR's) in the TAL, miR-9 and miR-374, which in turn cause an increase in CLDN14 expression level [43]. This process takes place under the direct regulation of the calcium sensing receptor (CaSR), which monitors the circulating Ca^{2+} levels and subsequently adjusts urinary excretion rates [43]. These findings nicely correspond with previous studies, which have demonstrated that paracellular Ca^{2+} reabsorption in the TAL can be inhibited by CaSR activation during hypercalcemia [44, 45].

To date, not much is known about the role of claudins in the intestinal absorption of Ca^{2+}. In vitro studies have shown that vitamin D induces an increase in paracellular Ca^{2+} transport in Caco-2 cells, a cell-line derived from intestinal epithelia cells [46]. In addition, in vivo studies have demonstrated that intestinal expression of claudin 2 and claudin 12 may be vitamin D-dependent [46]. Further studies are required to confirm these findings and investigate the role of these and other claudins in intestinal Ca^{2+} absorption. Literature does not provide any information on the involvement of claudins in paracellular intestinal Mg^{2+} absorption, therefore, their role in intestinal Mg^{2+} absorption remains to be determined.

Intestine
The fraction of dietary Ca^{2+} which is absorbed in the intestine depends on many factors, including bioavailability and bodily needs. As described before, intestinal absorption is the sum of two components: transcellular and paracellular absorption (Figure 3A) [47, 48]. When dietary Ca^{2+} supply is high, paracellular fluxes in the duodenum, jejunum and ileum are responsible for the main fraction (80-90%) of the intestinal Ca^{2+} absorption [49]. Under normal circumstances, the contribution of the transcellular pathway to total intestinal Ca^{2+} absorption is, therefore, relatively low. Transcellular absorption, which mainly takes place in the duodenum, is highly sensitive to 1,25-dihydroxyvitamin D_3 [50, 51]. Under certain circumstances, intestinal absorption via the transcellular pathway can be increased up to a level where it accounts for 50% of the total intestinal Ca^{2+} (Figure 3B). This occurs in cases of low dietary load or under circumstances of high Ca^{2+} requirements and prevents depletion of the bodily Ca^{2+} stores. The caecum and colon account for less than 10% of total Ca^{2+} uptake, presumably in both a paracellular and transcellular manner [49].
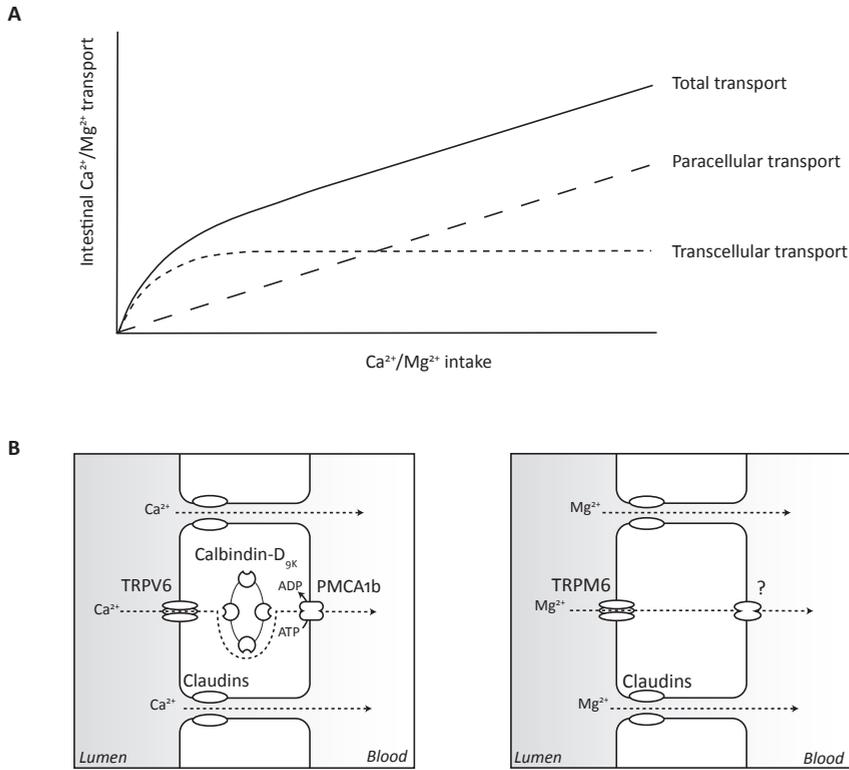
Figure 3 Total intestinal Ca^{2+} and Mg^{2+} absorption is the sum of transport via the paracellular pathway and the transcellular pathway. **A.** Transport via the paracellular pathway increases linearly, depending on the luminal concentration. Transport via the transcellular pathway is saturable, and predominant when luminal concentrations are low (adapted from [52]). **B.** Key players in intestinal absorption of Ca^{2+} and Mg^{2+}.

Between 25-75% of the Mg^{2+} from dietary sources is absorbed in the intestine, depending on the dietary availability as well as the needs of the body. When Mg^{2+} intake is normal the transcellular pathway, involving TRPM6, is responsible for approximately 30% of total absorption, a fraction that increases when dietary intake is low (Figure 3) [52]. The importance of TRPM6 in intestinal Mg^{2+} absorption is demonstrated in patients suffering from a condition named hypomagnesemia with secondary hypocalcemia (HSH). Schlingmann et al. have demonstrated that this autosomal-recessive disorder, which is characterized by low plasma Mg^{2+} levels due to diminished intestinal Mg^{2+} absorption and increased renal Mg^{2+}

excretion, is caused by mutations in the TRPM6 gene [53]. It was shown that transcellular intestinal Mg^{2+} absorption in these patients was greatly diminished, whereas paracellular absorption remained unchanged. As dietary Mg^{2+} is absorbed across the intestine by passive paracellular transport even with loss-of-function TRPM6 mutations, the treatment of HSH patients consists of high oral Mg^{2+} supplementation, which adequately corrects the hypomagnesemia. Intestinal paracellular transport depends on the transepithelial voltage, which is around 5 mV lumen positive with respect to the blood [32]. Luminal Mg^{2+} concentrations range from 1-40 mmol/L depending on dietary contents, generally providing a transepithelial chemical concentration gradient sufficient to further enhance absorption [32]. Paracellular transport is responsible for approximately 70% of Mg^{2+} absorption when luminal concentrations are high [52]. However, Mg^{2+}-specific intestinal paracellular channels have not yet been identified.

Kidney

In the kidney, the majority of the filtered Ca^{2+} is absorbed through paracellular reabsorption in the proximal tubule (50-60%) and to a lesser extent in the TAL (20-25%) (Figure 4) [20]. The absorption of Na^+ and water in the proximal tubule (PT) creates a chemical gradient across the epithelium, increasing the luminal concentration of Ca^{2+}, which allows it's paracellular absorption. At the apical side, Na^+ is reabsorbed from the pro-urine by the Na^+/H^+ exchanger 3 (NHE3), and subsequently extruded on the basolateral side via a Na^+-K^+-ATPase [18]. Water follows via aquaporin 1 (AQP1) waterchannels at both the apical and basolateral side of the PT cells. In the TAL, Na^+, K^+, and Cl^- are reabsorbed from the pro-urine via the Na^+-K^+-$2Cl^-$ co-transporter (NKCC2). A Na^+-K^+-ATPase at the basolateral side provides the driving force for this process. The absorbed Cl^- exits via the basolateral membrane via ClC-Kb channels, whereas the renal outer medullary K^+ channel 2 (ROMK2) allows for apical recycling of K^+ to the tubular lumen. This generates a lumen-positive electrochemical gradient, which drives the reabsorption of Ca^{2+} via the paracellular pathway in this segment [54]. The fine-tuning of the net urinary Ca^{2+} excretion takes place in the late distal convoluted (DCT) and connecting tubule (CNT), where a final 3-7% of Ca^{2+} is reabsorbed via a transcellular pathway involving TRPV5, calbindin-D_{28K}, and NCX1 [55]. This process is tightly regulated by a variety of mechanisms, including hormonal regulation. In the end, only 1-2% of the Ca^{2+} that was filtered from the blood into the pro-urine in the glomerulus is excreted via the urine [55].

Approximately 95% of the filtered Mg^{2+} load is reabsorbed along the different parts of the nephron via both paracellular and transcellular processes [56]. In the PT 10-30% of the filtered Mg^{2+} is reabsorbed via paracellular transport depending
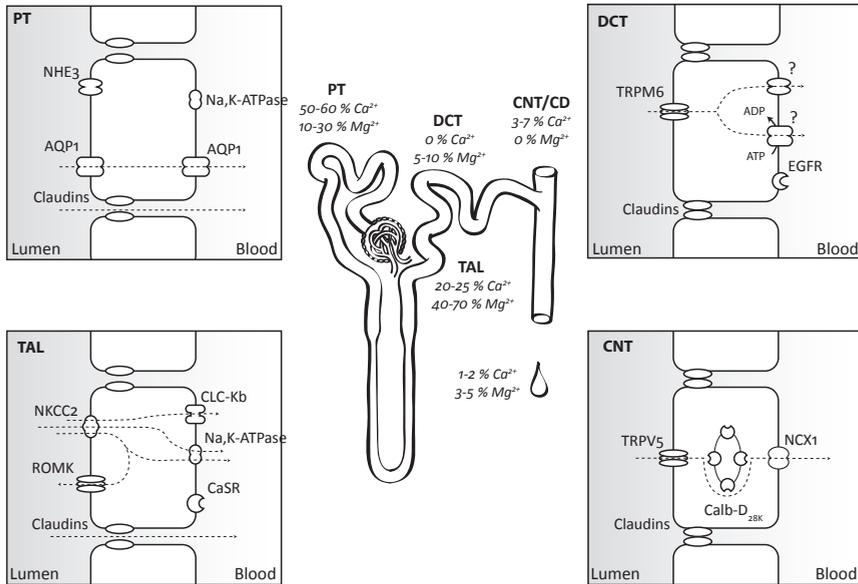
Figure 4 Key players in the reabsorption of Ca²⁺ and Mg²⁺ along different segments of the nephron. In the PT and TAL, Ca²⁺ and Mg²⁺ are mainly reabsorbed via the paracellular pathway. Reabsorption of Ca²⁺ and Mg²⁺ via the transcellular pathway mainly takes place in the CNT and DCT, respectively.

on Na⁺-driven water transport (Figure 4) [57-61]. Paracellular Mg²⁺ transport in the nephron predominates in the TAL, where 40-70% of the filtered Mg²⁺ is reabsorbed [62]. Here, Mg²⁺ reabsorption is mainly driven by the lumen-positive transepithelial voltage and is facilitated by claudin-16 and -19, that operate together to form a cation-permeable channel [63]. At the basolateral side, the CaSR modulates transport in response to changes in concentration of extracellular cations, reducing transport upon stimulation [44]. In the final 5-10% of Mg²⁺ is reabsorbed in an active transcellular manner in the DCT [64]. The tubular epithelium in this part of the nephron consists of a high-resistance epithelium with a lumen-negative voltage of approximately -5 mV. This is generated by the basolaterally localized Na⁺-K⁺-ATPase, which also provides a Na⁺ gradient for the Na⁺-Cl⁻-cotransporter (NCC) to facilitate transport of Na⁺ from the lumen into the cytoplasm. Cl⁻ and K⁺ are extruded on the basolateral side of the cell via ClC-Kb and Kir4.1 respectively. Apical entry of Mg²⁺ occurs via TRPM6, which can be stimulated via the basolateral epidermal growth factor receptor (EGFR) [65]. Mg²⁺ reabsorption

in the DCT defines the final urinary Mg^{2+} excretion, as there is no significant reabsorption of Mg^{2+} beyond the DCT.
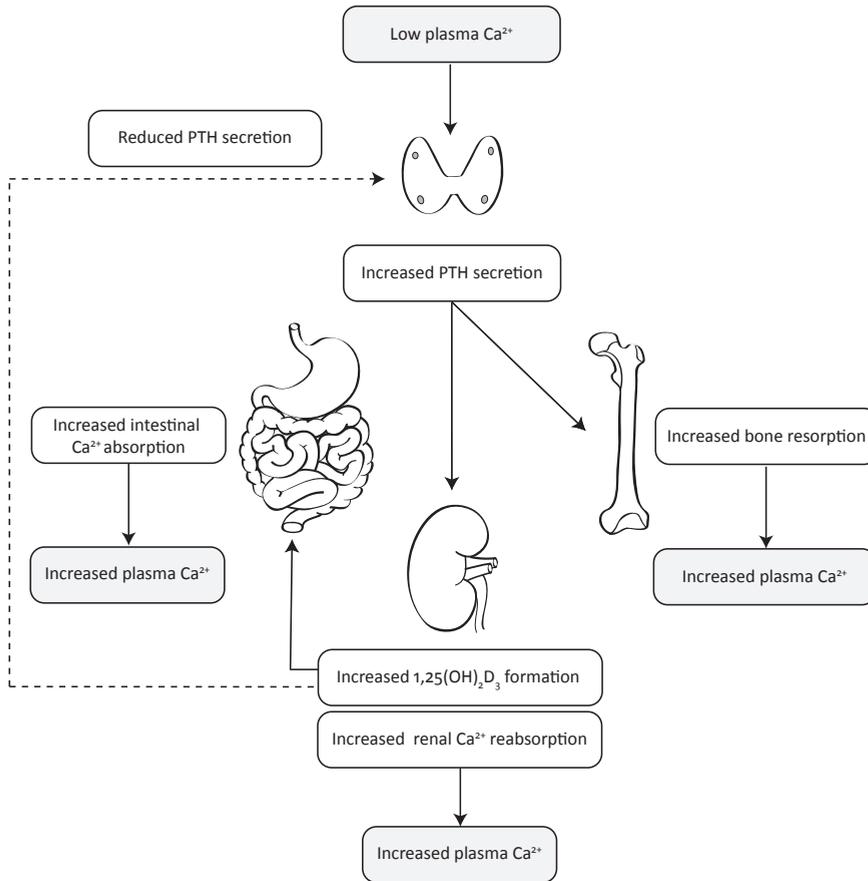
Bone
The maintenance of mineral stores in bone depends on the balance between bone mineralization by osteoblasts and bone resorption by osteoclasts. Various TRP channels, including TRPV4, TRPV5, and TRPV6, have been shown to be involved in Ca^{2+} homeostasis in the bone [66-68]. At the ruffled border membrane of osteoclasts, TRPV5 is involved in the removal of Ca^{2+} from the bone matrix, whereas TRPV4 regulates intracellular Ca^{2+} concentrations both in the osteoclast and osteoblast [66, 68]. TRPV6 is also expressed mainly at the luminal side of the osteoclast and osteoblasts, however, it does not seem crucial for bone mineralization in mice [67]. Expression studies in bone have also reported CaSR transcripts in osteoblasts as well as in osteoclasts [69]. The role of the osteoblast CaSR in bone development, mineralization, and resorption, was demonstrated using a mouse model with an osteoblast specific ablation of CaSR. These mice display severe bone defects, which are independent of systemic calciotropic hormones and rely only on local regulatory events involving the CaSR in bone tissue [70]. So far, it remains unknown if and how the CaSR in bone affects the expressed TRP channels. To date, our understanding of the molecular mechanisms underlying Mg^{2+} handling in bone is limited. Several studies have demonstrated a positive correlation between dietary Mg^{2+} intake and bone density. Dietary depletion leads to reduced bone Mg^{2+} contents without affecting plasma Mg^{2+} levels, indicating that bone acts as a storage from which Mg^{2+} is released in the situation of low Mg^{2+} supply. TRPM6 and TRPM7 are expressed in various osteoblast cell lines [71]. Extracellular Mg^{2+} concentrations have been demonstrated to stimulate osteoblast differentiation via TRPM7 in vitro [72]. The physiological relevance of this observation for Mg^{2+} transport in bone is not yet clear. The role of other Mg^{2+} transporters and sensors in this process remains to be determined as well.

Hormonal regulation of Ca^{2+} and Mg^{2+} transport

Calciotropic hormones
Ca^{2+} balance is tightly regulated by a number of hormones. The two predominant hormones involved in Ca^{2+} homeostasis are parathyroid hormone (PTH) and vitamin D [73, 74]. Other hormones, such as calcitonin, adrenal corticosteroids, estrogens, thyroxine, somatotropin, and glucagon may, however, also contribute to the maintenance of Ca^{2+} homeostasis [7, 20].

The secretion of PTH from the parathyroid glands in response to hypocalcemia is controlled by the CaSR, which senses the plasma Ca^{2+} levels [75]. PTH helps to maintain Ca^{2+} homeostasis via three routes (Figure 5) [12, 14]. First, it stimulates bone resorption, releasing Ca^{2+} from the bone into the blood. Second, it stimulates the kidney to reabsorb Ca^{2+} from the pro-urine. Third, it stimulates the synthesis of active vitamin D by the kidney, which in turn leads to an increase in intestinal Ca^{2+} absorption. Once released into the circulation PTH can bind to PTH receptors, which are located amongst others in the intestine, bone and kidney [20].

Figure 5 Effects of PTH and vitamin D on Ca^{2+} homeostasis. PTH, released from the parathyroid glands, stimulates the production of active vitamin D_3 by the kidney, which in turn stimulates intestinal Ca^{2+} absorption. It also increases bone resorption and renal Ca^{2+} reabsorption, increasing plasma Ca^{2+} levels.

Our body can obtain vitamin D from two sources: it can be synthesized in the skin under the influence of ultraviolet light, or it can be absorbed from our diet [76]. Unless fortified, few foods contain vitamin D; therefore dermal synthesis is the major natural source of this vitamin. Previtamin D_3 (cholecalciferol) is synthesized non-enzymatically in skin from 7-dehydrocholesterol during exposure to the ultraviolet rays in sunlight (Figure 6). In the liver, it undergoes a hydroxylation process by an enzyme called 25-hydroxylase, turning it into 25-hydroxyvitamin D_3 (calcidiol) [14]. Further hydroxylation of 25-hydroxyvitamin D_3 into the physio-logically active vitamin D metabolite 1,25-dihydroxyvitamin D_3 (calcitriol) occurs in the kidney by an enzyme named 1-alpha-hydroxylase, which is encoded by the CYP27B1 gene. The kidney also plays a role in the breakdown of active vitamin D into inactive metabolites. With the help of an enzyme named 24-hydroxylase, encoded by CYP24A1, 1,25-dihydroxyvitamin D_3 is broken down to 24,25-dihy-droxyvitamin D, which is biologically inactive. CYP24A1 is down-regulated by PTH and upregulated by 1,25-dihydroxyvitamin D_3 in a regulatory feedback loop ensuring proper plasma 1,25-dihydroxyvitamin D_3 levels. The major functions of 1,25-dihydroxyvitamin D_3 are carried out in the intestine, where it stimulates the
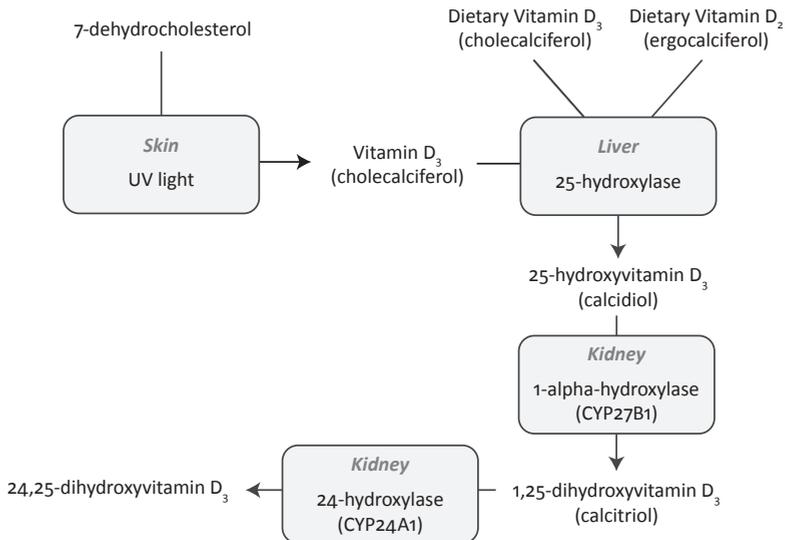
Figure 6 Overview of vitamin D metabolites and enzymes involved in their synthesis. The active vitamin D metabolite, 1,25 dihydroxyvitamin D_3, is synthesized from precursors by various enzymes including 1-alpha-hydroxylase. The enzyme 24-hydroxylase is responsible for the breakdown of active vitamin D to 24,25-dihydroxyvitamin D_3, an inactive metabolite.

absorption of Ca^{2+}, and in the parathyroid glands, where it inhibits the synthesis of PTH at the transcriptional level [12]. 1,25-dihydroxyvitamin D_3 can bind to the vitamin D receptor (VDR), which is a transcription factor. Upon binding to 1,25-dihydroxyvitamin D_3 the VDR heterodimerizes with other nuclear hormone receptors, in particular the family of retinoid X receptors. This complex subsequently binds to special DNA sequences called vitamin D responsive elements (VDRE) in the promoters of genes. These include TRPV5, TRPV6, calbindin-D_{9k}, and PMCA1b, which are strongly regulated by 1,25-dihydroxyvitamin D_3. The expression of renal transporters involved in Ca^{2+} transport is also regulated by 1,25-dihydroxyvitamin D_3, albeit to a lesser extent than the intestinal transporters [76, 77].

Magnesiotropic hormones

Like Ca^{2+}, Mg^{2+} has been suggested to be regulated by PTH and vitamin D. However, reports on their effects are conflicting and the exact role of these hormones in Mg^{2+} homeostasis remains unclear. The same holds true for many other hormones that have been proposed to have a regulatory role in Mg^{2+} homeostasis, such as vasopressin, aldosterone, estrogen and testosterone. Although the hormonal regulation of Mg^{2+} is not as well-defined as that of Ca^{2+}, several findings during the last decade have helped us to better understand how Mg^{2+} homeostasis is regulated.

In 2007, two Dutch sisters with isolated autosomal recessive hypomagnesmia (IRH) were diagnosed to have a mutation in the gene encoding the EGF precursor protein pro-EGF. It was shown that EGF, via activation of the EGF receptor (EGFR), stimulates Mg^{2+} transport via TRPM6 [78]. Supporting these findings, patients treated with the anticancer agent cetuximab, an EGFR antagonist, were also found to develop hypomagnesemia [79]. Taken together, these recent studies highlight an important role for EGFR signaling in the maintenance of Mg^{2+} homeostasis.

Recently, two common TRPM6 genetic variants (I1393V and K1584E polymorphisms) were associated with an increased risk of type 2 diabetes (DM2) in women with low Mg^{2+} intake [80]. Furthermore, it was shown that insulin activates TRPM6, and that when the described polymorphisms were introduced in TRPM6, this stimulatory effect was lost. In addition, patients with these polymorphisms were more likely to develop gestational diabetes mellitus (GDM), demonstrating the clinical relevance of these findings [81]. In the future, genetic variants of TRPM6 could potentially be used as biomarkers to identify individuals at risk for developing GDM/DM2-induced hypomagnesemia.

Clinical relevance

Under certain circumstances, the balance between absorption, storage and excretion of Ca^{2+} or Mg^{2+} can become disturbed. These disturbances can have various reasons. Sometimes, genetic defects in a gene encoding for one of the key players involved in Ca^{2+} or Mg^{2+} homeostasis cause abnormalities. In addition, the use of certain drugs can affect the balance of these divalents. The homeostatic disturbances may be relatively harmless when the body is able correct for them, however if Ca^{2+} or Mg^{2+} homeostasis are significantly disturbed, this may have serious clinical implications.

Hypocalcemia
Hypocalcemia can lead to various clinical manifestations, ranging from no symptoms at all or only a few symptoms if the hypocalcemia is mild, to life-threatening seizures and heart failure if it is severe. The rate of development of hypocalcemia and the duration of its presence will also influence the clinical manifestations. Muscle spasms, tetany, seizures and cardiac arrhythmia may occur in patients who develop hypocalcemia acutely, whereas cataracts, ectodermal changes and dental changes are features of chronic hypocalcemia [82].

The treatment of hypocalcemia varies with its severity and also depends on the underlying cause. Non-symptomatic patients, or patients with mild clinical manifestations should preferably be treated with oral supplements. Loop diuretics such as furosemide, inhibit NKCC2 consequently leading to reduced Ca^{2+} reabsorption in the TAL [82]. It is, therefore, advised to change hypocalcemic patients requiring diuretic treatment to a thiazide-type diuretic to prevent further renal Ca^{2+} loss. Intravenous administration of Ca^{2+} is only advised in severe cases where there is a need for acute treatment.

Hypercalcemia
Under normal circumstances, the body is able to dispose of an overload of Ca^{2+} by increasing the amount of Ca^{2+} storage in the bone and by increasing urinary Ca^{2+} excretion. Prolonged periods of hypercalciuria however can lead to nephrolithiasis as well as nephrocalcinosis. The severity of symptoms resulting from hypercalcemia depend on the degree of hypercalcemia as well as the rate at which it has developed. Hypercalcemia can lead to gastrointestinal symptoms, such as nausea, vomiting and constipation. In addition, it may lead to lethargy, muscle weakness, hypertension and shortening of the QT interval of the heart [12].

Selecting the right therapy to treat hypercalcemia requires a good differential diagnosis to determine the underlying cause. In some cases, however, immediate action is required. The safest, and most effective, way of treating hy'percalcemia in patients with normal cardiac and renal function is the intravenous administration of saline. The resulting volume expansion will reduce the reabsorption of Na^+, $Cl-$ and water in the PT, and will consequently also reduce paracellular Ca^{2+} absorption. Other possibilities include the use of loop diuretics like furosemide, the administration of biphosphonates (which reduced the release of Ca^{2+} from the bone by inhibiting osteoclast activity), calcitonin (which inhibits bone reabsorption and enhances renal Ca^{2+} excretion), glucocorticoids (which inhibit production of active vitamin D) and cinacalcet (which activates the CaSR, leading to reduced PTH release) [82].

Hypomagnesemia

Hypomagnesemia is defined as a plasma Mg^{2+} concentration below 0.70 mmol/L. Muscle cramps, tetany and muscular weakness are the main complaints of hypomagnesemic patients [83]. Cardiovascular abnormalities such as arrhythmias and convulsions have also been described. Hypomagnesemia is, however, often associated with multiple biochemical abnormalities such as hypokalemia and hypocalcemia. It is, therefore, difficult to ascribe specific clinical manifestations solely to hypomagnesemia. Chronic depletion of Mg^{2+} generally becomes clinically evident in patients at plasma Mg^{2+} concentrations of <0.40 mmol/L. Hypocalcemia (muscle cramps, tetany) and hypokalemia (muscle weakness), will contribute to the clinical phenotype when occurring secondary to hypomagnesemia. Hypokalemia associated with hypomagnesemia is often refractory to treatment by K^+, and can only be properly corrected when Mg^{2+} is co-administered. The decreased intracellular Mg^{2+} concentration resulting from Mg^{2+} deficiency, releases the Mg^{2+}-mediated inhibition of ROMK channels, thereby increasing K^+ excretion via the kidney, eventually resulting in hypokalemia [84]. Hypocalcemia secondary to hypomagnesemia has been hypothesized to originate from inappropriately low PTH secretion, the release of which depends on an intracellular signalling cascade that requires Mg^{2+}. Also the responsiveness of target organs to PTH stimulation seems to be reduced [85, 86]. Hypocalcemia secondary to hypomagnesemia with low parathyroid hormone secretion is frequently observed when plasma Mg^{2+} levels are extremely low [87]. Treatment is only successful when hypomagnesemia is addressed together with the hypocalcemia as Ca^{2+} supplementation by itself will not suffice [86].

Hypomagnesemic patients can be repleted in various ways. Depending on the severity of the clinical symptoms and the origin of the hypomagnesemia patients may be treated with oral supplements, with intramuscular injections or by intravenous infusions [88]. Intravenous administration is the most effective in restoring plasma Mg^{2+} to normal levels, and is, therefore, the best treatment in case of severe hypomagnesemia. The disadvantage is that patients have to visit the hospital on a regular basis if frequent treatment is required. Oral supplements do not require hospital visits, however, not all patients tolerate these Mg^{2+} supplements of due to their cathartic effect at higher dosages. Solubility and bio-availability vary greatly between various Mg^{2+} supplements. Organic Mg^{2+} salts have a higher solubility and bioavailability compared to inorganic Mg^{2+} salts, making them more suitable for oral Mg^{2+} replacement therapy. It should be noted that in case of severe hypomagnesemia or Mg^{2+} deficiency due to intestinal malabsorption, oral Mg^{2+} supplements may not be sufficient to restore plasma Mg^{2+} levels to normal.

Hypermagnesemia

Hypermagnesemia causes a broad variety of symptoms depending on plasma Mg^{2+} levels (Table 1) [83, 89, 90]. In case of a relatively mild degree of hypermagnesemia, patients may suffer from nausea, vomiting and flushing. Within the asymptomatic and mildly symptomatic stages of hypermagnesemia (between 1.1 and 3.0 mmol/L) there is also the therapeutic range in which hypermagnesemia can be used to control convulsions [91]. When the plasma Mg^{2+} levels increase further, however, symptoms become increasingly dangerous, eventually leading to a comatose state and/or asystole. Since the renal response to high Mg^{2+} levels is extremely efficient, hypermagnesemia is relatively rare and primarily observed in patients with renal insufficiency. However, in rare cases hypermagnesemia is found in individuals with normal renal function, mostly as a result of exogenous administration of high doses of Mg^{2+} via oral, intravenous or rectal routes [92].

Treatment of hypermagnesemia should primarily be aimed at lowering plasma Mg^{2+} levels. However, when serious complications of Mg^{2+} intoxication are present, intravenous administration of low doses of Ca^{2+} may quickly reduce severity of symptoms due to the antagonistic effect of Ca^{2+} to Mg^{2+}. It is, therefore, the advised initial treatment in case of life-threatening situations. Also, haemodialysis may be used to quickly reduce plasma Mg^{2+} levels in severe cases [93, 94]. Next, oral intake and/or intravenous administration of Mg^{2+} salts should be discontinued immediately to avoid further intoxication. Subsequently, renal Mg^{2+} excretion could be stimulated by intravenous administration of diuretics and saline to ensure high urine output and prevent volume depletion [95].

Table 1 Symptoms of hypermagnesemia.

Plasma Mg^{2+} level (mmol/L)	Symptoms
0.7-1.1	None, normal plasma level
1.1-2.0	Asymptomatic
2.0-3.0	Nausea, vomiting, cutaneous vasodilation, headaches, hyporeflexia, lethargy
3.0-5.0	Unresponsiveness, loss of deep tendon reflexes, hypotension, electrocardiographic changes, bradycardia
>5.0	Complete heart block, respiratory paralysis, coma, shock
>8.0	Asystole, death

Adapted from [83, 89, 90]

Intestinal absorption studies

Reports of scientists studying the absorption of nutrients in the intestine date back to the 18th century. Various experimental techniques were applied during that time, ranging from small perforated metal tubes filled with grass which were fed to sheep in order to determine of the contents would be digested, to linen bags filled with bread and meat which were ingested by researchers themselves and later collected from the feces. Approximately 250 years after these first experiments, a broad range of well established in vivo, ex vivo, in situ and in vitro methods to study intestinal absorption are available, which have contributed greatly to our understanding of transport processes in the gastrointestinal tract. The following paragraphs provide a summary of various methods that are presently available to study the intestinal absorption of ions in an in vivo or ex vivo setting.

Ussing chamber technique

The Ussing chamber method was developed in 1951 by Ussing and Zerahn as a tool to investigate active Na$^+$ transport by frog skin [96]. To date, Ussing chambers are still used to study transport across the intestinal epithelium. To this end, small sections of intestinal mucosa are clamped between two chambers, which are filled with bathing solutions on the mucosal and serosal sides. In addition, the experimental set-up of the Ussing chamber offers the possibility to monitor and regulate the transepithelial electrical resistance. Fluxes from the mucosal to serosal side and from serosal to mucosal side can be measured depending on the

content of the buffers that are used. This way, it is possible to distinguish between passive, paracellular transport and active, transcellular transport. A major advantage of the Ussing chamber technique is that it allows scientists to measure and compare transport in specific intestinal segments within and between different species. The limitations of this technique include the difficulty of maintaining tissue viability, the lack of an intact blood flow and the potential presence of residues of muscle- and serosal layers, which may disturb accurate measurements.

Everted gut sac technique

The everted gut sac technique was first described by Wilson and Wiseman in the 1950's [97]. For this ex vivo technique intestinal segments are isolated from an animal. The segment is then everted, filled with buffer, and tied on both sides to create a closed compartment. They are then suspended in an oxygenated buffer. With (radioactive) probes and non-absorbable markers transport from the outer, mucosal, side to the inner, serosal, side of the sac are measured. Paracellular and transcellular transport cannot be characterized by studying the bidirectional movement of solutes, as transport is measured in a unidirectional, mucosal to serosal way only. By determining whether the transport is saturable or non-saturable, sensitive to certain modifiers and metabolic inhibitors, and by studying competition it is nevertheless possible to distinguish between the different transport processes. There are, however, some disadvantages to the everted gut sac methods. First, the underlying musculature is not removed from the sample, which may act as a barrier and can therefore lead to an underestimation of the actual transport that would take place in vivo. Second, the volume of the serosal compartment is small; meaning concentrations of compounds within the sac can quickly rise, negatively influencing the reliability of the measurement. Similar to the Ussing chamber technique, tissue samples in the everted gut sac methods do not have blood supply and tissue viability should be carefully monitored.

Perfusion studies

Perfusion experiments are based on an in situ technique in which an intestinal loop is isolated in an anesthetized animal by cannulating the proximal and distal end of an intestinal segment. This method closely resembles the in vivo situation as the blood and lymph supply as well as the innervation remains intact. The contents of the perfusion solution (containing a non-absorbable marker) can be determined before and after passing the intestinal loop, in order to determine the amount of absorption by the intestinal segment. The sensitivity is a limiting factor in the applicability of this method; if less than 20% of the compound of

interest is absorbed, perfusion techniques are not considered to be accurate. This problem may be solved by measuring the concentration of the substance of interest in blood samples drawn from the portal vein. Anesthesia and surgical manipulation may influence intestinal motility and blood flow, thereby inducing changes in intestinal permeability reducing reliability.

Balance studies

In balance studies, intake and excretion of an ion are analyzed in order to determine, amongst others, intestinal absorption. By housing animals in metabolic cages it is possible to carefully monitor the individual intake of food and water, in addition it allows for separation of urinary and fecal samples. By calculating the difference between the intake of an ion via food and water and its excretion via the feces an estimation can be made of intestinal absorption. As this method does not take into account the excretion of ions from the blood back into the intestinal lumen it may lead to an underestimation of absorption. Also, it does not distinguish between paracellular and transcellular transport, nor does it provide information about the absorption in a specific intestinal segment.

Absorption studies

Intestinal absorption studies are traditionally performed using radioactive isotopes. After oral administration, the rate of absorption from the intestine into the blood is measured, providing accurate information on the rate and kinetics of absorption. For intestinal Ca^{2+} absorption studies in animals the radioactive ^{45}Ca isotope is frequently used. It emits a low energy beta radiation, which is completely absorbed by a layer of matter less than 1 mm thick, meaning its use is relatively safe. In addition, its long half-life of 163 days makes it easy to work with, whereas it still emits enough radiation to allow for accurate and easy quantification using a scintillation counter. There are 19 radioactive Mg^{2+} isotopes, with half-lives varying from 170 nanoseconds to approximately 21 hours. The short half-life and the resulting problems involving their availability, costs and applicability, makes the radioactive Mg^{2+} isotopes unsuitable for absorption-studies. Non-radioactive, stable isotopes of Mg^{2+} such as ^{25}Mg and ^{26}Mg can be distinguished from ^{24}Mg based on their weight using mass spectrometry techniques. The first report of the use of stable isotopes to study Mg^{2+} absorption dates back to 1975 [98]. However, they were mainly used in balance studies, teaching us little about the kinetics of intestinal Mg^{2+} absorption.

Outline of this thesis

The general aim of this thesis is to generate more insight in the physiological, pathophysiological and pharmacological regulation of intestinal Ca^{2+} and Mg^{2+} transport. TRPV6 is considered the primary protein responsible for transcellular intestinal Ca^{2+} absorption. In vitro studies have demonstrated that a negatively charged aspartic acid within the putative pore region of mouse TRPV6 (position 541) is critical for Ca^{2+} permeation of the channel. In chapter 2 the in vivo role of this amino acid in TRPV6 mediated Ca^{2+} transport is determined by the functional characterization of Ca^{2+} homeostasis in a TRPV6$^{D541A/D541A}$ knock-in mouse model. An increasing number of case-reports is published concerning patients suffering from hypomagnesemia due to the use of proton pump inhibitors. In chapter 3, the molecular the molecular mechanism underlying proton pump inhibitor induced hypomagnesemia is investigated in mice. The effect of the proton pump inhibitor omeprazole on Mg^{2+} homeostasis and expression levels of the colonic H^+,K^+-ATPase as well as magnesiotropic genes is addressed. Chapter 4 describes a method to measure intestinal Mg^{2+} absorption in an in vivo setting using stable isotopes. In addition, an innovative technique is described, with which local absorption of ions in the colon in mice can be measured using intestinal cannulas. In chapter 5 a unique set of human gastrointestinal biopsies is used to determine details expression patterns of a broad range of claudins. Also, the expression of claudins in patients suffering from inflammatory bowel disease is studied. Chapter 6 describes the clinical and biochemical characteristics of three patients with idiopathic infantile hypercalcemia. The potential role of CLDN3 and CLDN4 in the intestinal hyperabsorption of Ca^{2+} found in patients with this rare disease is investigated. In chapter 7 a young patient suffering from Williams-Beuren syndrome with infantile hypercalcemia is described and recent advances concerning the etiology of infantile hypercalcemia are discussed. Finally, the studies described in the chapters of this thesis are summarized in chapter 8, which also provides a detailed discussion placing the findings in the context of the current knowledge regarding intestinal transport of Ca^{2+} and Mg^{2+}.

References

1. Dimke H, Hoenderop JG, Bindels RJ: Hereditary tubular transport disorders: implications for renal handling of Ca^{2+} and Mg^{2+}. *Clin Sci (Lond)* 118: 1-18, 2009

2. Ferre S, Hoenderop JG, Bindels RJ: Sensing mechanisms involved in Ca^{2+} and Mg^{2+} homeostasis. *Kidney Int* 82: 1157-1166, 2012

3. Luft FC: Whither Magnesium? *Clinical Kidney Journal* 5: i1-i2, 2012

4. Jahnen-Dechent W, Ketteler M: Magnesium basics. *Clinical Kidney Journal* 5: i3-i14, 2012

5. Maguire ME, Cowan JA: Magnesium chemistry and biochemistry. *Biometals* 15: 203-210, 2002

6. Saris NE, Mervaala E, Karppanen H, Khawaja JA, Lewenstam A: Magnesium. An update on physiological, clinical and analytical aspects. *Clin Chim Acta* 294: 1-26, 2000

7. van de Graaf SF, Bindels RJ, Hoenderop JG: Physiology of epithelial Ca^{2+} and Mg^{2+} transport. *Rev Physiol Biochem Pharmacol* 158: 77-160, 2007

8. Wacker WEC: *Magnesium and man*, Harvard University Press, 1980.

9. Levine BS, Coburn JW: Magnesium, the mimic/antagonist to calcium. *N Engl J Med* 310: 1253-1255, 1984

10. Hartwig A: Role of magnesium in genomic stability. *Mutat Res* 475: 113-121, 2001

11. Pecoraro VL, Hermes JD, Cleland WW: Stability constants of Mg^{2+} and Cd^{2+} complexes of adenine nucleotides and thionucleotides and rate constants for formation and dissociation of MgATP and MgADP. *Biochemistry* 23: 5262-5271, 1984

12. Greenberg A, Cheung AK: *Primer on Kidney Diseases*, Elsevier Saunders, 2005.

13. Moe SM: Disorders involving calcium, phosphorus, and magnesium. *Prim Care* 35: 215-237, v-vi, 2008

14. Favus MJ, Goltzman D: Regulation of Calcium and Magnesium. In: *Primer on the Metabolic Bone Diseases and Disorders of Mineral Metabolism*. John Wiley & Sons, Inc., pp 171-179.

15. Schwaller B: The continuing disappearance of "pure" Ca^{2+} buffers. *Cell Mol Life Sci* 66: 275-300, 2009

16. Schrier RW: *Atlas of Diseases of the Kidney*, Wiley, 1999.

17. Allen LH: Calcium bioavailability and absorption: a review. *Am J Clin Nutr* 35: 783-808, 1982

18. Dimke H, Hoenderop JG, Bindels RJ: Molecular basis of epithelial Ca^{2+} and Mg^{2+} transport: insights from the TRP channel family. *J Physiol* 589: 1535-1542,

19. Hoenderop JG, Bindels RJ: Calciotropic and magnesiotropic TRP channels. *Physiology (Bethesda)* 23: 32-40, 2008

20. Hoenderop JG, Nilius B, Bindels RJ: Calcium absorption across epithelia. *Physiol Rev* 85: 373-422, 2005

21. Nijenhuis T, Hoenderop JG, Bindels RJ: TRPV5 and TRPV6 in Ca^{2+} (re)absorption: regulating Ca^{2+} entry at the gate. *Pflugers Arch* 451: 181-192, 2005

22. Bronner F: Mechanisms and functional aspects of intestinal calcium absorption. *J Exp Zool A Comp Exp Biol* 300: 47-52, 2003

23. Feher JJ: Facilitated calcium diffusion by intestinal calcium-binding protein. *Am J Physiol* 244: C303-307, 1983

24. Bindels RJ: Calcium handling by the mammalian kidney. *J Exp Biol* 184: 89-104, 1993

25. Chubanov V, Gudermann T, Schlingmann KP: Essential role for TRPM6 in epithelial magnesium transport and body magnesium homeostasis. *Pflugers Arch* 451: 228-234, 2005

26. Groenestege WM, Hoenderop JG, van den Heuvel L, Knoers N, Bindels RJ: The epithelial Mg^{2+} channel transient receptor potential melastatin 6 is regulated by dietary Mg^{2+} content and estrogens. *J Am Soc Nephrol* 17: 1035-1043, 2006

27. Chubanov V, Schlingmann KP, Waring J, Heinzinger J, Kaske S, Waldegger S, Mederos y Schnitzler M, Gudermann T: Hypomagnesemia with secondary hypocalcemia due to a missense mutation in the putative pore-forming region of TRPM6. *J Biol Chem* 282: 7656-7667, 2007

28. Chubanov V, Waldegger S, Mederos y Schnitzler M, Vitzthum H, Sassen MC, Seyberth HW, Konrad M, Gudermann T: Disruption of TRPM6/TRPM7 complex formation by a mutation in the TRPM6 gene causes hypomagnesemia with secondary hypocalcemia. *Proc Natl Acad Sci U S A* 101: 2894-2899, 2004

29. Berggard T, Miron S, Onnerfjord P, Thulin E, Akerfeldt KS, Enghild JJ, Akke M, Linse S: Calbindin $D2_{8k}$ exhibits properties characteristic of a Ca^{2+} sensor. *J Biol Chem* 277: 16662-16672, 2002

30. Quamme GA: Molecular identification of ancient and modern mammalian magnesium transporters. *Am J Physiol Cell Physiol* 298: C407-429, 2010

31. Flatman PW: Mechanisms of magnesium transport. *Annu Rev Physiol* 53: 259-271, 1991

32. Schweigel M, Martens H: Magnesium transport in the gastrointestinal tract. *Front Biosci* 5: D666-677, 2000

33. Gunzel D, Yu AS: Claudins and the modulation of tight junction permeability. *Physiol Rev* 93: 525-569,

34. Amasheh S, Fromm M, Gunzel D: Claudins of intestine and nephron - a correlation of molecular tight junction structure and barrier function. *Acta Physiol (Oxf)* 201: 133-140, 2011

35. Hou J: Lecture: New light on the role of claudins in the kidney. *Organogenesis* 8: 1-9, 2012

36. Krause G, Winkler L, Mueller SL, Haseloff RF, Piontek J, Blasig IE: Structure and function of claudins. *Biochim Biophys Acta* 1778: 631-645, 2008

37. Hou J, Rajagopal M, Yu AS: Claudins and the kidney. *Annu Rev Physiol* 75: 479-501, 2012

38. Simon DB, Lu Y, Choate KA, Velazquez H, Al-Sabban E, Praga M, Casari G, Bettinelli A, Colussi G, Rodri-guez-Soriano J, McCredie D, Milford D, Sanjad S, Lifton RP: Paracellin-1, a renal tight junction protein required for paracellular Mg^{2+} resorption. *Science* 285: 103-106, 1999

39. Konrad M, Schaller A, Seelow D, Pandey AV, Waldegger S, Lesslauer A, Vitzthum H, Suzuki Y, Luk JM, Becker C, Schlingmann KP, Schmid M, Rodriguez-Soriano J, Ariceta G, Cano F, Enriquez R, Juppner H, Bakkaloglu SA, Hediger MA, Gallati S, Neuhauss SC, Nurnberg P, Weber S: Mutations in the tight-junction gene claudin 19 (CLDN19) are associated with renal magnesium wasting, renal failure, and severe ocular involvement. *Am J Hum Genet* 79: 949-957, 2006

40. Angelow S, El-Husseini R, Kanzawa SA, Yu AS: Renal localization and function of the tight junction protein, claudin-19. *Am J Physiol Renal Physiol* 293: F166-177, 2007

41. Hou J, Renigunta A, Gomes AS, Hou M, Paul DL, Waldegger S, Goodenough DA: Claudin-16 and claudin-19 interaction is required for their assembly into tight junctions and for renal reabsorption of magnesium. *Proc Natl Acad Sci U S A* 106: 15350-15355, 2009

42. Thorleifsson G, Holm H, Edvardsson V, Walters GB, Styrkarsdottir U, Gudbjartsson DF, Sulem P, Halldorsson BV, de Vegt F, d'Ancona FC, den Heijer M, Franzson L, Christiansen C, Alexandersen P, Rafnar T, Kristjansson K, Sigurdsson G, Kiemeney LA, Bodvarsson M, Indridason OS, Palsson R, Kong A, Thorsteinsdottir U, Stefansson K: Sequence variants in the CLDN14 gene associate with kidney stones and bone mineral density. *Nat Genet* 41: 926-930, 2009

43. Gong Y, Renigunta V, Himmerkus N, Zhang J, Renigunta A, Bleich M, Hou J: Claudin-14 regulates renal Ca^{2+} transport in response to CaSR signalling via a novel microRNA pathway. *EMBO J* 31: 1999-2012,

44. Desfleurs E, Wittner M, Simeone S, Pajaud S, Moine G, Rajerison R, Di Stefano A: Calcium-sensing receptor: regulation of electrolyte transport in the thick ascending limb of Henle's loop. *Kidney Blood Press Res* 21: 401-412, 1998

45. Motoyama HI, Friedman PA: Calcium-sensing receptor regulation of PTH-dependent calcium absorption by mouse cortical ascending limbs. *Am J Physiol Renal Physiol* 283: F399-406, 2002

46. Fujita H, Sugimoto K, Inatomi S, Maeda T, Osanai M, Uchiyama Y, Yamamoto Y, Wada T, Kojima T, Yokozaki H, Yamashita T, Kato S, Sawada N, Chiba H: Tight junction proteins claudin-2 and -12 are critical for vitamin D-dependent Ca^{2+} absorption between enterocytes. *Mol Biol Cell* 19: 1912-1921, 2008

47. Bronner F: Mechanisms of intestinal calcium absorption. *J Cell Biochem* 88: 387-393, 2003

48. Hardwick LL, Jones MR, Brautbar N, Lee DB: Magnesium absorption: mechanisms and the influence of vitamin D, calcium and phosphate. *J Nutr* 121: 13-23, 1991

49. Khanal RC, Nemere I: Regulation of intestinal calcium transport. *Annu Rev Nutr* 28: 179-196, 2008

50. Wasserman RH: Vitamin D and the dual processes of intestinal calcium absorption. *J Nutr* 134: 3137-3139, 2004

51. Christakos S, Dhawan P, Porta A, Mady LJ, Seth T: Vitamin D and intestinal calcium absorption. *Mol Cell Endocrinol* 347: 25-29,

52. Quamme GA: Recent developments in intestinal magnesium absorption. *Curr Opin Gastroenterol* 24: 230-235, 2008

53. Schlingmann KP, Weber S, Peters M, Niemann Nejsum L, Vitzthum H, Klingel K, Kratz M, Haddad E,

Ristoff E, Dinour D, Syrrou M, Nielsen S, Sassen M, Waldegger S, Seyberth HW, Konrad M: Hypomagnesemia with secondary hypocalcemia is caused by mutations in TRPM6, a new member of the TRPM gene family. *Nat Genet* 31: 166-170, 2002

54. Dimke H, Hoenderop JG, Bindels RJ: Hereditary tubular transport disorders: implications for renal handling of Ca^{2+} and Mg^{2+}. *Clin Sci (Lond)* 118: 1-18, 2010

55. Boros S, Bindels RJ, Hoenderop JG: Active Ca^{2+} reabsorption in the connecting tubule. *Pflugers Arch* 458: 99-109, 2009

56. Quamme GA: Laboratory evaluation of magnesium status. Renal function and free intracellular magnesium concentration. *Clin Lab Med* 13: 209-223, 1993

57. Le Grimellec C, Roinel N, Morel F: Simultaneous Mg, Ca, P,K,Na and Cl analysis in rat tubular fluid. II. During acute Mg plasma loading. *Pflugers Arch* 340: 197-210, 1973

58. Le Grimellec C, Roinel N, Morel F: Simultaneous Mg, Ca, P,K,Na and Cl analysis in rat tubular fluid. I. During perfusion of either inulin or ferrocyanide. *Pflugers Arch* 340: 181-196, 1973

59. Greger R: Ion transport mechanisms in thick ascending limb of Henle's loop of mammalian nephron. *Physiol Rev* 65: 760-797, 1985

60. Le Grimellec C: Micropuncture study along the proximal convoluted tubule. Electrolyte reabsorption in first convolutions. *Pflugers Arch* 354: 133-150, 1975

61. Quamme GA, Smith CM: Magnesium transport in the proximal straight tubule of the rabbit. *Am J Physiol* 246: F544-550, 1984

62. de Rouffignac C, Corman B, Roinel N: Stimulation by antidiuretic hormone of electrolyte tubular reabsorption in rat kidney. *Am J Physiol* 244: F156-164, 1983

63. Hou J, Paul DL, Goodenough DA: Paracellin-1 and the modulation of ion selectivity of tight junctions. *Journal of Cell Science* 118: 5109-5118, 2005

64. Brunette MG, Vigneault N, Carriere S: Micropuncture study of magnesium transport along the nephron in the young rat. *Am J Physiol* 227: 891-896, 1974

65. Thebault S, Alexander RT, Tiel Groenestege WM, Hoenderop JG, Bindels RJ: EGF increases TRPM6 activity and surface expression. *J Am Soc Nephrol* 20: 78-85, 2009

66. Masuyama R, Vriens J, Voets T, Karashima Y, Owsianik G, Vennekens R, Lieben L, Torrekens S, Moermans K, Vanden Bosch A, Bouillon R, Nilius B, Carmeliet G: TRPV4-mediated calcium influx regulates terminal differentiation of osteoclasts. *Cell Metab* 8: 257-265, 2008

67. van der Eerden BC, Weissgerber P, Fratzl-Zelman N, Olausson J, Hoenderop JG, Schreuders-Koedam M, Eijken M, Roschger P, de Vries TJ, Chiba H, Klaushofer K, Flockerzi V, Bindels RJ, Freichel M, van Leeuwen JP: The transient receptor potential channel TRPV6 is dynamically expressed in bone cells but is not crucial for bone mineralization in mice. *J Cell Physiol* 227: 1951-1959, 2012

68. Hoenderop JG, van Leeuwen JP, van der Eerden BC, Kersten FF, van der Kemp AW, Merillat AM, Waarsing JH, Rossier BC, Vallon V, Hummler E, Bindels RJ: Renal Ca^{2+} wasting, hyperabsorption, and reduced bone thickness in mice lacking TRPV5. *J Clin Invest* 112: 1906-1914, 2003

69. Chang W, Tu C, Chen TH, Komuves L, Oda Y, Pratt SA, Miller S, Shoback D: Expression and signal transduction of calcium-sensing receptors in cartilage and bone. *Endocrinology* 140: 5883-5893, 1999

70. Chang W, Tu C, Chen TH, Bikle D, Shoback D: The extracellular calcium-sensing receptor (CaSR) is a critical modulator of skeletal development. *Sci Signal* 1: ra1, 2008

71. Abed E, Labelle D, Martineau C, Loghin A, Moreau R: Expression of transient receptor potential (TRP) channels in human and murine osteoblast-like cells. *Mol Membr Biol* 26: 146-158, 2009

72. Abed E, Martineau C, Moreau R: Role of melastatin transient receptor potential 7 channels in the osteoblastic differentiation of murine MC3T3 cells. *Calcif Tissue Int* 88: 246-253,

73. Hoenderop JG, Muller D, Van Der Kemp AW, Hartog A, Suzuki M, Ishibashi K, Imai M, Sweep F, Willems PH, Van Os CH, Bindels RJ: Calcitriol controls the epithelial calcium channel in kidney. *J Am Soc Nephrol* 12: 1342-1349, 2001

74. Renkema KY, Alexander RT, Bindels RJ, Hoenderop JG: Calcium and phosphate homeostasis: concerted interplay of new regulators. *Ann Med* 40: 82-91, 2008

75. Ferre S, Hoenderop JG, Bindels RJ: Sensing mechanisms involved in Ca^{2+} and Mg^{2+} homeostasis. *Kidney Int* 82: 1157-1166, 2012

76. Bouillon R, Lieben L, Mathieu C, Verstuyf A, Carmeliet G: Vitamin D action: lessons from VDR and Cyp27b1 null mice. *Pediatr Endocrinol Rev* 10 Suppl 2: 354-366, 2013

77. Cline J: Calcium and vitamin d metabolism, deficiency, and excess. *Top Companion Anim Med* 27: 159-164, 2012

78. Groenestege WM, Thebault S, van der Wijst J, van den Berg D, Janssen R, Tejpar S, van den Heuvel LP, van Cutsem E, Hoenderop JG, Knoers NV, Bindels RJ: Impaired basolateral sorting of pro-EGF causes isolated recessive renal hypomagnesemia. *J Clin Invest* 117: 2260-2267, 2007

79. Tejpar S, Piessevaux H, Claes K, Piront P, Hoenderop JG, Verslype C, Van Cutsem E: Magnesium wasting associated with epidermal-growth-factor receptor-targeting antibodies in colorectal cancer: a prospective study. *Lancet Oncol* 8: 387-394, 2007

80. Song Y, Hsu YH, Niu T, Manson JE, Buring JE, Liu S: Common genetic variants of the ion channel transient receptor potential membrane melastatin 6 and 7 (TRPM6 and TRPM7), magnesium intake, and risk of type 2 diabetes in women. *BMC Med Genet* 10: 4, 2009

81. Nair AV, Hocher B, Verkaart S, van Zeeland F, Pfab T, Slowinski T, Chen YP, Schlingmann KP, Schaller A, Gallati S, Bindels RJ, Konrad M, Hoenderop JG: Loss of insulin-induced activation of TRPM6 magnesium channels results in impaired glucose tolerance during pregnancy. *Proc Natl Acad Sci U S A* 109: 11324-11329, 2012

82. Hoorn EJ, Zietse R: Disorders of calcium and magnesium balance: a physiology-based approach. *Pediatr Nephrol* 28: 1195-1206, 2012

83. Topf JM, Murray PT: Hypomagnesemia and hypermagnesemia. *Rev Endocr Metab Disord* 4: 195-206, 2003

84. Huang CL, Kuo E: Mechanism of hypokalemia in magnesium deficiency. *J Am Soc Nephrol* 18: 2649-2652, 2007

85. Anast CS, Mohs JM, Kaplan SL, Burns TW: Evidence for parathyroid failure in magnesium deficiency. *Science* 177: 606-608, 1972

86. Yamamoto M, Yamaguchi T, Yamauchi M, Yano S, Sugimoto T: Acute-onset hypomagnesemia-induced hypocalcemia caused by the refractoriness of bones and renal tubules to parathyroid hormone. *J Bone Miner Metab*, 29(6):752-5, 2011

87. Schlingmann KP, Sassen MC, Weber S, Pechmann U, Kusch K, Pelken L, Lotan D, Syrrou M, Prebble JJ, Cole DE, Metzger DL, Rahman S, Tajima T, Shu SG, Waldegger S, Seyberth HW, Konrad M: Novel TRPM6 mutations in 21 families with primary hypomagnesemia and secondary hypocalcemia. *J Am Soc Nephrol* 16: 3061-3069, 2005

88. Agus ZS: Hypomagnesemia. *J Am Soc Nephrol* 10: 1616-1622, 1999

89. Birrer RB, Shallash AJ, Totten V: Hypermagnesemia-induced fatality following epsom salt gargles(1). *J Emerg Med* 22: 185-188, 2002

90. Kutsal E, Aydemir C, Eldes N, Demirel F, Polat R, Taspnar O, Kulah E: Severe hypermagnesemia as a result of excessive cathartic ingestion in a child without renal failure. *Pediatr Emerg Care* 23: 570-572, 2007

91. Lu JF, Nightingale CH: Magnesium sulfate in eclampsia and pre-eclampsia: pharmacokinetic principles. *Clin Pharmacokinet* 38: 305-314, 2000

92. Clark BA, Brown RS: Unsuspected morbid hypermagnesemia in elderly patients. *Am J Nephrol* 12: 336-343, 1992

93. Shah GM, Winer RL, Cutler RE, Arieff AI, Goodman WG, Lacher JW, Schoenfeld PY, Coburn JW, Horowitz AM: Effects of a magnesium-free dialysate on magnesium metabolism during continuous ambulatory peritoneal dialysis. *Am J Kidney Dis* 10: 268-275, 1987

94. Weisinger JR, Bellorin-Font E: Magnesium and phosphorus. *Lancet* 352: 391-396, 1998

95. Kraft MD, Btaiche IF, Sacks GS, Kudsk KA: Treatment of electrolyte disorders in adult patients in the intensive care unit. *Am J Health Syst Pharm* 62: 1663-1682, 2005

96. Ussing HH, Zerahn K: Active Transport of Sodium as the Source of Electric Current in the Short-Circuited Isolated Frog Skin. *Acta Physiologica Scandinavica* 23: 110-127, 1951

97. Wilson TH, Wiseman G: The Use of Sacs of Everted Small Intestine for the Study of the Transference of Substances from the Mucosal to the Serosal Surface. *Journal of Physiology-London* 123: 116-125, 1954

98. Currie VE, Lengemann FW, Wentworth RA, Schwartz R: Stable [26]Mg as an in vivo tracer in investigation of magnesium utilization. *Int J Nucl Med Biol* 2: 159-164, 1975

2

Functional TRPV6 channels are crucial for transepithelial Ca²⁺ absorption

Titia E. Woudenberg-Vrenken[1], Anke L. Lameris[1]*,
Petra Weißgerber[2]*, Jenny Olausson[2], Veit Flockerzi[2], René J.M. Bindels[1],
Marc Freichel[2,3], Joost G.J. Hoenderop[1]

* equally contributed to this work

[1] Department of Physiology, Radboud University Nijmegen Medical Centre, Nijmegen, The Netherlands,
[2] Experimentelle und Klinische Pharmakologie und Toxikologie, Universität des Saarlandes, Homburg,
Germany, [3] Pharmakologisches Institut, Universität Heidelberg, Heidelberg, Germany

Abstract

TRPV6 is considered the primary protein responsible for transcellular Ca^{2+} absorption. In vitro studies demonstrate that a negatively charged amino acid (D) within the putative pore region of mouse TRPV6 (position 541) is critical for Ca^{2+} permeation of the channel. To elucidate the role of TRPV6 in transepithelial Ca^{2+} transport *in vivo*, we functionally analyzed a TRPV6$^{D541A/D541A}$ knock-in mouse model. After weaning, mice were fed a regular (1% wt/wt) or Ca^{2+}-deficient (0.02% wt/wt) diet and housed in metabolic cages. Blood was sampled for Ca^{2+} measurements, and the expression of Ca^{2+} transport proteins was analyzed in kidney, duodenum and colon. Intestinal ^{45}Ca^{2+} uptake was measured in vivo by an absorption assay. Challenging the mice with the Ca^{2+}-deficient diet resulted in hypocalcemia in wild-type and TRPV6$^{D541A/D541A}$ mice. On a low-Ca^{2+} diet both mouse strains displayed increased expression of intestinal TRPV6, calbindin-D9K, and renal TRPV5. TRPV6$^{D541A/D541A}$ mice showed significantly impaired intestinal Ca^{2+} uptake compared with wild-type mice, and duodenal TRPV5 expression was increased in TRPV6$^{D541A/D541A}$ mice. On a normal diet, serum Ca^{2+} concentrations normalized in both mouse strains. Under these conditions, intestinal Ca^{2+} uptake was similar, and the expression levels of renal and intestinal Ca^{2+} transport proteins were not affected. We demonstrate that TRPV6$^{D541A/D541A}$ mice exhibit impaired transcellular Ca^{2+} absorption. Duodenal TRPV5 expression was increased in TRPV6$^{D541A/D541A}$ mice, albeit insufficient to correct for the diminished Ca^{2+} absorption. Under normal conditions, when passive Ca^{2+} transport is predominant, no differences between wild-type and TRPV6$^{D541A/D541A}$ mice were observed. Our results demonstrate a specific role for TRPV6 in transepithelial Ca^{2+} absorption.

Introduction

Two pathways of intestinal Ca^{2+} absorption exist, and the preferred route depends on dietary availability of Ca^{2+}. When dietary Ca^{2+} levels are high, the paracellular, passive pathway is the predominant absorption mechanism, while active, transcellular transport occurs if Ca^{2+} supply is restricted (5; 12). Transcellular Ca^{2+} absorption requires entry at the luminal side of the intestinal epithelium. The epithelial Ca^{2+} channel transient receptor potential vanilloid 6 (TRPV6) is hypothesized to be responsible for this luminal Ca^{2+} uptake. Active Ca^{2+} absorption occurs at the proximal part of the small intestine, while the concentration-dependent paracellular pathway arises gradually throughout the intestine (5; 15). Within the gastrointestinal tract of human, rat and mouse, high levels of TRPV6 are observed in the duodenum and colon (14; 20; 24), which is in line with its proposed function in intestinal Ca^{2+} entry. Inside the cell, Ca^{2+} binds to a Ca^{2+}-binding protein, calbindin-D_{9K}, enabling diffusion towards the basolateral side of the cell, where Ca^{2+} is extruded into the blood via the plasma membrane Ca^{2+}-ATPase (PMCA1b) (10). Despite the absence of known activity in the kidney, TRPV6 expression has been reported in human and mouse kidney epithelia (20; 23; 24; 26; 35) as well.

Previous *in vivo* experiments revealed a role for TRPV6 in placental Ca^{2+} transport (27). Consistent with this hypothesis is the finding that calbindin-D_{9K} gene expression is significantly reduced in placenta of TRPV6^{-/-} mice, while TRPV5 levels are unaffected, suggesting an association of TRPV6 and calbindin-D_{9k} in placental Ca^{2+} transport. Since a considerable amount of Ca^{2+} transport still occurs in TRPV6^{-/-} mice, it is implied that other channels contribute significantly to this process (27). Recently, gain-of-function polymorphisms of the TRPV6 gene have been found in Ca^{2+}-stone forming patients, which might contribute to absorptive hypercalciuria (28). These findings suggest that TRPV6 is one of the key players in intestinal Ca^{2+} absorption in humans, although further studies are required to elucidate its precise role.

Structural analysis of TRPV6 channels suggested the presence of a pore region between transmembrane domains 5 and 6, in which three negatively charged amino acids are situated (3; 4). An aspartate at position 542 in human TRPV6 (541 in mouse) was hypothesized to determine Ca^{2+} conductance. In mouse TRPV6, replacement of D541 with an alanine residue abrogated Ca^{2+} permeation and Mg^{2+} block in *in vitro* experiments, and similar results were obtained *in vitro* with rabbit TRPV5 (21; 34; 36). Expression of human TRPV6 D542A resulted in non-functional channels, despite equivalent cell surface expression as for wild-type TRPV6 (4; 34). This suggests that D542 or D541 is critical for Ca^{2+} permeation and/or channel activity. To address the specific role of TRPV6 in transepithelial Ca^{2+} permeation *in vivo*, we analyzed a mouse model with a specific mutation in

the pore region; the TRPV6$^{D541A/D541A}$ knock-in mouse (36). This mouse model is unique, compared to TRPV6$^{-/-}$ mice, since the mutation creates a non-functional TRPV6 channel with no effect on the channel's structure-, rather than a complete knock-down of the channel, which might affect other proteins as well. The TRPV6$^{D541A/D541A}$ knock-in mice show a marked reduction of Ca^{2+} uptake by epididymal epithelial cells and consequently, the mobility and fertility of sperm are significantly reduced (36). Bone microarchitecture and bone matrix mineralization were not affected in these mice (29), suggesting a minor role of TRPV6 in bone metabolism. In the present study, we determined serum Ca^{2+} concentrations and urinary Ca^{2+} excretion, and measured intestinal Ca^{2+} absorption in TRPV6$^{D541A/D541A}$ mice in comparison to wild-type littermates under both normal dietary circumstances and severe nutritional Ca^{2+} restriction to specifically study the role of TRPV6 in transepithelial transport.

Materials and methods

Animal studies
Generation of TRPV6$^{D541A/D541A}$ knock-in mice is described in (36). TRPV6 littermates were housed in a temperature- and light-controlled room with standard pellet chow (1% wt/wt Ca^{2+}, SSNIFF Spezialdiäten GmbH, Soest, Germany) or a Ca^{2+}-deficient diet (0.02% wt/wt Ca^{2+}, SSNIFF) and filter sterilized drinking water available *ad libitum*. They were fed their respective diets from weaning (age 3 weeks) until the experiment date. TRPV6 mice on the normal and Ca^{2+}-deficient diet, n=14 per group, were housed in metabolic cages and 24-hr urine was collected. Fresh urine was used for the pH determination. The animals were sacrificed at an age of 12-14 weeks. Blood samples were taken and kidney and duodenum tissues were sampled and snap-frozen in liquid nitrogen. All experiments were performed in compliance with the animal ethics board of the Radboud University Nijmegen (Ethical License number RU-DEC 2008-192, RU-DEC 2008-067).

Genotyping
Genotypes were determined by PCR as described in (36) to identify animals with wild-type or TRPV6$^{D541A/D541A}$ genotypes.

Analytical procedures
Serum and urine total Ca^{2+} concentrations were measured using a colorimetric assay kit as described previously (11). Serum albumin concentrations were measured using an ELISA kit according to the manufacturer's protocol (GenWay Biotech Inc. San Diego, CA, USA). Urine Mg^{2+} concentrations were determined

using a colorimetric assay kit, according to the manufacturer's protocol (Roche Diagnostics, Woerden, The Netherlands). Urine phosphate and Na^+ concentrations were analyzed on a Hitachi autoanalyzer (Hitachi, Laval, Quebec, Canada).

In vivo $^{45}Ca^{2+}$ absorption assay

Ca^{2+} absorption was determined by measuring serum $^{45}Ca^{2+}$ levels at early time points after oral gavage as described in (33). In summary, mice were fasted over night. At time-point 0, mice were administered a solution containing 0.1 mM $CaCl_2$, 125 mM NaCl, 17 mM Tris pH 7.5, 1.8 g/l fructose, enriched with 20 μCi $^{45}CaCl_2/ml$ (New England Nuclear, Newton, Massachusetts, USA); in a volume of 15 μL/g of body weight. Blood samples were obtained via orbital puncture at 1, 2, 3 and 4 minutes after oral gavage, and serum was analyzed by liquid scintillation counting.

Quantitative real-time PCR analysis

Total RNA was isolated from kidney, duodenum (proximal part) and colon using TriZol Total RNA Isolation Reagent (Gibco BRL, Breda, The Netherlands) as described previously (9). cDNA was subsequently used to determine TRPV5, TRPV6, calbindin-D_{9K}, calbindin-D_{28K}, Na^+/Ca^{2+} exchanger 1 (NCX1), PMCA1b, and 1αOHAse mRNA expression levels. mRNA expression of the housekeeping gene hypoxan-thine-guanine phosphorybosyl transferase (HPRT) was used as endogenous control. mRNA levels were quantified by qPCR on an ABI PRISM 7900 HT Sequence Detection System (Applied Biosystems, Nieuwerkerk a/d IJssel, The Netherlands). Primers and fluorescent probes were purchased from Biolegio (Malden, The Netherlands), the sequences are listed in (30; 32).

Statistical analysis

Data are expressed as mean ± SEM. Statistical comparisons were analyzed by one-way ANOVA with a Bonferroni correction; $p<0.05$ was considered statistically significant. All analyses were performed using the Statview Statistical Package software (Power PC version 4.51) on an Apple iMac computer.

Results

Ca²⁺ deprivation reduces serum Ca²⁺ concentrations in wild-type and TRPV6[D541A/D541A] mice

Feeding the mice a Ca^{2+}-deficient diet, from weaning until the experiment resulted in a serum Ca^{2+} concentration of 1.7 ± 0.1 mM for TRPV6[D541A/D541A] mice and 1.6 ± 0.1 mM for wild-type mice (Figure 1A). Ca^{2+} levels in both mouse strains were significantly lower
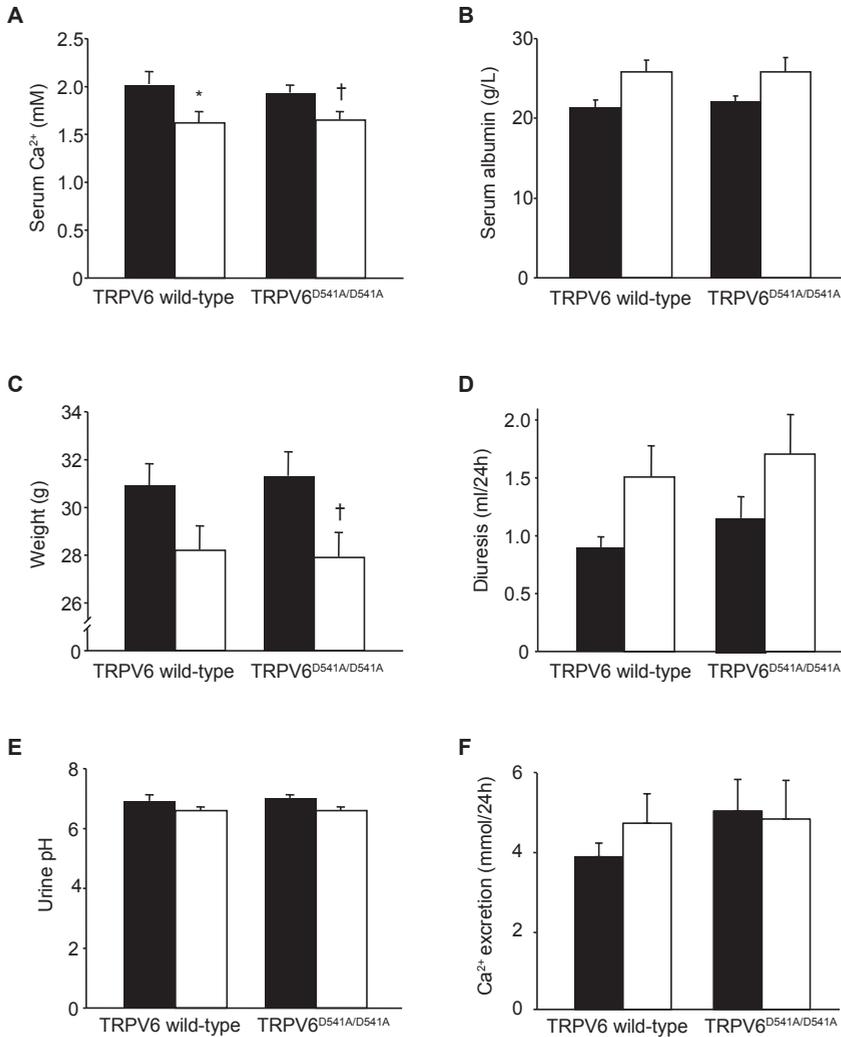
Figure 1 Effects of a Ca²⁺-deficient diet in wild-type and TRPV6[D541A/D541A] pore mutant mice. **A.** Serum Ca²⁺ concentration, **B.** serum albumin concentration, **C.** weight, **D.** diuresis, **E.** urine pH and **F.** total urinary excretion of Ca²⁺ of wild-type and TRPV6[D541A/D541A] mice on a regular 1% wt/wt Ca²⁺ diet (filled bars) or a Ca²⁺-deficient diet (0.02% wt/wt Ca²⁺, open bars). N=14 for each group. * P<0.05 versus wild-type mice on the regular diet. † P<0.05 versus TRPV6[D541A/D541A] mice on the regular diet.
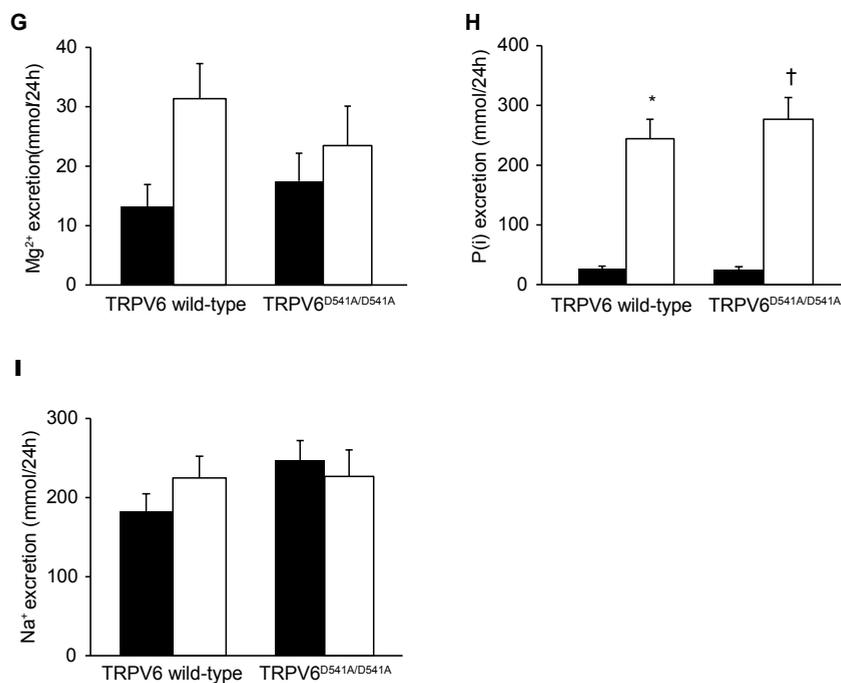
Figure 1 continued Effects of a Ca²⁺-deficient diet in wild-type and TRPV6$^{D541A/D541A}$ pore mutant mice. Total urinary excretion of *F.* Ca²⁺, *G.* Mg²⁺, *H.* P(i) and *I* Na⁺ of wild-type and TRPV6$^{D541A/D541A}$ mice on a regular 1% wt/wt Ca²⁺ diet (filled bars) or a Ca²⁺-deficient diet (0.02% wt/wt Ca²⁺, open bars). N=14 for each group. * P<0.05 versus wild-type mice on the regular diet. † P<0.05 versus TRPV6$^{D541A/D541A}$ mice on the regular diet.

compared to the same genotypes fed the normal Ca²⁺ diet (1.9 ± 0.1 mM and 2.0 ± 0.1 mM respectively, Figure 1A). Changes in serum Ca²⁺ concentration were not due to changes in the protein levels caused by a different dietary content, since serum albumin concentrations were similar for the four groups analyzed (Figure 1B). Ca²⁺-deficiency significantly reduced the body weight of TRPV6$^{D541A/D541A}$ mice to 27.9 ± 1.0 g compared with the weight of the same genotype on a regular diet of 31.3 ± 1.0 g (Figure 1C). Although the trend for wild-type mice was the same, the body weights were not significantly decreased in mice fed the Ca²⁺ deficient diet (28.2 ± 1.0 versus 30.9 ± 0.9 g, Figure 1C). The volume of urine voided by TRPV6$^{D541A/}$

^{D541A} and wild-type mice on both diets was not significantly different (Figure 1D), and both mice showed comparable urine pH values (Figure 1E). Renal Ca^{2+} excretion varied from 3.9 ± 0.4 - 5.0 ± 0.7 µmol/24h (Figure 1F), and was similar for the four groups studied. Urinary Mg^{2+} excretion (Figure 1G) was slightly increased in TRPV6 wild-type mice on the Ca^{2+}-deficient diet, but no significant changes could be observed caused by either the genotype or the diet. Ca^{2+} deprivation
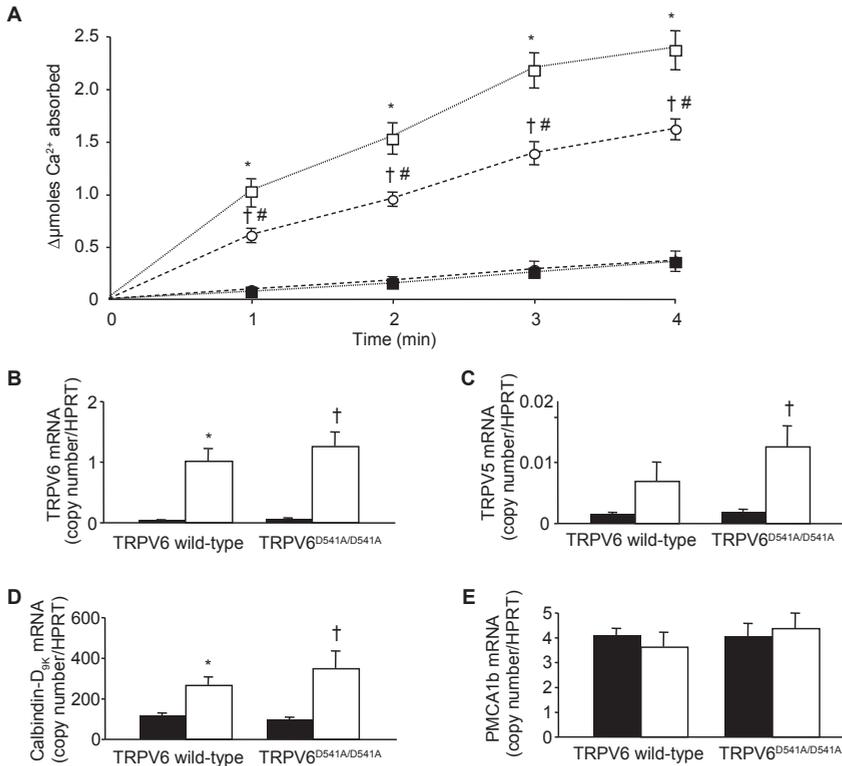
Figure 2 Intestinal Ca^{2+} absorption is reduced in TRPV6$^{D541A/D541A}$ mice on a Ca^{2+}-deficient diet. **A.** Serum Ca^{2+} changes within 4 minutes after ^{45}Ca^{2+} administration by oral gavage in wild-type (squares) and TRPV6$^{D541A/D541A}$ (circles) mice (N=12 per group) on a regular diet (1% wt/wt Ca^{2+}, filled symbols) or a diet deficient in Ca^{2+} (0.02% wt/wt Ca^{2+}, open symbols). **B.** Duodenal mRNA expression of TRPV6, **C.** TRPV5, **D.** calbindin-D$_{9K}$ and **E.** PMCA1b and **F.** TRPV6 expression in the colon (F) were measured and are expressed as a ratio to HPRT1. Data are presented as means ± SEM (N=6-8 per group). * P<0.05 versus wild-type mice on the regular diet. † P<0.05 versus TRPV6$^{D541A/D541A}$ mice on the regular diet. # P<0.05 versus wild-type mice on the Ca^{2+}-deficient diet.

F
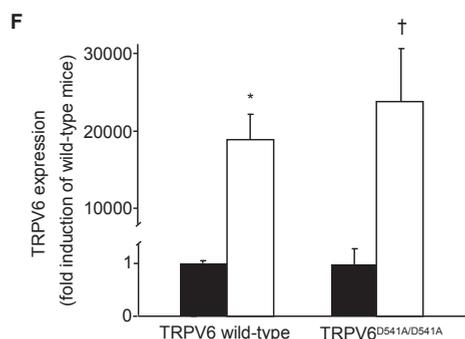
Figure 2 continued.

significantly enhanced urinary P(i) excretion 9.5-times in TRPV6 wild-type mice, and 11.2-fold change in TRPV6[D541A/D541A] mice (Figure 1H). Renal Na⁺ excretion was comparable for the four groups analyzed (Figure 1I).

Ca²⁺-deficient TRPV6[D541A/D541A] mice show impaired intestinal Ca²⁺ absorption
To study the functional consequences of the Ca²⁺-impermeable pore mutant on intestinal absorption, an *in vivo* ⁴⁵Ca²⁺ absorption assay was performed. A low Ca²⁺ diet resulted in a significantly increased Ca²⁺ absorption in TRPV6[D541A/D541A] and wild-type mice compared to mice on a regular diet (Figure 2A). At all time-points studied, TRPV6[D541A/D541A] mice displayed significantly reduced Ca²⁺ absorption compared with their wild-type littermates (Figure 2A, open symbols). On the regular diet, uptake of Ca²⁺ from the intestinal lumen was similar for TRPV6[D541A/D541A] and wild-type mice (Figure 2A).

Next, the gene expression of the Ca²⁺ transporters in the duodenum of these mice was examined by qPCR analysis. Ca²⁺ deprivation resulted in a 20-25-fold induction of TRPV6 expression (Figure 2B) in wild-type and TRPV6[D541A/D541A] mice. Interestingly, duodenal TRPV5 expression was significantly increased 6-times in TRPV6[D541A/D541A] mice on the Ca²⁺-deficient diet (Figure 2C), while a 3-fold change was induced by Ca²⁺-deficiency in wild-type mice (Figure 2C). Calbindin-D$_{9K}$ mRNA levels were 2.3 and 3.5 times up-regulated in wild-type and TRPV6[D541A/D541A] mice, respectively (Figure 2D). PMCA1b gene expression was not changed by the diet in either genotype (Figure 2E). Intestinal mRNA levels of TRPV6, TRPV5, calbindin-D$_{9K}$ and PMCA1b were similar for TRPV6[D541A/D541A] and wild-type mice on the regular diet (Figure 2B-E). Next, we analyzed TRPV6 mRNA levels in the colon, to study differences in expression in the large intestine. Ca²⁺-deficiency

significantly increased TRPV6 expression in TRPV6$^{D541A/D541A}$ and wild-type mice (23000 and 18000 fold, respectively, Figure 2F).

Regulation of the renal Ca^{2+} transporters by Ca^{2+} deprivation

Expression of renal Ca^{2+} transport proteins was then investigated. Ca^{2+}-deficiency resulted in a 2-fold up-regulation of TRPV5 mRNA levels (Figure 3A) in both TRPV6$^{D541A/D541A}$ and wild-type mice. Renal TRPV6 expression, which is quite low, was not increased compared with the mice on the regular diet (Figure 3B). Calbindin-D$_{28K}$ mRNA levels were significantly reduced in wild-type mice (Figure 3C),
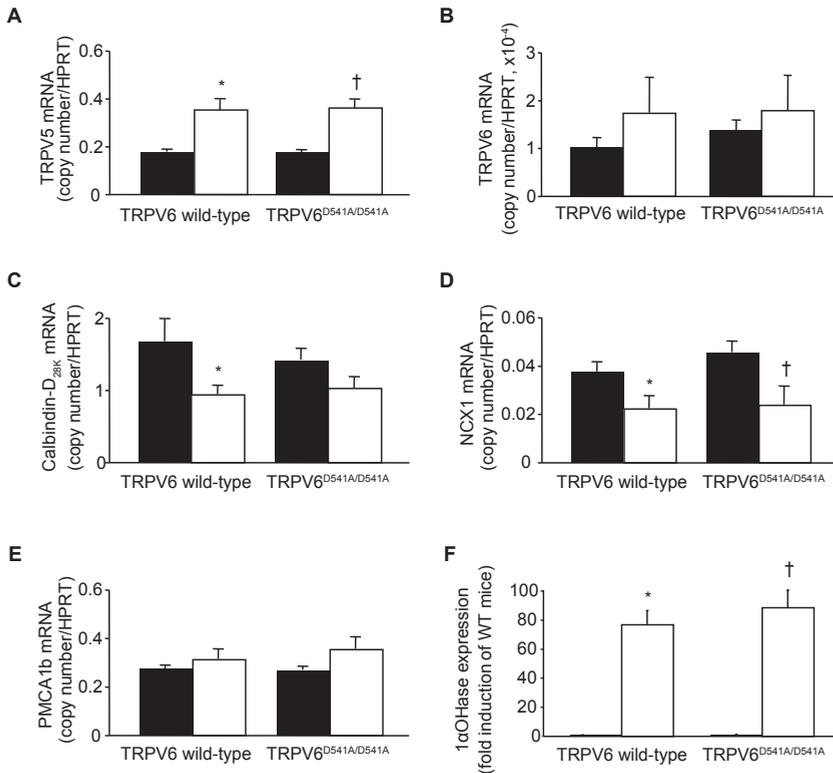
Figure 3 mRNA expression of renal Ca^{2+} transport proteins in TRPV6$^{D541A/D541A}$ pore mutant mice is comparable to wild-type mice. **A.** Renal mRNA expression of TRPV5, **B.** TRPV6, **C.** calbindin-D$_{28K}$, **D.** NCX1, **E.** PMCA1b, and **F.** 1αOHase of wild-type and TRPV6$^{D541A/D541A}$ mice on a regular 1% wt/wt Ca^{2+} diet (filled bars) or on a Ca^{2+}-deficient diet (0.02% wt/wt Ca^{2+}, open bars) were measured and are presented as ratio to HPRT1. Data are shown as means ± SEM. N=6-8 per group. * P<0.05 versus wild-type mice on the regular diet. † P<0.05 versus TRPV6$^{D541A/D541A}$ mice on the regular diet.

while the trend was the same for TRPV6$^{D541A/D541A}$ knock-in mice, no significant effect was detected in the kidneys of TRPV6$^{D541A/D541A}$ mice. NCX1 expression was decreased by almost 50% in both TRPV6$^{D541A/D541A}$ and wild-type mice (Figure 3D), but the levels of PMCA1b were not reduced compared with the mice on the regular diet (Figure 3E). Besides the different regulation of calbindin-D$_{28K}$ mRNA levels (Figure 3C), gene expression of renal Ca²⁺ transporters was identical in TRPV6$^{D541A/D541A}$ and wild-type mice (Figure 3A-E). On a regular diet, renal mRNA levels of TRPV5, TRPV6, calbindin-D$_{28K}$, NCX1 and PMCA1b were equal in TRPV6$^{D541A/D541A}$ and wild-type mice (Figure 3A-E). Expression of renal 1αOHase was studied to indicate changes in vitamin D homeostasis. In both TRPV6$^{D541A/D541A}$ and wild-type mice, 1αOHase expression was significantly increased by Ca²⁺ deprivation (Figure 3F), however no changes in expression between TRPV6$^{D541A/D541A}$ and wild-type mice could be observed (Figure 3F).

Discussion

This is the first study characterizing Ca²⁺ homeostasis in a mouse model in which TRPV6 channels are functionally inactivated by mutating the channel pore. Our results show that TRPV6 is specifically involved in transepithelial small intestinal Ca²⁺ transport. TRPV6$^{D541A/D541A}$ mice exhibit decreased duodenal Ca²⁺ uptake and increased intestinal TRPV5 gene expression compared to wild-type mice. Functional consequences on serum Ca²⁺ and the net urinary Ca²⁺ excretion were not observed, and the expression of Ca²⁺ transporters in the kidney was not affected.

The mice were challenged by a Ca²⁺-deficient diet to address the specific function of TRPV6 in transcellular Ca²⁺ transport. This resulted in a failure-to-thrive, emphasizing the importance of *in vivo* absorption assays to study functional consequences. Dietary Ca²⁺ restriction reduced intestinal absorption in TRPV6$^{D541A/D541A}$ knock-in mice, while the homeostasis of other electrolytes, measured by urinary excretion, was not significantly affected in TRPV6$^{D541A/D541A}$ knock-in mice. This implies a critical role for TRPV6 in transcellular Ca²⁺ transport specifically. This conclusion is supported by a gain-of-function haplotype in TRPV6, which is suggested to contribute to absorptive hypercalciuria in patients (28). Parallel to our study, Benn *et al.* (1) described a down-regulation of intracellular Ca²⁺ transport proteins in TRPV6$^{-/-}$ mice on a 0.02% wt/wt Ca²⁺-deficient diet but no differences in the same mice on a regular diet. However, impaired intestinal Ca²⁺ uptake for TPRV6$^{-/-}$ mice on a normal diet has been reported as well (2). This model is different from ours in that Bianco *et al.* (2) studied knock-out mice, while we analyzed knock-in mice with inactivated Ca²⁺ permeation, achieved by a

single amino acid replacement in the pore region of TRPV6. This latter study described TRPV6^{-/-} mice by a reduction in body weight, polyuria and hypercalciuria (2), while we showed that the phenotype of the TRPV6[D541A/D541A] mice on a regular diet is indistinguishable from wild-type mice. This is supported by the study of Benn *et al.* (1), who described the TRPV6^{-/-} mouse on a regular diet as normocalcemic with Ca^{2+} absorption comparable to wild-type mice. Both studies confirm the specific role of TRPV6 in transepithelial Ca^{2+} transport.

Ca^{2+} uptake was not completely absent in TRPV6[D541A/D541A] mice, implying that other mechanisms are critically involved. Vitamin D was found to regulate paracellular transport *in vitro* via direct effects on the expression of the tight junction complexes claudin-2 and claudin-12, and on the cell adhesion molecules claudin-3 and cadherin 17 (6; 7; 16). In the duodenum of TRPV6^{-/-} mice, vitamin D administration slightly increased expression of claudin-12, reduced levels of cadherin 17, while no changes in claudin-2 expression were detected. This suggests some stimulation of paracellular absorption, but *in vivo* proof is still not definite (1; 17). Therefore, other yet unidentified transport mechanisms might be compensating for the inactivation of TRPV6 in these TRPV6[D541A/D541A] mice, such as the L-type calcium channel $Ca_v1.3$. $Ca_v1.3$ is highly expressed in the apical membrane in jejunum and ileum of rat (19), and is supposed to function in glucose-mediated transcellular Ca^{2+} absorption under normal dietary conditions (18). It is interesting to study the effects of Ca^{2+}-deprivation on $Ca_v1.3$-mediated transport.

Changes in the expression of renal and intestinal Ca^{2+} transporters mediated by Ca^{2+}-deficiency in the TRPV6[D541A/D541A] and wild-type mice has been described before (1; 8). Remarkably, intestinal TRPV5 expression, which is generally low compared to TRPV6 expression in the duodenum of rodents (9; 13; 22; 32), was significantly enhanced in TRPV6[D541A/D541A] mice on the Ca^{2+}-deficient diet, and a minor, but not significant, increase was observed in wild-type mice. TRPV6 expression in the colon was not significantly changed in TRPV6[D541A/D541A] mice compared to wild-type mice. The changes in TRPV5 expression suggest the existence of a compensatory mechanism in TRPV6[D541A/D541A] mice, albeit insufficient to fully compensate for the loss of TRPV6 activity, as illustrated by the [45]Ca^{2+} absorption assay. Since these mice partially compensate for the reduced Ca^{2+} absorption in their duodenum, this confirms the involvement of TRPV6 in transcellular Ca^{2+} transport in the intestine.

Furthermore, on a Ca^{2+}-deficient diet both wild-type and TRPV6[D541A/D541A] display inappropriately high urinary Ca^{2+} excretion levels; e.g. within the normal range, despite being hypocalcemic. This phenomenon has been observed in knock out models associated with secondary hypervitaminosis D (25). TRPV5 expression is upregulated in the kidneys in an attempt to reabsorb more Ca^{2+}, but this is not

sufficient to correct the hypocalcemia. In addition, calbindin-D_{28K} and NCX1 expression are also decreased in the kidneys of these mice. This supports the theory of the renal dysfunction in wild-type and TRPV6$^{D541A/D541A}$ mice. Indeed, for wild-type mice on a Ca²⁺-deficient diet this has been described before (8). Furthermore, it is known that the expression of these renal Ca²⁺ transport proteins is down-regulated as a consequence of disturbed Ca²⁺ reabsorption via TRPV5 (31). In summary, our results demonstrate that TRPV6 specifically contributes to tran-sepithelial Ca²⁺ transport, as demonstrated by the significantly impaired intestinal ⁴⁵Ca²⁺ uptake in the TRPV6$^{D541A/D541A}$ knock-in mouse. Ca²⁺ absorption still occurs to some extent in these mice, suggesting a role for other transport mechanisms, either paracellular or yet unidentified transcellular transport mechanisms, and explains why the significantly diminished absorption is not reflected by a reduction in serum Ca²⁺ and/or urinary Ca²⁺ excretion.

Acknowledgements

Grants

Reference List

1. Benn BS, Ajibade D, Porta A, Dhawan P, Hediger M, Peng JB, Jiang Y, Oh GT, Jeung EB, Lieben L, Bouillon R, Carmeliet G and Christakos S. Active intestinal calcium transport in the absence of transient receptor potential vanilloid type 6 and calbindin-D9k. *Endocrinology* 149: 3196-3205, 2008.

2. Bianco SD, Peng JB, Takanaga H, Suzuki Y, Crescenzi A, Kos CH, Zhuang L, Freeman MR, Gouveia CH, Wu J, Luo H, Mauro T, Brown EM and Hediger MA. Marked disturbance of calcium homeostasis in mice with targeted disruption of the Trpv6 calcium channel gene. *J Bone Miner Res* 22: 274-285, 2007.

3. Bodding M. Voltage-dependent changes of TRPV6-mediated Ca²⁺ currents. *J Biol Chem* 280: 7022-7029, 2005.

4. Bodding M and Flockerzi V. Ca²⁺ dependence of the Ca²⁺-selective TRPV6 channel. *J Biol Chem* 279: 36546-36552, 2004.

5. Bronner F. Mechanisms and functional aspects of intestinal calcium absorption. *J Exp Zool A Comp Exp Biol* 300: 47-52, 2003.

6. Chirayath MV, Gajdzik L, Hulla W, Graf J, Cross HS and Peterlik M. Vitamin D increases tight-junction conductance and paracellular Ca²⁺ transport in Caco-2 cell cultures. *Am J Physiol* 274: G389-G396, 1998.

7. Fujita H, Sugimoto K, Inatomi S, Maeda T, Osanai M, Uchiyama Y, Yamamoto Y, Wada T, Kojima T, Yokozaki H, Yamashita T, Kato S, Sawada N and Chiba H. Tight junction proteins claudin-2 and -12 are critical for vitamin D-dependent Ca²⁺ absorption between enterocytes. *Mol Biol Cell* 19: 1912-1921, 2008.

8. Gkika D, Hsu YJ, van der Kemp AW, Christakos S, Bindels RJ and Hoenderop JG. Critical role of the epithelial Ca2+ channel TRPV5 in active Ca²⁺ reabsorption as revealed by TRPV5/calbindin-D28K knockout mice. *J Am Soc Nephrol* 17: 3020-3027, 2006.

9. Hoenderop JG, Hartog A, Stuiver M, Doucet A, Willems PH and Bindels RJ. Localization of the epithelial Ca²⁺ channel in rabbit kidney and intestine. *J Am Soc Nephrol* 11: 1171-1178, 2000.

10. Hoenderop JG, Muller D, Suzuki M, van Os CH and Bindels RJ. Epithelial calcium channel: gate-keeper of active calcium reabsorption. *Curr Opin Nephrol Hypertens* 9: 335-340, 2000.

11. Hoenderop JG, Muller D, van der Kemp AW, Hartog A, Suzuki M, Ishibashi K, Imai M, Sweep F, Willems PH, van Os CH and Bindels RJ. Calcitriol controls the epithelial calcium channel in kidney. *J Am Soc Nephrol* 12: 1342-1349, 2001.

12. Hoenderop JG, Nilius B and Bindels RJ. Calcium absorption across epithelia. *Physiol Rev* 85: 373-422, 2005.

13. Hoenderop JG, van der Kemp AW, Hartog A, van de Graaf SF, van Os CH, Willems PH and Bindels RJ. Molecular identification of the apical Ca²⁺ channel in 1, 25-dihydroxyvitamin D3-responsive epithelia. *J Biol Chem* 274: 8375-8378, 1999.

14. Karbach U and Feldmeier H. The cecum is the site with the highest calcium absorption in rat intestine. *Dig Dis Sci* 38: 1815-1824, 1993.

15. Kimberg DV, Schachter D and Schenker H. Active transport of calcium by intestine: effects of dietary calcium. *Am J Physiol* 200: 1256-1262, 1961.

16. Kutuzova GD and DeLuca HF. Gene expression profiles in rat intestine identify pathways for 1,25-dihydroxyvitamin D(3) stimulated calcium absorption and clarify its immunomodulatory properties. *Arch Biochem Biophys* 432: 152-166, 2004.

17. Lieben L, Benn BS, Ajibade D, Stockmans I, Moermans K, Hediger MA, Peng JB, Christakos S, Bouillon R and Carmeliet G. Trpv6 mediates intestinal calcium absorption during calcium restriction and contributes to bone homeostasis. *Bone* 47: 301-308, 2010.

18. Morgan EL, Mace OJ, Affleck J and Kellett GL. Apical GLUT2 and Cav1.3: regulation of rat intestinal glucose and calcium absorption. *J Physiol* 580: 593-604, 2007.

19. Morgan EL, Mace OJ, Helliwell PA, Affleck J and Kellett GL. A role for Ca(v)1.3 in rat intestinal calcium absorption. *Biochem Biophys Res Commun* 312: 487-493, 2003.

20. Nijenhuis T, Hoenderop JG, van der Kemp AW and Bindels RJ. Localization and regulation of the epithelial Ca²⁺ channel TRPV6 in the kidney. *J Am Soc Nephrol* 14: 2731-2740, 2003.

21. Nilius B, Vennekens R, Prenen J, Hoenderop JG, Droogmans G and Bindels RJ. The single pore residue Asp542 determines Ca²⁺ permeation and Mg²⁺ block of the epithelial Ca2+ channel. *J Biol Chem* 276: 1020-1025, 2001.

22. Okano T, Tsugawa N, Morishita A and Kato S. Regulation of gene expression of epithelial calcium channels in intestine and kidney of mice by 1alpha,25-dihydroxyvitamin D3. *J Steroid Biochem Mol Biol* 89-90: 335-338, 2004.

23. Peng JB, Brown EM and Hediger MA. Structural conservation of the genes encoding CaT1, CaT2, and related cation channels. *Genomics* 76: 99-109, 2001.

24. Peng JB, Chen XZ, Berger UV, Vassilev PM, Tsukaguchi H, Brown EM and Hediger MA. Molecular cloning and characterization of a channel-like transporter mediating intestinal calcium absorption. *J Biol Chem* 274: 22739-22746, 1999.

25. Renkema KY, Nijenhuis T, van der Eerden BC, van der Kemp AW, Weinans H, van Leeuwen JP, Bindels RJ and Hoenderop JG. Hypervitaminosis D mediates compensatory Ca²⁺ hyperabsorption in TRPV5 knockout mice. *J Am Soc Nephrol* 16: 3188-3195, 2005.

26. Suzuki M, Ishibashi K, Ooki G, Tsuruoka S and Imai M. Electrophysiologic characteristics of the Ca-permeable channels, ECaC and CaT, in the kidney. *Biochem Biophys Res Commun* 274: 344-349, 2000.

27. Suzuki Y, Kovacs CS, Takanaga H, Peng JB, Landowski CP and Hediger MA. Calcium channel TRPV6 is involved in murine maternal-fetal calcium transport. *J Bone Miner Res* 23: 1249-1256, 2008.

28. Suzuki Y, Pasch A, Bonny O, Mohaupt MG, Hediger MA and Frey FJ. Gain-of-function haplotype in the epithelial calcium channel TRPV6 is a risk factor for renal calcium stone formation. *Hum Mol Genet* 17: 1613-1618, 2008.

29. van der Eerden BC, Weissgerber P, Fratzl-Zelman N, Olausson J, Hoenderop JG, Schreuders-Koedam M, Eijken M, Roschger P, de Vries TJ, Chiba H, Klaushofer K, Flockerzi V, Bindels RJ, Freichel M and van Leeuwen JP. The transient receptor potential channel TRPV6 is dynamically expressed in bone cells but is not crucial for bone mineralization in mice. *J Cell Physiol* 227: 1951-1959, 2012.

30. van Abel M, Hoenderop JG, Dardenne O, St AR, van Os CH, Van Leeuwen HJ and Bindels RJ. 1,25-di-hydroxyvitamin D(3)-independent stimulatory effect of estrogen on the expression of ECaC1 in the kidney. *J Am Soc Nephrol* 13: 2102-2109, 2002.

31. van Abel M, Hoenderop JG, van der Kemp AW, Friedlaender MM, van Leeuwen JP and Bindels RJ. Coordinated control of renal Ca²⁺ transport proteins by parathyroid hormone. *Kidney Int* 68: 1708-1721, 2005.

32. van Abel M, Hoenderop JG, van der Kemp AW, van Leeuwen JP and Bindels RJ. Regulation of the epithelial Ca²⁺ channels in small intestine as studied by quantitative mRNA detection. *Am J Physiol Gastrointest Liver Physiol* 285: G78-G85, 2003.

33. van Abel M, Huybers S, Hoenderop JG, van der Kemp AW, van Leeuwen JP and Bindels RJ. Age-dependent alterations in Ca²⁺ homeostasis: role of TRPV5 and TRPV6. *Am J Physiol Renal Physiol* 291: F1177-F1183, 2006.

34. Voets T, Janssens A, Prenen J, Droogmans G and Nilius B. Mg²⁺-dependent gating and strong inward rectification of the cation channel TRPV6. *J Gen Physiol* 121: 245-260, 2003.

35. Weber K, Erben RG, Rump A and Adamski J. Gene structure and regulation of the murine epithelial calcium channels ECaC1 and 2. *Biochem Biophys Res Commun* 289: 1287-1294, 2001.

36. Weissgerber P, Kriebs U, Tsvilovskyy V, Olausson J, Kretz O, Stoerger C, Vennekens R, Wissenbach U, Middendorff R, Flockerzi V and Freichel M. Male Fertility Depends on Ca²⁺ Absorption by TRPV6 in Epididymal Epithelia. *Sci Signal* 4: ra27, 2011.

3

Omeprazole enhances the colonic expression of the Mg²⁺ transporter TRPM6

$$\text{Mg}^{2+}$$

Anke L. Lameris, Mark W. Hess, Ila van Kruijsbergen,
Joost G.J. Hoenderop, René J.M. Bindels

Department of Physiology, Radboud University Nijmegen Medical Centre, Nijmegen, The Netherlands

Abstract

Proton pump inhibitors (PPIs) are potent blockers of gastric acid secretion, used by millions of patients suffering from gastric acid-related complaints. Although PPIs have an excellent safety profile, an increasing number of case reports describe patients with severe hypomagnesemia due to long-term PPI use. As there is no evidence of a renal Mg^{2+} leak, PPI-induced hypomagnesemia is hypothesized to result from intestinal malabsorption of Mg^{2+}. The aim of this study was to investigate the effect of PPIs on Mg^{2+} homeostasis in an *in vivo* mouse model. To this end, C57BL/6J mice were treated with omeprazole, under normal and low dietary Mg^{2+} availability. Omeprazole did not induce changes in serum Mg^{2+} levels (1.48 ± 0.05 mmol/L and 1.54 ± 0.05 mmol/L in omeprazole-treated and control mice, respectively), urinary Mg^{2+} excretion (35 ± 3 μmol/24 h and 30 ± 4 μmol/24 h in omeprazole-treated and control mice, respectively) or fecal Mg^{2+} excretion (84 ± 4 μmol/24 h and 76 ± 4 μmol/24 h in omeprazole-treated and control mice, respectively) under any of the tested experimental conditions. However, omeprazole treatment did increase the mRNA expression level of the transient receptor potential melastatin 6 (TRPM6), the predominant intestinal Mg^{2+} channel, in the colon (167 ± 15% and 100 ± 7% in omeprazole-treated and control mice, respectively, *P < 0.05*). In addition, the expression of the colonic H^+,K^+-ATPase (cHK-α), a homolog of the gastric H^+,K^+-ATPase that is the primary target of omeprazole, was also significantly increased (354 ± 43% and 100 ± 24% in omeprazole-treated and control mice, respectively, *P < 0.05*). The expression levels of other magnesiotropic genes remained unchanged. Based on these findings, we hypothesize that omeprazole inhibits cHK-α activity, resulting in reduced extrusion of protons into the large intestine. Since TRPM6-mediated Mg^{2+} absorption is stimulated by extracellular protons, this would diminish the rate of intestinal Mg^{2+} absorption. The increase of TRPM6 expression in colon may compensate for the reduced TRPM6 currents, thereby normalizing intestinal Mg^{2+} absorption during omeprazole treatment in C57BL/6J mice, explaining unchanged serum, urine, and fecal Mg^{2+} levels.

3

Introduction

Proton pump inhibitors (PPIs) are indicated for gastric acid-related diseases like gastroesophageal reflux disease, Zollinger-Ellison syndrome, Barrett's esophagus, duodenal peptic ulcers, and gastritis [1]. All PPIs have a similar chemical structure and an identical mode of action. They are administered in the form of lipophilic, membrane-permeable, inactive pro-drugs [2]. PPIs are absorbed from the small intestine into the blood, after which they accumulate in the highly acidic canaliculi of the parietal cells of the stomach. Here, PPIs are protonated, which induces covalent binding between the PPI and specific cysteine residues of the gastric H^+,K^+-ATPase (gHK-α), resulting in potent inhibition of acid secretion [2]. Although PPIs are generally considered to have an excellent safety profile, over 65 cases of PPI-induced hypomagnesemia (PPIH) have been reported since 2006 [3-15]. In addition to these case reports, reduced serum Mg^{2+} levels associated with the use of PPI's were reported in a cohort of hospitalized patients [16]. A recently published study, based on reports submitted to the Adverse Event Reporting System of the US Food and Drug Administration, suggests that PPIH might concern several hundreds of patients since 2004 [17].

PPIH typically manifests after years of chronic PPI use, and patients present with symptoms common to severe Mg^{2+} depletion such as tetany, seizures, convulsions, and cardiac arrhythmia, often coinciding with secondary hypocalcemia. The causal link between the use of PPIs and the development of hypomagnesemia was shown in PPIH patients by a classical challenge-dechallenge-rechallenge protocol, leading to fast recovery from hypomagnesemia during dechallenge and fast reappearance of hypomagnesemia after rechallenge [3, 7, 14]. Intravenous Mg^{2+} loading tests indicate that PPIH patients are severely Mg^{2+} depleted, and determination of fractional Mg^{2+} excretion shows appropriate renal retention of Mg^{2+} [3, 4, 12, 14]. These findings implicate that intestinal malabsorption of Mg^{2+} plays a central role in the etiology of PPIH. This sets PPIH apart from many other forms of drug-induced hypomagnesemia which most frequently result from renal Mg^{2+} losses [18]. However, the exact molecular mechanisms underlying PPIH remain unknown.

Some authors speculate that PPIH might result from genetic variants in the epithelial Mg^{2+} channel transient receptor potential melastatin 6 (TRPM6) [3, 4, 12]. The vital role of TRPM6 in the maintenance of Mg^{2+} homeostasis has been well established [19]. The Mg^{2+} channel is expressed at the apical membrane of epithelial cells in the distal convoluted tubules of the kidney and at the luminal side of the gastrointestinal epithelium [20]. Recently, several magnesiotropic

hormones including epidermal growth factor, estrogen, and insulin have been described to influence Mg^{2+} absorption via TRPM6 [21-23]. In addition to the hormonal regulation, it is known that the presence of extracellular protons enhances inward currents via TRPM6, meaning that Mg^{2+} influx via this channel is strongly dependent on the extracellular pH [24].

The primary target of omeprazole, gHK-α, has a homologue named the colonic H^+,K^+-ATPase (cHK-α), which extrudes protons into the lumen of the intestine in exchange for potassium ions [25]. *In vitro* studies using guinea pig colonic crypts or colon tissue in Ussing chambers indicate that PPIs do not only reduce the activity of the gHK-α, but also that of the colonic H^+,K^+-ATPase (cHK-α) [26, 27]. Based on these observations, we hypothesize that omeprazole inhibits cHK-α activity, resulting in a lower amount of protons being extruded into the large intestine, subsequently leading to a reduced rate of intestinal Mg^{2+} absorption via TRPM6.

The aim of our study was, therefore, to create a mouse model of PPIH to test our hypothesis that omeprazole reduces TRPM6-mediated colonic Mg^{2+} absorption. To this end, we investigated the effect of omeprazole treatment on Mg^{2+} homeostasis *in vivo* by means of serum, urine, and fecal Mg^{2+} measurements and by determination of mRNA expression patterns of TRPM6 and cHK-α in the intestine and kidney.

Materials and methods

Animal studies
C57BL/6J mice (8 weeks old) were purchased from Charles River, the Netherlands. Animals were housed in a temperature- and light-controlled room with pelleted chow (SSNIFF Spezialdiäten GmbH, Germany) and drinking water available *ad libitum*. Omeprazole (Fagron, the Netherlands) was dispersed in a solution containing 0.5% (w/v) methylcellulose and 0.2% (w/v) $NaHCO_3$ (pH 9.0). Mice received a daily dose of 20 mg omeprazole per kilogram bodyweight, which was administered via oral gavage. For urine and feces collection, animals were individually housed in metabolic cages for 24 h. Blood was sampled from the submandibular facial vein at the end of the stay in the metabolic cages, and sera were collected for Mg^{2+} measurements. All experiments were performed in compliance with the animal ethics board of the Radboud University Nijmegen.

For the first experiment, animals were randomly divided into an omeprazole group (n=10) and a control group (n=10), receiving vehicle only. They were fed a standard chow with normal Mg^{2+} content (0.2% w/w Mg^{2+}, SSNIFF Spezialdiäten GmbH, Germany) during 28 days. A second experiment was performed, in which both groups of mice were fed a Mg^{2+}-deficient diet (0.02% w/w Mg^{2+}, SSNIFF Spezialdiäten GmbH, Germany) for 22 days followed by a recovery period of 2 days in which the mice were reintroduced to a diet with normal Mg^{2+} content.

Tissue collection and pH measurements

At the end of each experiment, blood was collected and animals were sacrificed via cervical dislocation under isoflurane anesthesia. Kidneys, duodenum, and colon segments were extracted, cleaned, and snap frozen in liquid nitrogen. In addition, stomach pH was analyzed using diagnostic test strips (Merck, Germany).

Analytical procedures

Before analysis, fecal samples were homogenized and digested in 65% nitric acid (Sigma-Aldrich, USA) for 2 h at 70 °C, followed by an overnight incubation at room temperature. Serum, urinary, and fecal Mg^{2+} concentrations were determined by a colorimetric xylidyl-II blue method (Cobas Roche Diagnostics, UK) on a Nanodrop 2000c spectrophotometer (Thermo Fisher Scientific, USA) at 600 nm wavelength and were verified using a commercial serum standard (Precinorm U, Roche, Switzerland).

Quantitative real-time PCR

Total RNA was extracted from tissues using TRIzol□ reagent (Invitrogen, UK) according to the manufacturer's protocol. The obtained RNA was subjected to DNase treatment (Promega, USA) to prevent genomic DNA contamination. Subsequently, RNA was reverse transcribed with murine leukemia virus reverse transcriptase. The obtained cDNA was used to determine mRNA expression levels of various magnesiotropic genes and H^+,K^+-ATPases, as well as mRNA levels of glyceraldehyde 3-phosphate dehydrogenase (GAPDH) as an endogenous control. The mRNA expression levels were quantified by real-time PCR on a CFX69 real-time detection system (BioRad, USA) using SYBR Green (BioRad, USA). Primers (Biolegio, the Netherlands) were designed with Primer 3 software (Whitehead Institute for Biomedical Research, USA) and are listed in Table I.

Table 1 Primer sequences used for real-time PCR.

Gene	NCBI ref.	Forward primer	Reverse primer
GAPDH	NM_008084.2	5'-TAACATCAAATGGGGTGAGG-3'	5'-GGTTCACACCCATCACAAAC-3'
TRPM6	NM_153417.1	5'-AAAGCCATGCGAGTTATCAGC-3'	5'-CTTCACAATGAAAACCTGCCC-3'
cHK-α	NM_138652.2	5'-GCTAAGGCAACGCGCGTCCT-3'	5'-CTGTTTTCCGGCGCATACTGTGA-3'
TRPM7	NM_021450.2	5'-GGTTCCTCCTGTGGTGCCTT -3'	5'-CCCCATGTCGTCTCTGTCGT-3'
EGF	NM_010113.3	5'-GAGTTGCCCTGACTCTACCG-3'	5'-CCACCATTGAGGCAGTATCC-3'
EGFR	NM_207655.2	5'-CAGAACTGGGCTTAGGGAAC-3'	5'-GGACGATGTCCCTCCACTG-3'
Kv1.1	NM_010595.3	5'-CTGTGACAATTGGAGGCAAGATC-3'	5'-GAGCAACTGAGCCTGCTCTTC-3'
CNNM2	NM_033569.3	5'-GGAGGATACGAACGACGTG-3'	5'-TTGATGTTCTGCCCGTACAC-3'
HNF1B	NM_009330.2	5'-CAAGATGTCAGGAGTGCGCTAC-3'	5'-CTGGTCACCATGGCACTGTTAC-3'
gHK-α	NM_018731.2	5'-TCCAGCAGGGATTCTTCAGGAAC-3'	5'-AGCCAATGCAGACCTGGAACAC-3'

Statistics

Values are expressed as means ± SEM. Differences between single groups of omeprazole-treated mice and controls were tested using a two-tailed, unpaired Student's t test. Comparison of multiple groups was performed by a one-way ANOVA with a Bonferroni correction. Differences between groups were considered to be statistically significant when $P < 0.05$. Analysis of the datasets was performed using GraphPad Prism (Macintosh version, 4.51).

Results

Effect of omeprazole on serum Mg^{2+} levels as well as 24-h urinary and fecal Mg^{2+} excretion under normal and low dietary Mg^{2+} availability

To study the effect of omeprazole on serum Mg^{2+} levels as well as 24-h urinary and fecal excretion of Mg^{2+}, mice were treated with 20 mg/kg body weight omeprazole (or vehicle) via oral gavage once a day. Serum Mg^{2+} levels, 24-h urinary Mg^{2+} excretion as well as 24-h fecal Mg^{2+} excretion were determined at the start of the experiment and after 28 days of treatment. There were no significant differences in body weight, food and water intake, diuresis, and fecal weight between the omeprazole-treated mice and vehicle-treated controls ($P > 0.2$ for all parameters) during their stay in the metabolic cages (Table 2). Serum Mg^{2+} levels (Figure 1A) were unaltered in omeprazole-treated mice compared to the vehicle-treated controls (1.48 ± 0.05 mmol/L and 1.54 ± 0.05 mmol/L in omeprazole-treated versus vehicle-treated mice, respectively, $P > 0.2$). The urinary excretion of Mg^{2+} (Figure

Table 2 Characteristics of vehicle-treated controls and omeprazole-treated mice.

	Control	Omeprazole
Body weight (g)	30.1 ± 0.9	30.2 ± 1.1
Food intake (g/24 h)	3.1 ± 0.2	3.0 ± 0.3
Water intake (mL/24 h)	4.2 ± 0.3	4.2 ± 0.2
Diuresis (mL/24 h)	1.2 ± 0.2	1.4 ± 0.2
Fecal weight (g/24 h)	1.6 ± 0.2	1.5 ± 0.2

3
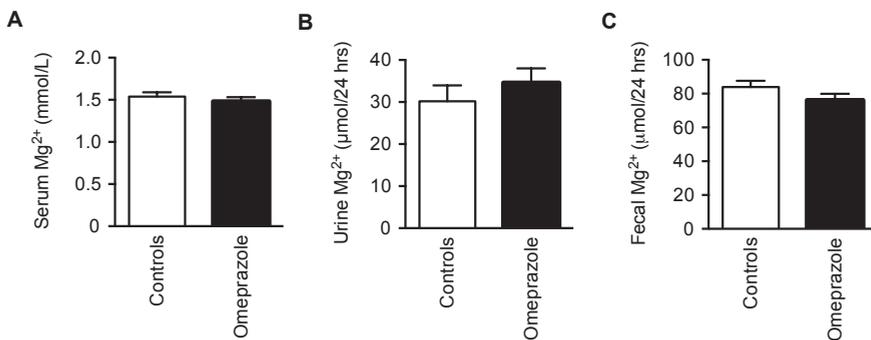
Figure 1 Effect of omeprazole treatment on Mg²⁺ homeostasis in CB57BL/6J mice. **A.** Serum Mg²⁺ concentration **B.** 24-h urinary Mg²⁺ excretion and **C.** 24-h fecal Mg²⁺ excretion in vehicle-treated controls (white bars) and omeprazole-treated mice (black bars) are shown. Data are presented as means ± SEM.

1B) did not significantly differ between the omeprazole group and the control group (35 ± 3 μmol/24 h and 30 ± 4 μmol/24 h for omeprazole-treated and vehicle-treated mice, respectively, $P > 0.2$). In addition, fecal Mg²⁺ excretion (Figure 1C) was not significantly different in omeprazole-treated mice compared to the vehicle-treated controls (76 ± 4 μmol/24 h and 84 ± 4 μmol/24 h in omeprazole-treated and control mice, respectively, $P > 0.2$).

To determine whether the effect of omeprazole on Mg²⁺ homeostasis is influenced by dietary Mg²⁺ availability, a subsequent experiment was performed in which mice were fed a Mg²⁺-deficient diet in addition to the treatment with omeprazole or vehicle. This diet induced a significant decline in serum Mg²⁺ values; however, no differences were observed between omeprazole- and vehicle-treated mice after 8 or 20 days of treatment (Figure 2). After 22 days on the Mg²⁺-deficient diet, the animals were reintroduced to a diet with normal Mg²⁺

content, to investigate the recovery rate between the two groups of mice. Within 2 days serum Mg^{2+} levels normalized to baseline values with no differences between omeprazole-treated animals and controls (1.42 ± 0.02 mmol/L and 1.44 ± 0.02 mmol/L for omeprazole-treated and vehicle-treated controls, respectively, *P > 0.2*).
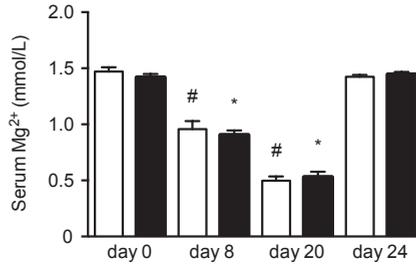
Figure 2 Effects of dietary Mg^{2+} restriction and omeprazole on serum Mg^{2+} in CB57BL/6J mice. Vehicle-treated controls (white bars) and omeprazole-treated mice (black bars) were fed a Mg^{2+}-deficient diet (0.02% w/w Mg^{2+}) for 22 days and then switched to a normal diet (0.2% w/w Mg^{2+}) to monitor recovery. * # *P < 0.05* compared to the corresponding group on day 0.

Effect of omeprazole treatment on gastric pH

To confirm the effect of omeprazole treatment on gastric acid secretion in our mouse model, we measured the pH in the gastric lumen using pH indicator strips (Figure 3). Four hours after administration of omeprazole, the intragastric pH was pH 6.7 ± 0.2 indicating that gastric acid production was effectively inhibited by omeprazole. Twenty-eight hours after the last dose of omeprazole was administered, the stomach pH remained significantly elevated with a pH 4.4 ± 0.4 in omeprazole-treated mice compared to a pH of 2.6 ± 0.3 in vehicle-treated mice (*P < 0.05*). These findings indicate that the omeprazole treatment ensured a continuous suppression of gastric acid secretion throughout the experiment.

Co-expression of TRPM6 and colonic H^+,K^+-ATPase in the colon

To confirm the co-localization of TRPM6 and cHK-α, their mRNA expression levels were determined in a murine gastrointestinal tissue panel (Figure 4). TRPM6 mRNA expression was found predominantly in the caecum and throughout the colon, while expression levels in the duodenum were negligible. cHK-α mRNA expression was low in the duodenum and caecum whereas in the colon, expression increased from the proximal towards the distal end.
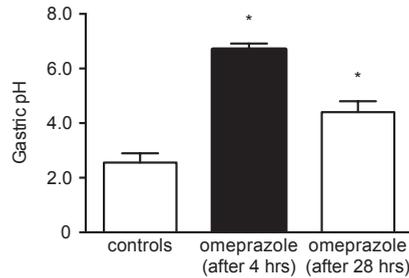
Figure 3 Effects of omeprazole treatment on gastric acid production. Effect of omeprazole treatment on gastric pH, 4 or 28 h (black bars) after administration of the last dose. Data are presented as means ± SEM. * $P < 0.05$ compared to vehicle-treated controls (white bars)
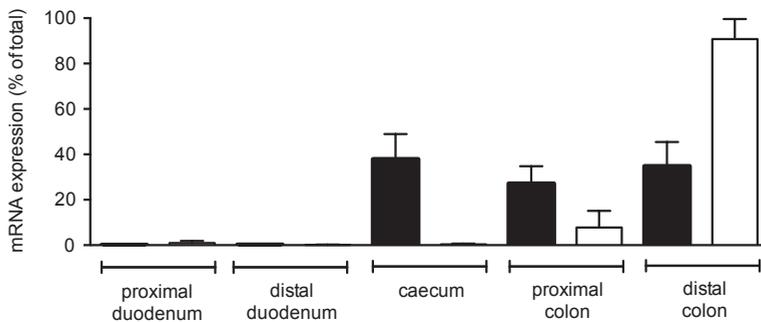
Figure 4 Gastrointestinal expression pattern of TRPM6 and cHK-α mRNA. mRNA expression levels of TRPM6 (black bars) and cHK-α (white bars) in the different segments of the gastrointestinal tract of CB57BL/6J mice as determined by real-time PCR. Expression levels are shown as a percentage of total gastrointestinal expression and were corrected for GAPDH expression. Data are presented as means ± SEM.

Omeprazole treatment specifically enhances mRNA expression of TRPM6 and cHK-α in the colon

Next, we investigated whether omeprazole affected TRPM6 and cHK-α mRNA expression levels in the colon (Figure 5A and B). Since the mRNA expression of both genes overlaps in the proximal as well as the distal colon, TRPM6 and cHK-α mRNA expression levels were analyzed in both colonic segments, to determine if they are affected by omeprazole treatment. The expression of TRPM6 in the

proximal segment of the colon was not significantly increased (127 ± 17% and 100 ± 4% in omeprazole-treated and control mice, respectively, *P > 0.2)*. There was, however, a significant upregulation of cHK-α in omeprazole-treated mice compared to vehicle-treated controls (257 ± 55% and 100 ± 7% in omeprazole-treated and control mice, respectively, *P < 0.05)*.

In the distal colon, the expression level of TRPM6 mRNA was increased ~1.5 times in omeprazole-treated mice compared to the vehicle-treated controls (167 ± 15% and 100 ± 7% for omeprazole-treated and vehicle-treated mice, respectively, *P < 0.05)*. Similar to our findings in the proximal colon, cHK-α mRNA expression
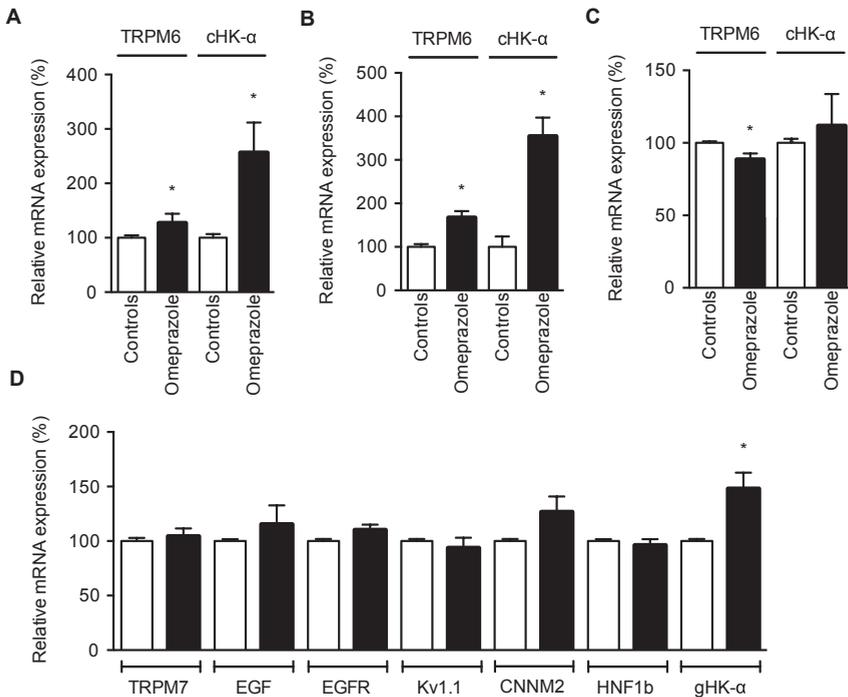
Figure 5 Effects of omeprazole treatment on mRNA expression levels of various magnesiotropic genes and H^+-K^+-ATPases in the colon and kidney. Relative mRNA expression levels (corrected for GAPDH) of TRPM6 and cHK-α in vehicle-treated controls (white bars) and omeprazole-treated mice (black bars) in **A.** the proximal and **B.** the distal colon, as well as in **C.** the kidney. **D.** Expression levels of various magnesiotropic genes and the gHK-α in the distal colon of vehicle-treated controls and omeprazole-treated mice. Data are presented as means ± SEM, * *P < 0.05* compared to vehicle-treated controls.

levels in the distal colon were ~3.5 times higher in omeprazole-treated mice compared to controls (354 ± 43% and 100 ± 24% for omeprazole-treated and vehicle-treated mice, respectively, $P < 0.05$).

In the kidney (Figure 5C), TRPM6 mRNA expression was significantly lower in omeprazole-treated mice compared to the controls (89 ± 4% and 100 ± 1% for omeprazole-treated and vehicle-treated mice, respectively, $P < 0.05$). The levels of cHK-α mRNA were unaltered by the omeprazole treatment (112 ± 22% and 100 ± 3% for omeprazole-treated and vehicle-treated mice, respectively, $P > 0.2$).

The mRNA expression levels of magnesiotropic genes other than TRPM6 could function as important negative controls as they could demonstrate the specificity of the upregulation of TRPM6 and cHK-α in the colon in reaction to omeprazole treatment. Therefore, we determined the expression levels of the following well-known magnesiotropic genes in the distal colon of omeprazole- and vehicle-treated mice: TRPM7, epidermal growth factor (EGF), EGF receptor (EGFR), potassium voltage-gated channel subfamily A member 1 (Kv1.1), Cyclin M2 (CNNM2) and hepatocyte nuclear factor 1 homeobox B (HNF1B) (Figure 5D).

The mRNA expression level of TRPM7, the closest homologue of TRPM6 and therefore the most important negative control, was unaltered in the distal colon of omeprazole-treated mice compared to the expression in vehicle-treated controls (104 ± 7% and 100 ± 3% for omeprazole-treated and vehicle-treated mice, respectively, $P > 0.2$). The expression levels of the other tested magnesiotropic genes were also not significantly altered by omeprazole treatment. In addition to the magnesiotropic genes, we have also analyzed the expression levels of the gHK-α. There was a small but significant increase in the expression of gHK-α in omeprazole-treated mice versus vehicle-treated controls (148 ± 15% and 100 ± 2% in omeprazole-treated and control mice, respectively, $P < 0.05$).

Discussion

This study demonstrates for the first time that omeprazole treatment enhances the colonic expression levels of both TRPM6 and cHK-α mRNA suggesting that omeprazole indeed influences intestinal Mg²⁺ absorption. However, prolonged exposure to omeprazole had no effect on either serum Mg²⁺ levels, urinary Mg²⁺ excretion, or fecal Mg²⁺ excretion in C57BL/6J mice under normal or low dietary Mg²⁺ conditions. Moreover, omeprazole did not affect the development of hypomagnesemia under dietary Mg²⁺ restriction, nor the recovery from hypomagnesemia under normal dietary Mg²⁺ conditions.

Under conditions of normal dietary Mg^{2+} availability, the majority of intestinal Mg^{2+} absorption takes place in the small intestine via a passive, paracellular pathway. When dietary Mg^{2+} concentrations are low, or when bodily needs are high, active transcellular transport via TRPM6 becomes more important [28]. By performing our experiments both under normal and low dietary Mg^{2+} availability, we aimed to distinguish between the effect of omeprazole on the paracellular and transcellular absorption pathways. Although there was no effect of omeprazole treatment on serum Mg^{2+} levels nor on urinary and fecal Mg^{2+} excretion, there was a significant increase in both TRPM6 and cHK-α mRNA levels in the distal colon of omeprazole-treated mice. The difference in the effect of omeprazole on TRPM6 mRNA expression in the proximal and distal colon is most likely the result of the lower baseline cHK-α expression in the proximal segment (as shown in figure 4), the net increase in cHK-α expression is therefore much lower in the proximal colon, consequently resulting in a less robust effect on TRPM6. The mRNA expression levels of several other known magnesiotropic genes, including the TRPM6 homologue TRPM7, were not affected, indicating that the effect of omeprazole treatment on TRPM6 expression in the colon is highly specific.

In addition to the effect in the colon, omeprazole treatment also slightly decreased TRPM6 mRNA expression in the kidney; however, the renal expression of cHK-a remained unchanged. Importantly, the unaltered urinary Mg^{2+} excretion of the mice indicates that the final renal Mg^{2+} balance was not compromised by the slight decrease of renal TRPM6 expression.

The increased expression of cHK-α mRNA in the colon upon treatment with omeprazole was very distinct. We also found a small, but statistically significant, increase in gHK-α mRNA expression in the distal colon of omeprazole-treated mice compared to the vehicle-treated controls. The expression levels of gHK-α in the colon are, however, very low, so the functional relevance of this small increase is disputable. Previous studies have described an increase in mRNA expression level of the gHK-α in the stomach induced by omeprazole treatment [29]. Most likely, the increased mRNA levels of the H^+,K^+-ATPases in the colon represent an adaptation mechanism to restore acid secretion. There is clear evidence from *in vivo* models that omeprazole can indeed accumulate in the colonic epithelium, although this accumulation is not as strong as in the stomach [30, 31]. As described before, omeprazole is a lipophilic pro-drug which easily passes the plasma membrane. In the presence of protons, the pro-drug is converted into an active form, trapping it into the cell. The conversion of the PPI, which causes its accumulation in the cell, also enables the binding of the PPI to intracellular

cystein residues of the gHK-α, thereby inhibiting the extrusion of protons [32]. The fact that omeprazole accumulates in the colon indicates that the colonic cells have a sufficiently low pH to allow for omeprazole activation, potentially leading to inhibition of cHK-α. The function and pharmacological sensitivity of the various HK-αs depends on the species, tissues, and systems in which they are studied [33, 34]. The inhibitory effect of omeprazole on cHK-α was shown in fractionized membranes of guinea pig distal colon, in which omeprazole was found to reduce cHK-α activity by 30% [26]. Furthermore, studies in Ussing chambers indicated that omeprazole inhibits cHK-α activity in the colon [27]. Inhibition of cHK-α by omeprazole would lead to a reduction of proton secretion into the lumen of the colon. Importantly, it has been shown that extracellular protons enhance inward currents via TRPM6, indicating that Mg²⁺ influx via TRPM6 is strongly dependent on the extracellular pH [24]. We therefore hypothesized that the effect of omeprazole on intestinal Mg²⁺ absorption is the result of an indirect effect of omeprazole on TRPM6, elicited via a reduction of cHK-α-mediated proton secretion. This hypothesis is in line with findings from previous studies which show that fermentable substrates, such as carbohydrates, stimulate intestinal Mg²⁺ absorption [35]. The fermentation of these substrates by bacteria leads to an acidification of the caecum and colon, without influencing systemic acid/base homeostasis. Interestingly, increasing the amount of fermentable substrate in the food results in increased intestinal Mg²⁺ absorption, whereas the absorption of other minerals such as calcium, iron, and zinc remains unchanged. Several human studies have confirmed the enhancing effect of fermentable oligo- or pol-ysaccharides on Mg²⁺ absorption [35]. These findings are in line with our hypothesis that changes in pH can influence Mg²⁺ absorption in the colon.

A tissue panel of the mouse intestinal tract shows abundant TRPM6 mRNA expression in the caecum as well as the colon, which is in line with earlier observations from our group [23]. cHK-α mRNA expression was predominantly found in the colon, where its expression increases towards the distal end, that is in accordance with the fact that active potassium absorption predominantly takes place in the distal part of the colon [36]. The co-expression of TRPM6 and cHK-α along the entire colon supports our hypothesis. The concurring upregulation of TRPM6 and cHK-α mRNA expression could represent a compensatory mechanism aiming to maintain sufficient Mg²⁺ absorption by counteracting the inhibitory effects of omeprazole on cHK-α-mediated proton secretion and TRPM6-mediated Mg²⁺ absorption. This would explain the lack of an effect of omeprazole on serum Mg²⁺ levels as well as urinary and fecal Mg²⁺ excretion in our mouse model.

Recently, a mathematical model simulating intestinal Mg^{2+} absorption has been described, aiming to explain PPIH. According to this model, PPI treatment reduces Mg^{2+} absorption, leading to a 5% decrease of serum Mg^{2+} [37]. In a study with healthy volunteers, administration of omeprazole (40 mg) once a day for 7 days reduced Mg^{2+} absorption by 1% [38]. Bai *et al.* showed that a 1% reduction of Mg^{2+} absorption could lead to an 80% depletion of Mg^{2+} stores over the course of 1 year. The minute changes described might go undetected in clinical practice or experimental conditions but could, over longer periods, result in PPIH. This is in line with the fact that most PPIH patients described so far are indeed long-term (>1 year) PPI users [5].

Several questions concerning the development of PPIH in human patients remain unanswered. The incidence of PPIH is still unknown, although there are indications that the case reports only represent the tip of the iceberg [17]. A simple explanation may be found in the dietary intake of Mg^{2+}; as the changes in Mg^{2+} absorption due to omeprazole treatment are small, they are easily corrected by a higher intake of Mg^{2+}, which could explain why certain patients develop PPIH whereas others do not [37]. The low incidence could, however, also indicate that patients will only develop PPIH if they are in some way predisposed. For example, a recent study shows a strong correlation between PPIH and the combined use of PPIs and diuretics [39]. Another possibility, outlined in case reports, is that the presence of mutations or single-nucleotide polymorphisms (SNPs) in magnesiotropic genes such as TRPM6 contributes to the development PPIH. In a single case of PPIH, TRPM6 was sequenced, but no abnormalities were found in exonic regions of TRPM6 [8]. Another study excluded the presence of mutations in SLC12A3, which is one of the genes involved in Gitelman syndrome [12]. However, these individual cases do not exclude the involvement of SNPs in magnesiotropic genes, and larger studies are needed in order to confirm or exclude the involvement of predisposing factors in the development of PPIH.

In conclusion, this study provides new insights in the effect of omeprazole on Mg^{2+} homeostasis in an *in vivo* setting, which could potentially shed light on the molecular aspects of the etiology of PPIH. A significant and specific effect of omeprazole treatment on TRPM6 and cHK-α mRNA expression levels in the distal colon was found, while the serum Mg^{2+} levels, 24-h urinary Mg^{2+} excretion as well as 24-h fecal Mg^{2+} excretion were not affected. The stimulation of mRNA levels was distinct in the colon, whereas in the kidney, little or no changes occurred. This is in line with the clinical findings indicating that PPIH results from reduced intestinal Mg^{2+} absorption and not from renal Mg^{2+} wasting. Further research, both on a clinical as well as a fundamental level, is needed to fully understand and prevent PPIH in the near future.

Acknowledgements

3

References

1. McKeage K, Blick SK, Croxtall JD, Lyseng-Williamson KA, Keating GM: Esomeprazole: a review of its use in the management of gastric acid-related diseases in adults. *Drugs* 68: 1571-1607, 2008

2. Olbe L, Carlsson E, Lindberg P: A proton-pump inhibitor expedition: the case histories of omeprazole and esomeprazole. *Nat Rev Drug Discov* 2: 132-139, 2003

3. Broeren MA, Geerdink EA, Vader HL, van den Wall Bake AW: Hypomagnesemia induced by several proton-pump inhibitors. *Annals of internal medicine* 151: 755-756, 2009

4. Cundy T, Dissanayake A: Severe hypomagnesaemia in long-term users of proton-pump inhibitors. *Clin Endocrinol* 69: 338-341, 2008

5. Cundy T, Mackay J: Proton pump inhibitors and severe hypomagnesaemia. *Curr Opin Gastroen* 27: 180-185, 2011

6. Doornebal J, Bijlsma R, Brouwer RM: [An unknown but potentially serious side effect of proton pump inhibitors: hypomagnesaemia]. *Nederlands tijdschrift voor geneeskunde* 153: A711, 2009

7. Epstein M, McGrath S, Law F: Proton-pump inhibitors and hypomagnesemic hypoparathyroidism. *N Engl J Med* 355: 1834-1836, 2006

8. Fernandez-Fernandez FJ, Sesma P, Cainzos-Romero T, Ferreira L: [Hypomagnesemia related to the use of omeprazole with negative result for mutation in the TRPM6 gene]. *Medicina clinica* 137: 188-189, 2011

9. Fernandez-Fernandez FJ, Sesma P, Cainzos-Romero T, Ferreira-Gonzalez L: Intermittent use of pantoprazole and famotidine in severe hypomagnesaemia due to omeprazole. *The Netherlands journal of medicine* 68: 329-330, 2010

10. Furlanetto TW, Faulhaber GA: Hypomagnesemia and proton pump inhibitors: below the tip of the iceberg. *Archives of internal medicine* 171: 1391-1392, 2011

11. Hoorn EJ, van der Hoek J, de Man RA, Kuipers EJ, Bolwerk C, Zietse R: A case series of proton pump inhibitor-induced hypomagnesemia. *American journal of kidney diseases : the official journal of the National Kidney Foundation* 56: 112-116, 2010

12. Kuipers MT, Thang HD, Arntzenius AB: Hypomagnesaemia due to use of proton pump inhibitors--a review. *The Netherlands journal of medicine* 67: 169-172, 2009

13. Mackay JD, Bladon PT: Hypomagnesaemia due to proton-pump inhibitor therapy: a clinical case series. *Qjm-Int J Med* 103: 387-395, 2010

14. Regolisti G, Cabassi A, Parenti E, Maggiore U, Fiaccadori E: Severe Hypomagnesemia During Long-term Treatment With a Proton Pump Inhibitor. *American Journal of Kidney Diseases* 56: 168-174, 2010

15. Hmu C, Moulik P, Macleod A: Severe hypomagnesaemia due to lansoprazole. *BMJ case reports*: published online 17 December 2009, 2009

16. Gau JT, Yang YX, Chen R, Kao TC: Uses of proton pump inhibitors and hypomagnesemia. *Pharmacoepidemiology and drug safety*: Article first published online: 15 FEB 2012 DOI: 2010.1002/pds.3224, 2012

17. Tamura T, Sakaeda T, Kadoyama K, Okuno Y: Omeprazole- and Esomeprazole-associated Hypomagnesaemia: Data Mining of the Public Version of the FDA Adverse Event Reporting System. *International journal of medical sciences* 9: 322-326, 2012

18. Lameris AL, Monnens LA, Bindels RJ, Hoenderop JG: Drug-induced alterations in Mg2+ homoeostasis. *Clin Sci (Lond)* 123: 1-14, 2012

19. Schlingmann KP, Waldegger S, Konrad M, Chubanov V, Gudermann T: TRPM6 and TRPM7 - Gatekeepers of human magnesium metabolism. *Bba-Mol Basis Dis* 1772: 813-821, 2007

20. Alexander RT, Hoenderop JG, Bindels RJ: Molecular determinants of magnesium homeostasis: insights from human disease. *Journal of the American Society of Nephrology : JASN* 19: 1451-1458, 2008

21. Nair AV, Hocher B, Verkaart S, van Zeeland F, Pfab T, Slowinski T, Chen YP, Schlingmann KP, Schaller A, Gallati S, Bindels RJ, Konrad M, Hoenderop JG: Loss of insulin-induced activation of TRPM6 magnesium channels results in impaired glucose tolerance during pregnancy. *Proceedings of the National Academy of Sciences of the United States of America* 109: 11324-11329, 2012

22. Thebault S, Alexander RT, Tiel Groenestege WM, Hoenderop JG, Bindels RJ: EGF increases TRPM6 activity and surface expression. *Journal of the American Society of Nephrology : JASN* 20: 78-85, 2009

23. Groenestege WM, Hoenderop JG, van den Heuvel L, Knoers N, Bindels RJ: The epithelial Mg2+ channel transient receptor potential melastatin 6 is regulated by dietary Mg²⁺ content and estrogens. *Journal of the American Society of Nephrology : JASN* 17: 1035-1043, 2006

24. Li M, Jiang J, Yue L: Functional characterization of homo- and heteromeric channel kinases TRPM6 and TRPM7. *J Gen Physiol* 127: 525-537, 2006

25. Cougnon M, Planelles G, Crowson MS, Shull GE, Rossier BC, Jaisser F: The rat distal colon P-ATPase alpha subunit encodes a ouabain-sensitive H+, K+-ATPase. *J Biol Chem* 271: 7277-7280, 1996

26. Watanabe T, Suzuki T, Suzuki Y: Ouabain-Sensitive K+-Atpase in Epithelial-Cells from Guinea-Pig Distal Colon. *Am J Physiol* 258: G506-G511, 1990

27. Rechkemmer G, Frizzell RA, Halm DR: Active potassium transport across guinea-pig distal colon: Action of secretagogues. *J Physiol-London* 493: 485-502, 1996

28. Quamme GA: Recent developments in intestinal magnesium absorption. *Curr Opin Gastroen* 24: 230-235, 2008

29. Tari A, Wu V, Sumii M, Sachs G, Walsh JH: Regulation of Rat Gastric H+/K+-Atpase Alpha-Subunit Messenger-Rna by Omeprazole. *Biochimica Et Biophysica Acta* 1129: 49-56, 1991

30. Phillips DH, Hewer A, Osborne MR: Interaction of omeprazole with DNA in rat tissues. *Mutagenesis* 7: 277-283, 1992

31. Nakamura M, Matsui H, Serizawa H, Tsuchimoto K: Lansoprazole Novel Effector Sites Revealed by Autoradiography: Relation to Helicobacter pylori, Colon, Esophagus and Others. *J Clin Biochem Nutr* 41: 154-159, 2007

32. Sachs G, Shin JM, Vagin O, Lambrecht N, Yakubov I, Munson K: The gastric H,K ATPase as a drug target: past, present, and future. *Journal of clinical gastroenterology* 41 Suppl 2: S226-242, 2007

33. Swarts HG, Koenderink JB, Willems PH, De Pont JJ: The human non-gastric H,K-ATPase has a different cation specificity than the rat enzyme. *Biochim Biophys Acta* 1768: 580-589, 2007

34. Shao J, Gumz ML, Cain BD, Xia SL, Shull GE, van Driel IR, Wingo CS: Pharmacological profiles of the murine gastric and colonic H,K-ATPases. *Biochimica et biophysica acta* 1800: 906-911, 2010

35. Coudray C, Demigne C, Rayssiguier Y: Effects of dietary fibers on magnesium absorption in animals and humans. *J Nutr* 133: 1-4, 2003

36. Sorensen MV, Matos JE, Praetorius HA, Leipziger J: Colonic potassium handling. *Pflugers Arch* 459: 645-656, 2010

37. Bai JP, Hausman E, Lionberger R, Zhang X: Modeling and Simulation of the Effect of Proton Pump Inhibitors on Magnesium Homeostasis. 1. Oral Absorption of Magnesium. *Molecular pharmaceutics* 9 pp 3495–3505, 2012

38. Serfaty-Lacrosniere C, Wood RJ, Voytko D, Saltzman JR, Pedrosa M, Sepe TE, Russell RR: Hypochlorhydria from short-term omeprazole treatment does not inhibit intestinal absorption of calcium, phosphorus, magnesium or zinc from food in humans. *J Am Coll Nutr* 14: 364-368, 1995

39. Danziger J, William JH, Scott DJ, Lee J, Lehman LW, Mark RG, Howell MD, Celi LA, Mukamal KJ: Proton-pump inhibitor use is associated with low serum magnesium concentrations. *Kidney Int*: Epub ahead of print, 2013
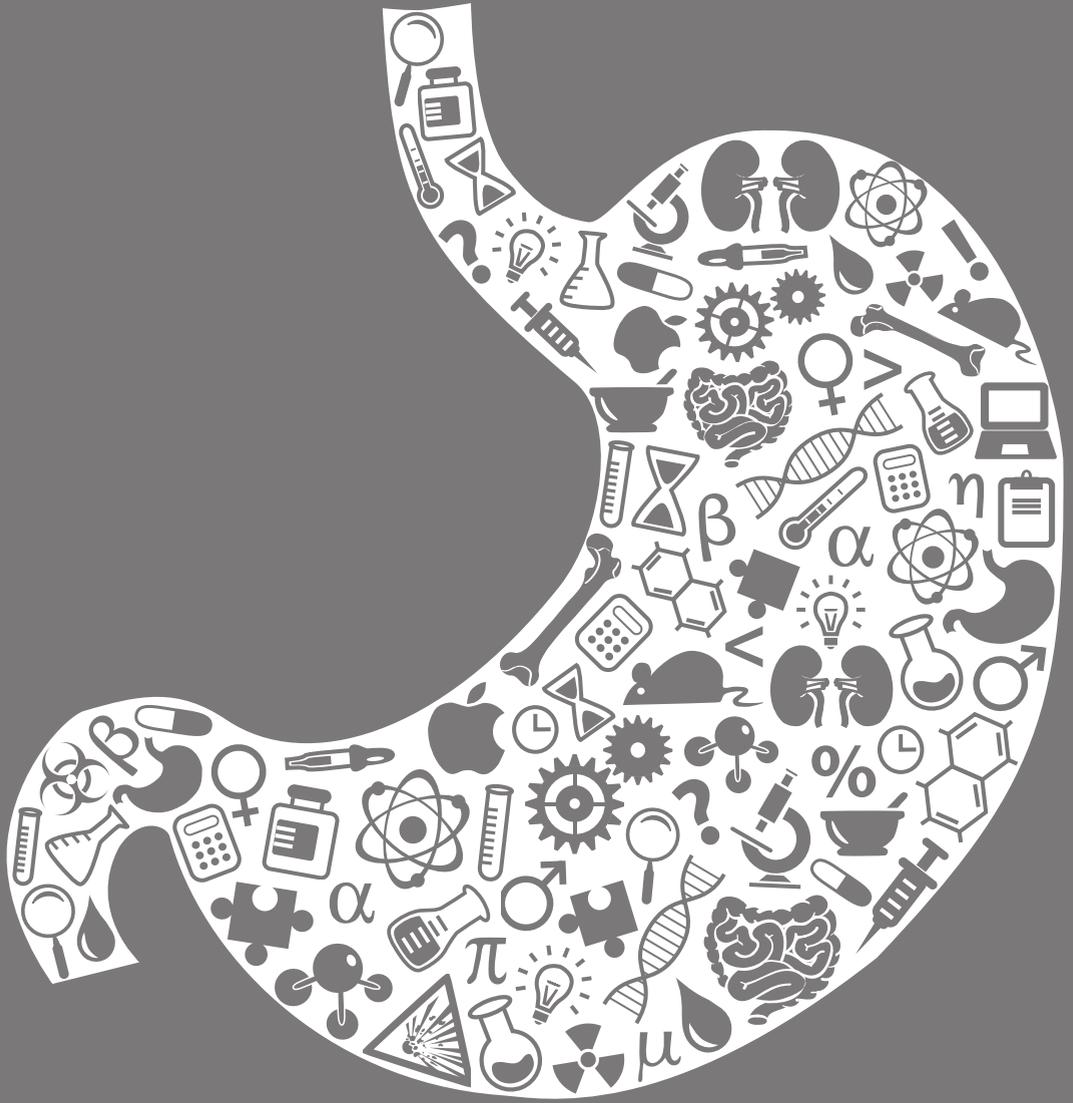
4

Segmental transport of Ca^{2+} and Mg^{2+} along the gastrointestinal tract

Anke L. Lameris[1], Pasi I. Nevalainen[2,3], Daphne Reijnen[4],
Ellen Simons[1], Jelle Eygensteyn[5], Leo A. Monnens[1], René J.M. Bindels[1],
Joost G.J. Hoenderop[1]

[1] Department of Physiology, Radboud University Nijmegen Medical Centre, Nijmegen, The Netherlands,
[2] School of Medicine, University of Tampere, Tampere, Finland, [3] Department of Internal Medicine,
Tampere University Hospital, Tampere, Finland,
[4] Central animal facility, Radboud University Nijmegen Medical Centre, Nijmegen, The Netherlands,
[5] Department of General Instrumentation, Faculty of Sciences, Radboud University Nijmegen

Abstract

Calcium (Ca^{2+}) and magnesium (Mg^{2+}) ions are involved in many vital physiological functions. Since dietary intake is the only source of minerals for the body, intestinal absorption is essential for normal homeostatic levels. The aim of this study was to characterize the absorption of Ca^{2+} as well as Mg^{2+} along the gastro-intestinal tract at a molecular, functional and physiological level. The expression patterns of transient receptor potential vanilloïd subtype 6 (TRPV6) and transient receptor potential melastatin subtype 6 (TRPM6) along the gastrointestinal tract of humans as well as mice was determined. A method was established to measure the rate of Mg^{2+} absorption from the intestine using $^{25}Mg^{2+}$ in a time-dependent manner. In addition, local absorption in different segments of the intestine was determined using surgically implanted intestinal cannulas. With these methods, the absorption of Ca^{2+} and Mg^{2+} in the proximal and distal segments of the intestine was determined at different concentrations. In addition, the effect of dietary Mg^{2+} content and vitamin D on intestinal Mg^{2+} absorption was investigated. In humans, TRPV6 is expressed in the proximal intestinal segments and TRPM6 in the distal parts of the intestine. In mice, similar expression patterns were observed, although both transporters are also expressed in the caecum. Intestinal absorption of Mg^{2+} is regulated by dietary needs in a vitamin D-independent manner. In line with the expression patterns of TRPV6 and TRPM6, it was shown that transcellular Ca^{2+} transport mainly takes place in the proximal segments of the intestine. On the other hand, transcellular Mg^{2+} absorption predominantly occurs in the distal part of the gastrointestinal tract. Vitamin D treatment of mice increased serum Mg^{2+} levels and 24-hr urinary Mg^{2+} excretion, but not intestinal absorption of $^{25}Mg^{2+}$. Further research is necessary to determine the exact role of vitamin D on intestinal Mg^{2+} absorption. Segmental cannulation of the intestine and time-dependent absorption studies using $^{25}Mg^{2+}$ provide new ways to study intestinal Mg^{2+} absorption. These methods can be used to address longstanding scientific questions with regard to the intestinal absorption of Mg^{2+}, such as the effect of magnesiotropic hormones.

Introduction

Calcium (Ca²⁺) and magnesium (Mg²⁺) are essential for many physiological functions, such as muscle contraction, neuronal excitability, bone formation, and enzymatic activity. It is, therefore, of vital importance that the concentration throughout the body is tightly regulated. For Ca²⁺ as well as Mg²⁺, this regulation takes place by the concerted action of the intestine, where these divalents are absorbed from our diet, the bones, where Ca²⁺ and Mg²⁺ are stored, and the kidneys, where they are filtered from the blood and reabsorbed from the pro-urine [1].

Since our dietary intake is the only source of minerals for the body, intestinal absorption is of key importance for the maintenance of normal homeostatic levels. Intestinal absorption of Ca²⁺ and Mg²⁺ can take place via a paracellular and a transcellular pathway [2]. Paracellular transport takes place via tight-junctions and is driven by the electrochemical gradient across the epithelium. The transepithelial electrical potential difference is around 5 mV, lumen positive with respect to the interstitial compartment [3]. In addition, the luminal concentrations of Ca²⁺ and Mg²⁺ depend on their dietary contents and are in general sufficient to provide a transepithelial chemical concentration gradient which further enhances absorption [3]. Transcellular absorption of Ca²⁺ and Mg²⁺ from the intestinal lumen is facilitated by members of the transient receptor potential (TRP) ion channel family. Intestinal absorption of Ca²⁺ is mediated via TRP vanilloïd type 6 (TRPV6), whereas absorption of Mg²⁺ takes place via TRP melastatin type 6 (TRPM6) [1]. The relative contribution of the paracellular and transcellular pathway to the total amount of Ca²⁺ and Mg²⁺ that is absorbed from the intestine depends on dietary supply and bodily needs [2]. Under normal circumstances paracellular absorption seems predominant [3, 4]. When paracellular absorption cannot meet the daily need of the body, transcellular absorption becomes essential [2, 5]. Specific transport proteins, located in the luminal and basolateral membrane of the epithelial cells, govern this latter process [3, 6]. Previous studies in mice have shown that TRPV6 is primarily expressed in duodenum, caecum and colon, whereas TRPM6 was only found in caecum and colon [7]. This finding suggests that transcellular Ca²⁺ and Mg²⁺ absorption takes place only in distinct segments of the gastrointestinal tract. Functional data supporting this hypothesis is, however, lacking.

The aim of the present study was, therefore, to characterize the absorption of Ca²⁺ and Mg²⁺ along the gastrointestinal tract at the molecular, functional and physiological level. To this end, the expression patterns of TRPV6 and TRPM6 along the gastrointestinal tract of humans as well as mice were determined. In addition, methods were developed to measure the rate of Mg²⁺ absorption from

various segments of intestine in a time-dependent manner. To this end, a technique was developed to measure local absorption at different segments of the intestine using surgically implanted intestinal cannulas. The intestinal absorption of Ca^{2+} was studied with the use of the radioactive $^{45}Ca^{2+}$ isotopes. $^{45}Ca^{2+}$ emits a low energy beta radiation, meaning its use is relatively safe. In addition, its long half-life (more than 5 months) allows for accurate and easy quantification using a scintillation counter. Although there are ample radioactive Mg^{2+} isotopes, none of them is particularly suitable for absorption studies due to their short half-lives, which range from nanoseconds to hours [8]. In addition to the radioactive isotopes, three stable Mg^{2+} isotopes exist. These stable isotopes, i.e. ^{24}Mg, ^{25}Mg and ^{26}Mg, have a respective natural abundance of 79, 10 and 11% and can be distinguished using inductively coupled plasma mass-spectrometry (ICP-MS) [9]. Enriched ($\pm99\%$) preparations of a $^{25}Mg^{2+}$ or $^{26}Mg^{2+}$ are commercially available. The stable isotope technique is based on the measurement of a change in the ratio between the three isotopes in a sample of interest, such as urine, blood or feces. Absorption of the enriched Mg^{2+} isotope will change the isotopic ratio compared to the normal natural abundance [10]. Both $^{25}Mg^{2+}$ and $^{26}Mg^{2+}$ have been used to study Mg^{2+} homeostasis in humans as well as in animal models [11, 12]. The most commonly used and well-established method to determine Mg^{2+} absorption by stable isotopes techniques is via fecal monitoring [12, 13]. After oral administration, excretion of the isotope via the feces is monitored over a certain period of time, subsequently, the difference between the amount of isotope that was administered and the amount that was excreted via the feces can be used to determine how much Mg^{2+} was absorbed. However, this technique will underestimate intestinal absorption since part of the absorbed Mg^{2+} is secreted into the intestinal lumen via for example bile or pancreatic excretions. To correct for intestinal secretion, the double labeling technique has been developed [10]. In this latter approach, enriched isotopes are administered via two routes: one isotope is given orally, while the other one is injected intravenously. Net absorption can then be measured by correcting for fecal excretion of the intravenously administered isotope. Both the single- and the double labeling technique are laborious and, more importantly, neither of the techniques provides detailed information on time-dependent absorption kinetics. Thus, in the present study stable $^{25}Mg^{2+}$ isotopes were employed to measure intestinal Mg^{2+} absorption in a time- and concentration dependent manner. The effect of dietary Mg^{2+} content on intestinal absorption was determined. In addition, with the use of intestinal cannulas the absorption of Ca^{2+} as well as Mg^{2+} was analyzed at in the proximal and distal regions of the gastrointestinal tract, at several concentrations, to determine the location of paracellular and transcellular absorption. Finally, the effect of vitamin D on Mg^{2+} homeostasis was analyzed.

Materials and methods

Patient selection, sample collection and ethical considerations
For the expression gradients human mucosal gastrointestinal (GI) biopsies were obtained from subjects undergoing gastroscopy and/or colonoscopy in the context of indefinite gastric or colonic complaints. In more detail, a mucosal biopsy was collected from each site, comprising the esophagus, fundus, antrum, duodenum (3-5 centimeter beyond the pylorus), terminal ileum, ascending colon, transverse colon, descending colon, sigmoid colon and rectum. The jejunum could not be reached for sample collection. All biopsies were taken from healthy mucosa. Patients were selected during routine patient care in Finland (Tampere University Hospital). Exclusion criteria included active hyperparathyroidism, kidney insufficiency (serum creatinine >200 umol/L) and liver insufficiency (INR spontaneously >1.5). Gastroscopies and colonoscopies were performed during routine patient care when needed by clinical diagnosis. The additional biopsy samples taken for the study did not increase the complication risk of patients significantly. This study was approved by the ethical committee of Tampere University Hospital, Finland. Written informed consent was obtained from each subject.

Quantitative real-time PCR
Total RNA was extracted from tissues using TRIzol□ reagent (Invitrogen, Paisly, UK) according to the manufacturer's protocol. The obtained RNA was subjected to DNase treatment (Promega, Leiden, The Netherlands) to prevent genomic DNA contamination. Subsequently, RNA was reverse transcribed with murine leukemia virus reverse transcriptase. The obtained cDNA was used to determine mRNA expression levels of various calciotropic and magnesiotropic genes, as well as mRNA levels of glyceraldehyde 3-phosphate dehydrogenase (GAPDH) as an endogenous control. The mRNA expression levels were quantified by real-time PCR on a CFX69 real-time detection system (BioRad, Veenendaal, The Netherlands) using SYBR Green (BioRad, Veenendaal, The Netherlands). Primers (Biolegio, Nijmegen, the Netherlands) were designed with Primer 3 software (Whitehead Institute for Biomedical Research, Cambridge, USA) and are listed in Table I.

Animal studies
C57BL/6J mice (8 weeks old) were purchased from Harlan, the Netherlands. For the tissue panels, animals were sacrificed by cervical dislocation. Subsequently, intestinal segments were isolated, cleaned and snap frozen in liquid nitrogen. For all other studies mice were housed in a temperature- and light-controlled room with pelleted chow and drinking water available *ad libitum*. For the diet studies,

Table 1 Primer sequences used for real-time PCR.

Gene	Species	Forward primer	Reverse primer
GAPDH	*Homo Sapiens*	5'-GGAGTCAACGGATTTGGTCGTA-3'	5'-GGCAACAATATCCACTTTACCAGAGT-3'
TRPV6	*Homo Sapiens*	5'-GCTTTGCTTCAGCCTTCTATATCAT-3'	5'-TGGTAAGGAACAGCTCGAAGGT-3'
TRPM6	*Homo Sapiens*	5'-GCGGACATGGCATAAAATCTTC-3'	5'-TTGAGCAGCTCTTTGTTGTTGAA-3'
GAPDH	*Mus musculus*	5'-TAACATCAAATGGGGTGAGG-3'	5'-GGTTCACACCCATCACAAAC-3'
TRPV6	*Mus musculus*	5'-CTTTGCTTCAGCCTTCTATATCAT-3'	5'-TGGTAAGGAACAGCTCGAAGGT-3'
TRPM6	*Mus musculus*	5'-AAAGCCATGCGAGTTATCAGC-3'	5'-CTTCACAATGAAAACCTGCCC-3'
TRPV5	*Mus musculus*	5'-CCACAGTGATGCTGGAGAGG-3'	5'-GGATTCTGCTCCTGGTGGTG-3'
1αOHase	*Mus musculus*	5'-CGGATTGCTAACGGCGGA-3'	5'-GGCGCCTTAGTCGTCGCA-3'
CLDN2	*Mus musculus*	5'-TGGTGGGCATGAGATGCA-3'	5'-CTCCACCCACTACAGCCACTCT-3'
CLDN12	*Mus musculus*	5'-TCACATTCAACAGAAACGAGAAGAA-3'	5'-CCATCATACCGGGCACACTT-3'

GAPDH, glyceraldehyde 3-phosphate dehydrogenase; TRPV6, transient receptor potential vanilloïd type 6; TRPM6, transient receptor potential melastatin type 6; TRPV5, transient receptor potential vanilloïd subtype 5, 1αOHase, 1-alpha-hydroxylase; CLDN2, claudin 2, CLDN12, claudin 12.

mice were fed a low Mg^{2+}-deficient diet (0.02% w/w Mg^{2+}) a high Mg^{2+} diet (0.48% w/w Mg^{2+}) or a normal diet (0.25% w/w Mg^{2+}). All diets were purchased from SSNIFF Spezialdiäten (SSNIFF Spezialdiäten GmbH, Soest, Germany). For urine and feces collection, animals were individually housed in metabolic cages for 24 h. Blood was sampled from the submandibular facial vein at the end of the stay in the metabolic cages, and sera were collected for Mg^{2+} measurements. For studies on vitamin D, animals received daily intraperitoneal injections with 1,25-dihydroxyvitamin D_3 (100 pg/g bodyweight (BW)/day) or vehicle. All experiments were performed in compliance with the animal ethics board of the Radboud University Nijmegen (Ethical License number RU-DEC 2010-143, RU-DEC 2010-204, RU-DEC 2011-165).

Placement of intestinal cannulas

Cannulas were made using PE50 polyethylene tubing (Instech laboratories, Plymouth Meeting, USA), with an inner diameter 0.58 mm and outer diameter of 0.97 mm. Suture bulbs with a diameter of approximately 2 mm were created on the end of pieces of PE tubing using Dow Corning 723 flowable sealant silicone elastant (Dow Corning, Midland, USA). Mice were anesthetized using 1 µg/g BW medetomidine-hydrochloride (Sedastart, ASTfarma, Oudewater, The Netherlands) and 0.08 mg/g body weight (BW) ketamine (Nimatek, Eurovet, Bladel, The Netherlands), both administered via subcutaneous injection. The abdominal skin

was opened via a lateral incision, after which the muscle layer was cut along the linea alba (Figure 1A). Next, the caecum or stomach was localized, a small hole was created, a pouch suture was placed around the hole after which the tip of the cannula was inserted into the lumen (Figure 1B-F). The suture was closed around the cannula, in-between the suture bulbs, fixing the canule in place. The tubing was passed through the muscular layer of the intestinal wall on the lateral side, after which the abdominal cavity was closed with a running stitch using Vicryl Plus 5.0 sutures (Johnson & Johnson Medical, Amersfoort, The Netherlands) (Figure 1G-H). A pocket was created between the muscular layers and the skin. A SIP22/4 miniature injection port (Instech laboratories, Plymouth Meeting, USA) was attached to the cannula and placed in the subcutaneous pocket on the vetrolateral side of the animal (Figure 1I-J). The wound was closed using a running stitch and covered with wound clips to prevent post-surgical opening of the wound. Medetomidine anesthesia was reversed with a subcutaneous injection of 1 µg/g BW atipamezolhydrochloride (Sedastop, ASTfarma, Oudewater, The Netherlands). The cannula was accessible via the skin and was flushed every other day with saline to prevent clogging (Figure 1K). During the first 3 days after surgery, animals received 0.05 µg/g BW Buprenorphine hydrochloride (Temgesic, Reckitt Benckiser, West Ryde, Australia) twice a day via subcutaneous injection to prevent post-operative pain. Animals were allowed to recover for a minimum of 7 days, before absorption experiments were performed. In general, the mice fully recover during this period, as indicated by their return to their pre-operative weight (Figure 1M).

Ca²⁺ and Mg²⁺ determinations in serum, urine and feces

Serum and urine total Ca²⁺ concentrations were measured using a colorimetric assay as described previously [14]. Serum and urine Mg²⁺ concentrations were determined using a colorimetric assay kit, according to the manufacturer's protocol (Roche Diagnostics, Woerden, The Netherlands). Within-run precision and accuracy was controlled by means of an internal control Precinorm U (Roche Diagnostics, Almere, The Netherlands).

In vivo ²⁵Mg²⁺ absorption assay

Intestinal absorption of Mg²⁺ was measured by analyzing serum ²⁵Mg²⁺ levels. In short, animals were fasted (food, not water) overnight on wire-mesh raised floors to prevent coprophagia. At time-point 0, mice were administered a solution containing 44, 10 or 1.8 mM ²⁵Mg²⁺ (MgO, isotopic enrichment of >98%, CortectNet, Voisins-Le-Bretonneux, France), 125 mM NaCl, 17 mM Tris-HCl pH 7.5, 1.8 g/L fructose. Animals were administered a volume of 15 µL/g BW via oral gavage or via the subcutaneously placed injection ports. Subsequently, blood was
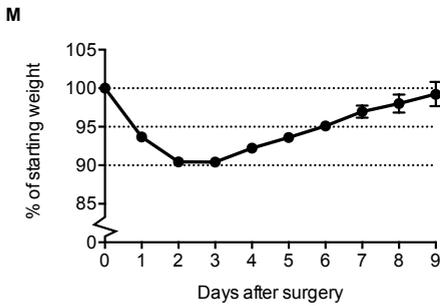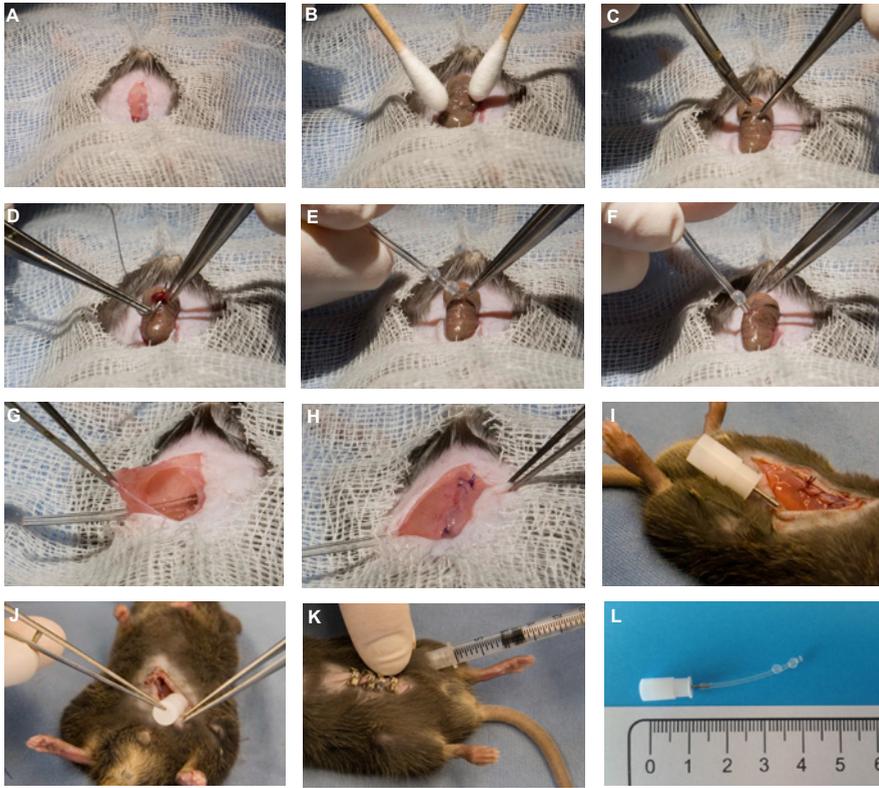
Figure 1 Surgical procedure to place intestinal cannulas connected to a subcutaneously positioned injection port. For a detailed description see "Placement of intestinal cannulas" in the materials and methods section. **A.** Opening of the abdominal cavity. **B.** Localization of the stomach or duodenum. **C.** Creating of an opening for the insertion of the cannula. **D.** Placement of a pouch suture around the opening. **E.** Insertion of the cannula in the intestine. **F.** Tightening the pouch-suture around the cannula in between the suture bulbs, fixing the cannula

in place. **G.** The cannula is passed through the muscular layer of the abdomen to the lateral side of the mouse. **H.** The abdominal cavity is closed. **I/J.** The injection port is attached to the cannula and placed in a subcutaneous pocket. **K.** The abdominal skin is closed and the cannula is flushed via the injection port. **L.** Cannula with suture bulbs and injection port. **M.** Weight development of the mice throughout experiments (n=81).

withdrawn at serial time-points via orbital puncture or via a small cut in the tail and collected in Microvette serum tubes (Sarstedt, Etten-Leur, The Netherlands). After collecting the serum from the coagulated blood samples, samples were digested in nitric acid (65% concentrated, Sigma, Zwijndrecht, The Netherlands) for 1 hour at 70 °C followed by an overnight incubation at room temperature. Subsequently, samples were diluted in milliQ and subjected to ICP-MS analysis (X1 series, Thermo Fisher Scientific, Breda, The Netherlands.

Calculations

The three stable isotopes of Mg^{2+} have the following natural abundance: ^{24}Mg 78.9%, ^{25}Mg 10.0%, ^{26}Mg 11.1%. The isotopic ratios at baseline are therefore: ^{25}Mg : ^{24}Mg = 0.1267 and ^{26}Mg : ^{24}Mg = 0.1407. The percentage of isotopic enrichment in the serum, urine and fecal samples was calculated using the following equation: (measured ^{25}Mg : ^{24}Mg ratio – baseline ^{25}Mg : ^{24}Mg ratio) / (baseline ^{25}Mg : ^{24}Mg ratio) * 100.

In vivo $^{45}Ca^{2+}$ absorption assay

Mice were fasted (food, not water) overnight on wire-mesh raised floors to prevent coprophagia. At time-point 0, mice were administered a solution containing 0.1, 10 or 44 mM $CaCl_2$, 125 mM NaCl, 17 mM TrisHCl pH 7.5, 1.8 g/L fructose, enriched with 20 μCi $^{45}CaCl_2$/ml (New England Nuclear, Newton, USA); in a volume of 15 μL/g of body weight. The solution was administered via the subcutaneously placed injection-port. Blood samples were obtained via orbital puncture at serial time-points after isotope administration via orbital puncture. Blood was collected in Microvette tubes, after clotting serum was removed and serum $^{45}Ca^{2+}$ levels were analyzed by liquid scintillation counting.

Statistical analysis

Values are expressed as means ± SEM. Statistical comparisons were analyzed by one-way ANOVA with a Bonferroni correction, or using an unpaired Student's *t* test. Differences between groups were considered to be statistically significant at *P < 0.05*. Statistical analysis was performed using GraphPad Prism (Macintosh version, 4.51).

Results

TRPV6 and TRPM6 expression along the gastrointestinal tract in humans and mice

In the human gastrointestinal tract, TRPV6 is expressed predominantly in the stomach and duodenum (Figure 2A). Along the murine gastrointestinal tract, the expression pattern of TRPV6 is slightly different. In addition to the expression in the stomach and the duodenum, TRPV6 is also strongly expressed in the caecum as well as in the distal regions of the colon (Figure 2B). TRPM6 is expressed in the distal regions of the gastrointestinal tract of human subjects and mice (Figure 2C-D). Interestingly, like TRPV6, TRPM6 in mice is expressed strongly in the caecum (Figure 2D).
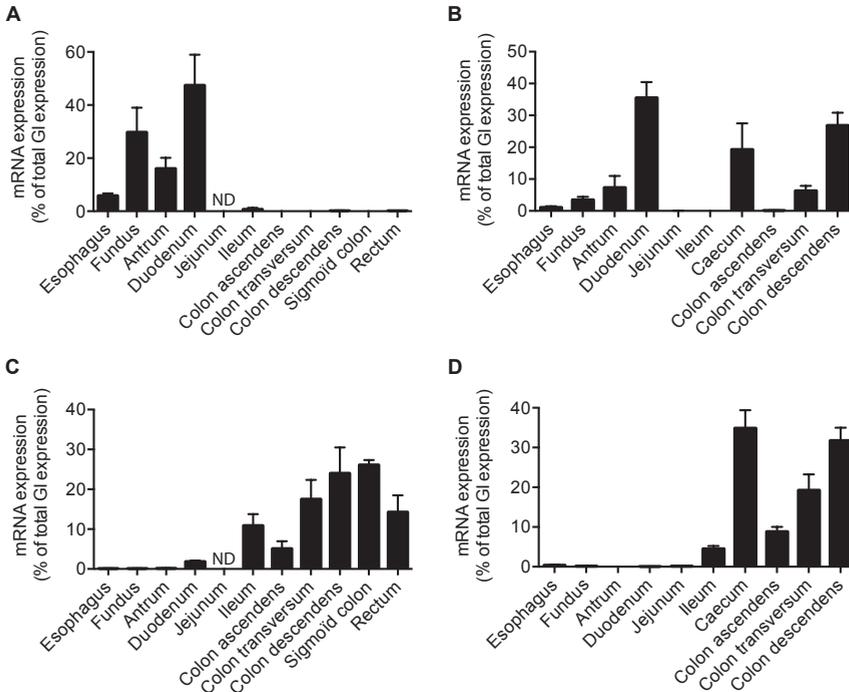
Figure 2 Localization of TRPM6 and TRPV6 along the gastrointestinal tract in humans and mice. Total gastrointestinal mRNA expression of TRPV6 (A/B) and TRPM6 (C/D) corrected for GAPDH expression, in human (**A/C**) and murine (**B/D**) samples (n=5). Data is expressed as a percentage of total gastrointestinal (GI) expression and presented as means ± SEM. ND, not determined.

Time dependent absorption of $^{25}Mg^{2+}$ after administration via oral gavage

To determine the sensitivity of our measurements in various types of samples, mice were given $^{25}Mg^{2+}$ (0.7 µmol/g BW) via oral gavage and placed in a metabolic cage for urine and feces collection, in addition, blood was collected. After 24 hrs, high levels of enrichment of $^{25}Mg^{2+}$ were found in both the urine and the feces, while in serum the enrichment was lower (Figure 3A). To determine the time dependence of $^{25}Mg^{2+}$ absorption from the intestine mice were given (0.7 µmol/g BW) $^{25}Mg^{2+}$ via oral gavage. Subsequently, blood was collected at serial time-points (Figure 3B). $^{25}Mg^{2+}$ was absorbed in a time-dependent manner, and reached a plateau-phase after approximately 2 hrs.

Proximal intestinal Mg^{2+} absorption is regulated by bodily needs

To investigate whether Mg^{2+} absorption, like Ca^{2+} absorption, is regulated by bodily needs, mice were fed a diet with a low (0.02% wt/wt Mg^{2+}), a normal (0.25% wt/wt Mg^{2+}) or a high (0.48% wt/wt Mg^{2+}) Mg^{2+} content for 2 weeks. After this period, the mice on the low Mg^{2+} diet had significantly lower serum Mg^{2+} levels compared to the group on the normal diet (Figure 4A). In addition, urinary Mg^{2+} excretion was diminished and fecal Mg^{2+} excretion was decreased (Figure 4B/C). Serum Mg^{2+} levels in mice receiving the high Mg^{2+} diet were not significantly different from the group on the normal diet (Figure 4A). Urinary and fecal Mg^{2+} excretion, however, were both significantly increased (Figure 4B/C). Interestingly, urinary excretion of Ca^{2+} was significantly decreased in the group receiving the
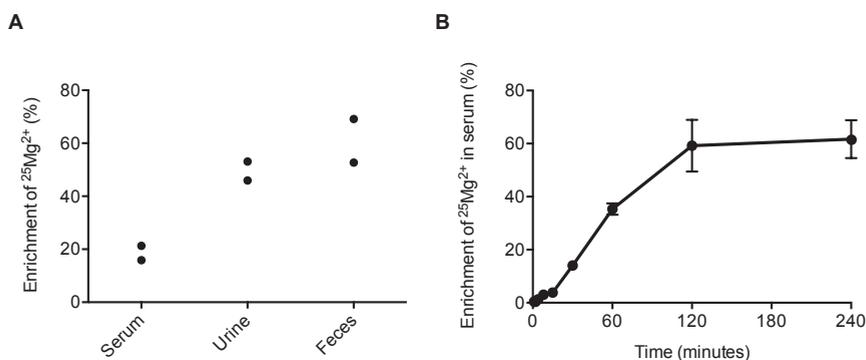
Figure 3 Time-dependent absorption of $^{25}Mg^{2+}$. **A.** Measurement of $^{25}Mg^{2+}$ in serum, urine and feces 24 hrs after administration of 0.7 µmol $^{25}Mg^{2+}$/g BW via oral gavage (n=2). **B.** Absorption of $^{25}Mg^{2+}$ from the intestine after administration via oral gavage (n=5). Data are presented as means ± SEM.

low Mg²⁺ diet, and significantly increased in the group receiving the high Mg²⁺ diet (Figure 4E). Serum Ca²⁺ levels and fecal Ca²⁺ excretion remained unchanged (Figure 4D/F).

Paracellular and transcellular absorption of Mg²⁺ in intestinal segments
To investigate the mineral absorption specifically in the proximal and distal intestinal segments, cannulas were surgically implanted in either the stomach or the caecum of mice. Subsequently, absorption of ⁴⁵Ca²⁺ or ²⁵Mg²⁺ was measured as a function of the luminal mineral concentration to distinguish between paracellular and transcellular transport. The Ca²⁺ absorption in the proximal
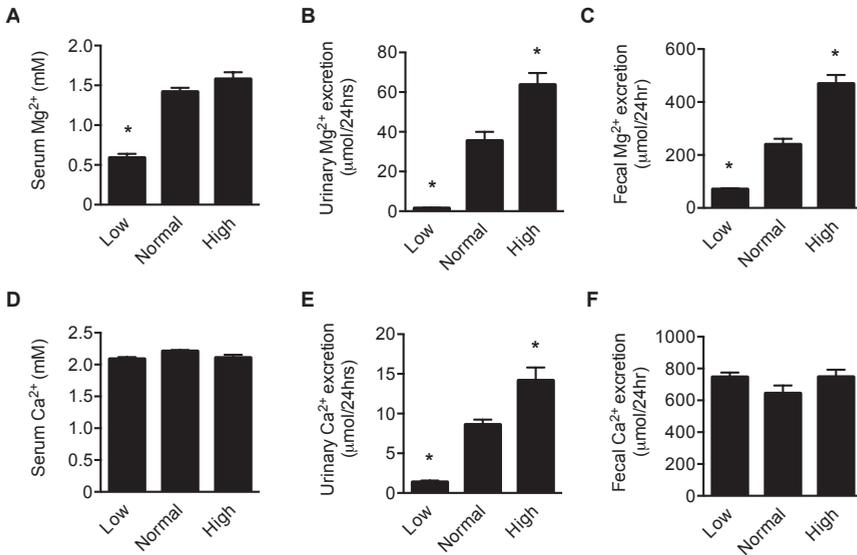
Figure 4 Effect of dietary Mg²⁺ on Intestinal Mg²⁺ absorption. **A.** Serum Mg²⁺ values of mice two weeks on diet with a low (0.02 % wt/wt Mg²⁺), a normal (0.25 % wt/wt Mg²⁺) or a high (0.48 % wt/wt Mg²⁺) Mg²⁺ content (n=5 for each group). **B.** Urinary Mg²⁺ excretion **C.** Fecal Mg²⁺ excretion. **D.** Serum Ca²⁺ levels. **E.** Urinary Mg²⁺ excretion. **F.** Fecal Mg²⁺ excretion. **G.** Intestinal absorption of ²⁵Mg²⁺, low- normal- and high Mg²⁺ diet groups are represented by dotted, filled and dashed lines, respectively. **H.** Average difference in intestinal absorption of ²⁵Mg²⁺ during four hours after isotope administration. **I.** TRPM6 mRNA expression levels in the colon, corrected for GAPDH expression and normalized to the normal Mg²⁺ diet group **J.** 1αOHase mRNA expression levels in the kidney, corrected for GAPDH expression and normalized to the normal Mg²⁺ diet group. Data are presented as means ± SEM. *P < 0.05* compared to normal Mg²⁺ diet.
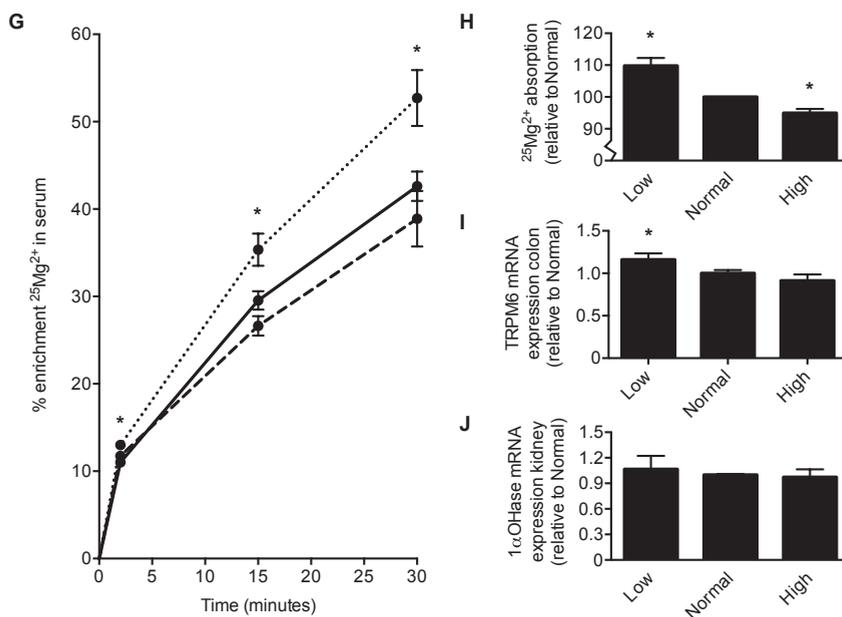
Figure 4 continued.

intestine was significantly higher compared to the more distal part at all luminal concentrations of Ca^{2+} tested (44, 10 and 0.1 mM), (Figure 5B/D/F). The proximal Mg^{2+} absorption was higher compared to the distal intestine at a high luminal concentration of Mg^{2+} (44 mM) (Figure 5A), but not at lower luminal concentrations (10 and 1.6 mM Mg^{2+}) (Figure 5C/E). The relationship between the absorption of $^{25}Mg^{2+}$ and the luminal Mg^{2+} concentration is displayed in figure 5G. In the proximal intestine, the absorption of $^{25}Mg^{2+}$ is linearly related to the buffer Mg^{2+} concentration, whereas in the distal intestine the absorption of Mg^{2+} is saturable at higher Mg^{2+} concentrations. The relation between $^{45}Ca^{2+}$ absorption and luminal Ca^{2+} concentration is comparable in the proximal and distal intestine, and consists of a saturable and a non-saturable, linear component (Figure 5H).

The effect of vitamin D on Mg²⁺ homeostasis

To determine whether vitamin D has an effect on Mg^{2+} homeostasis in general and more specifically on intestinal Mg^{2+} absorption, mice were treated with 1,25-dihydroxyvitamin D_3 (100 pg/g BW/day) for 7 days and subsequently the intestinal absorption of $^{25}Mg^{2+}$ was measured. Vitamin D treatment significantly increased serum Mg^{2+} and Ca^{2+} levels as well as 24 hr urinary Mg^{2+} and Ca^{2+}
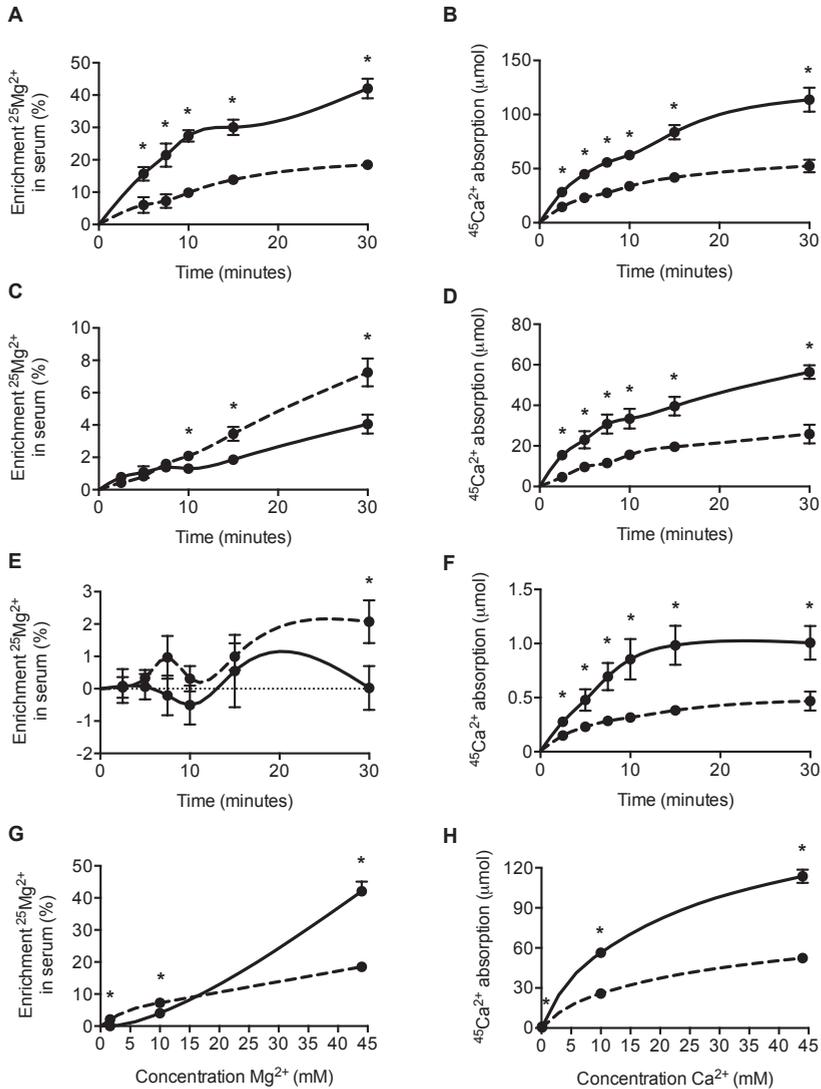
Figure 5 Paracellular and transcellular absorption of Mg^{2+} in intestinal segments. Solid lines represent mice with a cannula placed in the stomach, dashed lines represent mice with a cannula placed in the caecum. $^{25}Mg^{2+}$ absorption using a buffer containing **A.** 44 mM, **C.** 10 mM, or **E.** 1.6 mM Mg^{2+}. $^{45}Ca^{2+}$ absorption using a buffer containing **B.** 44 mM, **D.** 10 mM, or **F.** 0.1 mM. **G.** Relationship between luminal Mg^{2+} concentration and $^{25}Mg^{2+}$ absorption, and **H.** between luminal Ca^{2+} concentration and $^{45}Ca^{2+}$ absorption at t=30 minutes. Data are presented as means ± SEM, n=4-6. * $P < 0.05$ compared to the group with cannula placed in the stomach.

excretion (Figure 6A-D). Importantly, the Mg²⁺ absorption in the proximal was not significantly different between vehicle and vitamin D-treated mice (Figure 6E).
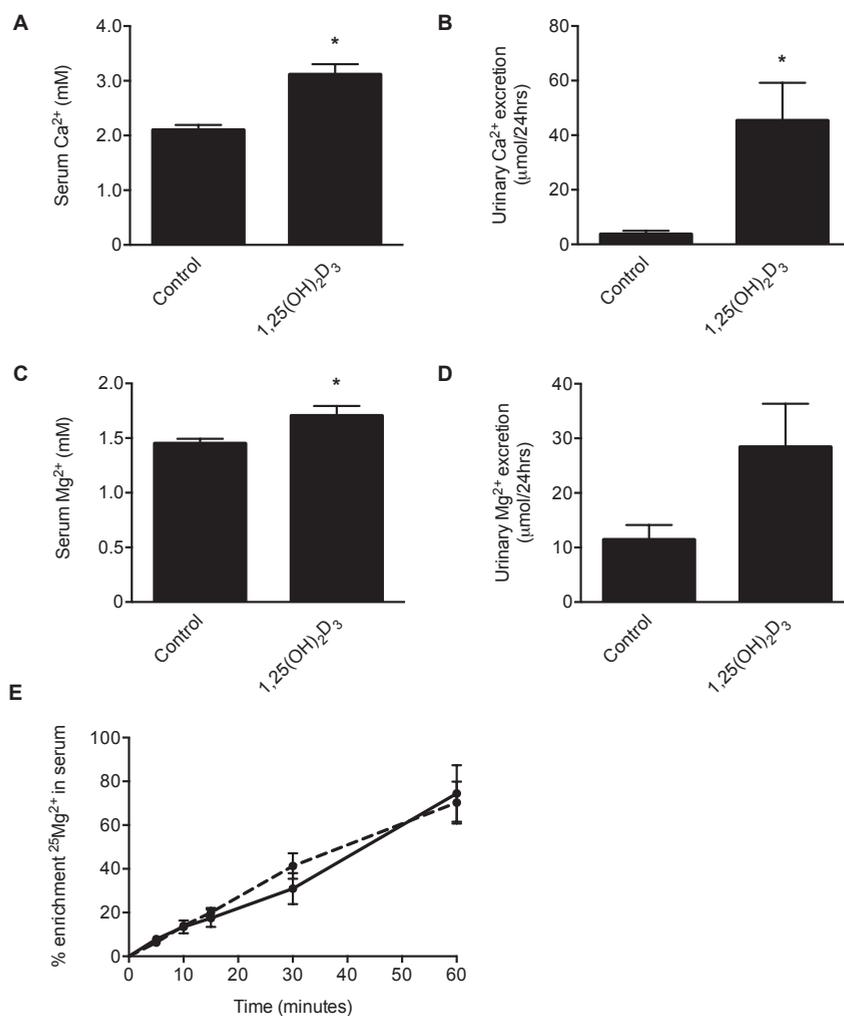
Figure 6 The effect of vitamin D on Mg²⁺ homeostasis. Mice were treated with vehicle (control) or 1,25-dihydroxyvitamin D₃ (100 pg/g BW/day) for 7 days **A.** Serum Ca²⁺ levels in controls and vitamin D-treated mice **B.** 24 hr urinary Ca²⁺ excretion **C**. Serum Mg²⁺ levels **D.** 24 hr urinary Mg²⁺ excretion **E.** Intestinal ²⁵Mg²⁺ absorption in control (solid line) and vitamin D (dashed line) treated mice. Data are presented as means ± SEM, n=5-7. * *P* < *0.05* compared to vehicle-treated controls.
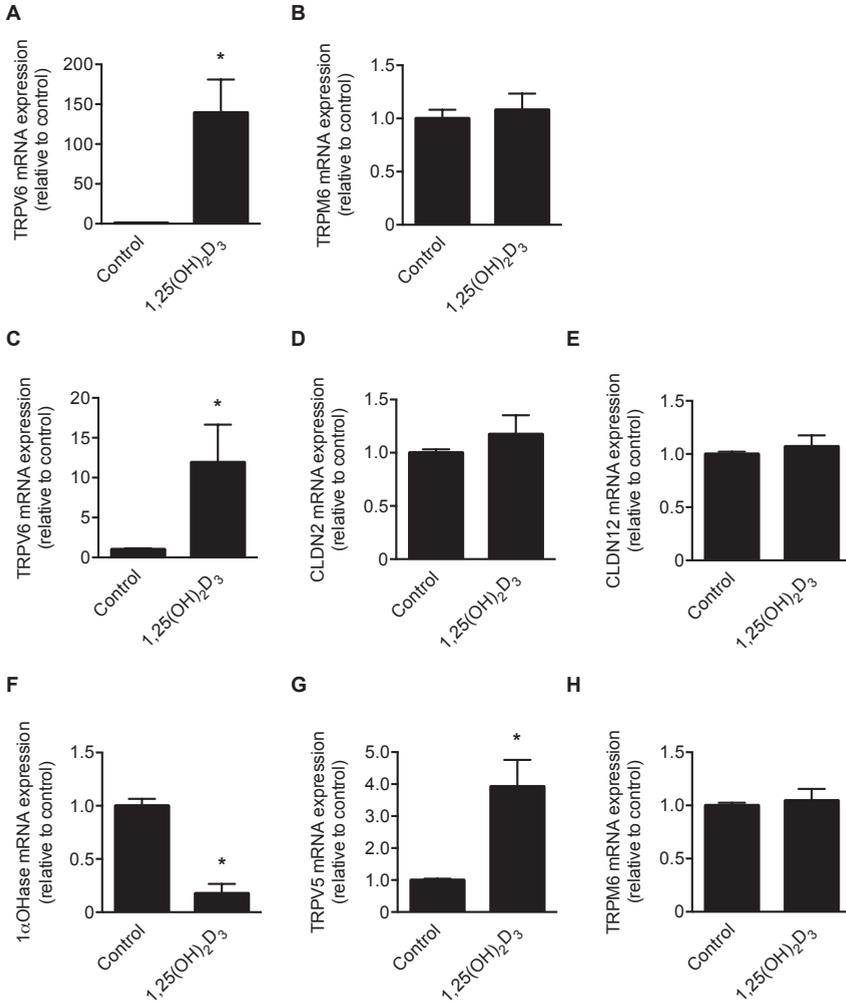
Figure 7 Expression of calciotropic genes, but not TRPM6, is regulated by vitamin D-treatment. mRNA expression levels of various calciotropic and magnesiotropic genes were determined in vehicle- treated controls and 1,25-dihydroxyvitamin D_3-treated mice. All values were corrected for GAPDH expression and were normalized to controls. **A.** TRPV6 and **B.** TRPM6 mRNA expression in colon. **C.** TRPV6, **D.** CLDN2, and **E.** CLDN12 mRNA expression in duodenum. **F.** 1αOHase, **G.** TRPV5 and **H.** TRPM6 mRNA expression in kidney. Data are presented as means ± SEM n=5-7. * *P < 0.05* compared to vehicle-treated controls.

Effect of vitamin D on intestinal Mg²⁺ absorption

The mRNA expression levels of TRPV6 in duodenum (Figure 7C) as well as the colon (Figure 7A) of vitamin D-treated mice were significantly increased compared to vehicle-treated controls. TRPM6 expression in the colon, however, remained unchanged (Figure 7B). The duodenal expression levels of CLDN2 and CLDN12 were analyzed to determine the effect of vitamin D on paracellular mineral transport. No significant differences in the expression levels were observed between vitamin D-treated mice and controls (Figure 7 D/E). In kidney, 1aOHase expression was significantly decreased in the vitamin D-treated group, indicating appropriate suppression of vitamin D synthesis by vitamin D treatment (Figure 7F). The renal TRPV5 expression of vitamin D-treated mice was significantly augmented compared to controls, while no changes were observed in renal TRPM6 expression between both groups.

Discussion

Compared to Ca²⁺, little is known about Mg²⁺ absorption in the intestine, including hormones regulating this process. The aim of this study was, therefore, to investigate the absorption of Mg²⁺ along the gastrointestinal tract on a molecular, a functional and a physiological level. Our findings indicate that: *i*) mRNA expression of TRPV6 is predominant in the proximal part of the human gastro-testinal tract, whereas TRPM6 is mainly expressed in the distal segments; *ii*) in the murine gastrointestinal tract expression patterns of TRPV6 and TRPM6 are similar to those observed in humans. In addition, TRPV6 and TRPM6 are both highly expressed in the caecum and TRPV6 is also present in the distal segments; *iii*) Ca²⁺ is predominantly absorbed in the proximal parts of the intestine, irrespective of its luminal concentration; *iv*) only at high luminal concentrations, Mg²⁺ is predominantly absorbed in the proximal parts of the intestine, compared to the distal intestinal segments.

The epithelial divalent channels, TRPV6 and TRPM6, form the gate-keepers of Ca²⁺ and Mg²⁺ absorption, respectively, along the gastrointestinal tract [15]. In humans, TRPV6 is expressed predominantly in the stomach and duodenum, whereas TRPM6 is mainly expressed in the ileum and colon. In mice, TRPV6 was also expressed in caecum and distal segments of the colon, while TRPM6 was in addition to ileum and colon also abundantly detected in caecum. The discrepancy between the expression patterns of these TRP's in human and mice might be explained by the morphological and functional differences between their gastro-intestinal tracts. Mice are non-ruminant herbivores that have a large caecum

compared to humans [16]. Their caecum houses many types of micro-organisms, which aid in the digestion of plant material by breaking down cellulose [17]. Plant material is an important source of Ca^{2+} and Mg^{2+}, which is only released if cellulose is digested. Since the digestion of cellulose takes place in the caecum of mice, these nutrients are released from the plant material in the more distal segments of the intestine.

Intestinal absorption of Ca^{2+} is strictly regulated by bodily need; increased when dietary Ca^{2+} supply is limited and decreased when Ca^{2+} is abundantly available [18]. To determine whether the same holds true in case of Mg^{2+}, the effect of dietary Mg^{2+} supply on intestinal absorption of Mg^{2+} was investigated. A low Mg^{2+} diet effectively induced a hypomagnesemia and urinary Mg^{2+} conservation. Conversely, enhanced renal Mg^{2+} excretion indicated that the high Mg^{2+} diet resulted in a surplus of Mg^{2+} in the body. Absorption of $^{25}Mg^{2+}$ was significantly increased in mice receiving the low Mg^{2+} diet, whereas Mg^{2+} absorption in the high Mg^{2+} diet group was reduced. This indicates that the rate of Mg^{2+} absorption, like for Ca^{2+}, nicely follows the dietary body needs. These alterations in Mg^{2+} absorption were accompanied by a slight, but significant, effect on the expression of TRPM6 in the mice on the low Mg^{2+} diet but not the high Mg^{2+} diet. This could be explained by the fact that the adaptation in Mg^{2+} was relatively mild. This findings contrast mice challenged with a Ca^{2+} deficient diet who showed a strong increase in intestinal Ca^{2+} transport, which was facilitated by the increased expression of proteins involved in Ca^{2+} transport, including TRPV6 [18, 19]. Renal expression of 1αOHase, the enzyme responsible for the production of active vitamin D, was unchanged during the various dietary Mg^{2+} regimes. This suggests that the process of intestinal Mg^{2+} absorption is vitamin D-independent. Alternatively, new magnesiotropic hormones, including the epidermal growth factor (EGF) and insulin, have been identified and shown to regulate Mg^{2+} reabsorption via TRPM6 in the kidney [20, 21]. These hormones could potentially play a role in the regulation of intestinal Mg^{2+} absorption. Another possible player is the Ca^{2+}-sensing receptor (CaSR), which senses the extracellular concentration of both Ca^{2+} and Mg^{2+} to control for instance, TRPV5 activity [22]. Interestingly, the dietary Mg^{2+} content also affected renal excretion of Ca^{2+}. The coupling between the Ca^{2+} and Mg^{2+} balance has previously been observed [7, 23], but the underlying mechanism remains under debate [23-26].

Paracellular absorption of Ca^{2+} and Mg^{2+} mainly takes place in the duodenum and jejunum. Based on the expression patterns of TRPV6 and TRPM6 observed in the gastrointestinal tracts of humans and mice, we hypothesized that transcellular Ca^{2+} absorption mainly takes place in the proximal parts of the intestine and

potentially also in the caecum and distal part of the colon in mice, whereas transcellular Mg^{2+} absorption is restricted to the distal parts of the gastrointestinal tract. To address this hypothesis with functional measurements, intestinal cannulas were placed in either the stomach or the caecum of mice, to allow local *in vivo* measurements of mineral absorption. Indeed, Ca^{2+} absorption in the proximal intestine was significantly higher compared to the more distal parts at all luminal concentrations of Ca^{2+} that were tested. Mg^{2+} absorption on the other hand was higher compared to the distal part of the intestine at a high luminal concentration of Mg^{2+}, but not at lower luminal concentrations. Absorption of Ca^{2+} in both the proximal and distal intestine consisted of two components; a nonsaturable, linear component, representing transport via the paracellular route, and a saturable component, corresponding to transport via the transcellular pathway. In contrast, absorption of $^{25}Mg^{2+}$ in the proximal intestine was linearly correlated to the Mg^{2+} concentration of the uptake-buffer, indicating that the absorption takes place solely via the paracellular route. In the distal intestine on the other hand, absorption of Mg^{2+} shows a curve consisting of both a linear and a saturable component, suggesting a combination of paracellular and transcellular absorption in this location. This is in line with the observed expression patterns of TRPV6 and TRPM6. These measurements indicate that transcellular intestinal absorption of Ca^{2+} and Mg^{2+} takes place at distinct locations along the gastrointestinal tract. Interestingly, at low luminal Ca^{2+} concentrations, the absorption of Ca^{2+} is approximately twice as high in the proximal intestine as in the distal part of the intestine. This is perfectly in line with the expression of TRPV6, which is almost twice as high in duodenum as in caecum of mice.

The observed expression patterns of TRPV6 and TRPM6 and the corresponding absorption of Ca^{2+} and Mg^{2+} is in line with clinical findings in patients that have undergone gastrointestinal resections of either the small or the large intestine. Patients that have small bowel resections often suffer from Ca^{2+} deficits due to reduced Ca^{2+} absorption [27]. Similarly, patients with Crohn's disease, mainly affecting the small intestine, are also known to have reduced serum Ca^{2+} levels [28]. Patients that have undergone large bowel resections on the other hand are more likely to display reduced serum Mg^{2+} levels [29-31]. The physiological reason for the spatial separation of Ca^{2+} and Mg^{2+} absorption remains to be determined. The stable isotope technique was successfully applied to measure time-dependent absorption of Mg^{2+} in the intestine. Since the measurements were performed in a relatively short time-scale, there was no need to correct for intestinal secretion or renal excretion. Double–labeling, which is the most commonly applied technique in fecal monitoring studies with isotope tracers, was, therefore, not applied. Thus, our method is more easily applicable and less costly [10]. The major limitation of

the present analysis is the reduced sensitivity because the relatively high natural abundance of $^{25}Mg^{2+}$ limits the reliability at low luminal concentrations.

Due to the similarities between Ca^{2+} and Mg^{2+} homeostasis, the calciotropic hormone vitamin D has often been suggested to play a role in Mg^{2+} handling [32]. To examine the effect of vitamin D on Mg^{2+} homeostasis, mice were treated with 1,25-dihydroxyvitamin D_3 for a week [32]. Vitamin D treatment increased serum Ca^{2+} levels as well as urinary Ca^{2+} excretion. Interestingly, serum Mg^{2+} levels and 24-hr urinary Mg^{2+} excretion were also significantly higher compared to controls, suggesting that intestinal absorption of Mg^{2+} was increased. However, changes in intestinal absorption were not detected using the $^{25}Mg^{2+}$ absorption assay. In order to gain more insight in the underlying molecular processes, mRNA expression levels or various genes were determined in duodenum, colon and kidney of the vehicle treated controls and vitamin D-treated mice. The expression of TRPV6 and TRPV5 in the intestine and kidney, respectively, were elevated in vitamin D-treated mice. TRPM6 expression, however, was unchanged both in colon and kidney, indicating that vitamin D does not affect transcellular absorption via TRPM6 at the transcriptional level. Vitamin D could also have an effect on paracellular transport of Ca^{2+} and Mg^{2+}. CLDN2 and CLDN12 are tight-junction proteins that have been suggested to play a role in paracellular absorption of Ca^{2+} in the intestine [33]. Their expression levels in the duodenum were however unchanged by vitamin D treatment in our study. Therefore, it is unlikely that they contributed to changes in intestinal Mg^{2+} absorption. So, despite the changes in serum Mg^{2+} levels and urinary Mg^{2+} excretion, no functional or molecular evidence was found that vitamin D affects intestinal Mg^{2+} absorption. High urinary Ca^{2+} levels may affect renal Mg^{2+} handling, explaining the hypermagnesiuria but not the observed hypermagnesemia [34, 35]. Alternatively, vitamin D induced mobilization of Mg^{2+} from bone could provide an alternative explanation for the increased serum Mg^{2+} levels and urinary Mg^{2+} excretion in vitamin D-treated animals [36]. Although Mg^{2+} homeostasis can be influenced by vitamin D in pharmacological doses, which is in line with previous findings, vitamin D seems to have no effect on Mg^{2+} homeostasis in the normal physiological range [32]. Indeed, 1αOHase knockout mice and klotho knockout mice, which are vitamin D deficient or display hypervitaminosis D, respectively, both have normal serum Mg^{2+} levels, urinary Mg^{2+} excretion and renal TRPM6 expression levels [7, 37].

In conclusion, transcellular Ca^{2+} and Mg^{2+} absorption in the intestine is spatially separated, as shown by $^{45}Ca^{2+}$ and $^{25}Mg^{2+}$ absorption studies. In addition, absorption of Mg^{2+} from the intestinal lumen is regulated by dietary supply. Further research is necessary to clarify the exact role of vitamin D in Mg^{2+} homeostasis. With the

use of $^{25}Mg^{2+}$ assays, this and many other scientific questions with regard to the absorption of Mg^{2+} can be addressed.

Acknowledgements

4

References

1. van de Graaf SF, Bindels RJ, Hoenderop JG: Physiology of epithelial Ca^{2+} and Mg^{2+} transport. *Rev Physiol Biochem Pharmacol* 158: 77-160, 2007

2. Schweigel M, Martens H: Magnesium transport in the gastrointestinal tract. *Front Biosci* 5: D666-677, 2000

3. Quamme GA: Recent developments in intestinal magnesium absorption. *Curr Opin Gastroenterol* 24: 230-235, 2008

4. Bronner F: Recent developments in intestinal calcium absorption. *Nutr Rev* 67: 109-113, 2009

5. Christakos S, Dhawan P, Porta A, Mady LJ, Seth T: Vitamin D and intestinal calcium absorption. *Mol Cell Endocrinol* 347: 25-29, 2011

6. Lieben L, Carmeliet G, Masuyama R: Calcemic actions of vitamin D: effects on the intestine, kidney and bone. *Best Pract Res Clin Endocrinol Metab* 25: 561-572, 2011

7. Groenestege WM, Hoenderop JG, van den Heuvel L, Knoers N, Bindels RJ: The epithelial Mg^{2+} channel transient receptor potential melastatin 6 is regulated by dietary Mg^{2+} content and estrogens. *J Am Soc Nephrol* 17: 1035-1043, 2006

8. Jahnen-Dechent W, Ketteler M: Magnesium basics. *Clinical Kidney Journal* 5: i3-i14, 2012

9. Schuette S, Vereault D, Ting BT, Janghorbani M: Accurate measurement of stable isotopes of magnesium in biological materials with inductively coupled plasma mass spectrometry. *Analyst* 113: 1837-1842, 1988

10. Coudray C, Pepin D, Tressol JC, Bellanger J, Rayssiguier Y: Study of magnesium bioavailability using stable isotopes and the inductively-coupled plasma mass spectrometry technique in the rat: single and double labelling approaches. *Br J Nutr* 77: 957-970, 1997

11. Coudray C, Rambeau M, Feillet-Coudray C, Gueux E, Tressol JC, Mazur A, Rayssiguier Y: Study of magnesium bioavailability from ten organic and inorganic Mg salts in Mg-depleted rats using a stable isotope approach. *Magnes Res* 18: 215-223, 2005

12. Abrams SA: Assessing mineral metabolism in children using stable isotopes. *Pediatr Blood Cancer* 50: 438-441; discussion 451, 2008

13. Coudray C, Feillet-Coudray C, Rambeau M, Tressol JC, Gueux E, Mazur A, Rayssiguier Y: The effect of aging on intestinal absorption and status of calcium, magnesium, zinc, and copper in rats: a stable isotope study. *J Trace Elem Med Biol* 20: 73-81, 2006

14. Hoenderop JG, Muller D, Van Der Kemp AW, Hartog A, Suzuki M, Ishibashi K, Imai M, Sweep F, Willems PH, Van Os CH, Bindels RJ: Calcitriol controls the epithelial calcium channel in kidney. *J Am Soc Nephrol* 12: 1342-1349, 2001

15. Dimke H, Hoenderop JG, Bindels RJ: Molecular basis of epithelial Ca^{2+} and Mg^{2+} transport: insights from the TRP channel family. *J Physiol* 589: 1535-1542, 2011

16. Mackie R, White B, Hume I: Fermentation in the Hindgut of Mammals. In: *Gastrointestinal Microbiology.* Springer US, pp 84-115, 1997

17. Fonty G, Gouet P: Fibre-degrading microorganisms in the monogastric digestive tract. *Animal Feed Science and Technology* 23: 91-107, 1989

18. Van Cromphaut SJ, Dewerchin M, Hoenderop JG, Stockmans I, Van Herck E, Kato S, Bindels RJ, Collen D, Carmeliet P, Bouillon R, Carmeliet G: Duodenal calcium absorption in vitamin D receptor-knock-out mice: functional and molecular aspects. *Proc Natl Acad Sci U S A* 98: 13324-13329, 2001

19. Woudenberg-Vrenken TE, Lameris AL, Weissgerber P, Olausson J, Flockerzi V, Bindels RJ, Freichel M, Hoenderop JG: Functional TRPV6 channels are crucial for transepithelial Ca^{2+} absorption. *Am J Physiol Gastrointest Liver Physiol* 303: G879-885, 2012

20. Groenestege WM, Thebault S, van der Wijst J, van den Berg D, Janssen R, Tejpar S, van den Heuvel LP, van Cutsem E, Hoenderop JG, Knoers NV, Bindels RJ: Impaired basolateral sorting of pro-EGF causes isolated recessive renal hypomagnesemia. *J Clin Invest* 117: 2260-2267, 2007

21. Nair AV, Hocher B, Verkaart S, van Zeeland F, Pfab T, Slowinski T, Chen YP, Schlingmann KP, Schaller A, Gallati S, Bindels RJ, Konrad M, Hoenderop JG: Loss of insulin-induced activation of TRPM6 magnesium channels results in impaired glucose tolerance during pregnancy. *Proc Natl Acad Sci U S A* 109: 11324-11329, 2012

22. Geibel JP, Hebert SC: The functions and roles of the extracellular Ca²⁺-sensing receptor along the gastrointestinal tract. *Annu Rev Physiol* 71: 205-217, 2009

23. Bonny O, Rubin A, Huang CL, Frawley WH, Pak CY, Moe OW: Mechanism of urinary calcium regulation by urinary magnesium and pH. *J Am Soc Nephrol* 19: 1530-1537, 2008

24. Carney SL, Wong NL, Quamme GA, Dirks JH: Effect of magnesium deficiency on renal magnesium and calcium transport in the rat. *J Clin Invest* 65: 180-188, 1980

25. Le Grimellec C, Roinel N, Morel F: Simultaneous Mg, Ca, P,K,Na and Cl analysis in rat tubular fluid. II. During acute Mg plasma loading. *Pflugers Arch* 340: 197-210, 1973

26. Quinn SJ, Thomsen AR, Egbuna O, Pang J, Baxi K, Goltzman D, Pollak M, Brown EM: CaSR-mediated interactions between calcium and magnesium homeostasis in mice. *Am J Physiol Endocrinol Metab* 304: E724-733, 2013

27. Hylander E, Ladefoged K, Madsen S: Calcium balance and bone mineral content following small-intestinal resection. *Scand J Gastroenterol* 16: 167-176, 1981

28. Krawitt EL, Beeken WL, Janney CD: Calcium absorption in Crohn's disease. *Gastroenterology* 71: 251-254, 1976

29. M'Koma AE: Serum biochemical evaluation of patients with functional pouches ten to 20 years after restorative proctocolectomy. *Int J Colorectal Dis* 21: 711-720, 2006

30. Shiga K, Hara H, Suzuki T, Nishimukai M, Konishi A, Aoyama Y: Massive large bowel resection decreases bone strength and magnesium content but not calcium content of the femur in rats. *Nutrition* 17: 397-402, 2001

31. Miranda SC, Ribeiro ML, Ferriolli E, Marchini JS: Hypomagnesemia in short bowel syndrome patients. *Sao Paulo Med J* 118: 169-172, 2000

32. Hardwick LL, Jones MR, Brautbar N, Lee DB: Magnesium absorption: mechanisms and the influence of vitamin D, calcium and phosphate. *J Nutr* 121: 13-23, 1991

33. Fujita H, Sugimoto K, Inatomi S, Maeda T, Osanai M, Uchiyama Y, Yamamoto Y, Wada T, Kojima T, Yokozaki H, Yamashita T, Kato S, Sawada N, Chiba H: Tight junction proteins claudin-2 and -12 are critical for vitamin D-dependent Ca²⁺ absorption between enterocytes. *Mol Biol Cell* 19: 1912-1921, 2008

34. Revusova V, Gratzlova J, Zvara V: Impaired renal tubular reabsorption of magnesium (TRMg) in Ca-containing kidney stone formers. *Int Urol Nephrol* 16: 237-242, 1984

35. Quamme GA: Effect of hypercalcemia on renal tubular handling of calcium and magnesium. *Can J Physiol Pharmacol* 60: 1275-1280, 1982

36. Lifshitz F, Harrison HC, Harrison HE: Effects of vitamin D on magnesium metabolism in rats. *Endocrinology* 81: 849-853, 1967

37. Woudenberg-Vrenken TE, van der Eerden BC, van der Kemp AW, van Leeuwen JP, Bindels RJ, Hoenderop JG: Characterization of vitamin D-deficient klotho(-/-) mice: do increased levels of serum 1,25(OH)2D3 cause disturbed calcium and phosphate homeostasis in klotho(-/-) mice? *Nephrol Dial Transplant* 27: 4061-4068, 2012

4

5

Expression profiling of claudins in the human gastrointestinal tract in health and during inflammatory bowel disease

Anke L. Lameris[1], Silvie Huybers[1], Katri Kaukinen[2,3],
T.H. Mäkelä[2], René J.M. Bindels[1], Joost G.J. Hoenderop[1], Pasi I. Nevalainen[3,4]

[1] Department of Physiology, Nijmegen Centre for Molecular Life Sciences,
Radboud University Nijmegen Medical Centre, The Netherlands
[2] Department of Gastroenterology and Alimentary Tract Surgery,
Tampere University Hospital, Tampere, Finland [3] School of Medicine,
University of Tampere, Tampere, Finland [4] Department of Internal Medicine,
Tampere University Hospital, Tampere, Finland

Abstract

Claudins, being part of the tight junction protein family, partially determine the integrity and paracellular permeability of the intestinal epithelium. The aim of this study was twofold. First, we set out to create an overview of claudin mRNA expression along the proximal-distal axis of the healthy human intestine. Second, we aimed to analyze expression levels of claudins in patients with active and inactive inflammatory bowel diseases (IBD) such as Crohn's disease (CD) or ulcerative colitis (UC).

Claudins show distinct expression patterns throughout the gastrointestinal tract. Some claudins show a proximal expression pattern, such as CLDN18 which is solely expressed in the stomach, and CLDN2 and -15 that are predominantly expressed in the proximal parts of the gastrointestinal tract. Other claudins such as CLDN3, -4, -7 and -8 are predominantly expressed in the distal parts of the gastrointestinal tract, or show a ubiquitous expression pattern throughout the entire gastrointestinal tract, which is the case for CLDN12. In addition, we show that changes in claudin expression in IBD are dependent on gastrointestinal location and inflammatory activity.

This study provides detailed mRNA expression patterns of various claudins throughout the human gastrointestinal tract. Analysis of expression levels of claudins in patients with CD, active- and inactive UC shows that changes in expression are confined to specific intestinal segments, and strongly depend on inflammatory activity.

Introduction

The intestinal epithelium forms the largest surface area and most important barrier between the internal and external environment of the body. For its integrity, the intestinal epithelium depends on three components: desmosomes, adherens junctions and tight junctions [1]. Tight junctions between epithelial cells play a dual role. First, they ensure cell polarity by inhibiting diffusion of membrane proteins from the apical to the basolateral side and vice versa. Second, they function as a gateway, determining the permeability of the epithelial cell layer via the paracellular pathway [1]. To this end epithelial cells are connected by tight junction strands. To date, several proteins have been identified within these tight junction strands, including occludin, claudins, tricellulin and marvel3D [2]. Consisting of a large family that comprises more than 24 isoforms, claudins have been shown to determine membrane integrity and form pore-like structures, which are responsible for size and charge selectivity of paracellular transport via tight junctions in a large variety of epithelia [3]. The different isoforms exhibit distinct tissue-, cell-, developmental stage-, and disease-specific expression patterns [4, 5].

Several studies have set out to determine the expression patterns of claudins in the intestine of mice or rats, showing expression of CLDN1, -2, -3, -4, -5, -7, -8, -12, -15, and -18. CLDN6, -9, -10, -11, -13, -14, -16, -17, and -19 were not detected in these studies [4, 6, 7]. In human intestine, however, expression of various claudins is less well established. Experimental data showing expression patterns throughout the human gastrointestinal tract is lacking.

In active inflammatory bowel diseases (IBD) such as Crohn's disease (CD) or ulcerative colitis (UC), a perturbed expression of tight junction proteins is a typical feature [8]. In accordance with this, IBD patients with inflamed gut epithelium may present with electrolyte disturbances [9]. Here, the pathophysiological relevance of claudins comes into play as changes in claudin expression influence epithelial integrity, thereby potentially leading to altered electrolyte absorption via tight junctions.

The aim of this study was twofold. First, we set out to create an overview of claudin mRNA expression along the proximal-distal axis of the healthy human intestine. Second, we aimed to analyze expression levels of claudin isoforms in patients with CD, active- and inactive UC to identify changes in expression that might explain the changes in epithelial integrity and electrolyte absorption.

Materials and Methods

Patient selection, serum and urine biochemistry

Patients were all selected during routine patient care in Finland (Tampere University Hospital). Included patients were undergoing coloscopy, gastroscopy or pouch/ileoscopy for medical indications. Diagnosis was confirmed based on both macro- and microscopical findings. Exclusion criteria included active hyperparathyroidism, kidney insufficiency (serum creatinine >200umol/L) and liver insufficiency (INR spontaneously >1.5). Biochemical analysis of blood and urine was routinely performed using standard techniques at the Laboratory Centre of the Pirkanmaa Hospital District, Finland. Three patients with active ulcerating colitis were unable to give urine samples because of diarrhea.

For the expression gradient study seven patients (2 males) with mean age 57 years (range 44-70) underwent gastroscopy and seven patients (2 males) with mean age 58 years (range 45-74) colonoscopy. Indications for gastroscopy were anemia, reflux, abdominal pain, Barrett's esophagus (n=2) and melena (n=2). Macroscopic findings included four normal, one Barrett's esophagus, one small ventricular ulcus and one patient had small erosions in duodenal bulbus. Of macroscopically normal gastroscopies two had helicobacter gastritis and one had Barrett's changes. Colonoscopies were done because of diarrhea (n=1), constipation (n=2), control of polypectomy (n=3) and control of inactive ulcerating proctitis (n=1). Three colonoscopy results were macro- and microscopically normal, 4 benign polyps were found in three patients, and the patient with previous proctitis had no inflammation with slightly atrophic sigmoid colon.

To investigate claudin expression in various patient groups human sigmoid and ileal biopsies were obtained from 27 patients (15 females, 12 males). Mean age was 41 years (range 18-73). CD and UC patients had mean disease history of 11 years (range 0-32). Four patients with CD had ileocolonic and 3 isolated colonic disease. Corticosteroid treatment was given to four patients with active UC (prednisolone 20 and 40 mg/day or intravenous methylprednisolone 60 mg/day), and one patient with inactive UC (prednisolone 20 mg started 6 weeks earlier for active disease). Mesalazine was used by 14 (median dose 2400 mg/day, range 1600-3200 mg), sulfasalazine by 2 (range 1000-1500 mg/day), azathioprine by 7 (median dose 150 mg/day, range 100-150 mg), and methotrexate by 3 patients (median dose 15 mg/week, range 15-20 mg/week). After colonoscopy three patients with active CD and six with active UC had their IBD medication increased.

Sample collection

For the expression gradients human mucosal gastrointestinal (GI) biopsies were obtained from subjects undergoing gastroscopy and/or colonoscopy in the context

of indefinite gastric or colonic complaints. In more detail, a mucosal biopsy was collected from each site, comprising the esophagus, fundus, antrum, duodenum (3-5 centimeter beyond the pylorus), terminal ileum, ascending colon, transverse colon, descending colon, sigmoid colon and rectum. The jejunum could not be reached for sample collection. All biopsies were taken from healthy mucosa.

The samples used to determine expression during IBD were taken during colonoscopy or pouch/ileoscopy. Biopsies for analyses of claudin expression were taken from macroscopically not inflamed terminal ileum and sigmoid colon or if inflammation was present from an area least inflamed and not from an area of an ulcer or spontaneous bleeding. Biopsies for diagnostic purposes were taken according to clinical decision of the gastroenterologist not always coinciding with study biopsies. Small bowel biopsy samples were taken in the terminal ileum. Colon biopsy samples were taken above the rectosigmoid junction when the colonoscope was ~30 centimeters ab ano. In patients with active UC or CD additional biopsy samples were taken from any part of colon: approximately 5 cm off from macroscopically healthy-inflamed margin to healthy side and to inflamed side. Tissue specimens were immediately snap-frozen in liquid nitrogen, to prevent mRNA degradation, and subsequently stored at -80°C.

Macro- and microscopic findings in colonoscopy
Control patients and inactive UC group had no macroscopic or microscopic inflammation. Five CD patients had slight macro- and/or microscopic inflammation in some part of colon, one macroscopically but not microscopically in ileum, and five macroscopically of whom three microscopically in sigmoid colon. All patients in active UC group had macro- and/or microscopic inflammation in some part of colon, two mild and five moderate to severe; none had inflammation in ileum, and in sigmoid colon one had mild and three moderate to severe macroscopic inflammation and microscopically two had mild and four had moderate to severe inflammation.

Quantitative real-time PCR analysis
Real-time analysis was performed according to MIQE guidelines [10]. In short, total RNA was extracted from intestinal mucosal biopsies using Trizol Total RNA Isolation Reagent (Life Technologies BRL, Breda, The Netherlands) according to manufacturers protocol. Obtained RNA was subjected to DNAse treatment (RQ1 RNase-free DNase, Promega, Madison, WI, USA) according to manufacturers protocol to prevent genomic DNA contamination. Quantity and quality of RNA was assessed by spectrophotometry on a Nanodrop 2000c spectrophotometer (Thermo Fisher Scientific, USA). Thereafter, 1.5 μg of RNA was reverse transcribed by Moloney-murine leukemia virus-reverse transcriptase (Life Technologies BRL),

an rt- sample (not containing reverse transcriptase) as well as a no-template control (not containing RNA) were included. The obtained cDNA was analyzed to determine mRNA levels of CLDN2, -3, -4, -7, -8, -12, -15, -18. The final volume of each reaction was 12,5 ul, consisting of 2,5 ul (5ng/ul) cDNA and 10 ul SybrGreen PCR master mix (Applied Biosystems, Foster City, CA, USA). Primers were designed with Primer 3 software (Whitehead Institute for Biomedical Research), and have a 95-105% amplification efficiency. Where possible, exon-spanning primers were used for amplification (Table 1). Glyceraldehyde 3-phosphate dehydrogenase (GAPDH) mRNA levels served as endogenous control for expression levels. Quantitative real-time PCR analysis was performed on an iQ5 iCycler Detection System (Bio-rad, Hercules, CA, USA). For figure 1, total GI expression was determined in the following way: For each segment the average relative expression was determined based on the delta Ct method using GAPDH as a reference gene. The total expression level of all segments was set to 100%, and the expression level of each segment is expressed as a percentage of this 100%. For figure 2 and 3, data is plotted in arbitrary units (AU), representing mRNA expression levels after correction with GAPDH and normalization to the control group.

Table 1 Primer sequences for SybrGreen real-time PCR

Gene	Accession	Forward primer (5'-3')	Reverse primer (5'-3')	Product size (bp)
GAPDH	NM_002046.3	GTCGGAGTCAACGGATTTGG	GGCAACAATATCCACTTTACCA-GAGT	78
CLDN2	NM_020384.3	CTCCTGGGATTCATTCCTGTTG	TCAGGCACCAGTGGTGAGTAGA	74
CLDN3	NM_001306.3	CCACGCGAGAAGAAGTACAC	GTAGTCCTTGCGGTCGTAGC	102
CLDN4	NM_001305.3	GGCTGCTTTGCTGCAACTG	AGAGCGGGCAGCAGAATACTT	71
CLDN7	NM_001307.5	ATCCCTACCAACATTAAGTAT-GAGTTTG	TGCACCTCCCAGGATGACTAG	84
CLDN8	NM_199328.2	TGCTGACGGCTGGAATCAT	ATTGGCAACCCAGCTCACA	71
CLDN12	NM_012129.4	CCTTTCCTTCCTGTGTGGAATC	AATTTTCTCCAGTTGGGAAGCA	75
CLDN15	NM_014343.2	TCCACATTCTGGCCGGTATC	GAAGTCCCGGGTGATGTTGA	71
CLDN18	NM_016369.3	TCATGTTCATTGTCTCAG-GTCTTTG	ACATCCAGAAGTTAGTCACCAG-CAT	81

Statistical analysis

Data is expressed as either mean ± SEM, or as box-plots. Data were statistically analyzed using SPSS statistics software (version 19) for Macintosh computers. A Levene test for Equality of Variance was used to assess equality of variance. Groups were compared using one-way ANOVA, followed by a Dunnett or a Dunnett T3 correction Post-test depending on the outcome of the Levene test.

Ethical considerations

Colonoscopies were performed during routine patient care when needed by clinical judgement. The additional biopsy samples taken for the study did not increase the complication risk of patients significantly. This study was approved by the ethical committee of Tampere University Hospital, Finland. Written informed consent was obtained from each subject.

Results

Profiling of claudin mRNA expression throughout the gastrointestinal tract

Real-time PCR analysis was performed to examine the expression patterns of claudins along the proximal-distal axis of the human intestine. Individual claudin show specific localization patterns in the GI tract, which vary strongly between the different isoforms (Figure 1). CLDN2 is mainly expressed in the proximal intestine and in the antrum, with less than 10% of total expression found beyond the ileum. Expression patterns of CLDN3 and -4 are almost identical, with approximately 90% of total mRNA expression located throughout the colon and rectum. CLDN7 expression resembles that of CLDN3 and -4, with predominant expression in the colon, sigmoid and rectum, and little expression in the esophagus, gastric region and proximal parts of the GI tract. CLDN8 shows a gradually increasing expression along the colon towards the rectum. CLDN12 is evenly expressed in the entire GI tract with exception of the esophagus. CLDN15 expression is confined predominantly to the duodenum and ileum where over 75% of its expression was found. CLDN18 was detected solely in the stomach.

Claudin expression in IBD

To evaluate whether claudin abundance is changed by either active or inactive IBD, mRNA expression levels of claudin isoforms were determined in several intestinal segments in various IBD patient groups and controls. We analyzed the expression of CLDN2, CLDN12, CLDN3 and CLDN4 in the ileum and sigmoid colon of control subjects compared to patients with CD, active UC, and inactive UC (Figure 2). In the ileum, CLDN2 expression was unchanged in IBD patient groups compared

5
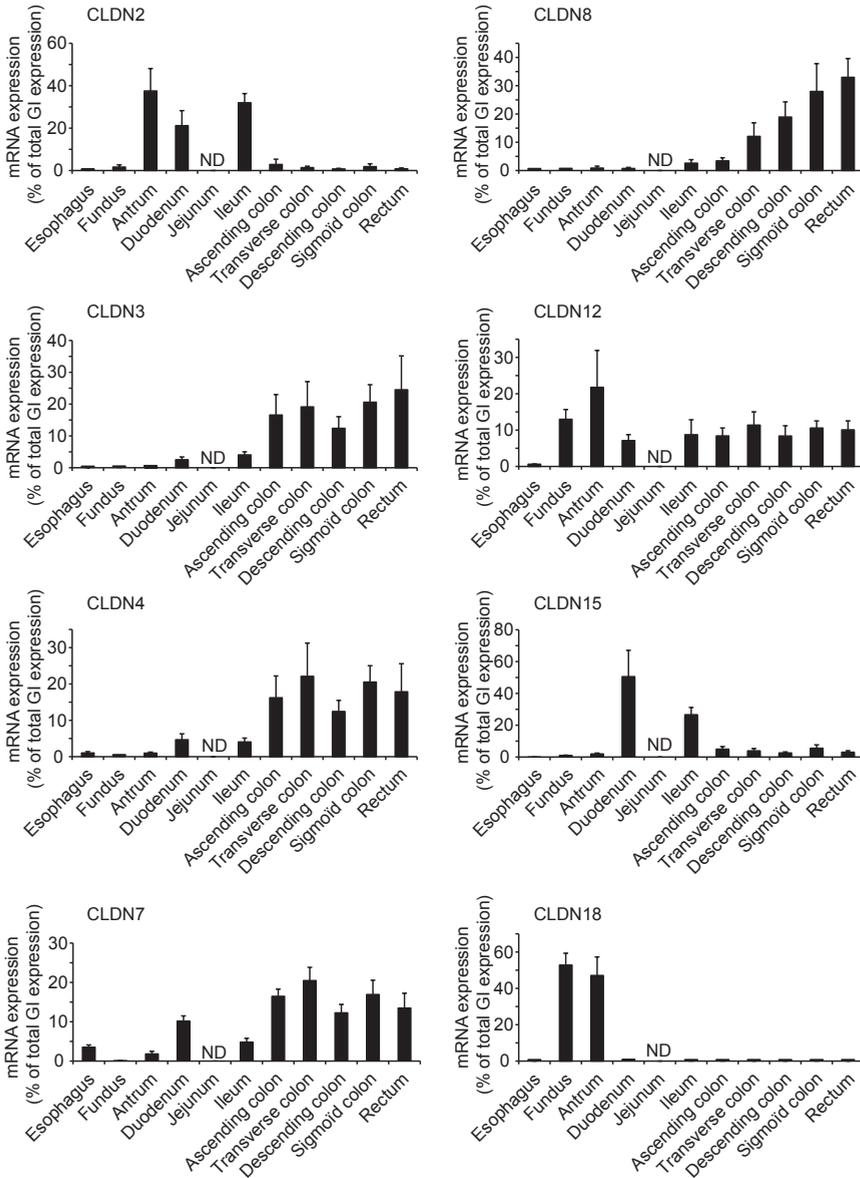
Figure 1 mRNA expression patterns of claudins along the human gastrointestinal tract. Claudins show specific localization patterns throughout the gastrointestinal tracts, varying strongly between the different isoforms. Results, corrected for GAPDH mRNA expression levels, are expressed as a percentage of total GI expression (mean ± SEM), ND; not determined.
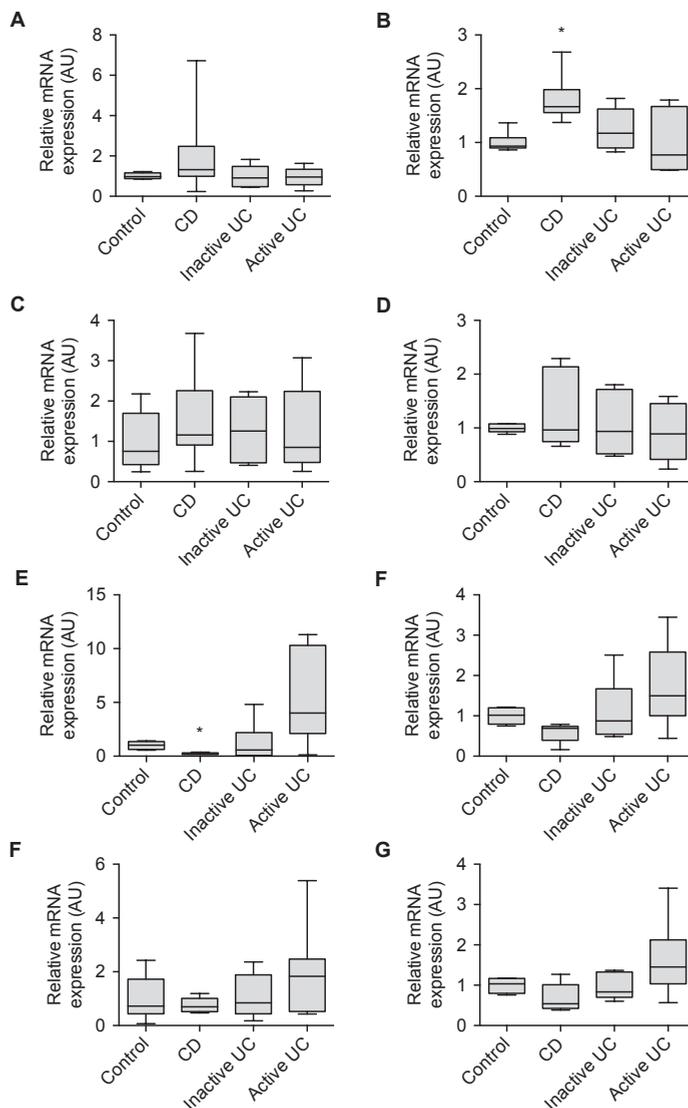
Figure 2 Expression of CLDN2, CLDN12, CLDN3 and CLDN4 in the ileum and sigmoid colon. mRNA expression of CLDN2, -12, -3 and -4 in the ileum (**A-D**) and sigmoid colon (**E-H**) of controls and IBD groups. Data is plotted in arbitrary units (AU), representing mRNA expression levels after correction with GAPDH and normalization with the control group. Results are expressed as Wiskers plots box showing the 5-95 percentile, lower quartile, median and upper quartile, significance was accepted at P<0.05.

to control subjects (Table 2) although some outliers, in whom expression was increased, were observed in the group of CD patients. CLDN12 mRNA expression was significantly upregulated in the ileum of CD patients (1.0 ±0.2 vs 1.8 ±0.4 AU, p<0.02), no changes were found between controls and UC patients. CDLN3 expression in the ileum was highly variable between individuals, both in the control group and in the IBD groups, consequently no differences in expression were observed between the groups. No significant changes were found in CLDN4 expression in the ileum. Interestingly, variance in the IBD groups compared to controls is significantly increased in all groups for both CLDN12 and CLDN4.

In the sigmoid colon (Figure 2), CLDN2 expression was significantly reduced by 5-fold in CD patients compared to controls (1.0 ±0.4 vs 0.2 ±0.1 AU, p=0.01). In addition, there is a trend towards increased expression in patients suffering from active UC. CLDN12 expression in the sigmoid colon was slightly decreased in CD patients (1.0 ± 0.2 vs 0.6 ± 0.2 AU, p=0.05). In the UC patient groups, no significant changes were found. Similar to the ileum, sigmoid colon expression of CLDN3 is highly variable, with no significant differences between the control subjects and subjects from any of the IBD groups. CLDN4 expression remains unchanged in IBD groups versus controls. In the sigmoid, significant differences between controls and IBD groups were found for CLD2, -4 and -12. Most notable is the increased variance in CLDN2 expression in active UC patients and in CLDN12 in all UC patients.

In the colon (Figure 3), expression of claudins was determined in biopsies taken from unaffected tissue and from inflammatory active areas as judged macroscopically. CLDN2 expression remains unchanged in CD, in UC patients there is a tendency towards increased expression (1.0 ± 0.4 vs 4.7 ±4.7 AU, p=0.24). CLDN12 is significantly downregulated (1.0 ±0.3 vs 0.4 ±0.2 AU, p=0.02) in CD patients compared to the nearby macroscopically more quiescent areas, in UC patients expression is unchanged. CLDN3 expression in the colon is highly variable, similar to expression in the ileum and sigmoid colon. However, a trend towards a downregulation in CD patients (1.0 ±0.7 vs 0.3 ±0.3 AU, p=0.08) was observed. For CLDN4 a significant downregulation (1.0 ±0.5 vs 0.2 ±0.2 AU, p=0.02) by macroscopic inflammation compared to healthy-appearing area is present in patients with CD.

Table 2 Overview of statistical parameters

			N	Mean	St.Dev.	Min.	Max.	Significance compared to Control
ILEUM	CLDN2	Control	6	1.0	0.2	0.8	1.2	/
		CD	7	2.2	2.2	0.2	6.7	0.24
		Inactive UC	5	1.0	0.6	0.5	1.8	1.00
		Active UC	5	1.0	0.5	0.3	1.6	1.00
	CLDN12 *	Control	6	1.0	0.2	0.9	1.4	/
		CD	7	1.8	0.4	1.4	2.7	0.01
		Inactive UC	5	1.2	0.4	0.8	1.8	0.75
		Active UC	5	1.0	0.6	0.5	1.8	1.00
	CLDN3	Control	6	1.0	0.7	0.3	2.2	/
		CD	7	1.5	1.1	0.3	3.7	0.69
		Inactive UC	5	1.3	0.8	0.4	2.2	0.94
		Active UC	5	1.3	1.1	0.3	3.1	0.95
	CLDN4 *	Control	6	1.0	0.1	0.9	1.1	/
		CD	7	1.3	0.7	0.7	2.3	0.80
		Inactive UC	5	1.1	0.6	0.5	1.8	1.00
		Active UC	5	0.9	0.6	0.2	1.6	1.00
SIGMOÏD COLON	CLDN2 *	Control	6	1.0	0.4	0.6	1.4	/
		CD	5	0.2	0.1	0.1	0.4	0.01
		Inactive UC	6	1.4	1.8	0.1	4.8	0.98
		Active UC	7	5.4	4.3	0.1	11.3	0.23
	CLDN12 *	Control	6	1.0	0.2	0.8	1.2	/
		CD	6	0.6	0.2	0.2	0.8	0.05
		Inactive UC	7	1.1	0.7	0.5	2.5	1.00
		Active UC	7	1.8	1.1	0.4	3.5	0.42
	CLDN3	Control	6	1.0	0.8	0.1	2.4	/
		CD	5	0.8	0.3	0.5	1.2	0.96
		Inactive UC	7	1.2	0.8	0.2	2.4	0.98
		Active UC	7	2.0	1.7	0.4	5.4	0.28
	CLDN4 *	Control	4	1.0	0.2	0.8	1.2	/
		CD	5	0.7	0.4	0.4	1.3	0.51
		Inactive UC	7	1.0	0.3	0.6	1.4	1.00
		Active UC	7	1.7	0.9	0.6	3.4	0.40

5

Table 2 Continued

			N	Mean	St.Dev.	Min.	Max.	Significance compared to Control
COLON	CLDN2 *	Unaffected IBD	8	1.0	0.4	0.4	1.4	/
		Inflamed CD	4	1.0	1.5	0.2	3.3	1.00
		Inflamed UC	6	4.7	4.4	0.6	12.5	0.24
	CLDN12	Unaffected IBD	9	1.0	0.3	0.6	1.4	/
		Inflamed CD	5	0.4	0.2	0.3	0.9	0.02
		Inflamed UC	5	1.2	0.5	0.7	1.8	0.59
	CLDN3	Unaffected IBD	8	1.0	0.7	0.0	2.2	/
		Inflamed CD	5	0.3	0.3	0.0	0.8	0.08
		Inflamed UC	5	0.7	0.5	0.2	1.5	0.51
	CLDN4	Unaffected IBD	8	1.0	0.5	0.1	1.8	/
		Inflamed CD	5	0.2	0.2	0.1	0.5	0.02
		Inflamed UC	5	0.6	0.4	0.3	1.4	0.49

* $p < 0.05$ Levene Test for equality of Variance

Discussion

In this study, we set out to analyze the expression patterns of claudins throughout the human gastrointestinal tract. The expression gradients observed in our study, can function as a standard for future research, showing which claudin isoforms are predominantly expressed in a certain region. In addition, we analyzed expression levels of claudins in patients with CD, active- and inactive UC to identify changes in expression that coincide with the changes in epithelial integrity and electrolyte absorption known to occur in IBD.

Based on function, claudins can be divided into three groups: barrier builders, pore formers, and claudins of ambiguous function [2]. Barrier builders decrease paracellular permeability and are also referred to as tightening claudins. CLDN1, -3, -4, -5, -8, -11, -14, and 19 are all considered to be part of this barrier building group. Pore formers enhance paracellular permeability in a size and charge
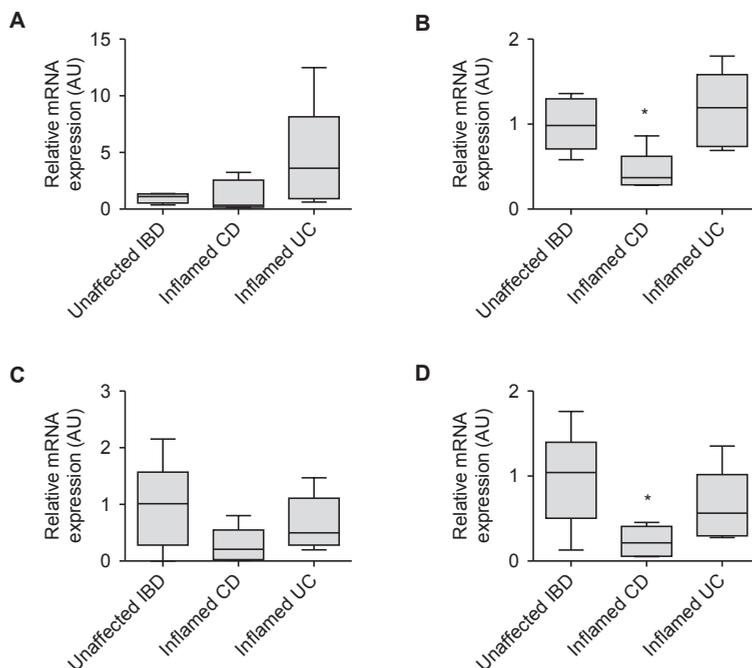
Figure 3 Expression of claudins in the colon in macroscopically active areas and nearby unaffected tissue of IBD patients. **A.** mRNA expression of CLDN2, **B.** CLDN12, **C.** CLDN3 and **D.** CLDN4 in the colon of IBD patients. Samples were obtained from macroscopically healthy (unaffected IBD) or inflamed tissue. Data is plotted in arbitrary units (AU), representing mRNA expression levels after correction with GAPDH and normalization with the group of macroscopically unaffected samples. Results are expressed as Wiskers plots box showing the 5-95 percentile, lower quartile, median and upper quartile, significance was accepted at P<0.05.

selective way and include CLDN2 and -10. Function of the remaining claudins such as claudin-7, -12, -15, and -16 is under debate or remains unclear [2]. The observed differential expression patterns of claudin isoforms in the human GI tract are likely to contribute to local diversity of transepithelial resistance and paracellular ion flow. We find an increased expression of the tightening claudin isoforms from proximal to distal sections of the GI tract. This is in line with previous studies by Markov *et al, which* showed that the transepithelial resistance in the rat intestine slightly decreases from duodenum towards the ileum, after which it strongly increases in colon [11]. According to our analysis, CLDN3 and CLDN4, both part of the barrier building group, are predominantly expressed in

the distal parts of the GI tract, but also show some expression in the duodenum. This is comparable to earlier findings by Holmes and Markov who found similar expression patterns in mice and rats, respectively [4, 11]. CLDN8, another barrier builder, gradually increases from proximal to distal GI sections, which is in line with the increasing epithelial resistance along this trajectory and previous finding indicating CLDN8 prevents backleak of absorbed Na^+ [12]. In addition, these results strongly resemble the expression pattern in mice, but not those of Markov *et al.* who found a high level of expression in the duodenum [4, 11]. The expression of CLDN7 is similar to the expression pattern of CLDN3 and CLDN4. Not much is known about its function in the intestine, however, in kidney it has been suggested to function as a paracellular Cl^- channel in the distal part of the nephron [13]. Remarkably, in kidney CLDN7 expression also overlaps with that of CLDN3, CLDN4 and CLDN8, similar to our findings in the intestine [13]. CLDN2, part of the previously discussed group of paracellular pore-formers, is predominantly expressed in the antrum, duodenum and ileum after which expression drops dramatically, which is in line with its pore-forming characteristics. Here our results are in line with Markov *et al.* whereas Holmes finds a constant level of expression throughout the entire intestinal tract [4, 11]. CLDN12 is ubiquitously expressed throughout the GI tract. Previous studies have shown that CLDN2 and CLDN12 are involved in vitamin D-mediated intestinal Ca^{2+} absorption *in vitro* as well as *in vivo* experiments [14, 15]. Ca^{2+} absorption is generally assumed to take place in the small intestine, an idea that matches perfectly with the expression pattern of CLDN2. Correlating these functional observations with the expression pattern of CLDN12 found in this study is more difficult. Some studies have suggested CLDN12 is part of the group of tightening claudins, responsible for decreasing epithelial permeability, deduced from it expression in blood vessels, the urine bladder and the brain [16, 17]. Potentially its function is variable, depending on interactions with other claudins as previously described for CLDN16 and CLDN19 [18, 19]. CLDN15 is essential for normal-sized morphogenesis of the small intestine, with knockout mice developing a mega-intestinal phenotype [20]. Additionally, it seems indispensable for small intestinal Na^+ and glucose absorption [21]. Based on our data, CLDN15 is mainly expressed in the duodenum and ileum, which matches with the previously described morphological, functional and pathological effects. CLDN18 expression is restricted to the stomach, and has been shown to prevent paracellular H^+ leakage [22]. In line with this function and the expression pattern we observed that CLDN18 is upregulated in Barrett's oesophagus epithelium during reflux disease, contributing to greater acid resistance [23, 24]. Our findings provide a detailed map displaying the predominant location of expression of various claudin isoforms in humans. As described above, expression patterns are in line with known isoform functions.

The expression profiles can thus be used to pinpoint the proper location for studying function/expression of claudin isoforms. In addition, human expression patterns of claudin seem to be quite similar to those in rodents, indicating that extrapolation of these results from animal models to a human setting is valid.

Since perturbed expression of tight junction proteins, including claudins, is a typical feature in IBD, the second aim of this study was to analyze mRNA expression levels of claudins in the intestinal tissues of patients with CD [8]. Our predominant finding in the ileum was a significant increase in CLDN12 abundance in CD patients compared to controls. In addition, variance is significantly increased in IBD groups compared to controls for CLDN12, and -4. Especially for CLDN4 the increased variance in IBD groups compared to the control group is pronounced. The larger heterogeneity in CLDN4 mRNA expression could result from local inflammatory processes, which were not macroscopically visible during the collection of the biopsies. CLDN4, but also CLDN5 and -8, have previously been shown to be redistributed from the tight junction to the subjunctional lateral membrane in CD, possibly adding to the observed variability in expression levels [25, 26]. No changes were found in CLDN3 expression. Notably, variance of CLDN3 expression is relatively high in all groups, including controls, compared to that of other genes.

In the sigmoid colon of the CD patients, CLDN2 is significantly downregulated compared to controls and a similar trend is present for CLDN12 expression. In sigmoid samples of active UC patients, a trend towards upregulation of CLDN12 abundance is observed and a clear increase in variance is found. As in the ileum, variance of CLDN3 is high, with no significant differences between controls and IBD patient groups. The increased variance in CLDN4 expression in sigmoid colon is less distinct in the ileum, no significant changes in mRNA expression between controls and IBD groups were found.

In the colon biopsies were taken from macroscopically healthy areas or inflamed tissue. No changes in expression of CLDN2 were found between healthy and inflamed areas in CD patients. A tendency towards CLDN2 upregulation was found in inflamed areas in UC patients, which is in line with findings from previous studies [27, 28]. CLDN12 is significantly downregulated in CD patients compared to controls, with no changes in UC patients. In the colon of CD patients CLDN4 is also significantly downregulated in inflamed tissue areas compared to macroscopically healthy areas, a similar trend is present for CLDN3 (p=0.084). Expression of CLDN3 and CLDN4 in areas of activity in UC is unchanged compared areas with no macroscopic inflammatory activity. These sample sets clearly show that major differences in expression are present in the same intestinal location, in this case colon, between macroscopically healthy and inflamed tissue. This could potentially explain the large variability we find in the samples from IBD patients compared to healthy controls.

5

Several studies have shown changes in CLDN expression in the intestinal epithelium of both CD and UC patients. CLDN2 expression has been shown to correlate positively with inflammatory activity [29]. In accordance with Zeissig *et al.* we observed that the CLDN2 expression in the sigmoid colon of UC patients is higher than expression in patients with CD, however, we find a decreased expression in CD patients compared to healthy controls which has not been described before [26]. Various other studies also show an increase in CLDN2 expression in cases of CD and UC. These studies have, however, sampled from macroscopically inflamed sigmoid colon or rectum [30]. This could explain the inconsistencies between their findings and the findings in our study, as we sampled locally from macroscopically healthy appearing tissue.

Adding to previous studies we also sampled the ileum of CD patients. In contrast to the decreased CLDN2 and CLDN12 in the sigmoid we observed an increased expression in the ileum not present in the UC patients or controls. None of the CD patients had inflammatory activity in the ileum which suggests our finding is related to the basic pathophysiology of CD or to be a reactive change in the non-inflamed areas in response to disease activity elsewhere. The increased expression of the pore-forming CLDN2 in the ileum coinciding with decreased expression elsewhere is not readily explained and requires further investigation. In the sigmoid colon, our study shows a reduced expression of CLDN3 and unchanged expression of CLDN4 in the sigmoid of active CD patients, but no changes in the inactive CD, which is in line with previous findings by Zeissig *et al.* [26]. In addition, we found a reduced expression of CDLN3 as well as CLDN4 in macroscopically inflamed colon tissue of patients with active CD compared to macroscopically healthy tissue. Reports on CLDN3 and CLDN4 expression in IBD are conflicting, with some groups showing reduced expression of CLDN3 with no changes in CLDN4 expression [26], others showing stable CLDN3 expression with reduced CLDN4 expression [28, 31], no significant changes at all [25, 30], or changes in cellular localization of proteins [25]. These differences may be the consequence of variations in sampling protocol, sample handling, and post-analysis corrections. In addition, it is not clear at which level the expression of claudins is regulated, inconsistencies may, therefore, also arise as some studies have analyzed mRNA expression whereas others have studied total protein levels [31] or protein localization [25, 27].

The discrepancy between findings in CD and UC patients can potentially be explained by the differences in etiology of these conditions. CD may involve any part of the gut including the ileum and the colon, but involvement of the rectum is seldom, UC on the other hand does not involve the ileum. This could explain that for UC patients, no significant changes in expression of any of the tested claudin isoforms were found in the ileum, as there are no inflammatory processes

present in this location. In addition, inflammation in CD is typically patchy and penetrates deep into the tissue, whereas UC is characterized by a more continuous area of inflammation, which is more superficially located in the mucosal layers [32]. The more superficial character of the inflammation in UC is likely to increase variation in expression analysis since the amount of inflamed tissue that is biopsied might vary. The increased variance in CLDN4 in the IBD groups compared to controls in the ileum is interesting as it indicates that, even in UC in which the ileum is supposedly unaffected, changes in expression in healthy area's can be observed. This could potentially be the result of compensatory mechanisms, aimed to counteract changes further along the GI tract.

The heterogeneous findings between the patient groups may be the result of local inflammatory processes releasing cytokines that exert a local effect. CD is a T-helper 1 inflammation producing interferon gamma and tumor necrosis factor alfa, whereas UC is a T-helper 2 inflammation producing interleucin-13 and interleucin-4 [33, 34]. In the sigmoid, we find a decrease CLDN2 expression in CD patients and an increased expression in active UC patients. This is in line with previous findings from Prasad *et al.* which showed in a series of *in vitro* experiments that interferon gamma decreases CLDN2, whereas interleucin -13 increases CLDN2 [25]. In addition, they show a significant upregulation of CLDN2 mRNA in the colon of UC patients, in the colon of CD patients, however, results were highly variable and not significant [25]. Our study shows a tendency towards downregulation of CLDN3 and -4 in the sigmoid and colon of CD patients, which was absent in UC patients. Again, this is in line with the study by Prasad *et al.*, which found no changes in CLDN3 and CLDN4 expression in reaction to interleucin-13, whereas exposure to tumor necrosis factor alpha and interferon gamma resulted in altered protein distribution patterns of CLDN3 and more particularly CLDN4.

In conclusion, this study provides a detailed map with mRNA expression patterns of claudins in the human gastrointestinal tract. Additionally, this study analyzed mRNA expression of CLDN2, -12, -3, and -4 in several intestinal segments in IBD patients compared to healthy controls, indicating that changes in mRNA expression of claudins are indeed correlated to IBD.

Acknowledgements:

References

1. Mitic LL, Van Itallie CM, Anderson JM: Molecular physiology and pathophysiology of tight junctions I. Tight junction structure and function: lessons from mutant animals and proteins. *Am J Physiol Gastrointest Liver Physiol* 279: G250-254, 2000

2. Amasheh S, Fromm M, Gunzel D: Claudins of intestine and nephron - a correlation of molecular tight junction structure and barrier function. *Acta Physiol (Oxf)* 201: 133-140, 2011

3. Will C, Fromm M, Muller D: Claudin tight junction proteins: novel aspects in paracellular transport. *Perit Dial Int* 28: 577-584, 2008

4. Holmes J, Van Itallie C, Rasmussen J, Anderson J: Claudin profiling in the mouse during postnatal intestinal development and along the gastrointestinal tract reveals complex expression patterns. *Gene Expr Patterns.* pp 581-588, 2006

5. Angelow S, Yu AS: Claudins and paracellular transport: an update. *Curr Opin Nephrol Hypertens* 16: 459-464, 2007

6. Fujita H, Chiba H, Yokozaki H, Sakai N, Sugimoto K, Wada T, Kojima T, Yamashita T, Sawada N: Differential expression and subcellular localization of claudin-7, -8, -12, -13, and -15 along the mouse intestine. *J Histochem Cytochem* 54: 933-944, 2006

7. Rahner C, Mitic LL, Anderson JM: Heterogeneity in expression and subcellular localization of claudins 2, 3, 4, and 5 in the rat liver, pancreas, and gut. *Gastroenterology.* 2001 pp 411-422.

8. Mankertz J, Schulzke JD: Altered permeability in inflammatory bowel disease: pathophysiology and clinical implications. *Curr Opin Gastroenterol* 23: 379-383, 2007

9. Seidler U, Lenzen H, Cinar A, Tessema T, Bleich A, Riederer B: Molecular mechanisms of disturbed electrolyte transport in intestinal inflammation. *Ann N Y Acad Sci* 1072: 262-275, 2006

10. Bustin SA, Benes V, Garson JA, Hellemans J, Huggett J, Kubista M, Mueller R, Nolan T, Pfaffl MW, Shipley GL, Vandesompele J, Wittwer CT: The MIQE guidelines: minimum information for publication of quantitative real-time PCR experiments. *Clin Chem* 55: 611-622, 2009

11. Markov AG, Veshnyakova A, Fromm M, Amasheh M, Amasheh S: Segmental expression of claudin proteins correlates with tight junction barrier properties in rat intestine. *J Comp Physiol B* 180: 591-598, 2010

12. Amasheh S, Milatz S, Krug SM, Bergs M, Amasheh M, Schulzke JD, Fromm M: Na+ absorption defends from paracellular back-leakage by claudin-8 upregulation. *Biochem Biophys Res Commun* 378: 45-50, 2009

13. Tatum R, Zhang Y, Salleng K, Lu Z, Lin JJ, Lu Q, Jeansonne BG, Ding L, Chen YH: Renal salt wasting and chronic dehydration in claudin-7-deficient mice. *Am J Physiol Renal Physiol* 298: F24-34, 2010

14. Christakos S, Dhawan P, Ajibade D, Benn BS, Feng J, Joshi SS: Mechanisms involved in vitamin D mediated intestinal calcium absorption and in non-classical actions of vitamin D. *J Steroid Biochem Mol Biol* 121: 183-187, 2010

15. Fujita H, Sugimoto K, Inatomi S, Maeda T, Osanai M, Uchiyama Y, Yamamoto Y, Wada T, Kojima T, Yokozaki H, Yamashita T, Kato S, Sawada N, Chiba H: Tight junction proteins claudin-2 and -12 are critical for vitamin D-dependent Ca^{2+} absorption between enterocytes. *Mol Biol Cell* 19: 1912-1921, 2008

16. Nitta T, Hata M, Gotoh S, Seo Y, Sasaki H, Hashimoto N, Furuse M, Tsukita S: Size-selective loosening of the blood-brain barrier in claudin-5-deficient mice. *J Cell Biol* 161: 653-660, 2003

17. Acharya P, Beckel J, Ruiz WG, Wang E, Rojas R, Birder L, Apodaca G: Distribution of the tight junction proteins ZO-1, occludin, and claudin-4, -8, and -12 in bladder epithelium. *Am J Physiol Renal Physiol* 287: F305-318, 2004

18. Hou J, Renigunta A, Gomes AS, Hou M, Paul DL, Waldegger S, Goodenough DA: Claudin-16 and claudin-19 interaction is required for their assembly into tight junctions and for renal reabsorption of magnesium. *Proc Natl Acad Sci U S A* 106: 15350-15355, 2009

19. Hou J, Renigunta A, Konrad M, Gomes AS, Schneeberger EE, Paul DL, Waldegger S, Goodenough DA: Claudin-16 and claudin-19 interact and form a cation-selective tight junction complex. *J Clin Invest* 118: 619-628, 2008

20. Tamura A, Kitano Y, Hata M, Katsuno T, Moriwaki K, Sasaki H, Hayashi H, Suzuki Y, Noda T, Furuse M, Tsukita S: Megaintestine in claudin-15-deficient mice. *Gastroenterology* 134: 523-534, 2008

21. Tamura A, Hayashi H, Imasato M, Yamazaki Y, Hagiwara A, Wada M, Noda T, Watanabe M, Suzuki Y, Tsukita S: Loss of claudin-15, but not claudin-2, causes Na$^+$ deficiency and glucose malabsorption in mouse small intestine. *Gastroenterology* 140: 913-923, 2011

22. Hayashi D, Tamura A, Tanaka H, Yamazaki Y, Watanabe S, Suzuki K, Sentani K, Yasui W, Rakugi H, Isaka Y, Tsukita S: Deficiency of claudin-18 causes paracellular H$^+$ leakage, up-regulation of interleukin-1beta, and atrophic gastritis in mice. *Gastroenterology*, 2012

23. Matsuda M, Sentani K, Noguchi T, Hinoi T, Okajima M, Matsusaki K, Sakamoto N, Anami K, Naito Y, Oue N, Yasui W: Immunohistochemical analysis of colorectal cancer with gastric phenotype: claudin-18 is associated with poor prognosis. *Pathol Int* 60: 673-680, 2010

24. Jovov B, Van Itallie CM, Shaheen NJ, Carson JL, Gambling TM, Anderson JM, Orlando RC: Claudin-18: a dominant tight junction protein in Barrett's esophagus and likely contributor to its acid resistance. *Am J Physiol Gastrointest Liver Physiol* 293: G1106-1113, 2007

25. Prasad S, Mingrino R, Kaukinen K, Hayes KL, Powell RM, MacDonald TT, Collins JE: Inflammatory processes have differential effects on claudins 2, 3 and 4 in colonic epithelial cells. *Lab Invest.* pp 1139-1162, 2005

26. Zeissig S, Bürgel N, Günzel D, Richter J, Mankertz J, Wahnschaffe U, Kroesen A, Zeitz M, Fromm M, Schulzke JD: Changes in expression and distribution of claudin 2, 5 and 8 lead to discontinuous tight junctions and barrier dysfunction in active Crohn's disease. *Gut.* pp 61-72, 2007

27. Das P, Goswami P, Das TK, Nag T, Sreenivas V, Ahuja V, Panda SK, Gupta SD, Makharia GK: Comparative tight junction protein expressions in colonic Crohn's disease, ulcerative colitis, and tuberculosis: a new perspective. *Virchows Arch* 460: 261-270, 2012

28. Oshima T, Miwa H, Joh T: Changes in the expression of claudins in active ulcerative colitis. *Journal of Gastroenterology and Hepatology.* pp S146-S150, 2008

29. Weber CR, Nalle SC, Tretiakova M, Rubin DT, Turner JR: Claudin-1 and claudin-2 expression is elevated in inflammatory bowel disease and may contribute to early neoplastic transformation. *Lab Invest* 88: 1110-1120, 2008

30. Amasheh S, Dullat S, Fromm M, Schulzke JD, Buhr HJ, Kroesen AJ: Inflamed pouch mucosa possesses altered tight junctions indicating recurrence of inflammatory bowel disease. *Int J Colorectal Dis* 24: 1149-1156, 2009

31. Burgel N, Bojarski C, Mankertz J, Zeitz M, Fromm M, Schulzke JD: Mechanisms of diarrhea in collagenous colitis. *Gastroenterology* 123: 433-443, 2002

32. Geboes: Histopathology of Crohn's disease and ulcerative colitis. In: *Inflammatory bowel disease* 4th ed ed. edited by SATSANGI J, S. L., Churchill Livingstone Elsevier , pp pp. 255–276, 2003

33. Fuss IJ, Heller F, Boirivant M, Leon F, Yoshida M, Fichtner-Feigl S, Yang Z, Exley M, Kitani A, Blumberg RS, Mannon P, Strober W: Nonclassical CD1d-restricted NK T cells that produce IL-13 characterize an atypical Th2 response in ulcerative colitis. *J Clin Invest* 113: 1490-1497, 2004

34. Wisner DM, Harris LR, Green CL, Poritz LS: Opposing regulation of the tight junction protein claudin-2 by interferon-gamma and interleukin-4. *J Surg Res* 144: 1-7, 2008

5

6

Involvement of claudin 3 and claudin 4 in idiopathic infantile hypercalcemia; a novel hypothesis?

Anke L. Lameris[1], Silvie Huybers[1], John R. Burke[2], Leo A. Monnens[3], René J.M. Bindels[1], Joost G.J. Hoenderop[1]

Department of [1] Physiology and [3] Pediatrics,
Radboud University Nijmegen Medical Centre, The Netherlands.
[2] Queensland Child and Adolescent Renal Service, Royal Children's Hospital and Mater Children's Hospitals, Brisbane, Queensland, Australia.

Abstract

Idiopathic infantile hypercalcemia (IIH) is a rare disease that generally resolves spontaneously between the age of 1- 3 years. Similar symptoms may occur in patients suffering from Williams-Beuren syndrome (WBS), which is caused by a microdeletion on chromosome 7. Two of the genes, named CLDN3 and CLDN4, located within this region are members of the claudin family that has been shown to be involved in paracellular calcium (Ca^{2+}) absorption. Based on the hemizygous loss of CLDN3 and CLDN4 in WBS and the function of these genes in paracellular Ca^{2+} transport we hypothesized that mutations in CLDN3 or CLDN4 could also be involved in IIH.

Biochemical characteristics, including calciotropic hormone levels, were obtained from three typical IIH patients. CLDN3 and CLDN4 sequences were also analyzed in these patients. The major intestinal Ca^{2+} transporter TRPV6 was also screened for the presence of mutations, since hypercalcemia in IIH and WBS has been shown to result from intestinal hyperabsorption. All three patients were also analyzed for the presence of deletions or duplications using a single nucleotide polymorphism (SNP) array for genomic DNA.

The serum Ca^{2+} levels of patients were 2.9, 3.3 and 3.8 mmol/L (normal <2.7 mmol/L). Levels of 25-hydroxyvitamin D_3 and 1,25-dihydroxyvitamin D_3 were normal, parathyroid hormone (PTH) and PTH-related peptide (PTHrP) levels were appropriately low. Sequencing of coding regions and intron-exon boundaries did not reveal mutations in CLDN3, CLDN4 and TRPV6. Identified SNPs were not correlated with the disease phenotype. A SNP array did not reveal genomic deletions or duplications.

Biochemical analysis did not reveal inappropriate levels of calciotropic hormones in IIH patients in this study. Furthermore, based on the lack of mutations in CLDN3, CLDN4 and TRPV6, we conclude IIH is neither caused by mutations in these candidate genes nor by deletions or duplications in the genome of these patients.

Introduction

Idiopathic infantile hypercalcemia (IIH) is a rare disorder of thus far unknown etiology with a reported prevalence of 1 in 50000 life births (patients with Williams Beuren syndrome, WBS, included) [1]. Children suffering from IIH usually present during their first year of life with clinical features of hypercalcemia, such as irritability, constipation, vomiting, increased thirst and a failure to thrive. Hypercalcemia in IIH patients is the result of intestinal hyperabsorption, which was shown by Barr *et al.* using oral calcium (Ca^{2+}) loading tests, and is emphasized by a cellulose phosphate treatment which normalizes the serum Ca^{2+} levels [2, 3]. Hypercalcemia generally resolves between the ages of 1 to 3 years, however hypercalciuria may persist up to the age of 12 [4, 5]. If diagnosed and treated in an early stage, the prognosis of IIH patients can be improved and the extent of nephrocalcinosis limited [5, 6].

IIH was first described in the United Kingdom in the 1950s by Lightwood and Fanconi [7, 8]. Originally, a subdivision of "mild" and "severe" IIH was made in order to distinguish between patients suffering solely from hypercalcemia and patients that also display additional abnormalities such as distinctive facial features [9]. The "severe" form has subsequently been shown to be part of a larger group of symptoms common to patients suffering from WBS [10]. WBS is nowadays known to result from a hemizygous microdeletion at 7q11.23 which arises from a recombination between misaligned repeat sequences flanking the region [11, 12]. The WBS deletion region encompasses 24 genes [13]. Among the genes located in the deleted region are CLDN3 and CLDN4, which encode tight junction proteins claudin 3 and 4, respectively [14, 15]. Members of the claudin protein family have been shown to be involved in paracellular Ca^{2+} absorption [16]. Also, they have been described to play an important role in the regulation of ion transport in both the intestine and the kidney [16]. The deletion of claudin 3 and 4 increases the permeability of the intestinal epithelium [17-20]. Changes in expression of various claudins in murine intestine throughout time indicate that the absence of a particular claudin can, in time, be compensated for by the maturation of other claudins [21].

Similarities in the course of development of hypercalcemia in IIH and WBS patients could be explained by a shared underlying mechanism such as a gene defect. The hemizygous loss of CLDN3 and -4 in WBS, combined with their function in ion transport, makes them good candidate genes underlying the similarities in disease phenotype in patients suffering from IIH and WBS. In order to validate this hypothesis, three typical IIH patients were analyzed for the presence of mutations in CLDN3 and CLDN4. Since the IIH phenotype is the result of intestinal hyperabsorption, the major intestinal Ca^{2+} transporter TRPV6 was also analyzed

6

in order to exclude changes in uptake due to mutational changes in this transporter. Finally, the presence of deletions and duplications was analyzed in all three patients using a single nucleotide polymorphisms (SNP) array.

Materials and methods

Patient selection and phenotype assignment
Patients 1 and 2 were selected and treated in Australia. They have been described in two previous Australian studies as patient III2 and III3 and as patient 1 and 10 [4, 22]. Observation and treatment of patient 3 took place in the Netherlands and this patient has not been previously described.

Serum and urine biochemistry
Biochemical analysis of blood and urine was routinely performed using standard laboratory techniques at the Royal Children's Hospital and Mater Children's Hospitals in Brisbane Australia (patient 1 and 2) or the Radboud University Nijmegen Medical Centre in the Netherlands (patient 3). Parathyroid hormone (PTH) measurements in both hospitals were performed using an immunometric assay measuring only intact PTH.

DNA extraction
DNA sample collection and storage were carried out according to standard methods. In short, 10 ml of peripheral blood was collected into ethylene-diamine-tetraacetic-acid (EDTA) containing tubes and centrifuged for 10 min at 3000 g to separate buffy coats and plasma. Total genomic DNA was isolated from the buffy coat using a standard blood and body fluid protocol. Extracted DNA was quantified by spectrophotometrical absorbance measurements and stored in aliquots.

Genotyping
Oligonucleotide primers (Biolegio, Malden, The Netherlands) for the amplification of genomic DNA by polymerase chain reaction (PCR) were developed based on genomic sequences. Since CLDN3 and CLDN4 both consist of one large exon, primers were designed to amplify overlapping parts of the exon and included intron-exon boundaries. For TRPV6, a similar approach was used. Because of short intron sequences between exons 2 and 3, 7 and 8, as well as 9 and 10, PCR amplification of these exons was combined and PCR-products were sequenced as single fragments. Primer sequences used for the amplification of CLDN3, CLDN4 and TRPV6 are listed in Table 1. PCR products were purified using a GenElute™ PCR Clean-up Kit (Sigma, St Louis, MO, USA). DNA sequencing was carried out by

standard procedures at the sequence facility of the Radboud University Nijmegen Medical Centre. Subsequently, patient sequences were aligned and compared with human CLDN3 (NM_001306), CLDN4 (NM_001305), or TRPV6 (NM_018646) mRNA sequences, obtained from the NCBI nucleotide database.

Table 1 Human primer sequences for CLDN3, CLDN4 and TRPV6

Gene	Exon_part	Forward primer	Reverse primer
CLDN3	1_1	5'-ACTGTCCTTAGGCCCTGGAG -3'	5'-AGATGTTCTGCGACGTGATG-3'
CLDN3	1_2	5'-GGCACCATCGTGTGCTGCG-3'	5'-CTTGGTGGCCGTGTACTTC-3'
CLDN3	1_3	5'-GTCGGCCAACACCATTATCC-3'	5'-TGAGGTTTCACAGTCCATGC-3'
CLDN3	1_4	5'-CTACGACCGCAAGGACTACG-3'	5'-GCTCAGCTTACAACCCCATC-3'
CLDN4	1_1	5'-AGCATGGGCTTTGAGGAAG-3'	5'-GCGATGCCCATTACCTGTAG-3'
CLDN4	1_2	5'-TGCACTCTGCGAACGTTAAG-3'	5'-CACCGGCACTATCACCATAAG-3'
CLDN4	1_3	5'-AACTGCCTGGAGGATGAAAG-3'	5'-CTTGGGAAGTTGTCCGAGTG-3'
CLDN4	1_4	5'-TGTTCTTCCCTGGACTGAGC-3'	5'-CTCTAAACCCGTCCATCCAC-3'
CLDN4	1_5	5'-ATCACCTCTGGGACTGTGC-3'	5'-CACCTCCACAGTTGAAATC-3'
TRPV6	1	5'-GCAGGTCTGTGGCTGGCCTG-3'	5'-CCTGGGAGCACCATCTGTCC-3'
TRPV6	2-3	5'-GCCTCTCCCTCCACAACTAGG-3'	5'-ACTGACTTGAAATACCCAACC-3'
TRPV6	4	5'-GAGGGACCCCCTGCAGGATCC-3'	5'-GCTGCCCAACAGATACGGCTG-3'
TRPV6	5	5'-GGAAGATAAGGCTGTCACTTG-3'	5'-GAAGGTCCCAGCCCCTCTCC-3'
TRPV6	6	5'-GGAGAGGGGCTGGGACCTTC-3'	5'-CACCTCTGTTTCTCCCAGGGC-3'
TRPV6	7-8	5'-CCTATCCACACTCTGTGACCG-3'	5'-AGTCTCTGAGGACAGAGAGCC-3'
TRPV6	9-10	5'-CCCTGGGCACCATGGAAATGC-3'	5'-CAGGAATCCAAGGAGTGGAAC-3'
TRPV6	11	5'-GGAGGCTGAATCTGCATGTGTGG-3'	5'-CCTGCAATGTCTACTGTTCTGCCC-3'
TRPV6	12	5'-CTGGATGGGGCAATTGCTTGCTTGG-3'	5'-CTCCTCCCCAAGTTTAGCCAG-3'
TRPV6	13	5'-GGACATGCACGCAGAGCCCGG-3'	5'-GCAGGTTCCTTGGTAGGAAGG-3'
TRPV6	14	5'-CTCAAGCTCTATCAACTCTCTCCC-3'	5'-ACACAGGCCTCCACAGGGAACCC-3'
TRPV6	15	5'-CCAGGGGATAACAGACAAGCATCC-3'	5'-CTGGAGATGAGACCTCTGG-3'

CLDN3, claudin 3; CLDN4, claudin 4; TRPV6, transient receptor potential vanilloid 6

Affymetrix NspI SNP array hybridisation and analysis

Microdeletion analyses were carried out on the Affymetrix GeneChip 250k (NspI) SNP array platform (Affymetrix, Inc., Santa Clara, CA), which contains 25-mer oligonucleotides representing a total of 262,264 SNPs. Hybridisations were performed according to the manufacturer's protocols. Copy numbers were determined using

6

the 2.0 version of the CNAG (Copy Number Analyzer for Affymetrix GeneChip mapping) software package, by comparing SNP intensities from patient DNA with those of a sex-matched pooled reference DNA sample (DNA from either ten healthy male or ten healthy female individuals) [23]. The average resolution of this array platform is 150-200 kb.

Results

Patient phenotype and biochemistry

An overview of selected clinical and biochemical characteristics of all patients and the corresponding reference ranges for infants under 12 months of age are provided in Table 2. Family background and clinical and biochemical characteristics of patient 1 and patient 2 have been described in previous publications [4, 22, 24]. In short, patient 1 and 2 both showed elevated serum Ca^{2+} levels and a urinary Ca/Cr ratio above normal reference range. PTH levels were below reference range in patient 1 and normal in patient 2. PTH-related peptide (PTHrP) levels were normal in both patients, as were 25-hydroxyvitamin D_3 levels. 1,25-dihydroxyvitamin D_3 levels were not changed in patient 1 and slightly elevated in patient 3.
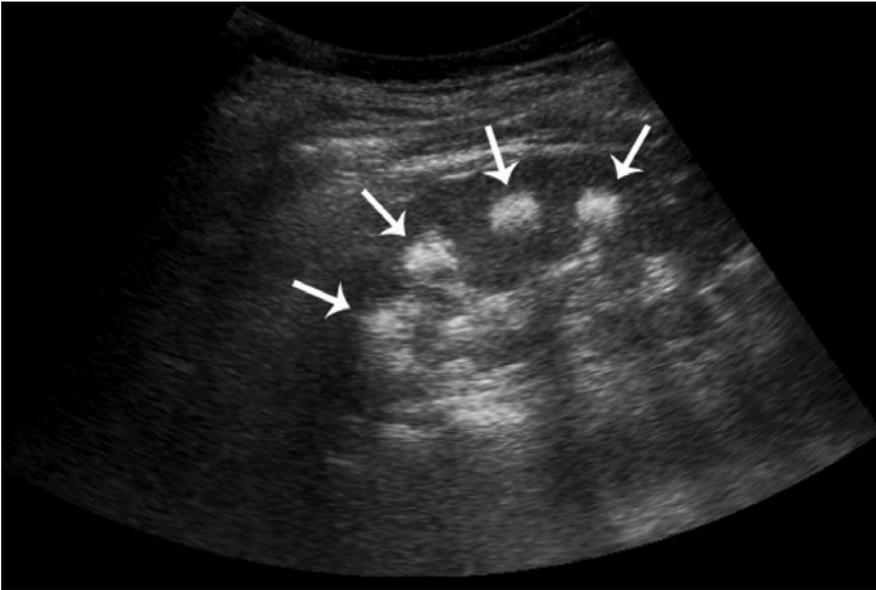
Figure 1 Ultrasound of the left kidney of patient 3 at the age of 2 months. Nephrocalcinosis in the medullar regions is indicated by white arrows.

Table 2 Selected clinical features and biochemical characteristics of included subjects

Patient	1	2	3	Ref. range
Age	8 months	3 months	2 months	<12 months
Clinical features	Failure to thrive	Family history	Failure to thrive	/
Ultrasound findings	Nephrocalcinosis	Normal	Nephrocalcinosis	/
Serum Ca²⁺ level (mmol/L)	3.34	2.9	3.76	<2.7
Ionized Ca²⁺ (mmol/L)	1.63	1.44	1.34	1.0-1.3
Random Ca/Cr ratio (mmol/mmol)	3.8	2	8.5	0.09-2.2
Intact PTH (pmol/L)	0.3	1.7	0.3	1.0-6.5
PTHrP (pmol/L)	0.22	N.D.	<0.3	<0.3
25-hydroxy-vit. D₃ (nmol/L)	57	99	51	35-100
1,25-dihydroxy-vit. D₃ (pmol/L)	61	220	132	50-150

N.D., not determined; Ca²⁺, calcium; Ca/Cr, calcium/creatinine; PTH, parathyroid hormone; PTHrP, PTH related peptide

6

Patient 3 was born at 40 weeks gestational age with normal birth weight of 3150 g. Both parents were healthy without consanguinity. Ultrasonography during pregnancy showed increased echogenicity of both kidneys of the fetus. She was first seen at our out-patient clinic at the age of 2 months because of failure to thrive and to evaluate the increased echogenicity observed before birth. An extensive nephrocalcinosis was observed (Figure 1). Clinical evaluation revealed no abnormalities, with blood pressure in the normal range. Biochemical analysis showed elevated levels of both total and ionized serum Ca^{2+}. The urinary Ca/Cr ratio was approximately four times. PTH levels were low, levels of PTHrP, 25-hydroxyvitamin D_3 and 1,25-dihydroxyvtamin D_3 were within normal reference range. Additional biochemical characteristics at the age of 2-3 months are shown in Table 3. Chromosomal examination showed a normal 46XX karyotype. Williams-Beuren syndrome was excluded based on the absence of a microdeletion in 7q11.23.

As the serum Ca^{2+} levels decreased spontaneously upon increase of fluid intake no other therapy was applied and her growth resumed at a normal rate. Since the age of two years she suffered from recurrent urinary tract infections. A cystogram
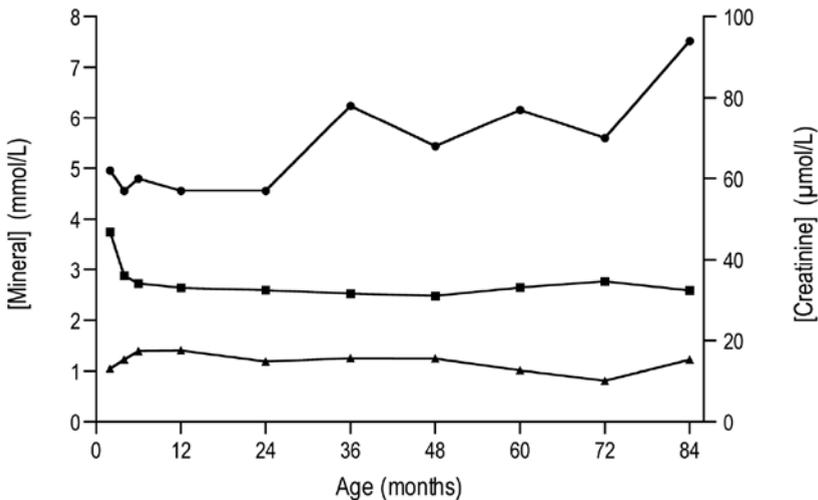
Figure 2 Development of serum Ca^{2+}, phosphate and creatinine levels in patient 3 throughout time. After an initial period of severe hypercalcemia serum Ca^{2+} levels (■) normalize in the upper percentiles of the normal reference range (<2.7 mmol/L). Serum phosphate levels (▲) are generally within reference range (1.2-2.2 mmol/L), but remain in the lower percentiles. Serum creatinine levels (●), right Y-axis) are within reference range (20-80 µmol/L) and seem to increase throughout time.

showed no reflux. Figure 2 depicts the development of Ca²⁺, phosphate and creatinine levels in patient 3 over time. After an initial period of extreme hypercalcemia, serum Ca²⁺ levels normalized at a level within normal range, but remained in the upper percentiles (2.6-2.7 mmol/L). At the age of 8 years her serum creatinine was 92 umol/l with an estimated creatinine clearance of 76 ml/min/1.73m². This slightly decreased clearance rate can be explained by the combination of recurrent urinary infections and nephrocalcinosis.

Table 3 Biochemical characteristics patient 3

Source	Analyzed compound	Patient 3	Normal reference range
Blood	Ca²⁺	3.41-3.76 mmol/L	<2.7 mmol/L
	Ionized Ca²⁺	1.26-1.34 mmol/L	1.0-1.3 mmol/L
	Mg²⁺	0.8 mmol/L	0.78-1.04 mmol/L
	Phosphate	1.05-1.14 mmol/L	1.20-2.2 mmol/L
	Alkaline Phosphatase	278-397 U/L	150-350 U/L
	Creatinine	46-62 μmol/L	20-80 μmol/L
	Intact PTH	0.3 pmol/L	1.0-6.5 pmol/L
	PTHrP	<0.3 pmol/L	<0.3 pmol/L
	25-hydroxy-vitamin D₃	51 nmol/L	35-100 nmol/L
	1,25-dihydroxy-vitamin D₃	132 pmol/L	50-150 pmol/L
	Calcitonin	5 pmol/L	<3.5 pmol/L
Urine	Ca/Cr ratio	8.2-8.7 mmol/mmol	0.09-2.2 mmol/mmol [34]
	Phosphate reabsorption	78-82%	78-96% [35]

Ca²⁺, calcium; Mg²⁺, magnesium; PTH, parathyroid hormone; PTHrP, PTH related peptide; Ca/Cr, calcium/creatinine

6

Sequence analysis

Analysis of coding regions and intron-exon boundaries of CLDN3, CLDN4, and TRPV6 genomic sequences revealed a number of SNPs in our three patients. Two SNPs were identified in CLDN3 of patient 1 and located in the 5' untranslated region (UTR) of the exon. CLDN4 showed five identical SNPs in both patient 2 and 3. One was located outside the exon near its 5' e nd, one in the 5' UTR and three in the 3' UTR. Sequence analysis of TRPV6 revealed one synonymous SNP in the coding region of exon 11 in patient 3. Table 4 provides an overview of all SNPs identified in our patients in CLDN3, CLDN4 and TRPV6. All SNP's found in this study were previously identified and are listed in single nucleotide polymorphism

(SNP) databases (http://ncbi.nlm.nih.gov/SNP/). SNP array analysis of genomic DNA from the patients did not reveal significant deletions or duplications.

Table 4 Sequence analysis of patients

Gene	Region	dbSNP allele	dbSNP cluster ID	Patient
CLDN3	Exon 1 → 5' UTR	C/G	rs7084	1
	Exon 1 → 5'UTR	A/G	rs6460054	1
CLDN4	5' near gene	A/G	rs4458741	2/3
	Exon 1 → 5'UTR	C/T	rs8629	2/3
	Exon 1 → 3'UTR	A/G	rs1127155	2/3
	Exon 1 → 3'UTR	C/T	rs1127156	2/3
	Exon 1 → 3'UTR	C/G	rs11316	2/3
TRPV6	Exon 11	C→T	rs4987704	3

CLDN3, claudin 3; CLDN4, claudin 4; TRPV6, transient receptor potential vanilloid 6; UTR, untranslated region

Discussion

To date the diagnosis IIH is still based on exclusion. Only if disorders such as Williams-Beuren syndrome, benign familial hypocalciuric hypercalcemia, primary hyperparathyroidism, thyroid disease, malignancy, excessive vitamin D and A intake, diuretic administration, sarcoidosis, and other granulomatous diseases are excluded the diagnosis IIH can be made [25]. No genetic defects causing IIH are known thus far.

Certain polymorphisms in TRPV6 have been associated with hypercalcemia due to intestinal hyperabsorption [26]. In IIH and WBS correlations between the absorptive hypercalcemic phenotype and mutations or polymorphisms in specific genes have not been identified thus far. Most studies on Ca^{2+} homeostasis in IIH and WBS patients have focused on abnormalities in Ca^{2+}, Ca^{2+}-regulating hormones including PTH and vitamin D. Studies consistently show that infants with IIH and WBS suffer from hyperabsorption of Ca^{2+} in the intestine and evidence for excessive vitamin D intake is generally lacking [1, 2, 27]. Although some reports show elevated levels of 25-hydroxyvitamin D_3 and 1,25-dihydroxyvitamin D_3, other studies were not able to confirm these findings [5]. We found no increased levels of 25-hydroxyvitamin D_3 in our patients. 1,25-dihydroxyvitamin D_3 levels were elevated

in one patient, however, in the two patients with the highest Ca^{2+} levels 1,25-dihy-droxyvitamin D_3 levels were normal. Alternative mechanisms to explain the hypercalcemia are an increased sensitivity for vitamin D, deficient suppression of PTH by hypercalcemia, or an increased release of PTHrP, which is highly similar to PTH in structure and function [5, 28-30]. PTH levels of our patients were below the normal reference range indicating an appropriate suppression of PTH in response to hypercalcemia. None of the patients described in this study had elevated PTHrP levels. PTHrP is, therefore, not likely to be involved in the increased intestinal Ca^{2+} absorption seen in IIH patients. Patient 3 showed slightly decreased serum phosphate concentrations and low renal phosphate reabsorption (Table 3). Decreased tubular phosphate reabsorption as a result of chronic hypercalcemia is a known phenomenon of unspecified etiology [31]. The correlation between serum phosphate and Ca^{2+} levels in patient 3 is also shown in figure 2.

The leading hypothesis on IIH and WBS pathogenesis is a genetic defect in Ca^{2+} homeostasis resulting in intestinal hyperabsorption of Ca^{2+}, which is compensated later in life [32, 33]. As described before CLDN3 and CLDN4, which are hemizygously deleted in WBS, are members of a large family of claudin proteins that are part of the tight junction complex regulating the paracellular permeability. Holmes *et al.* studied the expression of intestinal claudins in the mice of different ages and showed that some claudins are significantly up or down regulated throughout life [21]. The transient character of hypercalcemia in IIH and WBS patients could therefore potentially be explained by the altered expression of claudins that regulate the permeability of the intestinal epithelium. The partial loss of claudin 3 or claudin 4 expression would in this case be compensated for after a certain period of time, explaining the disappearance of hypercalcemia. This way our hypothesis would explain the clinical phenotype as observed in our patients on both a genetic and molecular level.

Patient DNA was analyzed for the presence of mutations in CLDN3 and CLDN4. Alternatively, the major intestinal Ca^{2+} channel TRPV6 was also analyzed to exclude the presence of gain of function mutations and activating polymorphisms that could be involved in the development of hypercalcemia. All SNP's found in this study were previously identified and are listed in single nucleotide polymorphism (SNP) databases (http://ncbi.nlm.nih.gov/SNP/). None of the polymorphisms is known to be related to disease, nor did our study indicate such a correlation. A SNP array did not reveal significant deletions or duplications in any of the patients. Together these results not only show that mutations in CLDN3 and CLDN4 are not involved in IIH, they also indicate that the IIH phenotype does not result from deletions or duplications in the genome of these patients.

In summary, this study showed no aberrant levels of vitamin D, PTH and PTHrP in IIH patients thereby invalidating a number of previous proposed

6

hypotheses. Furthermore, no mutations in CLDN3, CLDN4 and TRPV6 were found in these patients, who also did not have genomic deletions or duplications. The sporadic occurrence and general lack of a clear inheritance pattern in IIH, together with the limited number of patients known to suffer from IIH, complicates identification of genes involved in the development of transient hypercalcemia.

Acknowledgements

References

1.   Martin ND, Snodgrass GJ, Cohen RD: Idiopathic infantile hypercalcaemia-a continuing enigma. *Archives of disease in childhood* 59: 605-613, 1984

2.   Barr DG, Forfar JO: Oral calcium-loading test in infancy, with particular reference to idiopathic hypercalcaemia. *British medical journal* 1: 477-480, 1969

3.   Pak CY: Sodium cellulose phosphate: mechanism of action and effect on mineral metabolism. *J Clin Pharmacol New Drugs* 13: 15-27, 1973

4.   Huang J, Coman D, McTaggart SJ, Burke JR: Long-term follow-up of patients with idiopathic infantile hypercalcaemia. *Pediatric nephrology (Berlin, Germany)* 21: 1676-1680, 2006

5.   Pronicka E, Rowinska E, Kulczycka H, Lukaszkiewicz J, Lorenc R, Janas R: Persistent hypercalciuria and elevated 25-hydroxyvitamin D3 in children with infantile hypercalcaemia. *Pediatric nephrology (Berlin, Germany)* 11: 2-6, 1997

6.   Mitchell RG: The prognosis in idiopathic hypercalcaemia of infants. *Archives of disease in childhood* 35: 383-388, 1960

7.   Fanconi G, Girardet P, Schlesinger B, Butler N, Black J: [Chronic hyperglycemia, combined with osteosclerosis, hyperazotemia, nanism and congenital malformations.]. *Helvetica paediatrica acta* 7: 314-349, 1952

8.   Lightwood R: Idiopathic hypercalcaemia with failure to thrive. *Archives of disease in childhood* 27: 302–330, 1952

9.   Lightwood R, Stapleton T: Idiopathic hypercalcaemia in infants. *Lancet* 265: 255-256, 1953

10. Black JA, Carter RE: Association between Aortic Stenosis and Facies of Severe Infantile Hypercalcaemia. *Lancet* 2: 745-749, 1963

11. Nickerson E, Greenberg F, Keating MT, McCaskill C, Shaffer LG: Deletions of the elastin gene at 7q11.23 occur in approximately 90% of patients with Williams syndrome. *American journal of human genetics* 56: 1156-1161, 1995

12. Schubert C: The genomic basis of the Williams-Beuren syndrome. *Cell Mol Life Sci* 66: 1178-1197, 2009

13. Schubert C, Laccone F: Williams-Beuren syndrome: determination of deletion size using quantitative real-time PCR. *International journal of molecular medicine* 18: 799-806, 2006

14. Morita K, Furuse M, Fujimoto K, Tsukita S: Claudin multigene family encoding four-transmembrane domain protein components of tight junction strands. *Proceedings of the National Academy of Sciences of the United States of America* 96: 511-516, 1999

15. Paperna T, Peoples R, Wang YK, Kaplan P, Francke U: Genes for the CPE receptor (CPETR1) and the human homolog of RVP1 (CPETR2) are localized within the Williams-Beuren syndrome deletion. *Genomics* 54: 453-459, 1998

16. Van Itallie CM, Anderson JM: Claudins and epithelial paracellular transport. *Annual review of physiology* 68: 403-429, 2006

17. Hashimoto K, Oshima T, Tomita T, Kim Y, Matsumoto T, Joh T, Miwa H: Oxidative stress induces gastric epithelial permeability through claudin-3. *Biochem Biophys Res Commun* 376: 154-157, 2008

18. Hou J, Gomes AS, Paul DL, Goodenough DA: Study of claudin function by RNA interference. *The Journal of biological chemistry* 281: 36117-36123, 2006

19. Lamb-Rosteski JM, Kalischuk LD, Inglis GD, Buret AG: Epidermal growth factor inhibits Campylobacter jejuni-induced claudin-4 disruption, loss of epithelial barrier function, and Escherichia coli translocation. *Infect Immun* 76: 3390-3398, 2008

20. McLaughlin J, Padfield PJ, Burt JP, O'Neill CA: Ochratoxin A increases permeability through tight junctions by removal of specific claudin isoforms. *Am J Physiol Cell Physiol* 287: C1412-1417, 2004

21. Holmes JL, Van Itallie CM, Rasmussen JE, Anderson JM: Claudin profiling in the mouse during postnatal intestinal development and along the gastrointestinal tract reveals complex expression patterns. *Gene Expr Patterns* 6: 581-588, 2006

22. McTaggart SJ, Craig J, MacMillan J, Burke JR: Familial occurrence of idiopathic infantile hypercalcemia. *Pediatric nephrology (Berlin, Germany)* 13: 668-671, 1999

6

23. Nannya Y, Sanada M, Nakazaki K, Hosoya N, Wang L, Hangaishi A, Kurokawa M, Chiba S, Bailey DK, Kennedy GC, Ogawa S: A robust algorithm for copy number detection using high-density oligonucleotide single nucleotide polymorphism genotyping arrays. *Cancer Res* 65: 6071-6079, 2005

24. Mizusawa Y, Burke JR: Prednisolone and cellulose phosphate treatment in idiopathic infantile hypercalcaemia with nephrocalcinosis. *J Paediatr Child Health* 32: 350-352, 1996

25. Rodd C, Goodyer P: Hypercalcemia of the newborn: etiology, evaluation, and management. *Pediatric nephrology (Berlin, Germany)* 13: 542-547, 1999

26. Suzuki Y, Pasch A, Bonny O, Mohaupt MG, Hediger MA, Frey FJ: Gain-of-function haplotype in the epithelial calcium channel TRPV6 is a risk factor for renal calcium stone formation. *Human molecular genetics* 17: 1613-1618, 2008

27. Morgan HG, Mitchell RG, Stowers JM, Thomson J: Metabolic studies on two infants with idiopathic hypercalcaemia. *Lancet* 270: 925-931, 1956

28. Forbes GB, Bryson MF, Manning J, Amirhakimi GH, Reina JC: Impaired calcium homeostasis in the infantile hypercalcemic syndrome. *Acta Paediatr Scand* 61: 305-309, 1972

29. Langman CB BA, Sailer, Strewler GJ: Nonmalignant expression of parathyroid hormone-related protein is responsible for idiopathic infantile hypercalcemia. *J Bone Miner Res* 7: 593S, 1992

30. Karlowicz MG, Adelman RD: Renal calcification in the first year of life. *Pediatr Clin North Am* 42: 1397-1413, 1995

31. Brenner B: *The Kidney,* Philadelphia; PA, W.B. Saunders Company, 2008.

32. Alon U, Berkowitz D, Berant M: Idiopathic infantile hypercalcemia: rapid response to treatment with calcitonin. *Child Nephrol Urol* 12: 47-50, 1992

33. Bzduch V: Hypercalcemic phase of Williams syndrome. *J Pediatr* 123: 496, 1993

34. Matos V, van Melle G, Boulat O, Markert M, Bachmann C, Guignard JP: Urinary phosphate/creatinine, calcium/creatinine, and magnesium/creatinine ratios in a healthy pediatric population. *J Pediatr* 131: 252-257, 1997

35. Bistarakis L, Voskaki I, Lambadaridis J, Sereti H, Sbyrakis S: Renal handling of phosphate in the first six months of life. *Archives of disease in childhood* 61: 677-681, 1986

6

7

Importance of dietary calcium and vitamin D in treatment of hypercalcaemia in Williams-Beuren syndrome

Anke L. Lameris[1], Christel L.M. Geesing[2], Joost G.J. Hoenderop[1],
Michiel F. Schreuder[3]

Radboud University Nijmegen Medical Centre, Departments of [1] Physiology and
[3] Pediatric Nephrology, Nijmegen, The Netherlands
Bernhoven Hospital, [2] Department of Pediatrics, Oss, The Netherlands

Abstract

Williams-Beuren syndrome is a rare genetic disorder, caused by the deletion of 26-28 genes on chromosome 7. Fifteen percent of Williams-Beuren syndrome patients present with hypercalcaemia during infancy, which is generally mild and resolves spontaneously before the age of 4 years. The mechanisms underlying the transient hypercalcaemia in Williams-Beuren syndrome are poorly understood.

We report a case of severe symptomatic hypercalcaemia in a patient with Williams-Beuren syndrome, in which treatment with mild calcium restriction, hyperhydration and repeated bisphosphonate administration only resulted in short-lasting effects. Long-term lowering of serum calcium was only achieved after reducing calcium and vitamin D intake to the bare minimum.

This case illustrates the potential severity of hypercalcaemia in WBS, and demonstrates that both the cause as well as the solution of this problem may be found in the intestinal absorption of calcium. We hypothesize that the phenotypical resemblance between Williams-Beuren syndrome and transient idiopathic infantile hypercalcaemia can be explained by similarities in the underlying genetic defect. Patients suffering from transient infantile hypercalcaemia were recently described to have mutations in CYP24A1, the key enzyme in 1,25-dihydroxyvitamin D_3 degradation. In the light of this new development we discuss the role of one of the deleted genes in WBS, Williams Syndrome Transcription Factor, in the etiology of hypercalcaemia in Williams-Beuren syndrome.

Introduction

Williams-Beuren syndrome (WBS, OMIM 194050) is a rare genetic disorder, caused by a hemizygous deletion at 7q11.23 comprising approximately 26 to 28 genes [1]. WBS patients are generally characterized by distinctive facial dysmorphisms, mental retardation and cardiovascular abnormalities. In addition, approximately 15% of WBS patients present with hypercalcaemia during infancy, generally mild in nature. It resolves spontaneously before the age of 4 years, but sometimes reoccurs briefly during puberty [1]. The mechanisms explaining the transient hypercalcaemia are poorly understood. We report a case of severe symptomatic hypercalcaemia in a patient with WBS only resolving with a profound reduction of calcium and vitamin D intake, and present a potential mechanism for this metabolic abnormality.

Case report

An 18-months-old female patient was admitted to a local hospital to start tube feeding for treatment of failure to thrive due to feeding difficulties and persistent vomiting despite proton-pump inhibition. Three months earlier she was diagnosed with WBS with normal serum calcium levels (2.40 mmol/L), and was known with low birth weight, a cardiac murmur without a structural anomaly, and a developmental delay.

During her admission, her condition deteriorated, and she developed a hypercalcaemia (Table 1) and hypertension (up to 150/130 mmHg) for which she was transferred to the pediatric intensive care unit at the Radboud University Nijmegen Medical Centre. Her blood pressure was controlled with an intravenous calcium-antagonist, which was successfully switched to oral anti-hypertensive agents (amlodipine and labetalol). Extensive evaluation, excluding renal angiography, did not show an explanation for the hypertension, other than the hypercalcaemia and the underlying WBS.

The hypercalcaemia was treated with hyperhydration, furosemide and a reduced calcium intake. Laboratory tests ruled out other causes than the WBS for the hypercalcaemia (Table 1). To prevent nephrocalcinosis due to the subsequent hypercalciuria (urine calcium-creatinine ratio up to 3.0 mmol/mmol), potassium citrate was administered.

As this treatment just led to a small reduction in serum calcium (Figure 1), a bisphosphonate was administered, in a low dose to prevent hypocalcaemia. This resulted in only a short and mild reduction of the serum calcium, so repeated and increased doses of pamidronate were administered, all with only short-lasting effects (Figure 1). With every return of hypercalcaemia, the patient also showed

7

Table 1 Laboratory parameters at diagnosis and during follow-up.

Parameter	Normal range	Hospital admission for hypercalcaemia	3 months after admission	6 months after admission	Latest follow-up
Age		1 year, 6 months	1 year, 9 months	2 years 1 month	4 years, 6 months
Total calcium (mmol/L)	2.20-2.70	3.51	2.61	2.76	2.73
Calcium ion (mmol/L)	1.10-1.30	ND	1.33	1.37	1.26
Albumin (g/L)	35-50	45.0	44	52	ND
Phosphate (mmol/L)	1.5-2.2	1.5	1.72	1.54	1.26
eGFR (ml/min/1.73m^2)	90-120	41	129	114	ND
25-(OH)-vitamin D (nmol/L)	18-113	56.7	46	38	ND
1,25-(OH)-vitamin D (pmol/L)	47-130	18.7	ND	250	ND
PTH (pmol/L)	1.3-6.8	0.4	9.9	6.2	2.7
Urine calcium-creatinine ratio (mmol/mmol)	<1.5	1.15	<0.3	<0.3	0.55

ND, Not determined. eGFR, estimated glomerular filtration rate based on the Schwartz equation

an increase in blood pressure and vomiting. Therefore, calcium and vitamin D intake (drip-feed containing 588 mg Ca/d and 150 IE/d) was reduced to the bare minimum (68 mg/d and 0 IE/d, respectively) while maintaining adequate nutritional intake. With this treatment serum calcium was maintained at high-normal but stable levels that were clinically well accepted. Phosphate supplementation was initiated to treat her accompanying hypophosphataemia.

During follow-up, we found to our surprise a low renal calcium excretion and high PTH level during the calcium restriction. We interpreted this to be indicative of a more calcium-deficient state, despite the high-normal serum calcium, for which the calcium intake was gradually increased. No nephrocalcinosis is present at the latest ultrasound, and no hypercalciuria occurred during the gradual increase in calcium intake.
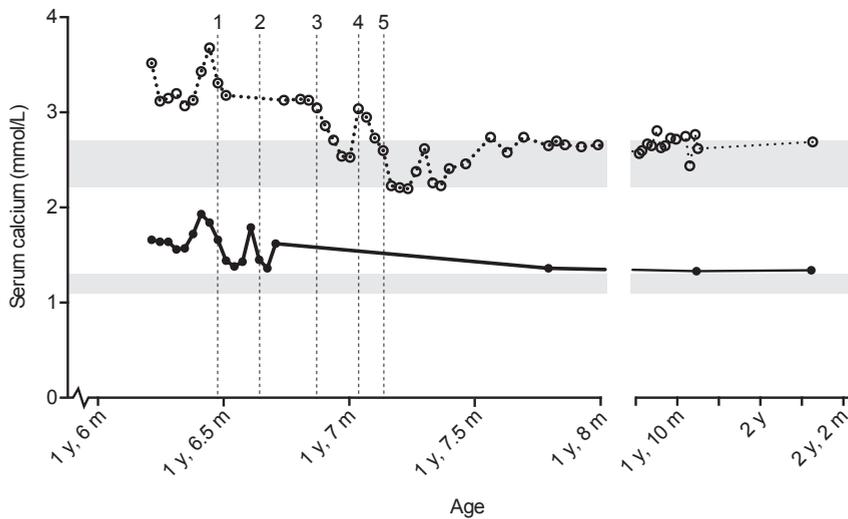
Figure 1 Time course of total calcium and ionized calcium levels in serum during treatment and follow-up. Grey area's indicate the normal range total serum calcium (2.20-2.70 mmol/L) and ionized calcium (1.10-1.30 mmol/L). The arrows indicate interventions. 1-4: i.v. administration of pamidronate, 0.25, 0.50, 1.0, and 1.0 mg pamidronate /kg bodyweight, respectively. 5: diet changed from drip-feed containing 588mg Ca/d and 150 IE 1,25-dihydroxyvitamin D_3 /d to a drip-feed with 68 mg Ca/d and 0 IE 1,25-dihydroxyvitamin D_3/d.

Discussion

In the past, various studies have been performed to try and elucidate the mechanism underlying hypercalcaemia in WBS. We hypothesize that increased intestinal absorption of calcium is the main factor in the pathogenesis of hypercalcaemia in these patients, as has been described in the past [2], potentially as a result of reduced break down of vitamin D. Most studies aimed to find changes in Vitamin D metabolism, with various degrees of success. Some groups find abnormalities in all patients suffering from WBS, whereas others only describe changes in vitamin D metabolism in WBS patients with hypercalcaemia, and some groups find no changes at all [2].

Bisphosphonate therapy (pamidronate) is recommended as an additional therapy when conventional measures (intravenous fluids, furosemide and dietary calcium restriction) fail to normalize serum calcium. However, the course of the hypercalcaemia in our patient seems to suggest no sustained effect of bisphosphonate treatment and suggests an intestinal cause of hypercalcaemia that can only be treated by (extensive) calcium and vitamin D restriction. Of note, our patient did not show extensive hypercalciuria at presentation (Table 1), which would be expected in hypercalcaemia However, renal function was reduced at that time with an estimated glomerular filtration rate of 41 ml/min/1.73m2 and hypercalciuria did present after optimizing renal function (urine calcium-creatinine ratio up to 3.0 mmol/mmol). The reduced renal function may explain the temporary absence of hypercalciuria, and may have contributed to the observed hypercalcaemia. The persisting hypercalciuria as well as hypercalcaemia that were observed when renal function was restored indicate that the hypercalcaemia in our patient is not solely explained by inappropriate renal calcium handling due to renal failure. Some of the features of our patient are not easily explained and may indicate an additional factor involved in the aetiology of hypercalcaemia in this particular patient. The high PTH levels observed after 3-6 months, when serum calcium levels are in the high-normal range could also indicate an altered set point of serum calcium, which is commonly associated with inactivating mutations in the calcium-sensing receptor (CaSR). Hypertension is, in addition to the hypercalcaemia, a well known feature in up to 50% of WBS patients and may be explained by elastin deficiency, a hallmark feature of WBS [1]. Alternatively, renal artery stenosis is described in some patients with WBS, which we did not fully exclude in our patient yet. As blood pressure was well controlled with the current medical therapy, renal ultrasound showed identical sized and normal structured kidneys, and renography showed a normal split renal function, no renal angiography was performed.

Our case of severe and sustained hypercalcaemia highlights that the underlying mechanism in WBS can be found, at least in part, in the uptake of calcium, as the long-term lowering of serum calcium was only obtained by a subtotal reduction of the calcium and vitamin D intake. Hypercalcaemia in WBS patient and patients suffering from idiopathic infantile hypercalcaemia (IIH) without WBS both have been shown to result from intestinal hyperabsorption of calcium, the contribution of potential changes in renal calcium handling to the observed hypercalcaemia remains to be determined [3].

Similar to our WBS patient, IIH patients were shown to benefit from dietary calcium and vitamin D restriction [4]. Patients should however by carefully monitored since long-term restriction of dietary calcium and vitamin D may induce rickets in these young patients [4, 5].

Based on these phenotypical similarities between patients with WBS and IIH patients we previously suggested there might be a common underlying genetic defect [6]. We hypothesized that claudin 3 and claudin 4, both involved in paracellular calcium absorption and located within the hemizygously deleted WBS region, might be responsible for the hypercalcaemia state of these patients. Unfortunately, we were not able to confirm this hypothesis in patients suffering from isolated infantile hypercalcaemia [6]. Letavernier et al have suggested that hypercalcaemia in WBS patients is the result of TRPC3 overexpression due to haploinsufficiency of the transcriptions factor TFII-I, which is located in the genomic region that is deleted in WBS patients [7]. Evidence that TRPC3 is involved in transepithelial calcium transport in the intestine however is lacking. Despite the earlier negative findings, our hypothesis remains valid. The similarities with regards to the transient hypercalcaemic phenotype of IIH and WBS patients suggest a common underlying genetic defect. Interestingly, the genetic defect causing IIH has recently been elucidated, shedding more light on the molecular mechanism underlying hypercalcaemia in these patients. Two independent studies have found that homozygous or compound heterozygous mutations and deletions in the CYP24A1 gene are responsible for the phenotype of patients suffering from idiopathic infantile hypercalcaemia. CYP24A1 encodes 25-dihydroxy-vitamin D 24-hydroxylase, which is the key enzyme in 1,25-dihydroxyvitamin D_3 degradation [8, 9]. Patients display hypercalcaemia, hypercalciuria, and suppressed PTH levels, whereas levels of 25-hydroxyvitamin D_3 and 1,25-dihydrox-yvitamin D_3 were within normal range. A third study describes patients with a heterozygous mutation in CYP24A1 that have a less severe clinical phenotype compared to the compound heterozygous patients, indicative of a haploinsufficiency or a dominant negative effect [10]. This study also shows that patients with CYP24A1 mutations have reduced levels of circulating 24,25-dihydroxyvitamin D_3 in line with a nonfunctional Cyp24a1 enzyme. Together, these studies indicate

7

that in IIH patients, intestinal hyperabsorption of calcium is the result of altered vitamin D catabolism.

Interestingly, a gene named Williams Syndrome Transcription Factor (WSTF) is located within the WBS deletion region. WSTF is a subunit of the ATP-dependent chromatin remodelling complex WINAC, whose activity facilitates ligand-dependent activation of CYP24A1 and repression of 25-hydroxyvitamin D_3-1-alpha hydroxylase (CYP27B1) by the vitamin D receptor (VDR) [11].

It has previously been hypothesized that hypercalcaemia in WBS is the result of loss of WINAC function, leading to reduced transcription of CYP24A1 and increased transcription of CYP27B1, theoretically resulting in increased 1,25-dihydroxyvitamin D_3 [12]. Lack of a clear increase in 1,25-dihydroxyvitamin D_3 levels in WBS patients seems to contradict this hypothesis. However, the phenotype of patients with CYP24A1 mutations clearly demonstrates that a lack of 25-dihydroxyvitamin D 24-hydroxylase may indeed lead to a hypercalcaemic phenotype without a clear increase in circulating 1,25-dihydroxyvitamin D_3 levels, only the patients receiving large doses of Vitamin D prophylaxis display elevated levels of circulating 1,25-dihydroxyvitamin D_3 [9]. As our patient was admitted for failure to thrive, it is safe to assume that her vitamin D intake was low. Similar observations have been made in *Cyp24a1* knockout (KO) mice, which have normal 1,25-dihydroxyvitamin D_3 levels at baseline, but show an impaired clearance of administered 1,25-dihydroxyvitamin D_3 [13]. The exact explanation for this finding remains to be determined, but it strengthens the hypothesis that the hemizygous deletion of WSTF could be responsible for the transient hypercalcaemia in WBS, despite a lack of clear alterations in 1,25-dihydroxyvitamin D_3. These data are in line with our hypothesis that deletion of WSTF in WBS patients leads to a reduced CYP24A1 activity, therefore a reduced catabolism of 1,25-dihydroxyvitamin D_3, which results in increased intestinal calcium absorption with subsequent hypercalcaemia.

In conclusion, our patient illustrates the potential severity of hypercalcaemia in WBS, and demonstrates that both the cause and the solution of this problem may be found in the intestinal absorption of calcium. Key to treatment of severe hypercalcaemia in WBS is subtotal restriction of calcium and vitamin D intake. Follow-up should include careful monitoring of serum and urinary calcium levels, to navigate between hypercalcaemia and calcium depletion.

References

1.   Pober BR: Williams-Beuren syndrome. *N Engl J Med* 362: 239-252, 2010

2.   Kruse K, Pankau R, Gosch A, Wohlfahrt K: Calcium metabolism in Williams-Beuren syndrome. *J Pediatr* 121: 902-907, 1992

3.   Barr DG, Forfar JO: Oral calcium-loading test in infancy, with particular reference to idiopathic hypercalcaemia. *Br Med J* 1: 477-480, 1969

4.   Martin ND, Snodgrass GJ, Cohen RD: Idiopathic infantile hypercalcaemia--a continuing enigma. *Arch Dis Child* 59: 605-613, 1984

5.   Gut J, Kutilek S: Idiopathic infantile hypercalcaemia in 5-month old girl. *Prague Med Rep* 112: 124-131,

6.   Lameris AL, Huybers S, Burke JR, Monnens LA, Bindels RJ, Hoenderop JG: Involvement of claudin 3 and claudin 4 in idiopathic infantile hypercalcaemia: a novel hypothesis? *Nephrol Dial Transplant* 25: 3504-3509, 2010

7.   Letavernier E, Rodenas A, Guerrot D, Haymann JP: Williams-Beuren syndrome hypercalcemia: is TRPC3 a novel mediator in calcium homeostasis? *Pediatrics* 129: e1626-1630, 2012

8.   Dauber A, Nguyen TT, Sochett E, Cole DE, Horst R, Abrams SA, Carpenter TO, Hirschhorn JN: Genetic defect in CYP24A1, the vitamin D 24-hydroxylase gene, in a patient with severe infantile hypercalcemia. *J Clin Endocrinol Metab* 97: E268-274, 2012

9.   Schlingmann KP, Kaufmann M, Weber S, Irwin A, Goos C, John U, Misselwitz J, Klaus G, Kuwertz-Broking E, Fehrenbach H, Wingen AM, Guran T, Hoenderop JG, Bindels RJ, Prosser DE, Jones G, Konrad M: Mutations in CYP24A1 and idiopathic infantile hypercalcemia. *N Engl J Med* 365: 410-421, 2011

10.   Tebben PJ, Milliner DS, Horst RL, Harris PC, Singh RJ, Wu Y, Foreman JW, Chelminski PR, Kumar R: Hypercalcemia, hypercalciuria, and elevated calcitriol concentrations with autosomal dominant transmission due to CYP24A1 mutations: effects of ketoconazole therapy. *J Clin Endocrinol Metab* 97: E423-427, 2012

11.   Barnett C, Krebs JE: WSTF does it all: a multifunctional protein in transcription, repair, and replication. *Biochem Cell Biol* 89: 12-23, 2011

12.   Yoshimura K, Kitagawa H, Fujiki R, Tanabe M, Takezawa S, Takada I, Yamaoka I, Yonezawa M, Kondo T, Furutani Y, Yagi H, Yoshinaga S, Masuda T, Fukuda T, Yamamoto Y, Ebihara K, Li DY, Matsuoka R, Takeuchi JK, Matsumoto T, Kato S: Distinct function of 2 chromatin remodeling complexes that share a common subunit, Williams syndrome transcription factor (WSTF). *Proc Natl Acad Sci U S A* 106: 9280-9285, 2009

13.   St-Arnaud R, Arabian A, Travers R, Barletta F, Raval-Pandya M, Chapin K, Depovere J, Mathieu C, Christakos S, Demay MB, Glorieux FH: Deficient mineralization of intramembranous bone in vitamin D-24-hydroxylase-ablated mice is due to elevated 1,25-dihydroxyvitamin D and not to the absence of 24,25-dihydroxyvitamin D. *Endocrinology* 141: 2658-2666, 2000

7

# 8

General discussion and summary

Introduction

Calcium (Ca^{2+}) and magnesium (Mg^{2+}) play an important role in many of our bodily functions, including bone formation, muscle contraction and relaxation, and enzymatic activity. It is, therefore, essential that plasma Ca^{2+} and Mg^{2+} concentrations are maintained within a narrow range. To this end, the plasma levels of both minerals are regulated by the concerted action of the intestine, bones and kidneys. Since dietary intake is the only source of Ca^{2+} and Mg^{2+} for our body, intestinal absorption is crucial for the maintenance of normal homeostatic levels. In the intestine, but also in the kidney, Ca^{2+} and Mg^{2+} are (re)absorbed via transcellular and paracellular pathways. Transcellular transport generally requires three consecutive steps, in which ions enter the cell via the apical membrane, diffuse through the cytoplasm, and exit the cell via the basolateral membrane. Two channels, transient receptor potential vanilloid type 6 (TRPV6) and transient receptor potential melastatin type 6 (TRPM6), facilitate the entry of these cations from the intestinal lumen into the cell, which is considered to be the rate-limiting factor in the transcellular transport pathway [4]. When transported via the paracellular pathway, ions do not cross the plasma membrane, but permeate the epithelium via the tight-junctions that are localized between the epithelial cells. The family of claudin proteins plays an important role in paracellular transport of Ca^{2+} and Mg^{2+} by determining the size- and charge selectivity of the paracellular route [5]. Hormones and other regulatory factors control transport via both the transcellular and the paracellular pathways. The studies described in this thesis were directed at further elucidating the molecular mechanisms involved in intestinal absorption of Ca^{2+} as well as Mg^{2+}. This chapter summarizes and discusses the major findings of this thesis.

The importance of TRPV6 in intestinal Ca^{2+} absorption

For both Ca^{2+} and Mg^{2+} the first step of transcellular transport, in which ions enter the cell by crossing the apical membrane, is facilitated by proteins from the transient receptor potential (TRP) family [6]. TRP proteins contain six membrane-spanning domains (S1–S6), a pore loop between domains S5 and S6, and intracellularly located carboxy- and amino termini [6]. Four TRP monomers are known to form a cation channel by assembling into homo- or heterotetramers (Figure 1). The epithelial Ca^{2+} channel TRPV6 is considered the primary protein responsible for transcellular intestinal Ca^{2+} absorption [7]. The pore region of each TRPV6 monomer contains a crucial aspartic residue at position 542 (position 541 in mouse). In the tetrameric channel, these negatively charged residues form a ring that facilitates Ca^{2+} conductance [8, 9]. Indeed, replacement of this aspartic acid by an alanine residue abrogated Ca^{2+} permeation in both human and mouse

8

TRPV6, suggesting that D542/D541 is critical for channel activity [9-11]. To address the specific role of TRPV6 in transepithelial Ca^{2+} permeation *in vivo*, a mouse model with a mutation in the pore region (the TRPV6[D541A/D541A] knock-in mouse) was used in the studies described in **Chapter 2** [12, 13]. This mouse model is unique since the mutation creates a non-functional TRPV6 channel while the general structure of the protein remains unchanged. In contrast, the conventional complete knockdown of the channel, such as in TRPV6 knockout (KO) mice, might also affect other proteins that would normally interact with the channel [14]. Under normal dietary Ca^{2+} conditions, no differences in Ca^{2+} homeostasis and mRNA expression levels of genes involved in Ca^{2+} homeostasis were observed between wild-type and TRPV6[D541A/D541A] mice. Presumably, under these conditions paracellular Ca^{2+} absorption prevailed, explaining the lack of differences between both genotypes. Importantly, when challenged with a Ca^{2+} deficient diet, TRPV6[D541A/D541A] mice showed decreased duodenal transcellular Ca^{2+} absorption compared to wild-type mice. This further substantiates that transcellular absorption becomes more important during dietary Ca^{2+} restriction.

Interestingly, Ca^{2+} absorption was not completely absent in TRPV6[D541A/D541A] mice, implying that other mechanisms are critically involved in transcellular Ca^{2+} absorption. Similar observations have been made in TRPV6 KO mice, in which it
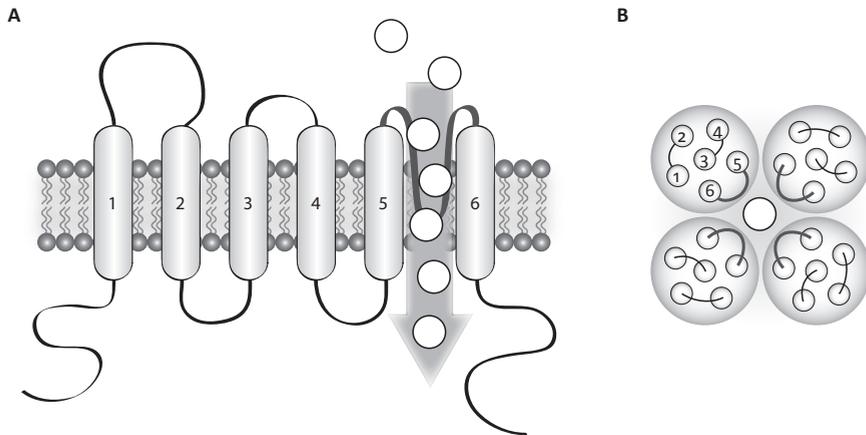
Figure 1 Structure of transient receptor potential (TRP) proteins. **A** Schematic representation of the six membrane-spanning domains (S1–S6) of a TRP protein, with the intracellular amino (N) and carboxy (C) termini. The pore loop (P) is located between domain 5 and 6. **B** Four TRP monomers assemble into a homo- or heterotetramer forming a functional cation channel.

was shown that in the absence of TRPV6, there is still a considerable amount of transcellular Ca^{2+} transport [14, 15]. These findings could indicate that other transport mechanisms can, under these specific circumstances, partially compensate for the loss of TRPV6. Indeed, during dietary Ca^{2+} restriction, the duodenal expression of TRPV5 was increased significantly in $TRPV6^{D541A/D541A}$ in our study. A smaller, albeit non-significant, increase of TRPV5 expression was also observed in wild-type mice. Since the expression of TRPV5 in the duodenum is low compared to that of TRPV6 (approximately 25 times lower under normal conditions and up to 150 times lower during dietary Ca^{2+} restriction), the physiological relevance of this increase in TRPV5 expression remains questionable. Another explanation for the remaining Ca^{2+} transport in absence of TRPV6 would be that an additional, potentially yet-unidentified, transporter plays an important role in transcellular Ca^{2+} transport. A potential candidate could be $Ca_v1.3$, an L-type calcium channel, which has been suggested to play a role in glucose-mediated transcellular Ca^{2+} absorption [16]. $Ca_v1.3$ is expressed in the duodenum but its presence is most prominent in the jejunum and ileum [17]. Although Cav1.3 KO mice have been generated, so far nothing has been reported concerning the maintenance Ca^{2+} homeostasis in these mice [18-20]. One study, however, did show that Cav1.3 KO mice have a smaller skeleton, lower body weight and lower bone mineral content compared to their wild-type littermates, which could be indicative of disturbed Ca^{2+} homeostasis [21]. To determine whether $Ca_v1.3$ indeed plays an important role in intestinal Ca^{2+} absorption *in vivo*, it would be interesting to study Ca^{2+} homeostasis in Cav1.3 KO mice. In addition, it could be useful to analyze the expression levels of $Ca_v1.3$ in the various KO models of calciotropic genes (such as TRPV6, calbindin-D_{9K}, and 1αOHase, vitamin D receptor, CaSR) under normal dietary circumstances as well as during Ca^{2+} deficiency. This would allow determining whether $Ca_v1.3$ can play a compensatory role, maintaining adequate levels of intestinal Ca^{2+} absorption in periods of low Ca^{2+} availability or in the absence of TRPV6. In order to get a complete picture of all the major players in transcellular intestinal Ca^{2+} absorption, it is important to determine whether Cav1.3 is indeed the "missing link" which is responsible for the remaining Ca^{2+} absorption seen in TRPV6 KO mice.

Understanding proton-pump inhibitor-induced hypomagnesemia

Proton-pump inhibitors (PPIs), a group of powerful suppressors of gastric acid secretion, have been on the market for more than two decades and are generally considered to have a good safety profile. In 2006, however, two cases of PPI-induced hypomagnesemia (PPIH) were reported in the *New England Journal of Medicine* [22]. This first report created awareness amongst physicians with regard to this potentially serious side effect, and in the following years more cases of PPIH were

8

described [22]. Subsequently, the United States Food and Drug Administration issued a warning, informing the general public that PPI's may cause hypomagnesemia if taken for a prolonged period of time [23]. As patients show no evidence of a renal Mg^{2+} leak, PPIH was hypothesized to result from intestinal malabsorption of Mg^{2+} [24, 25]. However, the exact mechanism underlying this defect in intestinal Mg^{2+} absorption remains unknown. In **Chapter 3**, we aimed to develop a mouse model of PPIH to study the underlying molecular mechanisms of this type of drug-induced hypomagnesemia. Although treatment with the PPI omeprazole did not cause hypomagnesemia in mice, it increased mRNA expression of TRPM6 in the colon. In addition, the mRNA expression of the colonic H^+,K^+-ATPase (cHK-α), a homologue of the gastic H^+,K^+-ATPase which is the primary target of PPI's, was also upregulated. We speculate that PPI's inhibit cHK-α, resulting in a diminished extrusion of protons into the lumen of the colon (Figure 2). Interestingly, an acidic environment is known to stimulate Mg^{2+} influx via TRPM6 [26]. Thus, reduced H^+ excretion via cHK-α as a consequence of its inhibition by omeprazole could, therefore, result in declined Mg^{2+} transport via TRPM6.

In the situation that reduced intestinal Mg^{2+} absorption resulting from PPI use is indeed caused by local pH changes in the colon, PPIH might be easily prevented by acidifying the colonic milieu. Coudray *et al.* have published a review describing
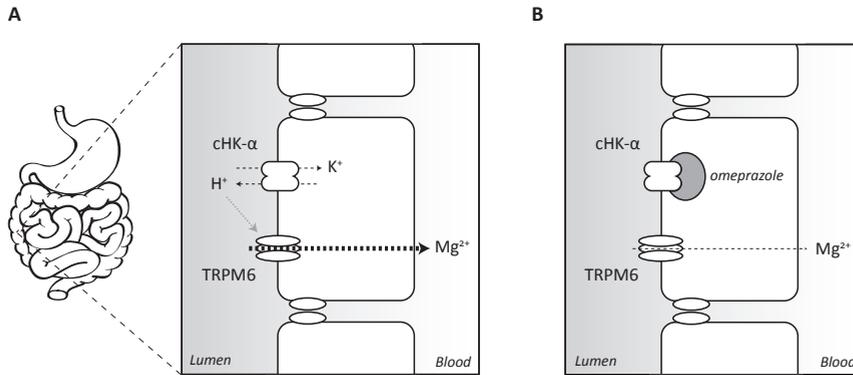
Figure 2 Schematic model of the hypothesized model for PPIH. **A.** Under normal circumstances, Mg^{2+} transport via TRPM6 is stimulated by protons. **B.** Omeprazole inhibits the colonic H^+,K^+-ATPase (cHK-α), resulting in reduced proton secretion into the intestinal lumen. When cHK-α is inhibited by omeprazole, the stimulatory effect on TRPM6 is diminished, resulting in a decrease of colonic Mg^{2+} absorption via TRPM6.

the effects of different types of fermentable carbohydrates on intestinal Mg^{2+} absorption [27]. Fermentation of carbohydrates by bacteria acidified the caecum and colon, and was shown to increase intestinal Mg^{2+} absorption in various animal models as well as in humans. These findings strengthen our hypothesis that local changes in pH can affect Mg^{2+} absorption in the colon. Interestingly, this simple dietary intervention could prevent the development of PPIH.

Despite the large number of PPI users worldwide, less than 100 cases have been reported to date. This does, however, not necessarily mean that the incidence is low. Hypomagnesemia often remains asymptomatic for a long period of time and many physicians are still unaware of this side effect of PPI's. In 2012, a retrospective study by Gau *et al.* showed that in a group of hospitalized patients, PPI use is associated with subclinically reduced serum Mg^{2+} levels [28]. Their study, however, did not take into account confounding factors commonly associated with hypomagnesemia including gastrointestinal illness, diarrhea, vomiting, chronic alcohol use, and chronic use of laxatives, diuretics or other drugs causing Mg^{2+} deficiency. The incidence of lower gastrointestinal illness was significantly higher in the PPI group compared to the control group, which may explain the increased incidence of hypomagnesemia since lower gastrointestinal disease may lead to reduced intestinal Mg^{2+} absorption and increased intestinal Mg^{2+} losses [29]. Other studies failed to find an association between PPI use and hypomagnesemia in their cohorts [30, 31]. This difference is most likely the result of the stricter exclusion criteria and correction for confounding factors in the latter studies compared to the study by Gau *et al.* [28]. The key to the correlation between PPI use and hypomagnesemia may indeed be found in these confounding factors, as was recently demonstrated by Danziger *et al.* who showed that the use of PPIs only correlated with lower serum Mg^{2+} levels in patients that also used diuretics. Among patients concurrently using diuretics, PPI use was associated with a significant higher incidence of hypomagnesemia (odds ratio 1.54). In addition, serum Mg^{2+} concentrations were slightly lower in diuretic users with PPI-treatment compared with diuretic users not taking PPI's. Interestingly, the association was strongest in those patients taking loop diuretics, followed by patients taking thiazides, both of which are known to reduce renal Mg^{2+} reabsorption [32]. Mobilization of Mg^{2+} from bone stores may maintain plasma concentrations, despite a net negative balance as a result of impaired intestinal absorption. This is in line with the fact that PPIH patients are often severely Mg^{2+} depleted upon presentation after long-term PPI use (>1 year).

Due to the, seemingly, low incidence of PPIH, authors of the case-reports often speculate on the potential involvement of mutations or SNP's in TRPM6 in the

8

development of PPIH. It is indeed possible that rare genetic variants of magnesiotropic genes, or of other genes such as cHK-α, contribute to PPIH. However, it is also possible that chronic PPI use slightly decreases intestinal Mg^{2+} absorption in all patients. The development of PPIH could, in that case, depend on a patient's Mg^{2+} intake, as well as on how well the patient is able to compensate for the reduced levels of intestinal absorption via, for example, increased renal Mg^{2+} reabsorption. Carefully designed balance studies are needed to address via which mechanisms PPIs negatively affect Mg^{2+} homeostasis. Meanwhile, physicians should be aware of this potentially serious side effect, particularly in "high-risk" patients, i.e. long-term PPI users who also take diuretics or other drugs that can contribute to the development of hypomagnesemia. By monitoring both serum and urinary Mg^{2+} levels in PPI users, susceptible patients can be identified in an early stage of PPIH development. In these patients, serious Mg^{2+} depletion can be prevented by dietary interventions or by the prescription of oral Mg^{2+} supplements.

Stable Mg^{2+} isotopes, applicability in absorption studies

As described in **chapter 3**, TRPV6 and TRPM6 are expressed at different segments of the gastrointestinal tract, indicating that transcellular absorption of Ca^{2+} and Mg^{2+} are spatially separated. In humans, TRPV6 is expressed predominantly in the stomach and duodenum, whereas TRPM6 is mainly expressed in the ileum and colon. In mice, TRPV6 was also expressed in caecum and distal segments of the colon, while TRPM6 was in addition to ileum and colon also abundantly detected in caecum (Figure 3). Mice are non-ruminant herbivores that have a large caecum compared to humans, which houses many types of microorganisms that play an important role in digestion of plant material by contributing to the enzymatic breakdown of cellulose [33, 34]. Since the digestion of cellulose in the caecum of mice takes place relatively far along the intestine, the animal would miss a lot of nutrients if it only can absorbed its nutrients in the proximal segment. This difference could explain the discrepancy between the expression pattern of TRPV6 in humans, which do not have a caecum aiding to the digestion of cellulose, and mice. The high expression levels of TRPV6 in the stomach are interesting, since the stomach is not generally considered to play a role in Ca^{2+} absorption. It has, therefore, been suggested that TRPV6 plays a role in maintaining intracellular Ca^{2+} balance in gastric cells after mucus secretion to refill the depleted Ca^{2+} stores [35]. In addition, TRPV6 has been shown to mediate capsaicin-induced apoptosis in gastric cells, the physiological relevance of this finding remains to be determined [36].

One of the reasons that knowledge with regard to intestinal absorption of Mg^{2+} is limited is the lack of proper tools to investigate the absorption processes. In

contrast to Ca^{2+}, Mg^{2+} does not have a radioactive isotope that is suitable for research. There are, however, two stable Mg^{2+} isotopes ($^{25}Mg^{2+}$ and $^{26}Mg^{2+}$) that can be distinguished from "normal" $^{24}Mg^{2+}$ by inductively coupled plasma mass spectrometry (ICPMS). These stable isotopes can be used as tracers in absorption studies [37, 38]. In a human setting, these isotopes have been applied to study Mg^{2+}
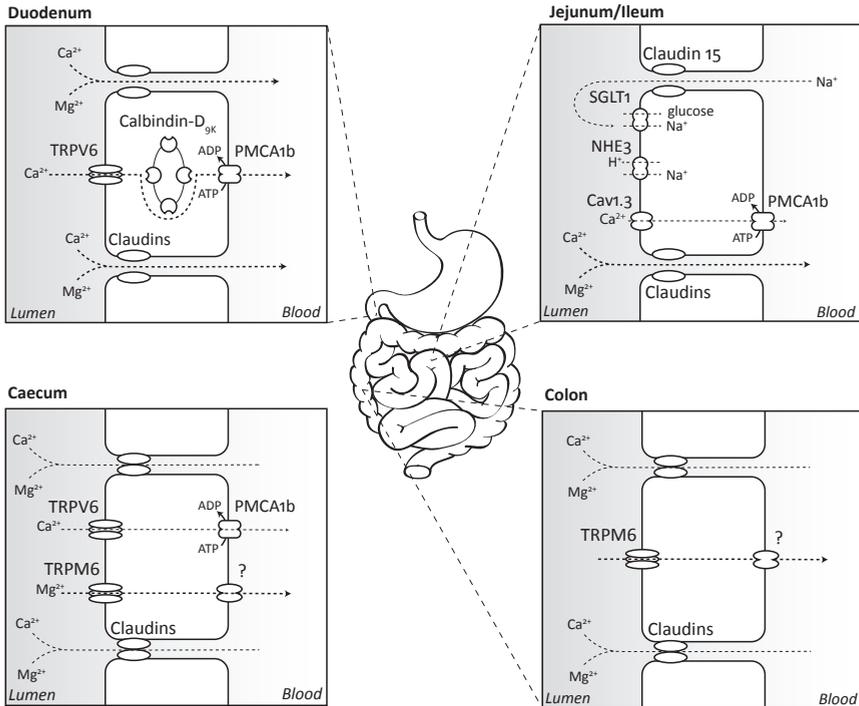
Figure 3 Schematic overview of paracellular and transcellular absorption of Ca^{2+} and Mg^{2+} along the gastrointestinal tract. In the duodenum, Ca^{2+} and Mg^{2+} are absorbed via the paracellular pathway involving claudins. In addition, transcellular Ca^{2+} absorption mediated via TRPV6, calbindin-D_{9K} and PMCA1b takes place in this segment. Transport of Ca^{2+} and Mg^{2+} in the jejunum and ileum are not yet clearly defined. In mice, the caecum and distal colon play an important role in transcellular absorption of Ca^{2+} and Mg^{2+} via TRPV6 and TRPM6. The basolateral extrusion mechanism for Mg^{2+} (?) remains to be defined. Despite the tight epithelium, paracellular transport can occur in these segments at high luminal concentrations. In the human colon, TRPV6 is not expressed, indicating that only Mg^{2+} is absorbed at this location via the transcellular pathway involving TRPM6.

8

absorption via faecal monitoring [39]. Similar methods have been applied in rodents [40]. However, extensive time-dependent studies following the actual absorption of Mg^{2+} from the intestinal lumen in time have not been published so far.

In **chapter 3**, a method to assess *in vivo* absorption of Mg^{2+} using the $^{25}Mg^{2+}$ isotope was developed. With this assay, it is possible to determine time-dependent absorption of Mg^{2+} from the intestine into the circulation. In addition, it was shown that intestinal Mg^{2+} absorption is regulated by bodily needs, exemplified by an increase in intestinal absorption when mice were placed on an Mg^{2+} deficient diet. These studies showed that Mg^{2+} depletion elicits a robust response in the kidneys, where the reabsorption of Mg^{2+} is increased to such extent that urinary Mg^{2+} excretion is virtually diminished. Intestinal absorption of Mg^{2+} changes in response to depletion, however the changes are relatively small. In sharp contrast, Ca^{2+} depletion leads to strong adaptations in intestinal absorption of Ca^{2+}, whereas the renal excretion of Ca^{2+} is much less affected [13].

Interestingly, Mg^{2+} depletion did not only decrease the urinary excretion of Mg^{2+}, but also that of Ca^{2+}. The debate concerning the molecular mechanism underlying this observation dates back to the early 20th century [41]. Recently, Bonny *et al.* have addressed this phenomenon in an elegant series of experiments [42]. These investigators showed that intravenous Mg^{2+} infusion significantly increases urinary Ca^{2+} excretion, indicating a renal effect. The outcome was not influenced by parathyroidectomy, nor by administration of furosemide, suggesting that the process is PTH independent and does not take place in the TAL. The authors postulate that Mg^{2+} directly inhibits the Ca^{2+} uptake by TRPV5 [42]. Ca^{2+} currents through TRPV5 are largely inhibited in the presence of 1mM extracellular Mg^{2+}, which is in line with luminal Mg^{2+} concentrations in the DCT/CNT [43, 44]. Alternatively, other studies using micropuncture have shown that the regulation of Ca^{2+} excretion by Mg^{2+} takes place in the TAL, where high luminal Mg^{2+} would compete with Ca^{2+} for paracellular reabsorption [45, 46]. A recent study by Quinn *et al.* has also addressed this issue by comparing the effect of Mg^{2+} loading and/or Ca^{2+} loading in wild-type mice, PTH KO mice and double KO mice lacking both PTH as well as the CaSR [47]. By measuring changes in the levels of both Mg^{2+} and Ca^{2+} in serum and urine, as well as the levels of hormones potentially participating in Mg^{2+} homeostasis, it was demonstrated that the altered regulation of both Mg^{2+} as well as Ca^{2+} during Mg^{2+} loading involves both PTH and the CaSR. Their results indicate that PTH as well as the CaSR, are important in the defence against oral Mg^{2+} loading. In their model, the concurring changes in Ca^{2+} metabolism seem to result, at least in part, from phosphate depletion, presumably due to the chelation of phosphate by Mg^{2+} in the gut.

Pi depletion will result in increased production of 1,25-dihydroxy-vitamin D_3 through a direct effect of Pi depletion on 1α-hydroxylase in the renal proximal tubule or via a decline in fibroblast growth factor 23 (FGF23)-mediated inhibition of 1α-hydroxylase activity. The increase in 1,25-dihydroxy-vitamin D_3 levels in turn result in increased intestinal Ca^{2+} absorption [47]. All in all, the results of the various studies are conflicting on several points, including the role the intestines and kidney in this phenomenon, as well as the involvement of hormones and the CaSR. Further research is required, as these findings may have important implications in, for example, the methods of supplementation of Ca^{2+} and Mg^{2+} during deficiencies.

Since TRPM6 is mainly expressed in the distal intestinal segments, normal absorption studies in which the isotopes are administered via oral gavage into the stomach are not suitable to study TRPM6 mediated intestinal absorption of Mg^{2+} *in vivo*. Therefore, we developed a surgical procedure to implant intestinal cannulas, which allows isotopes to be directly administered in the caecum. Combining these cannulas and the stable isotopes it was shown that transcellular and paracellular absorption of Ca^{2+} mainly takes place in the proximal regions of the intestine. For Mg^{2+}, paracellular transport is predominant in the proximal intestine whereas transcellular absorption mainly occurs in the colon. This absorption pattern of Ca^{2+} and Mg^{2+} is in line with the observed segmental expression of TRPV6 and TRPM6 indicating that transcellular Ca^{2+} and Mg^{2+} absorption take place at different locations along the intestine.

With the newly developed techniques, we can now address several unanswered questions concerning intestinal absorption of Mg^{2+}. For example, it would be interesting to investigate the action recently discovered magnesiotropic hormones like epidermal growth factor (EGF) and insulin [48, 49]. Both the EGF receptor and the insulin receptor are expressed in the intestine, however, due to a lack of histological information on the exact expression of TRPM6 it is unclear whether the receptors and TRPM6 are co-expressed within the same cells [50, 51]. In addition to the hormonal regulation, the intestinal effects of several drugs already known to influence renal Mg^{2+} handling can now be studied [52]. Their effect on intestinal Mg^{2+} absorption is rarely investigated, but could contribute significantly to development of hypomagnesemia. The interference of Mg^{2+} with Ca^{2+} reabsorption in the kidney also triggers questions with regard to the intestinal absorption of both cations. It is now timely to adequately address these issues, as well as many others.

8

Current views and future perspectives on claudins

Over the last decade, a paradigm shift has taken place concerning our scientific view of paracellular transport. With the identification of the family of claudin proteins, it became clear that paracellular transport is subject to regulation and much more specific and selective than scientists originally recognized. Tight junctions share biophysical properties with conventional ion channels, including size and charge selectivity, dependency of permeability on electrochemical gradients, competition between permeant molecules, anomalous mole-fraction behavior, and sensitivity to pH [53]. The current notion is that claudins form paracellular channels, making them a new class of channels that join two extracellular compartments and determine epithelial tightness by controlling paracellular transport between compartments.

Table 1 Putative ion permeability characteristics of claudin isoforms

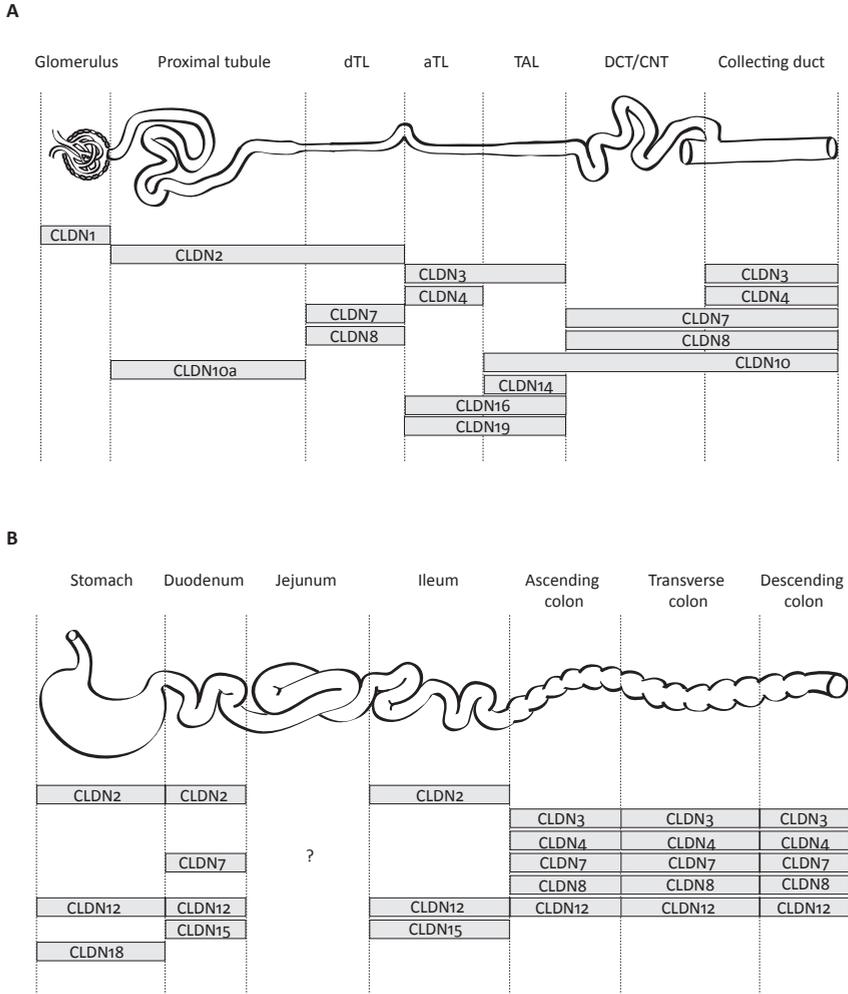| Claudin	
Cation selective	**Anion Selective**
Predominantly cation pore-forming	*Predominantly anion pore-forming*
Claudin 2	Claudin 7
Claudin 10	Claudin 10
Claudin 16	Claudin 17
Predominantly anion barrier-forming	*Predominantly cation barrier-forming*
Claudin 7	Claudin 1
Claudin 19	Claudin 3
	Claudin 4
	Claudin 5
	Claudin 6
	Claudin 9
	Claudin 14
	Claudin 18
Potential to form cation pore or anion barrier	*Potential to form anion pore or cation barrier*
Claudin 15	Claudin 4
	Claudin 8
	Claudin 11

Adapted from [2, 54]

By studying the functional consequences of mutations in CLDN16 and CLDN19, considerable progress has been made in our understanding of paracellular reabsorption of Ca^{2+} and Mg^{2+} in the kidney [55]. With regard to intestinal absorption of Ca^{2+} and Mg^{2+} via the paracellular pathway, however, little is known so far. In **chapter 5**, the expression of several claudin isoforms along the gastrointestinal tract was determined in a panel of human intestinal biopsy samples. Claudins were shown to have distinct expression patterns throughout the gastrointestinal tract. In addition, analysis of expression levels of claudins in patients with Crohn's disease, active, and inactive ulcerative colitis disclosed that changes in claudin expression in inflammatory bowel disease are confined to specific intestinal segments, and strongly depend on the inflammatory activity.

The intestine as well as the nephron display an overall decrease in paracellular permeability towards their distal end. However, individual segments also show major differences with respect to their specific physiological function. This is achieved at the molecular level by segment-specific expression of different claudins [56]. For the nephron, claudin expression patterns have been relatively well defined [57]. For example, segments that reabsorb large quantities of solutes and water such as the proximal tubule (PT) and thin descending limb (tDL), predominantly express pore-forming claudins, whereas tightening claudins are present in the water-impermeable thin ascending limb (tAL) [57]. Studying expression pattern of claudins can thus learn us important lessons about their function. This also applies to the intestine. CLDN18, for example, which is solely expressed in the stomach, has been shown to prevent paracellular H^+ leakage, which is essential for maintaining the low gastric pH [58]. Figure 4 presents an overview of the expression patterns of various claudins along the nephron and the gastrointestinal tract. Based on the expression patterns described in our study, CLDN2 and CLDN15 are interesting candidates that could play a role in intestinal absorption of Ca^{2+} and Mg^{2+}, as they are mainly expressed in the proximal intestinal segments, which are known to be responsible for the bulk of paracellular mineral absorption.

CLDN2 is known to function as a high-conductance, cation-permeable paracellular pore, which is permeable to, and inhibited by, Ca2+ [59, 60]. In the kidney, CLDN2 is highly expressed in the leaky PT, where up to 60% of the filtered Ca2+ load is reabsorbed from the pro-urine via the paracellular pathway. Interestingly, CLDN2 KO mice exhibit decreased proximal reabsorption of Na+, Cl- and water. In addition, CLDN2 KO mice display hypercalciuria, indicating that claudin-2 plays a role in paracellular Ca2+ transport in the PT [61]. In the intestine, CLDN2 expression was highest in the various segments of small intestine, which are relatively leaky

8

and the main site of paracellular Ca2+ and Mg2+ absorption. In contrast, CLDN2 is virtually absent in the colon, where the epithelium is generally considered to be tight [56, 62]. In vitamin D receptor KO mice, intestinal expression of CLDN2 and

A

B

Figure 4 Expression patterns of claudin isoforms along the nephron and gastrointestinal tract. **A.** Overview of the expression patterns of claudins along the nephron based on literature review. dTL, thin descending limb; aTL, thin ascending limb; TAL, thick ascending limb; DCT, distal convoluted tubule; CNT, connecting tubule. Adapted from [1-3]. **B.** Overview of the expression patterns of claudins along the gastrointestinal tract based on the studies described in chapter 5.

CLDN12 was significantly reduced compared to wild-type mice [63]. The expression of both genes was increased by 1,25-dihydroxyvitamin D3 in an intestinal epithelial cell line, Caco2 cells, coinciding with an increase in paracellular Ca2+ transport and a reduction of the transepithelial electrical resistance (TEER) [63]. These findings strongly suggest that tight junctions consisting of claudin 2 and/or claudin 12 form paracellular Ca^{2+} channels in intestinal as well as in renal epithelia. Importantly, they highlight a novel, vitamin D sensitive, mechanism participating Ca^{2+} homeostasis. Of note, the function of claudin 12 is not yet entirely clear. On one hand it has been proposed to increase paracellular permeability, potentially facilitating paracellular transport of Ca^{2+}, and on the other hand a role in epithelial tightening may be deduced from its expression within the blood vessels of the brain and the urinary bladder [64, 65]. The function of claudin 12 may be affected by the presence of other claudins, which would explain the distinct function in different tissues.

Several studies suggested that CLDN15 is responsible for prolactin-stimulated paracellular intestinal Ca^{2+} absorption [19, 66]. In NHE3 KO mice, which display various abnormalities in their Ca^{2+} homeostasis including reduced intestinal Ca^{2+} absorption, both CLDN2 and CLDN15 expression in jejunum is reduced, again linking CLDN15 to Ca^{2+} homeostasis [67]. Other studies, however, showed that the overexpression of CLDN15 does not increase paracellular Ca^{2+} transport in Caco-2 cells [63]. The phenotype of the CLDN15 KO mice is in this respect informative [68, 69]. Most strikingly, these mice have an enlargement of their small intestine [68]. Furthermore, the luminal Na^+ concentration in their small intestine was abnormally low, and glucose absorption was impaired [69]. It has, therefore, been suggested that CLDN15 could serve as a leaky Na^+ channel [69]. At the cellular level, claudin-15 is localized in close proximity to the sodium–glucose symporter SGLT1 and may contribute to the recirculation of Na^+ [69]. In line with the observed impairment of glucose absorption, the observed decrease in luminal Na^+ directly diminishes the activity of SGLT1 in the small intestine, particularly in the jejunum, which is the major site of glucose absorption [69]. Interestingly, this is also the site where $Ca_v1.3$ has been suggested to participate in transcellular Ca^{2+} absorption. CLDN15 is, therefore, not likely to be directly involved in paracellular Ca^{2+} transport. Instead, it probably facilitates the backleak of Na^+, which is important for SGLT1 and NHE3 function. The transport of Na^+ across the apical plasma membrane, facilitated by these proteins, most likely plays a role in Ca^{2+} transport, potentially by changing the transmembrane electrical potential. This change in potential could in turn affect Ca^{2+} transport via, for example, Cav1.3. Alternatively, transcellular Na^+ transport may contribute to the maintenance of a transepithelial electrochemical gradient facilitating paracellular Ca^{2+} transport (Figure 3).

8

Other interesting candidates in intestinal mineral transport would be CLDN10 and CLDN14. CLDN10 KO mice have been shown to suffer from hypermagnesemia and hypocalcemia, opposing the phenotype of CLDN16 KO mice, which display hypomagnesemia and hypercalciuria [70, 71]. Similarly, CLDN14 KO animals developed hypermagnesemia and hypocalciuria [72]. CLDN14 has been shown to regulate Ca^{2+} and Mg^{2+} absorption via an interesting mechanism, involving the CaSR and miRNA's. The expression of miR-9 and miR-374 is regulated by serum Ca^{2+} levels, which are sensed by the CaSR. MiR-9 and miR-374 determine the expression level of CLDN14, which in turn can block the paracellular cation channel formed by claudin 16 and 19, thereby reducing Ca^{2+} reabsorption in the TAL [73]. Extensive bioinformatical analysis with regard to miRNA target sites in claudins could reveal new players in renal, but most importantly, intestinal Ca^{2+} and Mg^{2+} absorption.

New perspectives of idiopathic infantile hypercalcemia

Idiopathic infantile hypercalcemia (IIH) is a potentially life-threatening disease. Interestingly, it is of a transient nature since symptoms usually resolve between the ages of 1 to 3 years. IIH was originally described in the United Kingdom in the 1950s by Lightwood and Fanconi [74, 75] who subdivided their cases into a "mild" and a "severe" type, to distinguish between patients suffering solely from hypercalcemia and patients who also displayed additional abnormalities such as distinctive facial features [76]. The "mild" form, also known as the Lightwood-type IIH, has become rare since many European countries forbade vitamin D fortification of dairy and food products after an outbreak of vitamin D intoxication in neonates. "Severe" IIH, also known as Fanconi-type hypercalcemia, is nowadays considered to be one of many symptoms that are part of the Williams-Beuren syndrome (WBS) phenotype. WBS is caused by a hemizygous microdeletion at 7q11.23, encompassing 24 genes [77] [78, 79]. In **chapter 4**, we hypothesized that the similarities in the course of development of hypercalcemia in isolated IIH patients and patients suffering from WBS can be explained by a shared underlying genetic defect. Figure 5 shows the genes located in the deleted chromosome region in WBS patients. A phenotype-genotype correlation has been demonstrated for only a few of the genes within this region, such as ELN and LIMK, which are linked to supravalvular aortic stenosis and impaired visuospatial constructive cognition respectively [79]. Based on this list of candidate genes, we hypothesized that the hemizygous deletion of two claudin genes (CLDN3 and CLDN4) can be responsible for the hypercalcemia in WBS patients, and could therefore also be responsible for the hypercalcemia in our IIH patients [80]. After careful analysis, we concluded that in our patients IIH is not caused by mutations in these candidate genes nor by deletions or duplications in the genome.

Recently, two groups described a new genetic defect in a large cohort of IIH patients and patients suspected to suffer from vitamin D intoxification [81, 82]. These studies confirm that loss of function of the vitamin D 24-hydroxylase enzyme (CYP24A1) can result in IIH. Since CYP24A1 is responsible for breakdown of active vitamin D into inactive metabolites, lack of CYP24A1 can result in
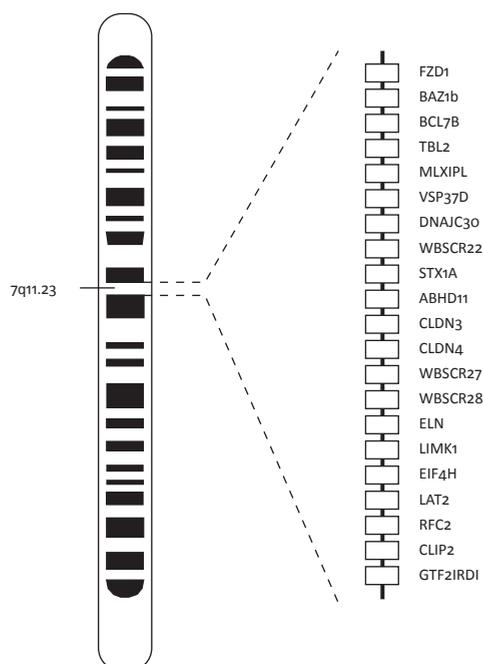
Figure 5 Overview of the genes localized in the WBS deletion region. WBS is characterized by the hemizygous microdeletion of the q11.23 region on chromosome 7. FZD1, frizzled family receptor 1; BAZ1B, bromodomain adjacent to zinc finger domain, 1B; BCL7B, B-cell CLL/lymphoma 7B; TBL2, transducin (beta)-like 2; MLXIPL, MLX interacting protein- like; VPS37D, vacuolar protein sorting 37 homolog D; DNAJC30, DnaJ (Hsp40) homolog, subfamily C, member 30; WBSCR22, Williams Beuren syndrome chromosome region 22; STX1A, syntaxin 1A; ABHD11, Abhydrolase domain-containing protein 11; CLDN3, claudin 3; CLDN4, claudin 4; WBSCR27, Williams Beuren syndrome chromosome region 27; WBSCR28, Williams Beuren syndrome chromosome region 28; ELN, elastin; LIMK1, LIM domain kinase 1; EIF4H, Eukaryotic translation initiation factor 4H; LAT2, linker for activation of T cells family, member 2; RFC2, Replication factor C subunit 2; CLIP2, CAP-GLY domain containing linker protein 2; GTF2IRDI, general transcription factor 2IRDI; WBSCR23, Williams Beuren syndrome chromosome region 28.

8

elevated levels of 1,25-dihydroxy-vitamin D_3 due to its reduced catabolism. Interestingly, serum 25-hydroxy-vitamin D_3 and 1,25-dihydroxy-vitamin D_3 levels were only elevated in those patients that were given a high bolus injection of 1,25-dihydroxy-vitamin D_3 (600,000 IU), while patients who received normal doses of 1,25-dihydroxy-vitamin D_3 prophylaxis (500 IU per day) displayed normal vitamin D levels, despite their lack of normal CYP24A1 to catabolize active vitamin D.

The transient nature of IIH remains to be explained. Interestingly, approximately half of the homozygous KO Cyp24a1 mice died before weaning due to severe hypercalcemia (20, 21). The homozygote mutants that survived past their weaning period had lower baseline circulating 1,25-dihydroxy-vitamin D_3 levels compared to wild-type controls. In addition, the surviving KO mice were found to have a decreased ability to clear 1,25-dihydroxy-vitamin D_3 from their blood (21). These mice also displayed decreased renal expression levels of Cyp27b1, which is responsible for the synthesis of active vitamin D (22). This compensatory mechanism could explain the lower circulating levels of baseline 1,25-dihydroxy-vitamin D_3 in the surviving homozygous mice and, if a similar mechanism is present in humans, may clarify why the hypercalcemia in IIH appears to improve over time (7). Another explanation of the transient nature of hypercalcemia in IIH patients can be found in patients suffering from Sotos syndrome. A subset of these hypercalcemic patients lack not only NSD1 but also SLC43A1 as a result of a microdeletion on chromosome 5q35 [83, 84]. SLC34A1 encodes NaPi2A, a renal phosphate transporter [85]. An interesting theory has been proposed with regard to the transient nature of hypercalcemia in these infants: impaired renal phosphate reabsorption leading to hypophosphatemia could result in activation of vitamin D and in turn, increased intestinal absorption of Ca^{2+} and phosphate, resulting in hypercalcemia and hypercalciuria [83]. The demand on renal phosphate reabsorption is highest during infancy, due to higher plasma levels and the phosphate requirement of the growing skeleton [85]. When phosphate handling matures, and therefore vitamin D requirement and production is diminished, intestinal hyperabsorption of Ca^{2+} ceases, normalizing Ca^{2+} homeostasis. This could provide an alternative explanation for transient hypercalcemia in IIH patients.

Although the biochemical characteristics of the patients described in **chapter 4** closely resembled those of the patients with a CYP24A1 mutation, they all tested negative for mutations in this gene (unpublished results). The mechanism underlying IIH in our patients, therefore, remains unresolved to date. Interestingly, there is another potential candidate gene within the region that is deleted in the WBS patients. BAZ1B, also known as Williams Syndrome Transcription Factor

(WSTF), is located within the WBS deletion region and encodes a subunit of the ATP-dependent chromatin remodelling complex WINAC, whose activity facilitates ligand-dependent activation of CYP24A1 and repression of CYP27B1 by the vitamin D receptor (VDR) [86]. Loss of WINAC function will lead to less transcription of CYP24A1 and increased transcription of CYP27B1 similar to CYP24A1$^{-/-}$ mice and patients with CYP24A1 mutations [87]. Lack of a significant increase in 1,25-dihydroxyvitamin D$_3$ levels in WBS patients seems to contradict this hypothesis. However, the phenotype of patients with CYP24A1 mutations demonstrates that a lack of 25-dihydroxyvitamin D 24-hydroxylase indeed leads to a hypercalcemic phenotype without a concomitant increase in circulating 1,25-dihydroxyvitamin D$_3$ levels [88]. Further investigations measuring vitamin D metabolism and catabolism in WBS patients will shed more light on the involvement of BAZ1B/WSTF and vitamin D metabolism in hypercalcemia in this group of patients. Furthermore, BAZ1B could be an interesting candidate for genetic screening in IIH patients negative for CYP24A1 mutations.

Conclusion and future perspectives

The general aim of this thesis was to generate more insight in the physiological, pathophysiological and pharmacological regulation of intestinal Ca^{2+} and Mg^{2+} transport. The studies presented in this thesis illustrate the importance of TRPV6 and TRPM6 in intestinal absorption of Ca^{2+} and Mg^{2+}, respectively. A new method was developed enabling the direct measurement of intestinal Mg^{2+} absorption using intestinal cannulas and stable Mg^{2+} isotopes. With this method, it is now possible to perform time-dependent, segment specific absorption studies in an *in vivo* setting. We applied this technique, showing the spatial separation of active Ca^{2+} and Mg^{2+} transport in the intestine. In order to gain more insight in the role of claudins in intestinal ion transport, the expression patterns of several claudins along the intestinal tract was determined. Three patients with IIH, were described, and using a candidate-based approach we tried to unravel the mechanisms underlying this phenotype. A case of a patient with WBS coinciding with hypercalcemia is described and a hypothesis with regard to the underlying molecular defect is discussed in the light of recent genetic findings in children suffering from IIH.

Recent studies have identified EGF and insulin as novel magnesiotropic hormones, while their effect on intestinal absorption remains unknown. These, and many other questions can now be addressed with the aid of the Mg^{2+} absorption technique established in this thesis. Although the importance of claudins in

8

paracellular Ca^{2+} and Mg^{2+} reabsorption in the kidney is now well defined, their role in intestinal transport remains largely unknown. Based on the intestinal expression pattern several candidates were selected and their relevance with respect to Ca^{2+} and Mg^{2+} absorption was discussed. More research is necessary to identify which claudin isoforms play a role in paracellular intestinal absorption of Ca^{2+} and Mg^{2+} and how they are regulated. Although our understanding of Ca^{2+} homeostasis is relatively well developed, especially when compared to our understanding of Mg^{2+} homeostasis, many questions remain to be answered. Recent findings have shed more light on the aetiology of IIH in some patients, however, the molecular mechanisms underlying other cases, like the ones described in this thesis, remain unclear.

Future research could provide insight in the missing pieces in our knowledge concerning intestinal Ca^{2+} and Mg^{2+} homeostasis. To this end, researchers should take advantage of recent developments in the field of genetics, which makes extensive screening of patients as well as large populations more accessible and cost efficient. This type of studies may lead to the identification of new genes involved in Ca^{2+} and Mg^{2+} homeostasis. Using the stable Mg^{2+} isotopes, it is now also feasible to directly measure Mg^{2+} absorption in cell and animal models. This will allow assessing the function of these newly indentified transport proteins. Ultimately, this will help the development of new therapeutic strategies to regulate the intestinal absorption of minerals. New therapies should aim to correct disturbances in intestinal absorption, and potentially compensate for pathological renal losses, both of an inherited or acquired nature.

References

1. Angelow S, Ahlstrom R, Yu AS: Biology of claudins. *Am J Physiol Renal Physiol* 295: F867-876, 2008
2. Hou J, Rajagopal M, Yu AS: Claudins and the kidney. *Annu Rev Physiol* 75: 479-501, 2012
3. Balkovetz DF: Tight junction claudins and the kidney in sickness and in health. *Biochim Biophys Acta* 1788: 858-863, 2009
4. Hoenderop JG, Bindels RJ: Calciotropic and magnesiotropic TRP channels. *Physiology (Bethesda)* 23: 32-40, 2008
5. Tsukita S, Furuse M: Overcoming barriers in the study of tight junction functions: from occludin to claudin. *Genes Cells* 3: 569-573, 1998
6. Woudenberg-Vrenken TE, Bindels RJ, Hoenderop JG: The role of transient receptor potential channels in kidney disease. *Nat Rev Nephrol* 5: 441-449, 2009
7. Peng JB, Chen XZ, Berger UV, Vassilev PM, Tsukaguchi H, Brown EM, Hediger MA: Molecular cloning and characterization of a channel-like transporter mediating intestinal calcium absorption. *J Biol Chem* 274: 22739-22746, 1999
8. Bodding M: Voltage-dependent changes of TRPV6-mediated Ca^{2+} currents. *J Biol Chem* 280: 7022-7029, 2005
9. Bodding M, Flockerzi V: Ca^{2+} dependence of the Ca^{2+}-selective TRPV6 channel. *J Biol Chem* 279: 36546-36552, 2004
10. Weissgerber P, Kriebs U, Tsvilovskyy V, Olausson J, Kretz O, Stoerger C, Vennekens R, Wissenbach U, Middendorff R, Flockerzi V, Freichel M: Male fertility depends on Ca^{2+} absorption by TRPV6 in epididymal epithelia. *Sci Signal* vol. 4 (171) pp. ra27, 2011
11. Voets T, Janssens A, Prenen J, Droogmans G, Nilius B: Mg^{2+}-dependent gating and strong inward rectification of the cation channel TRPV6. *J Gen Physiol* 121: 245-260, 2003
12. Weissgerber P, Kriebs U, Tsvilovskyy V, Olausson J, Kretz O, Stoerger C, Mannebach S, Wissenbach U, Vennekens R, Middendorff R, Flockerzi V, Freichel M: Excision of Trpv6 gene leads to severe defects in epididymal Ca^{2+} absorption and male fertility much like single D541A pore mutation. *J Biol Chem* 287: 17930-17941, 2012
13. Woudenberg-Vrenken TE, Lameris AL, Weissgerber P, Olausson J, Flockerzi V, Bindels RJ, Freichel M, Hoenderop JG: Functional TRPV6 channels are crucial for transepithelial Ca^{2+} absorption. *Am J Physiol Gastrointest Liver Physiol* 303: G879-885, 2012
14. Suzuki Y, Kovacs CS, Takanaga H, Peng JB, Landowski CP, Hediger MA: Calcium channel TRPV6 is involved in murine maternal-fetal calcium transport. *J Bone Miner Res* 23: 1249-1256, 2008
15. Benn BS, Ajibade D, Porta A, Dhawan P, Hediger M, Peng JB, Jiang Y, Oh GT, Jeung EB, Lieben L, Bouillon R, Carmeliet G, Christakos S: Active intestinal calcium transport in the absence of transient receptor potential vanilloid type 6 and calbindin-D9k. *Endocrinology* 149: 3196-3205, 2008
16. Morgan EL, Mace OJ, Affleck J, Kellett GL: Apical GLUT2 and Cav1.3: regulation of rat intestinal glucose and calcium absorption. *J Physiol* 580: 593-604, 2007
17. Morgan EL, Mace OJ, Helliwell PA, Affleck J, Kellett GL: A role for Ca(v)1.3 in rat intestinal calcium absorption. *Biochem Biophys Res Commun* 312: 487-493, 2003
18. Nakkrasae LI, Thongon N, Thongbunchoo J, Krishnamra N, Charoenphandhu N: Transepithelial calcium transport in prolactin-exposed intestine-like Caco-2 monolayer after combinatorial knockdown of TRPV5, TRPV6 and Ca(v)1.3. *J Physiol Sci* 60: 9-17, 2010
19. Charoenphandhu N, Nakkrasae LI, Kraidith K, Teerapornpuntakit J, Thongchote K, Thongon N, Krishnamra N: Two-step stimulation of intestinal Ca^{2+} absorption during lactation by long-term prolactin exposure and suckling-induced prolactin surge. *Am J Physiol Endocrinol Metab* 297: E609-619, 2009
20. Platzer J, Engel J, Schrott-Fischer A, Stephan K, Bova S, Chen H, Zheng H, Striessnig J: Congenital deafness and sinoatrial node dysfunction in mice lacking class D L-type Ca2+ channels. *Cell* 102: 89-97, 2000
21. Li J, Zhao L, Ferries IK, Jiang L, Desta MZ, Yu X, Yang Z, Duncan RL, Turner CH: Skeletal phenotype of mice with a null mutation in Cav 1.3 L-type calcium channel. *J Musculoskelet Neuronal Interact* 10: 180-187, 2010

8

66. Wongdee K, Teerapornpuntakit J, Siangpro C, Chaipai S, Charoenphandhu N: Duodenal villous hypertrophy and upregulation of claudin-15 protein expression in lactating rats. *J Mol Histol* 44: 103-109, 2013

67. Pan W, Borovac J, Spicer Z, Hoenderop JG, Bindels RJ, Shull GE, Doschak MR, Cordat E, Alexander RT: The epithelial sodium/proton exchanger, NHE3, is necessary for renal and intestinal calcium (re) absorption. *Am J Physiol Renal Physiol* 302: F943-956, 2011

68. Tamura A, Kitano Y, Hata M, Katsuno T, Moriwaki K, Sasaki H, Hayashi H, Suzuki Y, Noda T, Furuse M, Tsukita S: Megaintestine in claudin-15-deficient mice. *Gastroenterology* 134: 523-534, 2008

69. Tamura A, Hayashi H, Imasato M, Yamazaki Y, Hagiwara A, Wada M, Noda T, Watanabe M, Suzuki Y, Tsukita S: Loss of claudin-15, but not claudin-2, causes Na+ deficiency and glucose malabsorption in mouse small intestine. *Gastroenterology* 140: 913-923, 2011

70. Breiderhoff T, Himmerkus N, Stuiver M, Mutig K, Will C, Meij IC, Bachmann S, Bleich M, Willnow TE, Muller D: Deletion of claudin-10 (Cldn10) in the thick ascending limb impairs paracellular sodium permeability and leads to hypermagnesemia and nephrocalcinosis. *Proc Natl Acad Sci U S A* 109: 14241-14246, 2012

71. Will C, Breiderhoff T, Thumfart J, Stuiver M, Kopplin K, Sommer K, Gunzel D, Querfeld U, Meij IC, Shan Q, Bleich M, Willnow TE, Muller D: Targeted deletion of murine Cldn16 identifies extra- and intrarenal compensatory mechanisms of Ca^{2+} and Mg^{2+} wasting. *Am J Physiol Renal Physiol* 298: F1152-1161, 2010

72. Ben-Yosef T, Belyantseva IA, Saunders TL, Hughes ED, Kawamoto K, Van Itallie CM, Beyer LA, Halsey K, Gardner DJ, Wilcox ER, Rasmussen J, Anderson JM, Dolan DF, Forge A, Raphael Y, Camper SA, Friedman TB: Claudin 14 knockout mice, a model for autosomal recessive deafness DFNB29, are deaf due to cochlear hair cell degeneration. *Hum Mol Genet* 12: 2049-2061, 2003

73. Gong Y, Renigunta V, Himmerkus N, Zhang J, Renigunta A, Bleich M, Hou J: Claudin-14 regulates renal Ca^{2+} transport in response to CaSR signalling via a novel microRNA pathway. *EMBO J* 31: 1999-2012,

74. Fanconi G, Girardet P, Schlesinger B, Butler N, Black J: [Chronic hyperglycemia, combined with osteosclerosis, hyperazotemia, nanism and congenital malformations.]. *Helvetica paediatrica acta* 7: 314-349, 1952

75. Lightwood R: Idiopathic hypercalcaemia with failure to thrive. *Archives of disease in childhood* 27: 302–330, 1952

76. Lightwood R, Stapleton T: Idiopathic hypercalcaemia in infants. *Lancet* 265: 255-256, 1953

77. Schubert C, Laccone F: Williams-Beuren syndrome: determination of deletion size using quantitative real-time PCR. *International journal of molecular medicine* 18: 799-806, 2006

78. Nickerson E, Greenberg F, Keating MT, McCaskill C, Shaffer LG: Deletions of the elastin gene at 7q11.23 occur in approximately 90% of patients with Williams syndrome. *American journal of human genetics* 56: 1156-1161, 1995

79. Schubert C: The genomic basis of the Williams-Beuren syndrome. *Cell Mol Life Sci* 66: 1178-1197, 2009

80. Lameris AL, Huybers S, Burke JR, Monnens LA, Bindels RJ, Hoenderop JG: Involvement of claudin 3 and claudin 4 in idiopathic infantile hypercalcaemia: a novel hypothesis? *Nephrol Dial Transplant* 25: 3504-3509, 2010

81. Schlingmann KP, Kaufmann M, Weber S, Irwin A, Goos C, John U, Misselwitz J, Klaus G, Kuwertz-Broking E, Fehrenbach H, Wingen AM, Guran T, Hoenderop JG, Bindels RJ, Prosser DE, Jones G, Konrad M: Mutations in CYP24A1 and idiopathic infantile hypercalcemia. *N Engl J Med* 365: 410-421, 2011

82. Dauber A, Nguyen TT, Sochett E, Cole DE, Horst R, Abrams SA, Carpenter TO, Hirschhorn JN: Genetic defect in CYP24A1, the vitamin D 24-hydroxylase gene, in a patient with severe infantile hypercalcemia. *J Clin Endocrinol Metab* 97: E268-274, 2012

83. Kenny J, Lees MM, Drury S, Barnicoat A, Van't Hoff W, Palmer R, Morrogh D, Waters JJ, Lench NJ, Bockenhauer D: Sotos syndrome, infantile hypercalcemia, and nephrocalcinosis: a contiguous gene syndrome. *Pediatr Nephrol* 26: 1331-1334, 2011

84. Bergwitz C, Roslin NM, Tieder M, Loredo-Osti JC, Bastepe M, Abu-Zahra H, Frappier D, Burkett K, Carpenter TO, Anderson D, Garabedian M, Sermet I, Fujiwara TM, Morgan K, Tenenhouse HS, Juppner H: SLC34A3 mutations in patients with hereditary hypophosphatemic rickets with hypercalciuria

predict a key role for the sodium-phosphate cotransporter NaPi-IIc in maintaining phosphate homeostasis. *Am J Hum Genet* 78: 179-192, 2006

85. Levtchenko E, Schoeber J, Jaeken J: Genetic disorders of renal phosphate transport. *N Engl J Med* 363: 1774; author reply 1774-1775, 2010

86. Barnett C, Krebs JE: WSTF does it all: a multifunctional protein in transcription, repair, and replication. *Biochem Cell Biol* 89: 12-23, 2011

87. Yoshimura K, Kitagawa H, Fujiki R, Tanabe M, Takezawa S, Takada I, Yamaoka I, Yonezawa M, Kondo T, Furutani Y, Yagi H, Yoshinaga S, Masuda T, Fukuda T, Yamamoto Y, Ebihara K, Li DY, Matsuoka R, Takeuchi JK, Matsumoto T, Kato S: Distinct function of 2 chromatin remodeling complexes that share a common subunit, Williams syndrome transcription factor (WSTF). *Proc Natl Acad Sci U S A* 106: 9280-9285, 2009

88. Schlingmann KP, Kaufmann M, Weber S, Irwin A, Goos C, John U, Misselwitz J, Klaus G, Kuwertz-Broking E, Fehrenbach H, Wingen AM, Guran T, Hoenderop JG, Bindels RJ, Prosser DE, Jones G, Konrad M: Mutations in CYP24A1 and idiopathic infantile hypercalcemia. *N Engl J Med* 365: 410-421, 2011

8

9

Nederlandse samenvatting

Nederlandse samenvatting

Hoofdstuk 1: Introductie

Calcium (Ca^{2+}) en magnesium (Mg^{2+}) spelen een belangrijke rol bij veel processen die essentieel zijn voor het functioneren van ons lichaam, zoals spiercontractie, botvorming en enzymactiviteit. Het is daarom van groot belang dat hun concentratie in het lichaam goed wordt gereguleerd. Er zijn diverse overeenkomsten tussen de Ca^{2+} en de Mg^{2+} huishouding in het lichaam. Zo is er veel overlap in de organen die betrokken zijn bij hun opname en uitscheiding, de hormonen die hun transport reguleren, en de biologische sensoren die de concentratie van deze divalente kationen in het bloed waarnemen. De concentratie van Ca^{2+} en Mg^{2+} in ons bloed wordt nauwkeurig gereguleerd door *i*) de darmen, waar deze divalente kationen worden opgenomen; *ii*) het bot, waarin mineralen kunnen worden opgeslagen en waar vanuit ze kunnen worden afgegeven aan het bloed; *iii*) de nieren, die de uitscheiding van Ca^{2+} en Mg^{2+} via de urine faciliteren. Omdat ons voedsel de enige bron van mineralen voor ons lichaam is, is opname via de darmen essentieel voor de handhaving van een normale Ca^{2+} en Mg^{2+} huishouding. Er zijn 2 routes waarlangs Ca^{2+} en Mg^{2+} geabsorbeerd kunnen worden. Bij transport via de paracellulaire route passeren Ca^{2+} en Mg^{2+} het epitheel via kleine ruimtes tussen de cellen, de zogenaamde "tight junctions". Eiwitten uit de familie van claudines vormen een belangrijk onderdeel van deze tight junctions, omdat ze onder andere bepalen welke elektrolyten worden doorgelaten via deze paracellulaire route. Bij transport via de transcellulair route gaan de kationen door het apicale en basolaterale plasmamembraan van de cel heen, hetgeen mogelijk wordt gemaakt door specifieke ionkanalen en transporteurs. In de darm spelen de ionkanalen TRPV6 (Ca^{2+}) en TRPM6 (Mg^{2+}) bij dit proces een essentiële rol; ze faciliteren de opname van Ca^{2+} en Mg^{2+} zodat deze vanuit het lumen van de darm via de plasmamembraan de cel binnenkomen. Vanuit de cel kunnen deze ionen vervolgens via de basolaterale plasmamembraan naar het bloed worden getransporteerd. Het doel van het onderzoek beschreven in dit proefschrift, was om meer inzicht te krijgen in de fysiologische, pathofysiologische en farmacologische regulatie van Ca^{2+} en Mg^{2+} transport in de darm. Deze samenvatting geeft een kort overzicht van dit onderzoek en beschrijft op welke wijze het heeft bijgedragen aan ons begrip rondom de opname van deze twee divalente kationen in de darm en de processen die daarbij betrokken zijn.

9

Hoofdstuk 2: TRPV6 kanalen zijn essentieel voor de transcellulaire absorptie van Ca^{2+}

Het epitheliale Ca^{2+} kanaal TRPV6 bestaat uit 4 monomeren die samen als homotetrameer het transcellulaire transport van Ca^{2+} in de darm faciliteren. Iedere monomeer heeft 6 transmembraan domeinen, waarvan de hydrofobe regio tussen transmembraan domein 5 en 6 betrokken is bij de vorming van een porie waardoor Ca^{2+} via de apicale membraan de cel in kan diffunderen. Binnen deze regio bevinden zich negatief geladen aminozuren die er mede voor zorgen dat TRPV6 het positief geladen Ca^{2+} kan doorlaten. Wanneer één van deze aminozuren, namelijk een aspartaat op positie 541, wordt vervangen door een neutraal alanine residu is het ionkanaal niet meer functioneel. In hoofdstuk 2 werd onderzocht wat de rol is van dit aminozuur van TRPV6 in de Ca^{2+} huishouding door gebruik te maken van muizen met en zonder deze aminozuurverandering (respectievelijk $TRPV6^{D541A/D541A}$ en wild-type muizen). Wanneer de muizen via het voer een normale hoeveelheid Ca^{2+} binnenkregen waren er geen verschillen tussen de twee soorten muizen waarneembaar; zowel serum Ca^{2+} concentraties, renale Ca^{2+} uitscheiding als de expressie van genen betrokken bij Ca^{2+} huishouding waren onder deze omstandigheden gelijk. Wanneer de muizen echter op een dieet werden geplaatst waarin slechts zeer weinig Ca^{2+} aanwezig was, bleek de hoeveelheid Ca^{2+} die opgenomen werd vanuit de darm in $TRPV6^{D541A/D541A}$ muizen lager dan in wild-type muizen. Op basis van deze resultaten kon geconcludeerd worden dat TRPV6 kanalen essentieel zijn voor de opname van Ca^{2+} in de darm via de transcellulaire route.

Hoofdstuk 3: Omeprazol stimuleert de expressie van TRPM6 in het colon

Protonpomp remmers, zoals omeprazol, reduceren de secretie van maagzuur sterk en worden daarom veelvuldig voorgeschreven aan patiënten met maagzuur-gerelateerde klachten. Hoewel het gebruik van omeprazol over het algemeen als veilig wordt beschouwd, zijn er de afgelopen jaren bijna 100 casussen gepubliceerd over patiënten met een protonpompremmer-geïnduceerde hypomagnesiëmie. Aangezien er bij deze patiënten geen aanwijzingen zijn dat de hypomagnesiëmie wordt veroorzaakt door een renaal Mg^{2+} verlies, is de momenteel gangbare hypothese dat deze bijwerking het gevolg is van een verminderde intestinale opname van Mg^{2+}. In hoofdstuk 3 is het effect van omeprazol op de Mg^{2+} huishouding in de muis bestudeerd. Er werden geen verschillen in serum Mg^{2+} concentraties gemeten tussen muizen die waren behandeld met omeprazol en muizen die een placebobehandeling kregen. Ook de renale en fecale uitscheiding van Mg^{2+} was gelijk in beide groepen. Behandeling van muizen met omeprazol had echter wel een effect op de expressie van specifieke genen. In het colon van de

muizen die waren behandeld met omeprazol was de expressie van een waterstof/kalium pomp (cHK-α) sterk verhoogd ten opzichte van muizen die behandeld waren met placebo. cHK-α is een homoloog van de waterstof/kalium pomp in de maag die het primaire aangrijpingspunt van omeprazol is. Ook de expressie van TRPM6 nam toe in het colon van de met omeprazol behandelde muizen. Op basis van deze bevindingen is de hypothese geformuleerd dat omeprazol de werking van cHK-α in het colon remt, waardoor er minder protonen worden uitgescheiden in het lumen van de darm. Aangezien TRPM6 wordt gestimuleerd door extracellulaire protonen kan dit leiden tot een vermindering van het transport van Mg^{2+} via TRPM6. De toename van TRPM6 expressie kan potentieel compenseren voor het verminderde transport, waardoor de intestinale absorptie op peil blijft. Dit zou verklaren waarom de behandeling van muizen met omeprazol niet leidt tot veranderingen in serum Mg^{2+} concentraties, of tot een verandering in de uitscheiding van Mg^{2+} via de urine en feces.

Hoofdstuk 4: Segmentale absorptie van Ca^{2+} en Mg^{2+}

TRPV6 en TRPM6 hebben verschillende expressiepatronen in de humane darm. TRPV6 komt voornamelijk tot expressie in de proximale segmenten, zoals het duodenum, terwijl TRPM6 vooral in het colon voorkomt. Deze bevinding suggereert dat de transcellulaire absorptie van Ca^{2+} en Mg^{2+} op verschillende locaties in de darm plaatsvindt. Met behulp van stabiele Mg^{2+} isotopen werd aangetoond dat de intestinale Mg^{2+} absorptie afhankelijk is van de mate waarin het lichaam behoefte heeft aan Mg^{2+}. Zo neemt de opname van Mg^{2+} in de darm bijvoorbeeld toe wanneer er langere tijd weinig Mg^{2+} in het voedsel aanwezig is. Met behulp van canules, geplaatst in verschillende segmenten van de darm van muizen, werd aangetoond dat Ca^{2+} transport zowel bij lage als bij hoge luminale Ca^{2+} concentraties voornamelijk plaatsvindt in de dunne darm. Mg^{2+} transport daarentegen vindt bij hoge luminale Mg^{2+} concentraties vooral plaats in het duodenum, terwijl het bij lagere concentraties meer in het caecum en colon wordt opgenomen. Deze bevindingen sluiten aan bij eerder beschreven expressiepatronen van TRPV6 en TRPM6. Er is weinig bekend over de hormonale regulatie van de Mg^{2+} absorptie in de darm. Er wordt gesuggereerd dat vitamine D niet alleen een effect op de Ca^{2+} absorptie, maar ook op de Mg^{2+} opname heeft. Op basis van de studies in dit proefschrift lijkt er echter geen effect te zijn van vitamine D op de intestinale absorptie van Mg^{2+} of de expressie van de daarbij betrokken genen.

9

Hoofdstuk 5: Expressiepatronen van claudines in het humane gastro-intestinale stelsel

Als onderdeel van de tight junctions bepalen claudines voor een groot deel de permeabiliteit van het epitheel in onder andere de darmen en de nieren. Ze spelen daarom een belangrijke rol in het paracellulaire transport in deze organen. In hoofdstuk 5 zijn de mRNA expressiepatronen van diverse claudines binnen de verschillende segmenten van het gastro-intestinale stelsel van de mens onderzocht. Daarnaast is het effect van inflammatoire darmziekten zoals de ziekte van Crohn en Colitis Ulcerosa op de expressie van deze claudines bestudeerd. De verschillende claudines hebben ieder een specifiek expressiepatroon, veelal samenhangend met de functie van de desbetreffende transporteur en het intestinale segment. Zo komen de claudines die het epitheel permeabel maken voor water en elektrolyten veelal tot expressie in de dunne darm, terwijl de claudines die het epitheel minder doorlaatbaar maken juist meer voorkomen in de distale segmenten van de darm. Daarnaast werd aangetoond dat veranderingen in de expressie van claudines in patiënten met inflammatoire darmziekten afhankelijk is van het intestinale segment dat onderzocht wordt en van de lokale ontstekingsgraad.

Hoofdstuk 6: De rol van claudines in idiopathische infantiele hypercalciëmie

Idiopathische infantiele hypercalciëmie (IIH) is het gevolg van intestinale hyperabsorptie van Ca^{2+}. Het is een zeldzame ziekte die meestal voor het eind van het derde levensjaar vanzelf verdwijnt. Een vergelijkbaar beeld van tijdelijke hypercalciëmie komt voor bij patiënten die lijden aan het Williams-Beuren syndroom (WBS), waarbij een heterozygote microdeletie op chromosoom 7 heeft plaatsgevonden. Op basis van het Ca^{2+} fenotype in IIH en WBS patiënten werd verondersteld dat er een overeenkomstig onderliggend genetisch defect zou kunnen zijn. WBS-patiënten missen een gebied dat codeert voor meer dan 25 genen, waaronder CLDN3 en CLDN4. Deze 2 genen, die coderen voor claudine 3 en 4, zijn belangrijk bij het paracellulaire transport van ionen en komen tot expressie in de darm. Op basis van een grondige genetische analyse, uitgevoerd aan de hand van drie goed gekarakteriseerde IIH patiënten, werd aangetoond dat IIH niet veroorzaakt wordt door mutaties in CLDN3, CLDN4 of TRPV6, noch door deleties of duplicaties in het genoom.

Hoofdstuk 7: Het belang van een Ca²⁺ en vitamine D beperkt dieet in WBS

Een patiënt met ernstige hypercalciëmie in combinatie met WBS illustreert hoe belangrijk de beperking van zowel Ca²⁺ als vitamine D kan zijn wanneer de gebruikelijke behandeling met bijvoorbeeld bifosfonaten onvoldoende resultaat heeft. Overeenkomsten met betrekking tot de Ca²⁺ huishouding in WBS en IIH patiënten suggereren dat er een gezamenlijk onderliggend defect in deze patiënten aanwezig is. In een groot aantal patiënten is recentelijk aangetoond dat mutaties in CYP24A1, een belangrijk enzym in de degradatie van 1,25-dihydroxyvitamin D_3, kunnen leiden tot IIH. Opmerkelijk is dat een van de genen die ontbreekt in de aangedane chromosomale regio bij WBS-patiënten codeert voor Williams Syndrome Transcription Factor (WSTF). Het corresponderende eiwit is betrokken bij de transcriptie van twee enzymen (CYP24A1 en CYP27B1) die een essentiële rol vervullen in het vitamine D metabolisme. De heterozygote deletie van WSTF in WBS patiënten zou mogelijk het Ca²⁺ fenotype in deze patiënten en de overeenkomsten met IIH patiënten kunnen verklaren.

Hoofdstuk 8: Algemene discussie

De studies beschreven in dit proefschrift hebben inzicht gegeven in de fysiologische, pathofysiologische en farmacologische regulatie van Ca²⁺ en Mg²⁺ transport in de darm. In de diverse studies is het belang van het transcellulaire en paracellulaire transport, en de hierbij betrokken spelers zoals TRP-kanalen en claudines, op de absorptie van Ca²⁺ en Mg²⁺ in de darm onderzocht. Daarnaast werd een techniek ontwikkeld om met behulp van stabiele Mg²⁺ isotopen op een tijdsafhankelijke manier te bepalen hoeveel Mg²⁺ vanuit de darm wordt opgenomen. Door middel van canules, die in verschillende segmenten van de darm kunnen worden geplaatst, kan bovendien de absorptie in een specifiek deel van de darm bestudeerd worden.

Er zijn nog vele onbeantwoorde vragen omtrent de opname van Mg²⁺ in de darm. Zo is de rol van twee recentelijk geïdentificeerde magnesiotrope hormonen, namelijk de epidermale groei factor (EGF) en insuline, op de intestinale absorptie van Mg²⁺ nog onduidelijk. Ook zijn er veel medicijnen (zoals protonpompremmers, remmers van de EGF receptor, en diverse antimicrobiële middelen, calcineurine remmers en cytostatica) waarvan bekend is dat ze Mg²⁺ tekorten kunnen veroorzaken. De rol die Mg²⁺ absorptie, en de mogelijke verstoring hiervan door medicijnen, in de darm speelt bij het ontstaan van deze tekorten is tot op heden onderbelicht gebleven. De in dit proefschrift beschreven techniek voor het meten van intestinale Mg²⁺ absorptie zal in de toekomst bij kunnen dragen aan het beantwoorden en verder uitdiepen van deze en andere vraagstukken.

9

Door middel van technieken zoals exome sequencing is het mogelijk om nieuwe genen, betrokken bij Ca^{2+} en Mg^{2+} homeostase, te identificeren in patiënten met erfelijke afwijkingen in de mineraalhuishouding. Daarnaast maken genoom wijde associatie studies het mogelijk om in een groep patiënten een correlatie vast te stellen tussen genetische varianten in bepaalde genen en, bijvoorbeeld, de concentraties van mineralen in het bloed. Ook bij het bepalen van de functie van de op deze wijze geïdentificeerde genen of genetische varianten, is het gebruik van de stabiele Mg^{2+} isotopen waardevol ter aanvulling van de bestaande technieken zoals de patch-clamp techniek. Deze kennis kan uiteindelijk worden gebruikt om nieuwe therapieën te ontwikkelen voor de behandeling van zowel erfelijke als verworven ziekten die geassocieerd zijn met tekorten in de Ca^{2+} en Mg^{2+} huishouding als gevolg van een verminderde intestinale absorptie, maar ook ter compensatie van tekorten als gevolg van niet goed functionerende nieren.

9

10

List of abbreviations
Curriculum Vitae
List of publications
Dankwoord

List of abbreviations

1α-OHase	25-hydroxyvitamin-D_3-1α-hydroxylase
1,25(OH)$_2$D$_3$	1,25-dihydroxy-vitamin-D_3 / calcitriol
ANOVA	analysis of variance
AQP	aquaporin
ATP	adenosine 5'triphosphate
AU	arbitrary units
BW	body weight
$^{45}Ca^{2+}$	radioactive calcium isotope
Ca	calcium atom
Ca^{2+}	calcium ion
CaSR	calcium-sensing receptor
Cav1.3	L-type calcium channel
CD	collecting duct
CD	Crohn's disease
cDNA	complementary deoxyribonucleic acid
cHK-α	colonic H^+,K^+-ATPase
Cl^-	chloride ion
CLDN	gene encoding claudin
CNNM2	cyclin M2
CNT	connecting tubule
CYP24A1	cytochrome P450, family 24, subfamily A, polypeptide 1
CYP27B1	cytochrome P450, family 27, subfamily B, polypeptide 1
DCT	distal convoluted tubule
DM2	type 2 diabetes
ECF	extracellular fluid
EGF	epidermal growth factor
EGFR	epidermal growth factor receptor
ER	endoplasmic reticulum
FGF23	fibroblast growth factor 23
FHHNC	familial hypomagnesemia with hypercalciuria and nephrocalcinosis
GAPDH	glyceraldehyde 3-phosphate dehydrogenase
GDM	gestational diabetes mellitus
gHK-α	gastric H^+,K^+-ATPase
HNF1B	hepatocyte nuclear factor 1 homeobox B
HPRT	hypoxanthine-guanine phosphorybosyl transferase
HSH	hypomagnesemia with secondary hypocalcemia
IBD	inflammatory bowel diseases
IIH	idiopathic infantile hypercalcemia
IRH	isolated autosomal recessive hypomagnesmia
K^+	potassium ion
Kv1.1	K^+ voltage gated channel subfamily A, member 1
KO	knockout
Mg	magnesium atom
Mg^{2+}	magnesium ion
miR	microRNA
mRNA	messenger ribonucleic acid
Na^+	sodium ion
NCX1	Na^+/Ca^{2+} exchanger
NHE3	Na^+/H^+ exchanger 3
NKCC2	Na^+-K^+-$2Cl^-$ co-transporter

177

10

OMIM	online mendelian inheritance in man
PCR	polymerase chain reaction
PMCA1b	plasma membrane Ca^{2+}-ATPase
PPI	proton pump inhibitor
PPIH	PPI-induced hypomagnesemia
PT	proximal tubule
PTH	parathyroid hormone
PTHrp	parathyroid hormone-related peptide
RDA	recommended daily allowance
ROMK	inward rectifying ATP-sensitive K^+ channel
RT-PCR	reverse-transcriptase polymerase chain reaction
SEM	standard error of the mean
SNPs	single nucleotide polymorphisms
TAL	thick ascending loop of Henle
TRPV	transient receptor potential channel, subfamily vanilloid
TRPM	transient receptor potential channel, subfamily melastatin
UC	ulcerative colitis
VDR	vitamin D receptor
VDRE	vitamin D responsive elements

Curriculum Vitae

Anke Lameris werd geboren op 25 december 1984 te Grubbenvorst. Zij behaalde in 2002 haar VWO diploma aan het Blariacum college in Venlo. Vervolgens studeerde zij Medische Biologie aan de Radboud Universiteit Nijmegen. Tijdens deze opleiding doorliep zij een Bachelor stage van 3 maanden op de afdeling Psycho-neurofarmacologie (onder leiding van Dr. B. Ellenbroek en Prof. Dr. L. Cools). Gedurende haar Master opleiding Medische Biologie bracht ze 9 maanden door bij de afdeling Maag-, Darm- en Leverziekten voor een stageonderzoek, waarin ze onder begeleiding van Dr. E. Waanders en Prof. Dr. J. Drenth onderzoek verrichtte naar de samenstelling van cystevocht van patiënten die lijden aan polycysteuze leverziekte. Vervolgens liep ze gedurende 6 maanden stage bij de afdeling Fysiologie, waar ze zich onder leiding van Dr. T. de Groot en Prof. Dr. J. Hoenderop verdiepte in de celbiologie van het calciumkanaal TRPV5.

In augustus 2009 behaalde zij haar doctoraal examen met de toevoeging bene meritum. Ze startte reeds in januari 2009 als PhD student op de afdeling Fysiologie op een door ZonMW gesubsidieerd project, hetgeen heeft geleid tot het in dit proefschrift beschreven onderzoek. Ze werkte gedurende haar promotieonderzoek samen met diverse groepen in binnen- en buitenland, wat onder andere heeft geleid tot publicaties met collega's uit Duitsland, Finland en Australië. Tijdens haar promotie begeleidde ze diverse Bachelor- en Masterstudenten van de studies Moleculaire levenswetenschappen, Geneeskunde en Biomedische Wetenschappen. Daarnaast leverde ze, in de vorm van practica en werkgroepen, een bijdrage aan het onderwijs voor studenten Biomedische Wetenschappen en Geneeskunde. Vanaf oktober 2012 was ze bovendien actief als stagecoördinator, waarbij ze onder andere verantwoordelijk was voor de organisatorische zaken rondom de werving en begeleiding van studenten binnen de afdeling Fysiologie.

List of publications

Lameris AL, Monnens LA, Bindels RJ, Hoenderop JG. Segmental transport of Ca^{2+} and Mg^{2+} along the gastrointestinal tract. *Manuscript in preparation*

Arjona FJ*, de Baaij JH*, Schlingmann KP*, **Lameris AL**, van Wijk E, Flik G, Konrad M, Bindels RJ, Hoenderop JG. CNNM2 mutations cause impaired brain development and seizures in patients with hypomagnesemia. (*Submitted*) *contributed equally to this work

Lameris AL, Geesing CL, Hoenderop JG, Schreuder MF. Importance of dietary calcium and vitamin D in treatment of hypercalcaemia in Williams-Beuren syndrome. *J Pediatr Endocrinol Metab.* (*provisionally accepted), 2013*

Lameris AL, Hess MW, van Kruijsbergen I, Hoenderop JG, Bindels RJ. Omeprazole enhances the colonic expression of the Mg^{2+} transporter TRPM6. *Pflügers Arch.* In press, 2013

Lameris AL, Huybers S, Kaukinen K, Mäkelä TH, Bindels RJ, Hoenderop JG, Nevalainen PI. Expression profiling of claudins in the human gastrointestinal tract in health and during inflammatory bowel disease. *Scand J Gastroenterol.* 48: 58-69, 2013

Woudenberg-Vrenken TE, **Lameris AL***, Weißgerber P*, Olausson J, Flockerzi V, Bindels RJ, Freichel M, Hoenderop JG. Functional TRPV6 channels are crucial for transepithelial Ca^{2+} absorption. *Am J Physiol Gastrointest Liver Physiol.* 303: G879-885, 2012
*contributed equally to this work

Lameris AL, Monnens LA, Bindels RJ, Hoenderop JG. Drug-induced changes in Mg^{2+} homeostasis. *Clin Sci (Lond).* 123: 1-14, 2012

Lameris AL, Huybers S, Burke JR, Monnens LA, Bindels RJ, Hoenderop JG. Involvement of claudin 3 and claudin 4 in idiopathic infantile hypercalcemia: a novel hypothesis? *Nephrol Dial Transplant.* 25: 3504-3509, 2010

Waanders E, Van Krieken JHJM, **Lameris AL**, Drenth JPH. Disrupted cell adhesion but not proliferation mediates cyst formation in polycystic liver disease. *Mod Pathol.* 21: 1293-1302, 2008

Waanders E, **Lameris AL**, Den Camp HJMO, Pluk W, Gloerich J, Strijk SP, Drenth JPH. Hepatocystin is not secreted in cyst fluid of hepatocystin mutant polycystic liver patients. *J Proteome Res* 7: 2490-2495, 2008

10

Dankwoord

Zoals velen van jullie weten is het promoveren me niet altijd even makkelijk afgegaan. In januari 2009 begon ik, nog voordat ik goed en wel afgestudeerd was, aan dit promotie traject. Jong, naïef, en vol enthousiasme stortte ik me op de wetenschap. Nu, 5 jaar later en voor mijn gevoel 10 jaar ouder, is het dan eindelijk zover. Promoveren doe je niet alleen en er zijn dan ook heel veel mensen die ik in deze laatste pagina's van dit proefschrift graag wil bedanken.

Allereerst gaat mijn dank uit aan mijn promotoren Prof. Dr. Hoenderop en Prof. Dr. Bindels. Bedankt dat jullie me de kans hebben gegeven om binnen de afdeling Fysiologie mijn promotieonderzoek te doen. **Joost**, je deur staat altijd open voor een snel overleg, een peptalk of gewoon een grapje in het voorbijgaan. Het enthousiasme en de ongelofelijke hoeveelheid energie waarmee jij je in de wetenschap stort werken aanstekelijk en zijn een grote stimulans voor mij en vele andere jonge onderzoekers. Bedankt dat je steeds weer voor me klaarstond op de momenten dat ik het nodig had. **René**, ik heb veel van je geleerd. Ik heb enorm veel respect voor de manier waarop je je taken als scientific director van het NCMLS en als hoofd van onze afdeling weet te combineren. Je gestructureerde, georganiseerde manier van werken en je oog voor detail zijn ongeëvenaard en vormen het fundament voor het succes van onze afdeling.

Ook wil ik Prof. Dr. Monnens graag bedanken. Toen ik als PhD-studente begon bij de afdeling fysiologie werd mij door Joost en René verteld dat er een gepensioneerde kindernefroloog was die het leuk vond om nog wat bij de wetenschap betrokken te blijven. Onervaren als ik was, had ik geen flauw idee dat het een van de pioniers binnen het Nijmeegse onderzoek naar water- en zouttransport betrof. **Leo**, je enorme kennis, bevlogenheid, enthousiasme, betrokkenheid en goede neus voor interessante patiënten bewonder ik zeer. Graag wil ik je bedanken voor alles wat je voor me hebt gedaan de afgelopen jaren, ik had het niet beter kunnen treffen en kijk met veel plezier terug op onze overlegmomenten op je "kantoor".

Tijdens je PhD breng je veelal meer tijd op het lab door dan je lief is. Een goede sfeer en leuke, kundige collega's zijn dan ook onontbeerlijk voor het voltooien van een PhD-traject. Dankzij alle leuke collega's heb ik ontzettend veel goede herinneringen aan de afgelopen jaren.

Theun, onder jouw leiding startte ik mijn loopbaan bij Fysiologie als student, ik heb veel van je geleerd en denk nog steeds met heel veel plezier terug aan die tijd!

Titia, altijd stond je voor me klaar met goed advies en wijze raad. Wat heb ik je gemist toen terug naar Groningen ging! Ik ben blij dat ik de kans kreeg om je te helpen de V6-paper af te ronden, nu kunnen we toch nog zeggen dat we samen aan een project hebben gewerkt. Dankjewel voor al je hulp en lieve mailtjes de afgelopen jaren.

Mijn partners in crime voor verkleedpartijtjes: **Jenny** en **Leonie**. Wat hebben we een hoop lol gehad bij de diverse feestjes en etentjes. Dankjewel voor alle mooie herinneringen meiden! **Leonie**, we zijn zo verschillend maar soms ook zo gelijk. Ik ben blij dat we na je vertrek bij fysiologie contact hebben gehouden. Niets is zo goed voor het moraal als een avondje stAnneke: na het delen van lief, leed en broodjes met aioli ziet het leven er altijd ineens weer een stuk zonniger uit.

Bobby, meer dan eens heb ik me de afgelopen jaren afgevraagd of ik niet toch beter naar je had moeten luisteren. Gelukkig bel/mail je altijd op de momenten dat ik je peptalks het hardst nodig heb. Ik weet nog steeds niet of dat toeval is of dat je misschien een uiterst discrete spion op het lab hebt rondlopen? Het is in ieder geval altijd leuk om samen de nieuwste roddels en ontwikkelingen binnen ons veld te bespreken.

Silvia, good things come in small packages. Our trip to Milano where we stayed with your great family was an amazing experience. Over the years you taught me a lot about science, good food and cocktails ;) I hope that, after a bit of rest, you will "really really like magnesium" and science again. Wherever life may take you, I whish you all the best.

Sjoerd, Jeroen and Paco, the three musketiers from Unit 10. Never a dull moment when you are around! I will always cherish the memories of our fantastic trip to Cadiz! **Sjoerd**, altijd sta je klaar voor iedereen. Bij gebrek aan inspiratie heb je goede ideeën, bij problemen heb je wijze raad, bij verdriet heb je een opbeurend woordje en bij honger? Een boterhammetje cervelaat natuurlijk ;). Dankjewel voor al je hulp en de gezelligheid in de afgelopen jaren. Je bent altijd welkom in Gennep voor een middagje Ajax-PSV. **Paco**, it's always fun fighting the "kidney-people" in the lab together, one day we'll convince them that the kidney is not the only organ of importance in physiology/fishiology. Thanks for the many times we spent discussing science and all kind of other things, you are a great colleague and friend! **Jeroen**, de petit-prince, mijn favoriete golden-boy, mijn evil-twin, mijn vriendje! Je bent een van de weinigen die mijn ietwat sarcastische gevoel voor humor niet alleen weet te waarderen maar regelmatig zelfs weet te overtreffen! Je "politieke" talent is ongeëvenaard en ik heb de afgelopen jaren veel van je

mogen leren op dit vlak. Ik heb enorm veel bewondering voor de manier waarop jij je doelen nastreeft en waarmaakt. Het is mooi om te zien hoe je met volle overgave en een duidelijke visie werkt aan je wetenschappelijke carrière. Ik heb er het volste vertrouwen in dat al het harde werk van de afgelopen jaren zijn vruchten af gaat werpen in de toekomst. Dankjewel voor alle momenten dat je er de afgelopen jaren voor me was, en ik ben blij dat je op de dag van mijn verdediging aan mijn zij zal staan als paranimf.

Eline, ondanks alle tegenslagen ben je blijven vechten, nog even volhouden meid, je bent er bijna! Vergeet vooral niet in jezelf te geloven. Ik mis je op het lab, maar gelukkig is Arnhem dichtbij.

Liz en **Ellen/Evil** (in combinatie ook wel bekend als "het kippenhok") jullie hebben me zeer vakkundig door de laatste 1,5 jaar van mijn promotie heengesleept. Muffins, thee, gekke briefjes, horoscopen, ijsjes, PeterJan Rens en dansende bloemen: alles werd in de strijd gegooid wanneer het even tegenzat en ik opgebeurd moest worden. Thanks meiden! Nog even en dan zijn jullie aan de beurt, heel veel succes met jullie onderzoek, jullie komen er wel!

Mark H. Onze samenwerking verliep niet altijd even soepel, maar heeft uiteindelijk toch tot een prima publicatie geleid. Het is mooi om te zien hoe je inmiddels grote vorderingen maakt bij de verdere ontrafeling van PPIH in je patiëntenstudies, en ik waardeer het enorm dat je me nog steeds op de hoogte houdt van je nieuwste bevindingen. Succes met het afronden van je PhD.

Irene, wanneer je ziek of op vakantie bent blijkt altijd onmiddellijk weer hoe belangrijk je bent. Je bent de stille kracht die ons lab draaiende houdt. Bedankt voor het uitzoeken en bestellen van al mijn "exotische" producten.

AnneMiete, ik kan nog steeds niet helemaal geloven dat je echt met pensioen bent, het fysiologie-lab zonder jou is niet compleet! Bedankt voor al je hulp de afgelopen jaren.

Sjoeli, in no-time wist je jezelf onmisbaar te maken op de afdeling. Niet alleen vanwege je organisatorische talenten, maar vooral vanwege je vrolijke en gezellige persoonlijkheid. **Femke**, ook jij brengt het nodige leven in de brouwerij op het secretariaat fysiologie. Bedankt voor jullie hulp bij alle organisatorische zaken de afgelopen jaren, maar vooral voor alle leuke en gezellige momenten.

10

Joris, toen ik als student op het fysiologie lab rondliep kwam jij net terug uit Schotland. Met je baard, vreemde schotse accent en enorme hoeveelheid wetenschappelijke kennis vond ik je destijds een beetje eng. Een paar jaar, vele peptalks, knuffels, en een bekerglas vol chocotofs vermomd als muizenvoer later is dat wel over. Ik hoop dat je het naar je zin hebt in Groningen, hier in Nijmegen missen we je nog steeds.

Anne, de manier waarop jij, ondanks de vele wetenschappelijke tegenslagen, altijd positief bleef is bewonderenswaardig. Stiekem ben je daarin altijd een beetje een voorbeeld voor me geweest.

Erik, een vrolijke persoonlijkheid en een keiharde werker, je bent de Bom ;). Ook voor jou geldt: vergeet niet in jezelf te geloven!

Mijn studenten **Ila**, **Ellen**, en **Daisy**, ik hoop dat jullie net zo veel van mij hebben geleerd als ik van jullie, dank jullie wel voor alle hulp!

Mark de Graaf, Henrik, Marla, Laurianne, Maxime, Femke, Hans, Annelies, Ramon, Rick, Kuki, Sandor, Miyuki, Sabina, Ganesh, Johan, Christiane, Melissa, Marcel, Dennis, en alle andere mensen die ik hier waarschijnlijk nog vergeet: Bedankt voor jullie hulp, gezelschap en alle goede herinneringen die ik dankzij jullie heb aan mijn tijd op het lab!

Ook buiten de afdeling hebben vele mensen bijgedragen aan het tot stand komen van dit proefschrift.

Dr. **Pasi** Nevalainen; the unique set of biopsy samples you provided us with formed the basis for two of the papers in this thesis. Over the years, we've exchanged countless emails, discussed ideas and manuscripts via Skype, and even managed to meet once for a face-to-face discussion, thank you for all your help.

Dr. **Michiel** Schreuder; ook aan jou dank ik een van de hoofdstukken in dit proefschrift. Door de lange dagen in het lab vergeet je als onderzoeker soms waar je het allemaal voor doet, de verhalen en casussen uit de kliniek zetten dit allemaal echter meteen weer in perspectief. Ik vond het erg leuk om samen te brainstormen en te pogen om alle stukjes informatie die we hadden aan elkaar te puzzelen, bedankt!

Jelle Eygensteijn, alweer een aantal jaar geleden besloot ik dat het hoog tijd werd dat er binnen de afdeling fysiologie een nieuwe methode kwam om magnesium transport te bestuderen. Met veel geduld legde je mij de basis-principes van de ICPMS uit, en bekeken we samen de resultaten van mijn eerste experimenten. Ik hoop en verwacht dat er met behulp van deze techniek in de toekomst nog veel mooie functionele studies gedaan zullen worden op de afdeling fysiologie. Bedankt voor je hulp bij het opzetten en voor het analyseren van al mijn samples.

Wanneer je niet alleen dit dankwoord maar ook de rest van dit proefschrift hebt bekeken zul je gezien hebben dat ik nogal wat onderzoek met dieren heb gedaan. Dit was allemaal onmogelijk geweest zonder de hulp van de geweldige mensen van het CDL: **Henk** en **Jeroen M.**; toen ik net begon met mijn PhD stonden jullie altijd klaar om me met veel geduld de fijne kneepjes van het vak te leren. **Janneke, Thea, Wilma, Alex, Jeroen de B,** en **Denise**: dankzij jullie hulp verliepen niet alleen mijn experimenten goed maar was het bovendien altijd fijn om op de VGD te werken en even te ontsnappen aan het lab. **Bianca**, op de PRIME was ik af en toe te vinden voor het werk met radioactief calcium, het is een genot om te werken op je mooie en super soepel lopende afdeling. **Maikel**, een speciaal woordje voor jou: ondanks de lange drukke dagen en een naar muizen stinkende OK klaagde je nooit wanneer je me moest helpen...O wacht, dat deed je wel, en daarna zeurde je om taart ;) dankjewel voor alle hulp!

Daphne, dit proefschrift zou niet zijn wat het is zonder jou en je "gouden handjes". Onze samenwerking begon met een, wetenschappelijk gezien, teleurstellende trip naar Amsterdam. Bij gebrek aan een goed voorbeeld besloten we daarna met vereende krachten zelf de methode voor het aanleggen van de darmcanules op te zetten. Je zwangerschap dreigde even roet in het eten te gooien m.b.t. de planning van mijn experimenten, maar als jij iets in je hoofd hebt houdt niets je tegen. Nauwelijks meer achter de microscoop passend en tussen de harde buiken door opereerde je nog even 2 enorme series muizen zodat ik verder kon met mijn onderzoek tijdens je verlof. Ik ben je ongelofelijk dankbaar voor al je hulp, en kijk met plezier terug naar alle uren die we doorbrachten op het microscopen-labje, waar we tijdens de ok's kletsten over huizen, trouwen, babies, big fat gypsie weddings en de laatste roddels van zowel het CDL als het NCMLS ;)

En dan is er ook nog het leven buiten het lab, waar zoveel vrienden en familie onbewust hebben bijgedragen aan het tot stand komen van dit boekje.

Lieve **San**, meer dan eens gedurende de afgelopen jaren heb ik mezelf gaande gehouden onder het motto "niet zeuren Anke, Sandra heeft het nog veel zwaarder

en die leeft ook nog steeds". Onze telefoongesprekken vanuit de auto op weg naar huis om te klagen over bazen, collega's, patiënten, semi-artsen, reviewers en vriendjes hebben op wonderbaarlijke wijze nooit tot ongelukken geleid. Met dank aan de drukke agenda's is het niet altijd makkelijk om een gaatje te vinden om met z'n tweetjes of samen met Arjan en Sjoerd een avondje bij te kletsen, maar als het lukt is het altijd gezellig. Ik hoop dat je voor altijd jezelf en mijn vriendinnetje blijft! Dankjewel dat je me op de dag van mijn verdediging bij wilt staan als paranimf.

Fien, je hebt een geweldige zoon op de wereld gezet, dankjewel voor alle goede zorgen de afgelopen jaren. **Debby** en **Cliff**, het is altijd weer heerlijk om onder het genot van een glaasje wijn bij te kletsen en ondertussen te genieten van mijn liefste nichtje en neefje **Marit** en **Julian**. Bedankt dat jullie al die jaren steeds weer interesse hebben getoond in mijn saaie wetenschapsverhalen!

Miriam en **Joerie**, ook jullie verdienen hier een plekje. Lieve zus, het was altijd lekker om even aan de hectiek van het promoveren te ontsnappen door een middagje te helpen met het versieren van de klas of met het maken van nieuwe knutselwerkjes. Dankjulliewel voor de correcties van de Nederlandse gedeeltes van dit proefschrift en het aanhoren van de eerste versies van mijn leken-praatje!

Lieve **Opa**, ik vind het geweldig dat ik na al dat lange wachten nu eindelijk mijn boekje aan je kan overhandigen. Vaak vertelde je me hoe trots je op me bent en hoe je naar deze dag uitkeek. Maar ik ben ook trots; trots op mijn lieve, sterke en zorgzame en ontzettend eigenwijze Opa, van wie ik leerde om ondanks alles altijd door te zetten!

Lieve **Papp**a en **Mamma**, jullie staan altijd voor me klaar met een luisterend oor, een helpende hand, wijze raad of gewoon een hele dikke knuffel. Het is voor jullie niet altijd even gemakkelijk geweest om van een afstandje toe te moeten kijken en niet te kunnen (lees: mogen) helpen. Dankjewel voor jullie onvoorwaardelijke steun en liefde, zonder jullie was ik nooit zo ver gekomen.

Arjan, lieve sies, lang heb ik gezocht naar de juiste woorden en vele malen heb ik dit stuk herschreven om uiteindelijk tot de conclusie te komen dat woorden simpelweg tekort schieten. Ik ben de laatste jaren (en eigenlijk ook alle jaren daarvoor) niet de makkelijkste geweest. Desondanks sta je al 11 jaar altijd voor me klaar, maak je me steeds weer aan het lachen, en weet je me keer op keer weer te verassen. Dankjewel sies, ik kijk uit naar alles wat de komende jaren ons nog gaan brengen!

Anke Lameris